The Application and Assessment of Active Network Management Techniques for Distribution Network Power Flows

Michael James Dolan

A thesis presented in fulfilment of the requirements
for the degree of Doctor of Philosophy

Institute for Energy and Environment
Department of Electronic and Electrical Engineering
University of Strathclyde
Glasgow G1 1XW
Scotland UK

2012

This thesis is the result of the author's original research. It has been composed by the author and has not been previously submitted for examination which has led to the award of a degree.

“We make a living by what we get, but we make a life by what we give”

Sir Winston Leonard Spencer Churchill

(1874-1965)

Contents

Figures

Tables

Glossary of Abbreviations

AI	Artificial Intelligence
ACCM	Active Constrained Connection Manager
ADM	Active Distribution Management (synonymous with ANM)
ANM	Active Network Management (synonymous with ADM)
CLR	Current Limiting Reactors
CRIEPI	Central Research Institute of the Electric Power Industry (Japan)
CSP	Constraint Satisfaction Problem
DER	Distributed Energy Resources
DG	Distributed Generation
DGI	Distribution Generation Incentive
DGCG	Distribution Generation Co-ordinating Group (UK)
DPCR	Distribution Price Control Review (UK)
DNO	Distribution Network Operator
DTI	Department of Trade and Industry (UK)
DTR	Dynamic Thermal Rating
ED	Economic Dispatch
EGWG	Embedded Generation Working Group (UK)
EHV	Extra High Voltage
EICM	Equal Incremental Cost Method
EMR	Electricity Market Reform (UK)
EPRI	Electric Power Research Institute (USA)
FG	Firm Generation
FLI	Fault Location and Isolation
FSM	Fast Simulation & Modelling
GW	Giga Watt
HV	High Voltage
IEC	International Electrotechnical Commission
IED	Intelligent Electronic Device
IFI	Innovation Funding Incentive (UK)

LCNF	Low Carbon Network Fund (UK)
LV	Low Voltage
MFR	Multi-feeder Reconfiguration
MVA	Mega Volt-Ampere
MWh	Mega Watt Hour
NFG	Non-Firm Generation
NNFG	New Non-Firm Generation (synonymous with RNFG)
Ofgem	Office of Gas and Electricity Markets (UK)
OPC	Object Linking and Embedding for Process Control
OPF	Optimal Power Flow
RIG	Regulatory Instructions and Guidance (UK)
RNFG	Regulated Non-Firm Generation (synonymous with NNFG)
RO	Renewable Obligation (UK)
ROC	Renewable Obligation Certificate (UK)
RPZ	Registered Power Zone (UK)
SCADA	Supervisory Control and Data Acquisition
SFCL	Superconducting Fault Current Limiters
SHG	Self-Healing Grid
SPS	Special Protection System
SSFCL	Solid-State Fault Current Limiter
SVC	Static VAr Compensation
TSG	Technical Steering Group
UC	Unit Commitment
UKGDS	United Kingdom Generic Distribution System
VVC	Volt-VAr Control
WS	Work Streams

Abstract

The UK Government regards renewable energy technology deployment to be crucial in successfully meeting reduced greenhouse gas emission targets. As such, incentives promoting the connection of clean energy sources to the UK's electricity infrastructure are influencing a significant increase of distributed generation (DG) planning applications. With an abundance of the UK's indigenous energy resources being either rural or coastal large volumes of DG are seeking connection at the lower voltage distribution networks. Connecting large quantities of intermittent generation, to distribution networks, presents significant problems to the planning and operation of these traditionally passive networks due to bi-directional power flows creating voltage fluctuations and uncertainty in power flow magnitudes. In addition, conventional planning methods results in financial barriers that are preventing DG connections due to the high cost of reinforcing the existing infrastructure. One method of avoiding, or at least deferring, this high capital costs is to adopt an Active Network Management (ANM) approach.

This thesis presents and evaluates two novel ANM approaches that manage the real power output of multiple DG units, in real-time, such that distribution networks operate within thermal limits. Studies are conducted in a closed-loop simulation environment, with actual hardware, on two topologically different networks to demonstrate the flexibility of the novel application of the Optimal Power Flow (OPF) and the Constraint Satisfaction Problem (CSP) when applied to the Power Flow Management (PFM) problem. The performance of these model-based algorithms is assessed against their ability to detect thermal excursions, their solution computation time, their resilience to measurement error, their real power curtailment, their ability to conform to current DG commercial connection agreements and their ability to adapt to changes in network topology. Results reported in this thesis demonstrate the feasibility of these novel ANM approaches for PFM, and their applicability in terms of incorporating intelligence into the UK's future smart grids.

Acknowledgements

I would like to offer sincere thanks to Professor Jim McDonald for the opportunity of working within the Advanced Electrical Systems (AES) research group and carrying out this research work. Sincerest gratitude and thanks also goes to my supervisor, Professor Graham Ault, for his support, time and reassurance through the duration of this project. Also, to Professor Stephen McArthur for his guidance and additional support. To Dr Ivana Kockar whose door has always been open for invaluable advice and help, thank you!

My gratitude extends to UK Power Networks (formerly EdF Energy), Scottish Power, ABB, the Engineering and Physical Research Council (EPSRC) and the Autonomous Regional Active Network Management System (AuRA-NMS) consortium for their technical and financial support over the duration of this project.

Thanks go to all my colleagues within the AES research group especially to Euan Davidson for his patience, guidance and support that has undoubtedly inspired and help the progress of this work and to Dr Bob Currie whom I hold fully responsible for this pleasure!

To my mum, dad, sister and friends, thank you for all your encouragement over the years and supporting me in whatever I ventured out to do.

Special thanks go to my wife, Anna, and my son, Callum. Thank you so much for all your understanding, support and for being there to always brighten up my day!

Chapter 1

Introduction

1.1 Summary of Chapter 1

This chapter introduces the motivation for the research presented within this thesis in the context of overcoming the barriers for increased Distributed Generation (DG) connections and maximising DG access to the networks to combat climate change and meet national and global targets. The technical concerns of DG connections are highlighted and the incentives offered for generator connections at distribution level are stated. Active Network Management (ANM) is then introduced as a means of embedding intelligence into existing distribution networks to enable higher penetrations of DG to be connected to the distribution networks emphasising the role ANM can play in the wider picture of smart grid technologies. The focal point of this thesis, the development and demonstration of new ANM functionality for Power Flow Management (PFM), is then established and the techniques the author has applied to the PFM problem are discussed along with prior PFM developments reported within the literature. The methodology of the research undertaken in this thesis is then presented. The principal research contributions are stated followed by the author's journal and conference publication output along with the contributions made as a panellist and invited presenter. Finally, an overview of the subsequent thesis chapters is explained.

1.2 Research Introduction and justification

1.2.1 Climate Change

Climate change is well understood as being a global issue that requires global action. The United Nations Framework Convention on Climate Change (UNFCCC) [1.1], formed in 1992, encouraged industrialised nations to change their ways in a global effort to reduce greenhouse gases. The UNFCCC encouragement was positively received and led to a requirement for industrialised nations to commit to country-specific targets. The UNFCCC treaty is not a legally binding agreement in itself but is used as a platform for obtaining updates that inform the mandatory emission

targets. These updates or protocols are legally binding when endorsed. The 1997 Kyoto Protocol [1.2] came into force in February 2005 whereby 55 countries ratified the international agreement of global greenhouse gas reduction. This requires the UK to reduce harmful emissions by 12.5%, the base year being 1990, in the five year commitment period (2008-2012) of the protocol [1.3]. The UK exceeded this target comfortably. In 2009 the figure was reported to be a reduction of 21% [1.4]. In November 2008, the UK became the first country in the world to pass a Climate Change Bill [1.5], an ambitious legislative act, that legally bound the UK to reduce carbon dioxide ($CO_{2)}$ emissions by at least 26% by 2020 and by 80% by 2050 from the CO_2 base line set in 1990. The UK Government regards renewable energy technology deployment to be crucial in successfully meeting reduction targets [1.6] and has a legal obligation to meet a 15% target for energy sourced from renewables as set out by the EU Renewable Energy Directive [1.7].

1.2.2 Increased Connection of Distributed Generation (DG)

Distributed generators are generator units connected at the lower voltage distribution network and generally range from a few kilowatts (kW) up to 100 megawatts (MW) in size. The UK has vast natural resources in rural and coastal locations [1.8][1.9] and therefore away from the country's high voltage transmission network the number of renewable generators connecting to lower voltage distribution networks have seen a significant increase. The main support for the integration of large scale renewable generation was introduced by Ofgem in 2002 and was branded the Renewable Obligation Certificate (ROC) Scheme [1.10]. This scheme has enabled the successful deployment of DG units through a mechanism that requires a licensed energy supplier to source an annual percentage of clean energy from renewable generation. A ROC is awarded to a supplier for every megawatt hour (MWh) of renewable energy supplied. If any supplier fails to meet the target percentage a buy-out penalty is imposed. At the end of the year ROCs are redeemed and successful suppliers rewarded financially. In 2009, further to the Energy White Paper of 2007 [1.11], bandings were introduced that reflected the costs and scale of eligible generation and ROCs were assigned accordingly. For example, onshore wind was eligible for

1ROC/MWh whereas offshore wind was eligible for 2ROCs/MWh. Hence, promoting offshore technology deployments to capture the UK's vast offshore natural resources.

The technical concerns with the increasing penetrations of DG were published in 1998 by Econnect and ILEX [1.12] in a technical guide for the connection of embedded generators to the distribution networks. Within this technical guide the implications and effect of DG on distribution networks was documented as; changes in system steady state voltages or step voltage changes, increase of current flows, increase in prospective fault currents and transformers operating with reverse power flows. Jenkins *et al* discuss these technical concerns further in [1.13]. With increasing planning applications for DG connections and technical limitations becoming more apparent Ofgem set out regulatory mechanisms, within the Distribution Price Control Review 4 (DPCR4) [1.14], that would encourage Distribution Network Operators / Owners (DNOs) to invest in research and development. The principal objective being to further demonstrate new technologies as being cost efficient ways of accommodating and operating DG units on their networks. The Innovation Funding Incentive (IFI) [1.15] was offered to DNOs that embarked upon projects that enhanced the technical development of their distribution networks. This incentivised collaborative projects that paved the way for solutions to be developed that would address real world problems. The Registered Power Zone (RPZ) [1.15] incentive allowed for these DG connection solutions to be taken forward and deployed on the DNO's system demonstrating and building confidence in new technologies.

Connecting large quantities of generation to distribution networks presents significant problems to current planning and operating regimes employed by network operators as these networks were designed for delivery of power from grid supply points to bulk supply points and onto customer loads in a passive manner. With increased penetration of renewable generators the distribution networks can expect to be subjected to higher fault currents, be susceptible to more frequent voltage fluctuations and thermal constraint infringements due to the dispersed nature of the

numerous and various power injection points. This creates additional uncertainty, in a power system with limited monitoring and observability, which is further complicated by the intermittency and stochastic nature of most forms of renewable generation.

1.2.3 Active Network Management (ANM)

Active Network Management (ANM) is a real-time monitoring and control strategy that can be adopted to facilitate increased DG connections while avoiding high network reinforcement costs, or at least, reducing or deferring reinforcement capital expenditure [1.16]. In 2006, Ault *et al* [1.17], demonstrated that ANM of network power flows had the potential of increasing energy sourced from renewable generation threefold compared to that of maintaining traditional connection methods. Also presented was an economic cut off point for ANM that demonstrated the financial applicability of ANM schemes. In [1.18], Mutale corroborates that ANM, through active voltage control, is central to the cost effective integration of DG units in terms of the reduction of total system costs. Adoption of ANM can avoid the lengthy process of reinforcement planning applications by enabling DG units to utilise the existing network capacity headroom. Since inception ANM has evolved to include functionality to manage distribution network constraints in real-time. This includes the control of all 'active' devices from generators to the demand side that enable functionality such as voltage control, power flow management, fault level management, post-fault restoration, minimisation of power losses and load shifting to be achieved. Therefore, the ANM of network constraints through real-time control of DG units, Energy Storage Systems (ESS), on-line tap changer transformers (OLTCs) and demand side management / resources guarantees network service requirements are met. With communication infrastructures, sensors, actuators and management functionality in place, on distribution networks, real-time responsive and active networks will play a major role in building the necessary confidence in the operation of autonomous networks. State-of-the-art ANM functions will be presented in Chapter 2.

1.2.4 Active Network Management (ANM) in the Energy Networks of the Future

There is a concerted effort to predict and envisage future network requirements towards 2050 [1.19] where participants taking an 'active' role require the DNOs to increase the number of ANM schemes at all voltage levels. An era of increased distributed generation, automation, decision making, communications infrastructure and protocols is being entered into and central to these areas is a bid to facilitate a common vision of the electricity networks of the future, the 'smart grid' [1.20]. To attain the vision of a flexible, accessible, reliable and economic power infrastructure requires input and consolidation of views from academic and industrial experts, regulators, network operators, suppliers (electricity and equipment) and consumers.

With increasing consumer demand and diminishing finite resources of fossil fuels the impact on security and quality of supply are high priorities in conjunction with environmental assessments of new technologies. The displacement of traditional central generation by that of DG requires an incremental smart grid transition following a carefully planned framework that co-ordinates all of the power system stakeholders rather than the transition being coerced by a smart grid revolution. ANM can be viewed as an incremental step in achieving the smart grid ambitions [1.20] through planned and co-ordinated deployment standards that ensure an extensible, safe and secure energy network is delivered. This step-by-step approach will assist in building confidence and identify areas where further enhancements may be required.

1.2.5 Active Power Flow Management

This thesis focuses on the requirement for technical solutions categorised by [1.21] as network Power Flow Management (PFM). In terms of ANM functionality little has been published on the distribution PFM problem compared with that of voltage control. This is due to the conservative planning approach adopted by DNOs to ensure the security and quality of the electrical supply. In a bid to avoid heavy

penalties imposed by Ofgem in the form of Customer Interruption (CIs) and Customer Minutes Lost (CMLs) charges this planning approach is based upon the worst case period (i.e. the coincidence of maximum generation and minimum load) to protect network security however this leaves additional and unused capacity for DG connections at all other periods. Employing an ANM scheme for PFM offers real-time monitoring and control based upon actual system conditions and events. Therefore, active PFM not only allows increased levels of DG to be connected but also enables the DNOs to maximise the utilisation of their network assets whilst keeping them within thermal limits.

In 2003 short and long term PFM solutions were proposed [1.21] for the management of single and multiple DG units to facilitate increased DG connections through reinforcement of network assets, the monitoring and tripping / inter-tripping schemes and the dynamic control of DG output. These tripping schemes were categorised under 'pre-fault constraint' and 'post-fault constraint' conditions. The 'pre-fault constraint' was a planned level of DG connection to a particular network that took account of the loss of one circuit i.e. the first circuit outage (FCO) which is synonymous with the term 'n-1' (this circuit will have the highest export capacity and is the worst case FCO). Therefore this generation has a 'firm' connection that requires no ANM scheme for the FCO which means that generation could operate under 'n-1' conditions and need only be constrained under a second circuit outage (SCO) or 'n-2' condition. Due to the FCO being the worst case (the highest rated line) it was identified that there was potential to accommodate further levels of DG, 'post-fault constraint', when complemented with an inter-tripping scheme. This level of generation would have a 'non-firm' connection to the network and would be tripped off immediately following any circuit outage. These connection methods were the basis of the published Engineering Technical Report by the Electricity Association in 2005[1.22].

Kabouris *et al*, 2004, introduced interruptible generator contracts and DG power reduction control [1.23] in a bid to tackle increasing DG planning applications to the Greek network. The curtailment of DG power output, when network security

constraints occurred, was proposed to be carried out via programmable logic controllers (PLCs) and the existing SCADA system. The DG power set points were based on the maximum DG output that could be injected into the grid without raising security issues. The real time monitoring of power flows on a congested transmission line allowed the control actions to be instructed as either a preventative or corrective act. A preventative action was classified as a control action that ensures a predefined security margin is not exceeded whilst the corrective actions were control commands resulting from the actual security limits being breached. The predefined security margins are a result of off-line studies that are conducted for various contingency events and logged in a look-up table that can be accessed by the scheme to update the margin for the network conditions. The control algorithm cycles in a 30 second loop and operates in a closed-loop fashion to ensure that post DG responses alleviate the thermal excursion (otherwise a new control command is calculated and issued). The nature of the interruptible contracts for the 'must take' renewable energy introduces a 'regulated', rather than a 'guaranteed', approach to managing DG access to the network. The paper concludes that taking this approach can significantly increase the penetration of DG units.

Kabouris *et al*, 2004, suggested that DG curtailment could be distributed between continuously updated priority lists.

Liew *et al*, 2005, discussed an ANM scheme for power flow management that successfully provided the connection of a 76MW off-shore wind farm near Great Yarmouth, England [1.24]. This PFM scheme was deployed on a substation computing platform to manage power flows from the DG units to ensure that firm connection arrangement of a Combined Cycle Gas Turbine (CCGT) was not compromised. Curtailment signals from the control system were banded into 25% trim signals and allocated by the control algorithm based upon the available thermal capacity of the circuits. A number of off-line studies are required as it was identified that thermal overloads were likely to appear on unmonitored circuits. These conditions were identified via power flow studies taking account of the CCGT output and network loading and subsequent curtailment factors calculated for the DG units

to ensure thermal limits are not breached. It is concluded that the ANM scheme allowed the regulated output of a 76MW wind farm to be connected with a saving in the region of £3m (from that of the necessary network reinforcement works).

In 2008, in a letter presented to the IEEE [1.25], Currie *et al* discussed some of the key outcomes from the first multiple DG controlling distribution ANM scheme to be deployed in the UK on Orkney's distribution network. One of the observations documented from this closed-loop control scheme is that wind farm response rates are set around 4 – 5% of the DG units' rated output per minute. This publication shows that this active PFM schemes can successfully manage multiple DG curtailment and ensure that command instructions are enforced for the duration of the network constraint in real-time.

The work presented in this thesis contributes to the area of distribution PFM by examining two existing techniques, formulated around the PFM problem, and applies and extends them to disparate networks to evaluate the real-time performance. The novelty lies within the formulation and application of the techniques in a closed loop real-time test environment using a model based approach. The methods for active PFM investigated within this thesis are:

- The optimisation method of Optimal Power Flow (OPF)
- The artificial intelligence (AI) method of the Constraint Satisfaction Problem (CSP)

1.2.5.1 Optimal Power Flow (OPF) Technique

Optimal Power Flow (OPF) was first introduced circa 1960 [1.26] and has many existing publications detailing its potential use, mainly in the power systems planning domain. OPF consists of an objective function with the focus being either to minimise or maximise the function whilst meeting the bounds or constraints of the problem. These bounds are in the form of equality and inequality constraints that require an optimal solution to be found such that the constraints are imposed. More

recently, OPF focused approaches to DG connections and ANM have been published.

In 2005, Harrison *et al* presented an OPF method to evaluate the headroom available for planning DG connections using PTI's PSS/E power systems software combined with an IPLAN automation script removing the laborious task of manual data input for power system planners [1.27]. Modelling fixed power factor DG units as negative loads and utilising the OPF package's load shedding capability offered capacity solutions for time-series evaluations in less than one second per OPF run. Furthermore, thermal and voltage constraints were enforced within the planning tool. These timescales highlight the potential applicability of OPF within a real-time environment.

In 2008, Ochoa *et al* published a non-linear programming OPF approach adapted to determine the maximum DG connection capacities available whilst considering ANM variables and constraints [1.28]. The paper discussed the inclusion of co-ordinated voltage control, energy curtailment, network losses and fault levels in addition to the standard OPF constraints of thermal and voltage limitations. Augmentation of [1.28], in 2009, led to the evaluation of the potential DG capacity on a section of the Irish 38kV network [1.29] while including OLTC, power factor and energy curtailment variables within the bounds of the problem. These papers demonstrate the role of OPF and value of ANM functions for DNO planners to evaluate and increase DG capacity on their networks, respectively. In [1.30], published in 2010, the authors further demonstrate the applicability of OPF and ANM functions for evaluating and increasing DG access on distribution networks. Within this publication it is noted that DG contractual arrangements are not included in the bounds of the formulation. Enforcing current DG connections agreements and therefore curtailment/disconnection priorities are highlighted as important areas of research.

The OPF formulation discussed within this thesis takes account of the current UK DG connection philosophy of last-in, first off (LIFO). This is of importance for use

in the real-time control domain in meeting current commercial arrangements. The novelty of applying this approach is pertinent to the real-time control domain of power systems operation and is further discussed in Chapter 3, formulated in Chapter 4 and evaluated in Chapter 6.

1.2.5.2 Constraint Programming (CP) and the Constraint Satisfaction Problem (CSP)

Constraint Programming (CP) is a technique that can be applied to problems modelled as a Constraint Satisfaction Problem (CSP). CSP is a well known problem definition to computer scientists working on artificial intelligence (AI) applications. There are several classes of CSP (Boolean, integer, linear, finite, mixed) and research into CP has led to the development of a growing set of algorithms (e.g. backtracker, local search, constraint propagation) for solving these different problems [1.31]. A CSP follows no specific steps or procedures since the properties of a solution are pre-determined via declarative programming. Thus, the goal is specified without giving the route to achieving that goal. The particular class of CSP discussed in this thesis is a finite discrete domain CSP. There are few examples of this technique's use within the power sector.

In 1998, Kun-Yuan Huang *et al* proposed a CP algorithm that was applied to the unit commitment (UC) problem within powers systems [1.32]. The paper focuses on thermal generating units and the approach is demonstrated using part of the Taiwanese transmission network. The UC problem aims to provide a plan for economically dispatching central generating plant for a forecasted load in such a manner that the generators' operating constraints are reflected. The author sets up the UC problem through declarative programming (inherent with CP) and uses the CSP properties of backtracking, forward checking and looking ahead to prune the search space of the problem through constraint propagation in order to remove any infeasible solutions. The successive search space was then explored using a depth first, branch and bound approach. Conclusions drawn in the publication state that the many constraints involved in UC problems can be easily expressed via the

declarative programming nature and that CSP is very efficient at reducing the search space. The approach was compared to other algorithms applied to UC (dynamic programming (DP), Lagrangian relaxation (LR) and simulated annealing (SA)) and showed that the 'near-optimal' solution (SA returned the global optimum but with significant computational expense) can be returned in a short timescale.

In 2000 Chantler *et al* presented a model-based diagnostic system for diagnosing faults in electrical transmission systems [1.33]. The purpose of which could allow the scheduling of preventative maintenance based upon the anomaly detection of substation protective devices. Using fault recorder (FR) data it is possible to determine the behaviour of the protective devices, i.e. whether they operated when required or not, and the timescales in which they operated, i.e. identifying any deviation in the expected operating times. The off-line diagnostic system comprises two main elements, namely the 'Global Viewer' and the 'Diagnoser'. Within the 'Diagnoser' the FR data needs to be interpreted to determine the behaviour. The interpretation of this data is described as a search problem as the solution results in a number of paths for each transitional sequence. The state space can initially be built up using the FR digital/discrete signals and further refined using CSP to test temporal and other constraints.

The CSP formulation described within this thesis will be modelled to enable the representation of the current UK connection philosophy, LIFO. This approach is further discussed in Chapter 3, formulated in Chapter 5 and evaluated in Chapter 6.

The above techniques offer a network agnostic approach required for the population of "a toolbox of proven technical solutions that can be deployed rapidly and cost effectively" [1.20]. Latter chapters explain the formulation, application, demonstration and comparison of these recognised techniques for the real-time responsive control function of PFM.

1.3 Research Methodology

The research presented in this thesis took a systematic and iterative approach from the outset in the identification of the requirements through to the testing stage. Figure 1 illustrates the procedure. This structured design method was first introduced by Royce in 1970 [1.34] as a critical path for successful implementation of initial software concepts with the objective of avoiding costly errors through the process. The top-down nature of this model would later earn it the name 'the waterfall model'.

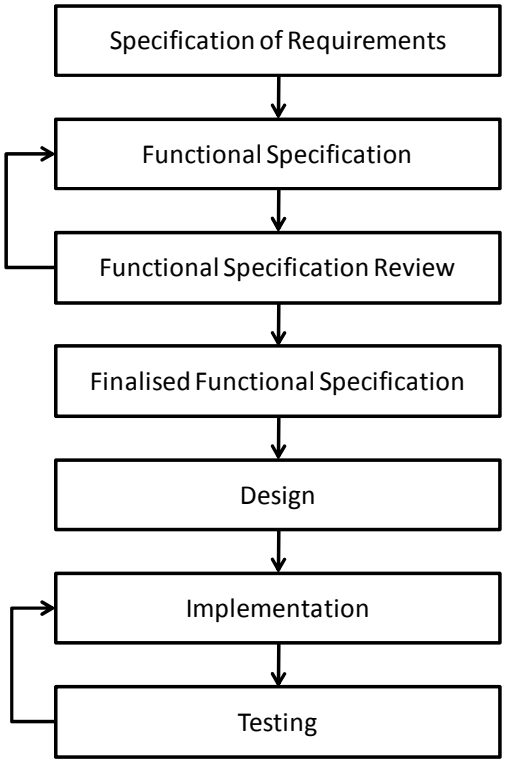

Figure 1 - Structured Development and Experimental Process Followed for Investigation of PFM Techniques

The 'Specification of Requirements' and the 'Functional Specification' are discussed in Chapter 3 prior to the introduction of both candidate approaches and the test environment. The sections below present an overview of the 'Design', 'Implementation' and 'Testing' phases of the work presented in this thesis.

1.3.1 Design

Understanding *what* the ANM scheme requirements are is crucial to deciding *how* they will be achieved. Therefore, the design stage asks the question *how* the PFM functions will be built and *how* the ANM system architecture will be constructed to meet the defined specifications. This thesis focuses on *how* the PFM algorithms will meet the specification of requirements with Chapter 3 explaining the suitability of the chosen techniques' characteristics and *how* they achieve the necessary goals. Chapters 4 and 5 demonstrate the operational characteristics of these approaches to the PFM problem.

1.3.2 Implementation

The implementation process requires the PFM function software to be deployed upon hardware that would be used in the ANM scheme. The purpose of which is to ensure network measurements can be collated, analysed and if necessary control signals sent to corresponding DG units in the field. To achieve this, a real-time laboratory environment was put in place that would emulate the field intelligent electronic devices (IEDs), e.g. the DG control unit that may be 'read from' and 'written to' over a local network. Chapter 3 describes and depicts this implementation environment.

1.3.3 Testing

Following on from the implementation of the hardware, software and the subsequent development of a real-time simulation environment a schedule of testing was created to evaluate the performance of the PFM algorithms under certain conditions; 'perfect measurement', 'erroneous measurement' and 'first circuit outage' conditions. The computation time, the number of control signals issued, the level of DG curtailment, conformity to LIFO and any ability to degrade gracefully can subsequently be examined. These tests were carried out across two differing network topologies to meet the network agnostic criterion.

1.4 Principal Research Contributions

The principal research contributions and novelty of this reported work can be summarised as follows:

- The formulation of a corrective power flow algorithm modelled as an Optimal Power Flow problem for real-time operational control of multiple generator units complete with the formulation of the relaxation of trim/trip commands for intermittent distributed energy resources
- The closed loop simulated demonstration of the corrective Optimal Power Flow management algorithm and reporting of the characteristics in relation to robustness, computation time, resilience to measurement error, graceful degradation and DG curtailment levels
- The formulation of a corrective power flow algorithm modelled as a Constraint Satisfaction Problem for real-time operational control of multiple generator units complete with the formulation of the relaxation of trim/trip commands for intermittent distributed energy resources
- The closed loop simulated demonstration of the corrective power flow Constraint Satisfaction Problem algorithm and reporting of the characteristics in relation to robustness, computation time, resilience to measurement error, graceful degradation and DG curtailment levels
- The inclusion of current UK DG contractual arrangements within each of the applied approaches and investigation of the implications of these connection arrangements
- Comparative practical analysis of the power flow management algorithms modelled as a Constraint Satisfaction Problem and Optimal Power Flow formulation for solving thermal constraint violations in real-time

These contributions will be discussed, developed and carefully examined in the following chapters. These contributions are highly valuable as they meet the needs of

current industry requirements and produce relevant new knowledge for operation within future energy networks.

In addition to the above contributions the author has also supported the development work to establish the sequential steady-state simulator used to investigate the operating characteristics of the candidate corrective power flow algorithms.

1.5 Published Work

The following sub-sections list the author's publications, conference panel sessions and workshop participation.

1.5.1 Journal Papers

The author has published the following academic journal papers, either as a main author or co-author:

1. Michael J. Dolan, Euan M. Davidson, Graham W. Ault, Stephen D. J. McArthur, Keith Bell, "Distribution Power Flow Management Utilising an Online Constraint Programming Technique", IEEE Transactions on Smart Grid, *under review*

2. Michael J. Dolan, Euan M. Davidson, Ivana Kockar, Graham W. Ault, Stephen D. J. McArthur, "Distribution Power Flow Management Utilising an Online Optimal Power Flow Technique", IEEE Transactions on Power Systems, Vol. 27, No. 2, pp. 790-799, May 2012

3. Simon Gill, Graham W. Ault, Michael J. Dolan, Damien Frame, "The Role of Electric Heating and District Heating Networks on the Integration of Wind Energy to Island Networks" , International Journal of Distributed Energy Resources Journal, Paper No. 2010-12-23-242

4. Michael J. Dolan, Ian M. Elders, Graham W. Ault, "Economic and Technical Evaluation of an Energy Storage System Connected to an Islanded Distribution Network", International Journal of Distributed Energy Resources Journal, Paper No. 2008-12-01-173

1.5.2 Conference Papers

In addition to the above journal publications the author has published the following academic conference papers, either as a main author or co-author:

1. Michael J. Dolan, Graham W. Ault, Damien F. Frame, Simon Gill, Ivana Kockar, Olimpo Anaya-Lara, Stuart Galloway, Colin Mathieson, Stewart Reid, Frank Clifton, Bryan O'Neill, Colin Foote, Andrejs Svalovs, "Northern Isles New Energy Solutions: Active Network Management Stability Limits", IEEE Power and Energy Society Innovative Smart Grid Technologies (Europe) 2012, Paper No. 378

2. Federico Coffele, Michael J. Dolan, Campbell Booth, Graham W. Ault, Graeme Burt, "Co-ordination of Protection and Active Network Management for Smart Distribution Networks", CIRED Workshop 2012, May 2012, Paper No. 0031

3. Ayodeji Owonipa, Michael J. Dolan, Euan M. Davidson, Victoria Catterson, Graham W. Ault, Stephen D. J. McArthur, "The Need for an Agent Arbitration Approach for Co-ordinated Control in Active Power Networks", 46th International Universities' Power Engineering Conference, Germany, 2011

4. Damien Frame, Kelvin Tembo, Michael J. Dolan, Scott M. Strachan, Graham W. Ault, "A Community Based Approach for Sustainable Off-Grid PV Systems in Developing Countries", IEEE PES General Meeting, Chicago, July 2011

5. Rachael L. Storry, Michael J. Dolan, Euan M. Davidson, Ivana Kockar, Graham W. Ault, "A Case for Losses Minimisation in Active Network Management Systems", CIRED, 21st International Conference on Electricity Distribution, June 2011, Paper No. 0247

6. Michael J. Dolan, Euan M. Davidson, Callum Morris, Graham W. Ault, Stephen D. J. McArthur, "Multi Agent Platform for Active Network Management", 4th International Conference on Integration of Renewable and Distributed Energy Resources, New Mexico, December 2010

7. Ivana Kockar, Euan M. Davidson, Graham W. Ault, Michael J. Dolan, "Distributed Generation Access and Power Flow Management", IEEE PES General Meeting, Minneapolis, July 2010

8. Euan M. Davidson, Michael J. Dolan, Graham W. Ault, Stephen D. J. McArthur, "AuRA-NMS: An Autonomous Regional Active Network Management System for EDF Energy and SP Energy Networks", IEEE PES General Meeting, Minneapolis, July 2010

9. Lynne McDonald, Rachael L. Storry, Alan Kane, Finlay, Graham W. Ault, Ivana Kockar, Stephen D. J. McArthur, Euan M. Davidson, Michael J. Dolan, "Minimisation of Distribution Network Power Losses using an Active Network Management System", 45th International Universities' Power Engineering Conference, Cardiff, 2010

10. Euan M. Davidson, Michael J. Dolan, Stephen D. J. McArthur, Graham W. Ault, "The use of Constraint Programming for the Autonomous Management of Power Flows". Proceedings of the 15th International Conference on Intelligent Systems Applications to Power Systems, Nov. 2009

11. Michael J. Dolan, Euan M. Davidson, Federico Coffele, Graham W. Ault, Ivana Kockar, James R. McDonald. "Using Optimal Power Flow for Management of Power Flows with Active Distribution Networks within Thermal Constraints". 44th International Universities' Power Engineering Conference, Glasgow, 2009

12. Euan M. Davidson, Stephen D. J. McArthur, Michael J. Dolan, James R. McDonald. "Exploiting Intelligent Systems Techniques within an Autonomous Regional Active Network Management System". IEEE PES General Meeting, Calgary, July 2009

13. Michael J. Dolan, Euan M. Davidson, Graham W. Ault, "Techniques for Actively Managing Distribution Network Power Flows within Thermal Constraint", CIRED, 20th International Conference on Electricity Distribution, June, 2009, Paper 0736

14. Phil Taylor, Tao Xu, Stephen D.J. McArthur, Graham W. Ault, Euan M. Davidson, Michael J. Dolan, Cherry Yuen, M. Larsson, Duncan Botting, David Roberts, Peter Lang, "Integrating voltage control and power flow management in AuRA-NMS", CIRED Seminar 2008: SmartGrids for Distribution, June 2008, Paper 0035

15. Robert A. F. Currie, Michael J. Dolan, Graham W. Ault, Jim R. McDonald, "Assessing the Impact of Active Power Flow Management on SCADA Alarm Volume", CIRED, 19th International Conference on Electricity Distribution, May 2007, Paper 0176

1.5.3 Panel Sessions and Workshops

The author has presented at the following panel sessions and lectures:

1. "Contributions of Intelligent Systems on Smart Grids", The 15th International Conference on Intelligent Systems Applications to Power Systems, Curitiba Brazil, November 2009

2. "Integrating Renewables to the Grid", CITYNET Consortium, University of Strathclyde, October 2009

3. "Exploiting Intelligent Systems Techniques within an Autonomous Regional Active Network Management System", IEEE PES General Meeting, Calgary, July 2009

4. "Engineers without Borders - UK Scottish Conference", Workshop on "Sustainable Energy Development", University of Strathclyde, February 2010

5. "Grid Training - Community Energy Scotland", University of Strathclyde, November 2010

6. "Models for Sustainable Renewable Energy development: The Gambia Project", Centre for Lifelong Learning, University of Strathclyde, November 2011

1.6 Overview of Thesis Chapters

Chapter 2 of this thesis includes background information of the UK's evolving distribution networks and examines the incentives and drivers that have led to the proliferation of distributed generator connections. The developments in ANM are

discussed in terms of overcoming the technical barriers associated with DG connections with examples of deployed ANM schemes discussed. ANM is discussed within the context of the vision of future energy networks and the role that ANM solutions will play in the transition to smart grid technologies. Finally, the existing UK connection philosophy currently used in practice is described. Consequently, this chapter presents the challenges in making the transition from well established 'fit and forget' distribution network operating regimes to the ANM solutions required to meet the needs of the future energy networks.

In Chapter 3 the 'Specification of Requirements' and the 'Functional Requirements' of the ANM scheme are introduced prior to presenting the characteristics of the PFM approaches in their general forms. The real-time test environment used for the evaluation of the power flow management software is described, depicted and illustrated in the context of future electricity networks. The case study networks are introduced along with the relevant load and generation profiles necessary to evaluate the PFM algorithms.

Chapter 4 discusses the optimal power flow (OPF) approach and identifies the formulation required to tackle the PFM problem with OPF. Results are presented from the real-time test environment of the ability of the algorithms to detect network thermal excursions, to send control signals to limit and relax DG units' outputs, to conform to the LIFO principle, to enable the computation time of control signals sent to the DG units to be examined and to inspect the method's robustness when faced with sensor/measurement errors.

In Chapter 5 the Constraint Satisfaction Problem (CSP) approach to PFM is discussed in terms of the CSP attributes for the PFM problem. The formulation of the CSP PFM problem is then introduced. Results are then presented that demonstrate the real-time applicability of this method. The ability to detect network thermal excursions, to send control signals to limit and relax DG unit outputs, to conform to the LIFO principle, to meet the real-time computation requirements of calculating

control signals sent to the DG units and an inspection of the method's robustness when faced with sensor/measurement errors are each investigated and documented.

Chapter 6 forms the discussion based on the results of Chapter's 4 and 5. These results are further scrutinised to identify the relevant accuracies in the form of 'over' and 'under' curtailment when compared to the base case (the perfect measurement scenario) and the subsequent impact of these on DNOs and DG owners. Conclusions are then drawn that identify the PFM approach's conformity to the prescribed user and functional requirements that demonstrate the potential use of OPF and CSP based approaches for PFM. Finally, potential future avenues for this research are documented.

In Chapter 7 conclusions of the work presented in this thesis are discussed in terms of the high level implementation issues surrounding an ANM scheme. In addition, the ability of each of the PFM approaches to meet the general and user requirements are presented. Finally, the future work for this research is discussed.

1.7 Chapter 1 References

[1.1] United Nations, "Framework Convention on Climate Change: Handbook", 2006 UNFCCC, http://unfccc.int/resource/docs/publications/handbook.pdf, accessed on 12th October 2010

[1.2] United Nations, "Kyoto Protocol to the United Nations Framework Convention on Climate Change", 1998, http://unfccc.int/resource/docs/convkp/kpeng.pdf, accessed on 12th October 2010

[1.3] HM Government, "The Energy Challenge: Energy Review Report", Department of Trade and Industry, July 2006, http://webarchive.nationalarchives.gov.uk/+/http://www.dti.gov.uk/files/file31890.pdf, accessed on 12th October 2010

[1.4] HM Government, "The UK Low Carbon Transition Plan: National Strategy for Climate and Energy", Department of Energy and Climate Change, July 2009, http://centralcontent.fco.gov.uk/central-content/campaigns/act-on-copenhagen/resources/en/pdf/DECC-Low-Carbon-Transition-Plan, accessed on 12th October 2010

[1.5] HM Government, "Climate Change Act 2008: Impact Assessment", Department of Energy and Climate Change, March 2009, http://www.decc.gov.uk/assets/decc/85_20090310164124_e_@@_climatechangeactia.pdf, accessed on 12th October 2010

[1.6] HM Government, "The UK Renewable Energy Strategy", Department of Energy and Climate Change, July 2009, http://www.decc.gov.uk/assets/decc/what%20we%20do/uk%20energy%20supply/energy%20mix/renewable%20energy/renewable%20energy%20strategy

/1_20090717120647_e_@@_theukrenewableenergystrategy2009.pdf, accessed on 12th October 2010

[1.7] European Commission, "National Renewable Energy Action Plan for the United Kingdom", Article 4 of the Renewable Energy Directive 2009/28/EC, http://www.decc.gov.uk/assets/decc/what%20we%20do/uk%20energy%20supply/energy%20mix/renewable%20energy/ored/25-nat-ren-energy-action-plan.pdf, accessed on 12th October 2010

[1.8] Renewable UK (Formally the British Wind Energy Association, BWEA), http://www.bwea.com/images/misc/noabl_c.gif Wind Energy Resource Map, accessed on 2nd March 2011

[1.9] Renewable UK (Formally the British Wind Energy Association, BWEA), http://www.bwea.com/marine/atlas.html. Marine Energy Resource Atlas. Accessed on 2nd March 2011

[1.10] "The Renewables Obligation Order 2002", No. 914, available at http://www.legislation.gov.uk/uksi/2002/914/made. Accessed on 2nd March 2011

[1.11] HM Government, "Energy White Paper 2007: Meeting the Energy Challenge", Department of Trade and Industry, May 2007

[1.12] "A Technical Guide for the Connection of Embedded Generators to the Distribution Network", Econnect & ILEX, November 1998

[1.13] Jenkins, N., Allan, R., Crossley, P., Kirschen, D. and Strbac, G. (2000); "Embedded Generation"; IEE Power and Energy Series 31, The Institution of Electrical Engineers, London, United Kingdom

[1.14] Office of the Gas and Electricity Markets (Ofgem), "Electricity Distribution Price Control Review - Final Proposals" November 2004 265/04

[1.15] Office of the Gas and Electricity Markets (Ofgem), "Distributed Generation Incentive, Innovation Funding Incentive, Registered Power Zones - Regulatory Instructions and Guidance - Version 2", April 2007

[1.16] D. Roberts, SP Power Systems LTD, 2004, "Network Management Systems for Active Distribution Networks – A Feasibility Study", DTI Distributed Generation Programme, Contract Number: K/EL/00310/00/00

[1.17] G.W. Ault, R.A.F. Currie, J.R. McDonald, "Active Power Flow Management Solutions for Maximising DG Connection Capacity**",** IEEE PES General Meeting, Montreal, October 2006

[1.18] J. Mutale, "Benefits of Active Management of Distribution networks with Distributed Generation", IEEE PES Power Systems Conference and Exposition, October 2006

[1.19] G. W. Ault, D. Frame, N. Hughes, N. Strachan, "Electricity Network Scenarios for Great Britain in 2050 Final Report for Ofgem's LENS Project", November 2008, Ref. No. 157a/08

[1.20] SmartGrids. "Vision and strategy for Europe's electricity networks of the future" Available: http://www.smartgrids.eu, accessed on 6th May 2012

[1.21] A. Collinson, F. Dai, A. Beddoes, Crabtree, J. "Solutions for the Connection and Operation of Distributed Generation"; DTI Distributed Generation Programme (Contractor: EA Technology) K/EL/00303/00/01/REP; 2003

[1.22] Energy Networks Association (2004); "Guidelines for Actively Managing Power Flows associated with the Connection of a Single Distributed

Generation Plant", Working draft: Engineering Technical Report 124 (ver-005), February 2004

[1.23] J. Kabouris and C. D. Vournas; "Application of Interruptible Contracts to Increase Wind-Power Penetration in Congested Areas"; IEEE Transactions on Power Systems, Volume: 19, Issue: 3, P1642 – 1649, August 2004

[1.24] S. N. Liew and T. Moore; "Design and Commissioning of Active Generator Constraint for an Offshore Windfarm"; Proceedings 18th International Conference on Electricity Distribution, Turin, Italy, 6-9 June, 2005

[1.25] R. A. F. Currie, G. W. Ault, R. W. Fordyce, D. F. MacLeman, M. Smith and J. R. McDonald; "Actively Managing Wind Farm Power Output"; IEEE Letter, Transactions on Power Systems, Volume: 23, Issue: 3, 1523- 1524, August 2008

[1.26] J. Carpentier, "Contribution a l'Etude du Dispatching Economique", Bulletin de la Society Francaise des Electricien 8 3 (1962), pp. 431–447

[1.27] G.P. Harrison and A.R. Wallace, "Optimal power flow evaluation of distribution network capacity for the connection of distributed generation", IEE Proceedings Generation, Transmission & Distribution. vol. 152, 115-122, 2005

[1.28] L.F. Ochoa, C.J. Dent, and G.P. Harrison, "Maximisation of intermittent distributed generation in active networks", CIRED Seminar 2008: SmartGrids for Distribution, Frankfurt, 2008

[1.29] L.F. Ochoa, A. Keane, C.J. Dent, and G.P. Harrison, "Applying Active Network Management Schemes to an Irish Distribution Network for Wind Power Maximisation", CIRED: 20th International Conference on Electricity Distribution, Prague, 2009

[1.30] L.F. Ochoa, C.J. Dent, and G.P. Harrison, "Distribution Network Capacity Assessment: Variable DG and Active Networks", IEEE Transactions on Power Systems, vol. 25, no. 1, February 2010

[1.31] K. R. Apt. "Principles of Constraint Programming", Cambridge University Press, 2003

[1.32] Kun-Yuan Huang Hong-Tzcr Yang, Ching-Lien Huang, "A New Thermal Unit Commitment Approach Using Constraint Logic Programming", IEEE Transactions on Power Systems, Vol. 13, No. 3, pp. 936-945, August 1998

[1.33] M. Chantler, P. Pogliano, A. Aldea, G. Tornielli, T. Wyatt, A. Jolley. "Use of fault-recorder data for diagnosing timing and other related faults in Electricity Transmission Networks" IEEE Trans. on Power Systems, Vol. 15, No. 4, pp. 1388-1393, November 2000

[1.34] W. W. Royce, "Managing the development of large software systems," Proceedings, IEEE WESCON, pp. 1-9, August 1970

Chapter 2

Evolving Distribution Networks and Active Distribution Network Management

2.1 Summary of Chapter 2

This chapter provides the basis of change to the UK distribution systems and the evolutions that are taking place to facilitate and overcome the technical obstacles of DG integration. Each of the technical issues and their associated solutions are communicated along with the role and potential of ANM research into each of these areas of DG integration. The incentives that are required to assist the DNOs and DG operators/owners to overcome the technical barriers in a bid to meet national targets for renewable generation are discussed. Addressing these hurdles with incentivised technical solutions is highlighted as being fundamental to ensuring cost effective network access for DG plant is achieved. Current state-of-the-art advancements and deployments in ANM are presented. The characteristics of the smart grid vision are documented and the function that ANM techniques and strategies can play in energy networks of the future is examined. Finally, the UK's current contractual arrangement for DG unit connections is discussed.

2.2 The United Kingdom's Evolving Distribution Networks

Electrical distribution systems (132/33/11kV in England and 33kV/11kV in Scotland) were traditionally passive networks that delivered unidirectional power from bulk supply points, received via the high voltage active transmission networks (400/275kV), to dispersed load centres. With most of the UK's renewable resources (wind, wave, tidal) being located in rural, less densely populated areas [2.1] the closest and most economic point of connection for DG is at the electrically weaker, lower voltage, distribution level. The increasing interest and focus on connecting more renewable generation to distribution networks means that the networks are subjected to bidirectional power flows. This results in an increase in power flow magnitudes and adds to the uncertainty in predicting the actual power flowing due to the intermittency of the connected renewable generator units. Distribution Network Operators/Owners (DNOs) are obliged to operate their power delivery systems in a safe and secure manner and must operate within statutory voltage and frequency

limits as well as within plant thermal capacities. With heavy penalties [2.2] imposed, by Ofgem for customer minutes lost (CML) and customer interruptions (CI), the DNO's focus is primarily on security of the electrical supply. In a bid to preserve system security, strict connection agreements, set by DNOs, must be adhered to by Distributed Generator Operators/Owners (DGO) or they are penalised by disconnection from the network. These stringent connection rules are generally developed from worst case scenarios which result in underutilised network capacities for all periods with the exception of the worst case scenario which the connection would have been based upon.

To fully utilise the distribution network capacity and capability, with increased DG connections, the current operating methods requires a degree of scrutiny and decisive action should be taken to move the management of the networks in line with the current and emerging technologies.

Under the current connection framework, planned under Engineering Recommendation P2/5 [2.3] and now P2/6 [2.4], the DGO is generally required to pay a deep connection cost that may include network reinforcement costs to ensure quality of supply standards are met. Taking an active role in system management has been shown to increase the connection of DG to the existing network infrastructure [2.5][2.6][2.7]. The primary concerns are the issues that arise from the bidirectional power flows and the associated changing magnitudes of power flow through the connection of distributed generators (DG). These concerns and barriers fall under three main technical, interconnected and often conflicting categories:

- Voltage Control
- Fault Level Management
- Power Flow Management

To accommodate DG and the inherent technical concerns it is preferable to develop intelligent distribution systems capable of the real-time monitoring and control that address the above technical challenges. This thesis presents two real-time monitoring

and control methods that focus on offering technical solutions to power flow management problem. The approaches investigated meet today's network requirements and offer flexible and extensible traits that can advance in parallel with the UK's evolving electrical delivery systems and mechanisms.

2.3 Addressing the Barriers Associated with Distributed Generation (DG) Connections

The Embedded Generation Working Group (EGWG) identified in 2001 that distributed and renewable generation schemes were experiencing major barriers that required intervention at government level [2.8][2.9][2.10]. With this in mind, the DTI and Ofgem set-up the Distribution Generation Co-ordinating Group (DGCG) in 2002. The task of the DGCG was to investigate and recommend, to the government, how the barriers faced by distributed energy developers could be removed. To aid the DGCG on advising how to allow fair and open access to the distribution networks, they established a Technical Steering Group (TSG). Under the TSG a number of Work Streams (WS) were setup and called upon to investigate solutions to overcome the hurdles faced. WS3 and WS5 had particular focus on distribution automation activities. One of the focuses of WS3 was to address solutions to three of the technical barriers of DG connections [2.11] voltage control, power flow and fault level management. The solutions developed within WS3 included Active Distribution Management (ADM) schemes for individual generator applications, which were based on existing isolated examples and technology. WS5's focus was on longer-term solutions to DG connections in areas of fault level, voltage control, active management, security, islanding, supplementary services, power quality, network design, safety, new technology and network losses. The two deemed to be at the focal point of future distribution networks were active management and network design. WS5's Active Management group was responsible for coordinating research and development activities which were supported by industrial suppliers, DNOs, generation developers, consultants and academics.

Addressing the barriers of DG integration and examining solutions has been acknowledged at the highest levels. The short term active network management solutions, for single generator cases, are not appropriate for significant levels of DG penetration as multiple bespoke constraint management systems would unfold adding further complexity to network control. The approaches discussed within this thesis monitor and control multiple DG units in a decentralised way to ensure power flows remain within thermal limits. The applicability and scalability of these approaches provides significant knowledge for implementing active management solutions, for multiple generators, in the current distribution network operating framework. Furthermore, the application of these approaches offer valuable information about what the requirements of the longer term solution would need to provide in terms of flexibility and extensibility.

2.4 Drivers and Incentives for the Connection of Distributed Generation (DG)

The main driver for renewable DG connections stems from increasing pressure to combat global warming and reduce greenhouse gas emissions from the electricity sector and society as a whole.

The UK Department of Trade and Industry's (DTI) Energy White Papers of 2003 [2.12] and 2007 [2.13] were written from past experience of, and research carried out for, the facilitation of renewable connections. A 50 year strategic plan of UK specific targets and challenges was communicated through the 2003 paper. Three challenges were identified and fell under the following categories:

- 'Environmental'- which was to address climate change
- 'The Decline of the UK's Indigenous Energy Supplies'
- 'Update much of the UK's Energy Infrastructure'

The environmental challenge stated a target reduction of CO_2 emissions of 20% by 2010, based on the CO_2 levels measured in 1990. This target goes beyond the objective of the ratified and now legally binding Kyoto Protocol which states the target of cutting CO_2 levels by 12.5% between 2008 and 2012 [2.19]. Developed countries have a legal obligation to reduce greenhouse gas emissions by 5% between 2008 and 2012. The target of energy supplied from renewable energy sources stands at 10% by 2010.

Investment in renewable technologies required incentives to try to balance the risks that DNOs faced. Regulatory Instructions and Guidance (RIGs) were put in place in April 2005, by Ofgem, to encourage developers to help meet government renewable targets. The majority of renewable generation connections were predicted to be made to the distribution network. Therefore, regulatory schemes offered as an incentive to DNOs were initiated to spark innovative technology deployment. Figure 2, below illustrates the innovation process, from the high risk research period through the development, trial and pilot stages that leads to full deployment at a reduced risk levels.

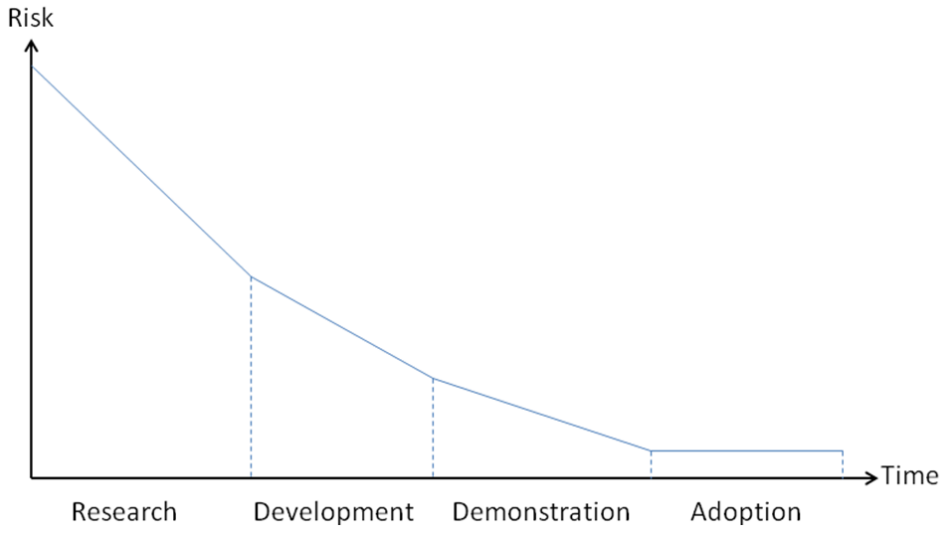

Figure 2 - Innovation Process Depicting the Levels of Risk Associated to each Fundamental Procedure of the Process

The Distribution Generation Incentive (DGI) is an economic incentive designed to encourage DNOs to connect DG. The connection, capital and network reinforcement costs incurred by new DG developments were not attractive to either DNOs or the proposed developers. DGI has complex details but the overall view was that it hoped to entice new interest in connections. The DNO is to receive, over a period of 15 years through system use charges, 80% of the capital cost (above the connection charge) for accommodating DG connections. There is also an added £/kW motivation or incentive rate to encourage the facilitation of economical and efficient DG connections.

The Innovation Funding Incentive (IFI) was put in place to encourage DNOs to lead research projects into the development stages. Companies are part funded for each project they conduct. It also persuades annual reporting of projects, on an open basis, for others to identify the state of the art and best practices to adopt.

Registered Power Zones (RPZ) are focused specifically for the connection of DG onto distribution networks. The Distribution Price Control Review 4 (DPCR4) suggested that 10GW of renewable generation could be connected in the next five years. This can be made up from generators producing kWs to machines exporting MWs connected at all distribution voltage levels. This requires new system designs and overcoming operating challenges. Therefore, the RPZ schemes are intended to encourage DNOs to develop and demonstrate new more cost effective solutions to connecting and operating generation. The solutions should offer specific benefits to new DG operators and broader benefits to consumers. The DPCR4 takes into account the risks that the DNO faces when using new innovations.

The Renewable Obligation (RO) offers licensed electricity suppliers to source an increasing proportion of sales from renewable energy sources or pay a penalty. Renewable generator operators sell Renewable Obligation Certificates (ROCs) to suppliers for every megawatt hour (MWh) of electricity they buy. These certificates can be redeemed annually and the money accrued from penalties is shared among the suppliers that can provide ROCs.

The publication, in 2007, of the UK DTI's second Energy White Paper reiterated the intention of successfully meeting the target of energy sourced from renewables. The 2003 Energy White Paper's recommendations were successful in bringing forward the most cost-effective renewable technologies under the Renewable Obligation (RO) scheme. This is noticeable from the rise in renewable penetration after the document's publication – it took 14 years for the first GW of wind energy to be connected and only 20 months for the second GW [2.13]. There is recognition that existing incentives put in place to meet this challenge must be revisited and reinforced to encourage the deployment of emerging technologies. Principally, this means schemes that encourage offshore resources to be exploited by using up-and-coming offshore generation technologies (the cost of which soared unexpectedly) but the general message is strong – renewable energy is still high on the agenda.

Ofgem set up the Low Carbon Network Fund (LCNF) [2.14], under the DPCR5 [2.15], to build understanding of what DNOs will need to provide to achieve a secure low carbon economy. The scheme runs from 2010 to 2015 and will allow ground breaking projects, sponsored by DNOs, to be funded from the £500m fund. The scheme is split into two separate tiers. Tier 1 focuses on small scale projects and enables DNOs to recover a proportion of the expenditure incurred to demonstrate innovative ideas. Tier 2 has an annual allocation budget of £64m and is distributed among projects on a competitive basis. Successful Tier 2 project bids have included deployment of new technologies, along with development and demonstration of new operating and commercial arrangements. Since the outset of the scheme, Ofgem has awarded funds to ten Tier 2 projects. Under the current LCNF plan, the allocation of funds across the two tiers stands at £80m for Tier 1 projects, £320m for Tier 2 and £100m for discretionary rewards. The latter is awarded for successfully deployed projects that bring understanding of the new investments, operating and commercial frameworks necessary to provide a safe and secure electricity supply in Britain's low carbon future.

In 2010 Ofgem announced RIIO (Revenue = Incentives + Innovation + Outputs) [2.16] to recognise that network companies must have long term flexible plans for future investments that can respond to uncertain future network demands. These investments are envisaged to be in the region of £30billion over the coming decade. The RIIO model, focused on electricity transmission [2.17] and gas distribution, seeks to encourage and reward companies in support of forward thinking strategies and ensure that consumers fund the required investments at a fair price. The performance measured model will financially punish inefficient companies that do not meet the performance targets that result from consultations with consumers and network users. The long term planning required by network companies not only focuses on investments, under the RIIO model, but also ensures that a low carbon future is achieved through the operation of smarter grid technologies.

The Electricity Market Reform (EMR) White Paper [2.18] was published in 2011 to address the decommissioning and closure of a quarter of the UK's generating assets (20GW of coal and nuclear plants) in the next decade and promote investments in sources of clean energy. The predicted cost of securing supply and the decarbonisation of generation is £110billion. The principal components of the reform package include: a carbon price floor, long-term contract, emission performance standard and a capacity mechanism. These key elements ensure that a fair carbon price is set, a stable and predictive revenue stream for renewable generators is in place and that annual emission caps are set for new fossil fuelled generators. The last element, the capacity mechanism, requires further consultations to ensure that future energy security issues are addressed and that participating generators and demand side resources are incentivised. Fundamentally, this reform seeks to put measures in place that are strong incentives to invest in low carbon generation technologies.

The government level drivers and incentives and having de-regulated distribution networks for generation opened the market for generation of all sizes and technologies. This spawned interest for renewable generators which resulted in the UK's attention being focused on research and development of projects that aid facilitation of DG onto distribution networks.

It is clear that the incentives being offered will aid the development of more clean energy sources and as such the technical barriers need to be addressed. The significant numbers of renewable deployments require the investigation of rigorously tested novel approaches to combat the increasing technical constraints associated with the envisaged growth of DG. The following sections discuss the three main technical concerns and methods published in the literature that seek to overcome them. The subsequent chapters develop and test approaches specifically addressing the power flow management area.

2.5 Technical Concerns Associated with Distributed Generation (DG)

The following section gives an overview of each of the three main technical issues that require to be addressed with the connection of DG onto a distribution network. In 2000 these issues were published and discussed by Jenkins *et al* in [2.20].

2.5.1 Voltage Control

Voltage control has been at the forefront of DG integration since conception of the idea of embedded generation due to the statutory obligation of a DNO to maintain system voltages within limits. DNOs have different obligations to supply a voltage within certain limits to different customers. The requirements for these terminal voltages are: +10%/-6% for circuits at 230V (LV supply), +6%/-6% for circuits less than 132kV (HV networks) and +10%/-10% for circuits above 132kV (EHV networks). The connection of DG units results in a voltage rise at the point of connection and various methods exist for resolving voltage fluctuations due to the intermittency of individual DG units within the distribution network. Each solution comes with implications for the generator, DNO and consumer. Collinson *et al* [2.11] documented the methods of voltage control as being:

- Line re-conductoring
- Use of a dedicated network
- Single generator reactive and real power control
- On-line tap changer
- Active voltage control
- Line voltage regulation

These solutions are further discussed in the following sub-sections.

2.5.1.1 Line Re-conductoring

This approach can be viewed as a 'planned' management of voltage control as lines can be re-placed with lower resistance cable over a specific timescale or at planned maintenance outages. The lower resistance cable allows more distributed generation to be connected as voltage regulation along that conductor is improved. This is a costly solution and could only be effective over a long period of time. The capital cost required for this solution can act as a disincentive to the connection of DG, particularly small DG units.

2.5.1.2 Dedicated Networks

These could be particularly beneficial in rural areas where distributed generation is likely to greatly exceed any local load requirements and vast amounts of exported power are produced. The customers would be isolated from the distribution network and therefore not be subjected to the voltage fluctuations that arise from the embedded generation. The cost implication would be high and would also require careful planning to ensure that the network is utilised to the best of its design along with a maximum return to the DNO. Again, the cost associated with this solution can act as a barrier to the connection of DG.

2.5.1.3 Generator Reactive and Real Power Control

Switched capacitor and reactor banks, transformer tap changers, Static VAr Compensation (SVC) or statcoms can be used to control distributed generator reactive power flows. All these solutions are used and have been established on conventional generators. They are often used to regulate the voltages at the bus that the generator is connected to by controlling reactive power flow. Reactive power absorbed by DG units can help reduce the voltage rise effect and would be deemed a preferential, by the DG operator, method compared with that of real power control (real power export being the source of revenue for a DG owner). It is notable that at distribution level reactive power control is less effective than at transmission level where circuits generally have a higher X/R ratio.

Regulating the real power output of DG units is an effective way of allowing more DG connections and managing feeder voltage profiles. However, as the sale of real power is the income stream for DG operators, in a competitive market, the DG operators would want to maintain the levels of network capacity that they had contracted to them.

2.5.1.4 On-line Tap Changer (OLTC)

OLTC devices regulate the magnitude of the voltage at the busbars by systematically changing the primary and secondary coil ratio of the transformer (usually the change is made on the primary winding) connected to the network. They are generally found within the distribution substation. These electrically operated mechanical devices sense load changes and start to operate in a hierarchical manner until a stable voltage, to meet statutory limits, at the secondary side of the transformer is achieved. These devices can take up to several minutes to operate.

2.5.1.5 Active Voltage Control

Active voltage control with remote sensing was the basis of the GenAVC system that was developed for area voltage control. The principal role of active voltage control with remote sensing is to establish busbar voltages based upon some real system measurements and pseudo measurements derived from historical data. The output of active voltage control would be to initiate OLTC operations, via a control block, to maintain area voltages within statutory limits.

2.5.1.6 Line Voltage Regulation

Long transmission lines have high reactance, higher than that of the distribution network reactances, and will comprise more losses and higher voltage drop along that conductor. One method of solving this voltage problem is to incorporate a transformer, with a one to one ratio, at an optimal point along the cable. This will ensure that at the point where the voltage could fall below an unacceptable value the transformer can act to increase the secondary voltage up to a sufficient level to meet with the requirements of the statutory limits at the receiving end. This concept has been used on rural 11kV circuits in the Welsh distribution network to maintain acceptable voltage profiles.

2.5.2 Fault Level Management

Distribution networks can expect to see an increase in prospective fault levels with the connection of DG [2.11] and as such prospective fault currents place limitations on the expansion of DG connections due to the cost of upgrading switchgear. Assets that are already close to the fault current limit are in danger of being damaged if subjected to higher fault currents which could result in mal-operation of the equipments' desired functions. This result has direct implications for network security and the safety of public and personnel. The cost of the necessary upgrade of circuit breakers and switchgear to cope with increased fault currents could be extremely high and under current UK policies would be met by the distributed

generator. In terms of increasing potential DG connection whilst avoiding the cost of switch gear replacement the impact of current limiting devices and network splitting has been investigated.

Present methods of obstructing the fault current flow are to place high impedance devices between generators and loads such as transformers and reactors or to increase impedance through changes in network topology, network splitting [2.11] [2.21].

Wu *et al*, 2003, [2.22] discussed the implications of having a high fault current level as indicating that a network is robust and strong. A high fault level suggests that network impedance is low and therefore voltage drop along feeders/lines will be reduced offering a better voltage profile. It is discussed that there is a trade off between the cost of high fault current breaking switchgear and the level of desired robustness. Therefore, the main technologies/techniques for limiting fault currents, the alternative to uprating of switchgear, are identified as being:

- Current limiting reactors (CLR)
- Is-limiter (ABB product)
- Superconducting fault current limiters (SFCL)
- Solid-state fault current limiter (SSFCL)
- Network splitting

Current limiting reactors, the Is-limiter, superconducting fault current limiters and the solid-state fault current limiter introduce additional impedances to the system and hence reduce fault currents. Wu et al, 2003, discuss the merits and applications of these devices and highlight the negative impact on voltages (CLR), the cost of procuring and installing (SFCL), the complexity of the device's auxiliary system (SSFCL) and concludes that network splitting offers the most economical technical solution for the reduction of fault currents.

Foote et al, 2005, [2.23] provided analysis based upon four generic UK distribution networks that illustrated the benefits and costs associated with network splitting

configurations. This valuable guidance into the performance of network splitting used power quality and reliability indicators as a base measurement to assess the cost of network splitting arrangements when switching out one of the parallel transformers from service and splitting busbar sections. The authors highlight that the results illustrate the impact of network splitting and discuss the requirement for further detailed analysis for the application of network splitting for specific distribution systems. The paper shows that for the generic distribution networks examined that the removal of transformers, where permissible, from operation resulted in the allocation of additional headroom for prospective fault currents. The authors noted that this has, in some occasions, a significant negative impact on reliability and power quality. It was reported that the splitting of buses offered some additional headroom which did not impact reliability or power quality as drastically. The paper concludes that operation, maintenance and control issues are also required to be explored when using network splitting for management of fault currents and the impact of impedance changes, through network splitting, on protection systems, DG transient stability and transformer loading requires specific investigation.

2.5.3 Power Flow Management (PFM)

Network power flows are influenced by the characteristics of power injection and consumption, as well as the impedance of the connecting circuits. By introducing DG units into distribution networks, there is a move away from the traditional unidirectional power flow that distribution networks were originally designed to accommodate. The resultant bidirectional power flows bring added uncertainty to the direction and magnitude of flows in a distribution network and may pose significant risk to network security. Monitoring of power flows ensure that the thermal rating of the associated network components are not exceeded. Thermal overloading of these components can affect the correct operating criteria and the lifespan of these expensive assets. Tripping of over current protection schemes has a financial implication for the DNO in terms of CIs and CML. Current conservative planning measures ensure that DG export onto any network or feeder does not compromise the security of the system. A robust solution for managing power flows would provide

system security without the DNO being financially penalised by the regulator. As the penetration of DG increases so does the risk of tripping circuits when thermally overloaded and with a strong desire from DNOs to protect the lifespan of their aged assets PFM offers the ability to support network security by protecting the operating margins of system plant.

In terms of research the focus has been on active Power Flow Management (PFM) approaches and techniques.

In 2005 Currie *et al* [2.24] presented a novel active network management concept that enabled increased DG connections and optimised the Orkney networks existing capacity. This paper presented the idea of New-Non-Firm Generation (NNFG) above that of the limitations imposed by traditional planning connection arrangements, Firm Generation (FG) and Non-Firm Generation (NFG). Power system analysis studies identified that 25MW of load following NNFG capacity could be connected without exceeding network fault limits with system voltages supported through existing and planned compensation devices. Currie identified that this level of connection would result in thermal limits being exceeded and the requirement for regulating the NNFG connections through an ANM scheme.

The solution Currie proposed entailed the Orkney network being split into “zones” or “cells”. The idea being that each zone had its own control logic that looked to maximise the DG export subject to the zones maximum export capacity with two defined operating margins. The operating margins ensured that sequential trimming (for a larger margin) and sequential tripping (for a smaller margin) of the NNFG connections can be carried out. Under the operation of this active power flow management scheme if a generator does not respond to a trimming signal it will be tripped after a pre-defined timescale. Currie explains the complexity involved in defining the margins due to them being dependent on the ramp rates of generating units, the communication and control delays, the logic processing, capacity and characteristics of online generation and network demand characteristics.

The successful operation of Orkney's ANM scheme required direct MVA measurements to determine the export capacity from each of the control zones. The proposed location for the control logic for each zone was within the central control centre (as opposed to distributed control centres).

Currie discusses the impact of an ANM scheme on DNOs, generators and consumers.

In 2006, Ault *et al* [2.6], demonstrated that the active PFM scheme discussed in [2.24] could facilitate up to three times more generation capacity than traditional firm generation approaches. Half-hourly load and generation profiles were used to determine the NNFG constraints and record the MWh per MW of connected NNFG units using two sets of operating margins. Studies were conducted up to and beyond the maximum permissible generator connection capacity, identified as 72MW (inclusive of FG, NFG and NNFG). Furthermore, an economic cut-off point (ECOP) was presented, for the two operating margin scenarios, based upon the assumed investment costs, revenue from energy sales and Renewable Obligation Certificates. Ault emphasises that ANM schemes, managing multiple DG units, are crucial to meeting UK renewable targets in a cost effective way.

Currie *et al* [2.25], 2006, review the current generator connection philosophies and incorporates Regulated Non-Firm Generation (RNFG, synonymous with NNFG) as a new connection philosophy. A 13-step method to determine the economic cut-off point (ECOP) for the RNFG capacity is presented. Under this economic assessment the importance of future electricity market prices and the Renewable Obligation Certificate (ROC) scheme is presented as playing a crucial role in the connection of DG above and beyond the traditional FG and NFG capacity limits. The paper concludes that under current pricing and national incentives the active PFM functionality discussed can play a vital role in the economic harnessing of renewable energy. However it is stressed that further work is required to determine the trim and trip operating margins of the scheme to ensure system security is maintained and that the specific assessment of DG curtailment levels are achieved.

In 2007, Currie *et al* [2.26] published a method for determining the active PFM scheme's operating margins and discussed the importance of the performance of the communications links in defining the operating margins. The operating margins are separated into two categories, a trim margin and a trip margin. The trip margin is described as the last of the ANM scheme's operation to preserve system security and must take account of DG ramp rates to maintain system voltages, timescale of control operation, short-term/emergency line ratings. Under normal operating conditions the trim margin is defined as the safe export capacity of the control zone and takes into consideration the timescales involved ramping down DG output to avoid moving into the trip margin region. Having demonstrated the calculation of the operating margins power system studies were carried out on a UKGDS [2.27] model to determine the annual DG energy yields and a subsequent economic evaluation carried out. The results indicated for the levels of DG connected (17-23MW) at a RNFG level that little in terms of curtailment was experienced.

Jupe, 2008 [2.28], discusses the technical considerations and economics of a number of solutions that allow greater connections of DG to operate at distribution network levels. It is observed that thermal ratings of power system plant and circuits are not a static quantity and vary throughout the year in line with meteorological conditions. It is discussed and shown that taking advantage of the dynamic rating phenomena, in terms of active management, that increased DG yields can be sought. Jupe adopts the term Active Constrained Connection Manager (ACCM) for this Dynamic Thermal Rating (DTR) approach to manage a single DG unit. The publication concludes that the long term return on investment costs for an ACCM system that uses DTRs outweighs traditional reinforcement, ACCM based upon seasonal ratings and ACCM based upon static ratings.

Candidate control strategies for the power flow control of multiple DG units are discussed and energy yields quantified by Jupe, 2009 [2.29]. The methods developed and modelled are based upon sensitivity analysis of network power flow change due to the change of DG power injection at DG buses. The current control strategy of last

in, first off (LIFO) is presented as the current UK connection strategy that control schemes should meet. It is proposed that a 'LIFO sensitivity based' control approach could be taken on each DG unit to meet contractual agreements. In addition to applying the 'LIFO sensitivity based' control approach, the author proposed and demonstrated three further control strategies. These control approaches included:

- the "percentage of total DG output" where the DG with the largest power output would take the most responsibility for alleviating congestion;
- the "equal percentage reduction of present power output" where each DG unit would curtail output in equal proportions to their present output;
- the "most appropriate technical strategy" where the DG with the most technical ability to resolve the congestion is curtailed.

Simulations are conducted to evaluate the aggregated annual energy yield gains through implementation of each of the control strategies. The paper concludes that the greatest energy yields were associated to the "most appropriate technical strategy" however it is acknowledged that incentives would need to be in place for individual DG owners to accept curtailment to ensure higher overall energy yields are achieved. In 2010, Jupe *et al* [2.30] focus on the Power Flow Sensitivity Factors (PFSFs) approach to managing network power flows and examines the resultant energy yields from each of the schemes in a UK field trial. It is discussed that a similar approach could be applied to distribution network voltages.

In 2009, Jupe [2.31] presents the development stages of the power flow management scheme for controlling the output of multiple DG units using sensitivity based analysis and DTR. The four stage process includes: off-line analysis to determine susceptible parts of a network to power flow excursions with DG connections, quantify the headroom gains of the susceptible network area with the inclusion of a DTR scheme, development of the real-time DTR scheme and the incorporation of the DTR scheme with a sensitivity based DG power output control schemes. The thermal vulnerability process is proven to provide valid results for all types of network topologies. This approach has been used to identify monitoring investments on a trial

network. The calculation of sensitivity factors has been deemed to be network topology specific and as such any changes in topology require the calculation of new DG power output sensitivity factors. The paper concludes that a sensitivity based power flow management scheme is feasible when vulnerable components and necessary instrumentation is identified.

In 2010, Currie *et al* [2.32], published an overview of the active PFM scheme deployed on Orkney network, Scotland. Within this publication the lessons learned and review of the ANM scheme were discussed in terms of moving towards a smart grid. The ANM scheme deployed on Orkney operates in parallel with the existing Supervisory Control and Data Acquisition (SCADA) system. The flexibility of the ANM scheme is highlighted as being able to accommodate further DG connections, network topology changes and upgrades in plant which are desired characteristics by the DNOs. Another desirable characteristic implemented within the ANM is the graceful backing-off of the RNFG units should communications be lost. Currie also makes reference to other approaches, such as optimisation and artificial intelligence techniques, and discusses several areas of work required when moving away from the deterministic approach deployed on the island of Orkney. The paper concludes with recommendations for ANM scheme developments based upon the learning obtained from the live Orkney scheme.

The approaches developed and presented, within this thesis, for power flow management builds upon the existing research knowledge in the field. These reported alternative approaches for managing multiple DG units are demonstrated to maintain networks within thermal limits and increase the DG access compared to that of traditional inter-tripping techniques and are therefore in line with other ANM solutions.

2.6 United Kingdom Developments in Active Network Management (ANM)

In the early stages of ANM, introduced through the DGCG, bespoke solutions were applied to single generator cases to meet the particular power network requirement. The increased number of granted DG applications means levels of DG access is set to rise bringing a need to develop and implement solutions for multiple generator connections. This requires co-ordination between the distribution network and embedded generators through active planning, real-time monitoring and management.

A "Register of Active Management Pilots, Trials, Research, Development and Demonstration Activities" was put together in February 2006 and updated in January 2008 [2.33]. The purpose of which, was to inform DNOs, industry, policy makers, and academics of the status of ongoing active management projects. Various projects are identified within this document with the majority of activity being in the initial R&D stages (approximately 78%). 14% of projects are described as being in full deployment with the remaining percentage in the trial and pilot stages.

It is clear that the technical focus, of the majority, of projects is limited to one or two of the technical problems instigated by DG connections. Within the ANM Register an ongoing Econnect project, entitled "Embedded Controller", addresses three of the main issues; voltage control, fault level management and power flow management. With one other, entitled "Demand Area Power System" led by the Central Research Institute of the Electric Power Industry (CRIEPI), focusing on four areas; power flow management, voltage control, demand side management and protection systems.

Within the UK ANM of the distribution system is emerging as the preferred solution to the connection and operation of DG. Ofgem incentives, such as Innovation Funding Incentive (IFI) and Registered Power Zones (RPZ), are intended to stimulate change and bring innovative technical solutions to distribution networks.

2.6.1 Active Network Management (ANM) Examples

Circuits are limited by their thermal ratings. To avoid overloading of circuits static line ratings are calculated based on the worst case scenario. This generally leaves a safety margin of unused available capacity at the worst case and an even higher available capacity when at the other end of the spectrum. A new approach of utilising dynamic line ratings is focusing on using this available capacity to avoid circuit reinforcement. Central Networks are the first DNO to be granted RPZ status by Ofgem [2.34]. Their scheme, under development, will enable the existing 132kV lines from Skegness to Boston to accommodate up to 90MW of additional generation above the existing 227MW capacity. The scheme will use local temperature and real-time load data to calculate new dynamic line ratings. Curtailment of generation would be subject to breaching these dynamic line ratings. This enables lines to carry extra power, from wind farms, by making real-time decisions rather than relying on the static line rating values.

The abundant renewable resources found on the Orkney Islands have made them the focus of increased DG connections. However, at times of minimum demand the export capacity, of the two 33kV submarine cables, reaches its maximum when the existing generating plant operates at rated output. Due to this any further generator connections would require the submarine interconnection to be uprated. An ANM investigative project was undertaken by the University of Strathclyde, for SSE, to develop an innovative facilitation method of connecting more DG without expensive reinforcement works. The approach of expanding NFG connections was addressed through zoning of the existing Orkney network. Each zone was assigned where new Regulated Non-Firm Generation (RNFG, also referred to as New Non-Firm Generation (NNFG)) connections were to be made and where some thermal, load and generation conditions were met. The result was sequential trimming/tripping/inter-tripping of RNFG units at times where export power flows reached a threshold. A pilot scheme has been successfully implemented on the Orkney network (granted RPZ status for the innovative solution) led by the research work conducted by Currie [2.26].

The GenAVC controller project was led by Econnect and developed in the University of Manchester. The principal objective of this scheme was to increase the export of energy onto the distribution networks while managing network voltages. GenAVC is an ANM device that regulates the voltage on 11kV circuits. Voltage control was achieved by gathering real-time measurement from network points (UK Power Networks, formerly EdF Energy, and United Utilities networks were used for pilot schemes) and utilised state estimation to fill in the unknowns. The comparison would be made of actual voltages, against system voltage set points and the tap ratios on the controlled distribution transformers changed accordingly. These controllers are available on the market. Results of a GenAVC application are available at [2.35]. Figure 3 illustrates the measurement and control loops required by GenAVC.

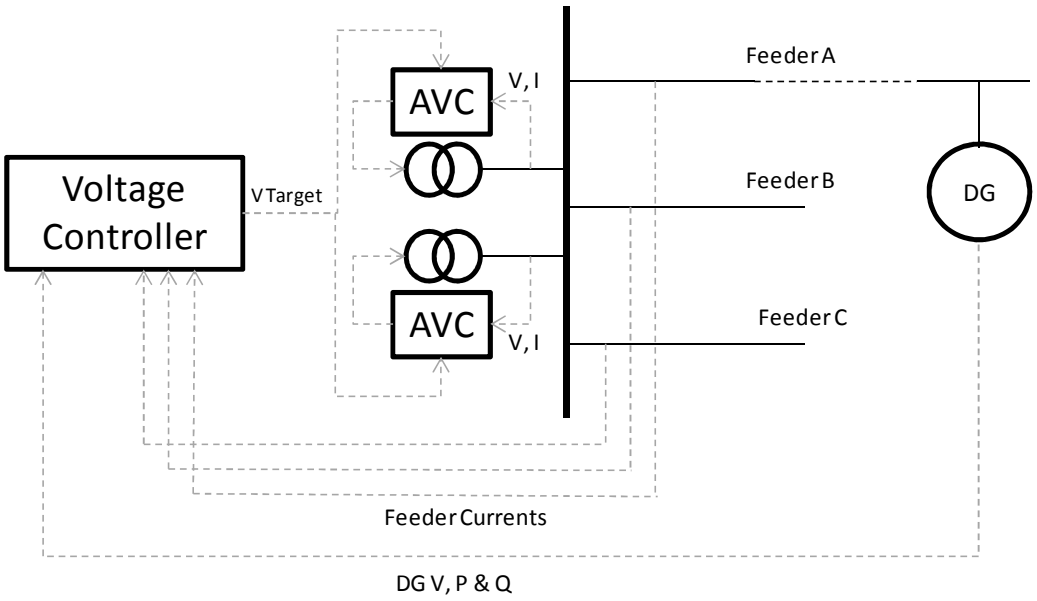

Figure 3 - Illustration of GenAVC Measurement and Control Loops

The target voltage set points, calculated within the voltage controller, are communicated to the transformer AVRs at the local substation. The calculated set points are based upon voltage measurements at the local substation busbar and current measurements on the connected feeders along with the voltage and power

output at remote buses with DG connections. Distribution state estimation is employed to evaluate voltages throughout the network (using any additional strategically placed measurements devices) to determine the required change in AVR voltage set points.

In [2.36] Fila presents a comparison of the most commonly used AVR schemes in UK distribution networks and an advanced voltage control options for active distribution networks implemented in the SuperTAPP n+ AVR. The objective of SuperTAPP n+ AVR is to ensure that a co-ordinated voltage control solution is achieved. The calculations of voltage set points rely upon local feeder current measurements and the load shared by these feeders to estimate the output of connected DG units. This removes the requirement for a direct communications link to the DG units. The studies undertaken demonstrate that increased levels of DG can cost effectively connect to distribution networks when using distribution state estimation techniques and local voltage controllers compared to that of standard AVC schemes.

An ongoing and ambitious project, Intelligrid [2.37] led by the Electric Power Research Institute (EPRI), has produced an Architecture Guidebook that brings together the 'energy' world and the 'information technology' world. The Fast Simulation & Modelling (FSM) part of the project will be designed to provide the mathematical underpinning and look-ahead capability for a Self-Healing Grid (SHG). SHG should be capable of automatically anticipating and responding to power system disturbances, while continually optimising its own performance. The FSM is aimed at developing real time software based on an open platform that would be used to help operators to make decision to operate complex power systems. This aims to tackle the power delivery system issues by means of using local actuators and thinking globally to perform the following functions:

- Volt-VAr control function (VVC)
    - Maintain power quality
    - Improve power systems stability

- Multi-feeders reconfiguration (MFR)
    - Reduction of CML's
    - Transfer loads
    - Re-energise circuits
- Fault location and isolation (FLI)
    - Reduction of outage duration through quick reconfiguration
- Special protection systems (SPS)
    - Adapt and optimise protection set-points
    - Ensure optimisation and safe reconfiguration

Other aspects of the continuing work of the Intelligrid consortium are projects called Communication Protocols for Distributed Energy Resource and Consumer Portal. There are several standards for handling blocks of information sent over a communication networks. DNP3, Modbus, LON-LAG, IEC 60870-5, IEC 61850 and several proprietary protocols are typical examples of communication protocols that are used for power system automation and control. The existence of numerous protocols may hinder or prohibit the integration of new or different vendor devices within a network due to interoperability conflicts or through commercial barriers arising from large "monopoly" vendors. The Communication Protocols for Distributed Energy Resource project recognises the requirement to standardise communications and enable different devices and controllers to 'talk' to one another. The project is looking to develop open communication networks that will be able to support the growing number of devices connected to power delivery systems in a plug and play manner. It is envisaged that standardising data exchanges on these open communication networks will allow the incorporation of small scale generation plant and storage devices over a period of time without the need for custom redesign. The Consumer Portal aspires to empower consumers and reduce utility costs. The services could include; demand response, net metering, real-time pricing, automated meter reading, energy management and appliance management. In 2006 EPRI included Advanced Monitoring Systems within the remit of IntelliGrid.

Utilities are looking for smarter ways in which to get more from the network's existing assets and are gaining confidence in trialling newly established monitoring and control strategies. The research presented within this thesis aimed to establish a monitoring and control strategy that could be trialled on today's networks and be flexible enough for future energy networks.

2.7 Energy Networks of the future

As discussed the present day, 'fit and forget', operation of the distribution network restricts the flexibility of the network. In order to provide an economic, flexible and secure network DG connections at distribution level requires a new connection philosophy, 'connect and manage', to ensure maximum benefit is attained for all stakeholders. The European Commission formed the European Technology Platform (ETP) for Electricity Networks of the Future whereby current and emerging commercial, environmental and technical issues could be addressed to enable a unified vision of the European energy infrastructure looking towards 2020 and beyond. The ETP started work in 2005 and published the ETP 'Vision and Strategy for European Electricity Networks of the Future' [2.38] document in April 2006. This document was to serve as the catalyst to ensure all parties involved in electricity generation and delivery (transmission and distribution) expressed their views on the direction that the energy business would take in the coming years to meet the needs of Europe's future.

Within this document the primary enabling elements of the vision were highlighted:

- "Creating a proven toolbox of technical solutions"
- "Harmonising regulatory and commercial frameworks"
- "Establishing shared technical standards and protocols"
- "Development of information, computing and communication systems"
- "Ensuring successful interfacing of new and old technologies"

The recognition that future electricity networks need to be flexible, accessible, reliable and economic requires the expertise from industrialists, academics and regulatory authorities to work in harmony to achieve the consolidated goals of each of the stakeholders. Research, development and demonstration of technologies will play a key role in 'smart grid' developments.

In 2007 the ETP produced the "Strategic Research Agenda" [2.39] which exposed the main areas to be explored. Technical and non-technical areas were split into five main research streams with a total of nineteen sub tasks. By placing the network users at the centre of all the research ideas it is envisaged that customer active participation will drive developments as and when the user requirements surface and are fully understood. In 2010 the "Strategic Deployment Document" [2.40] was produced in which a time line is set out for priority innovative deployments and the respective benefits to stakeholders highlighted.

2.8 Future of Active Network Management (ANM)

Regulatory and market forces are predominantly going to be the influences that guide the way for ANM schemes. The signals sent out by the DECC and Ofgem are positive. They will pave the way for adopting the strategies required for the essential advancements required to evolve to active management solutions for distribution networks and the smart grid.

ANM research areas have produced beneficial techniques for addressing certain power system needs using a real-time approach. Therefore, there are existing technologies and products available and with current and emerging incentives network deployment and trial schemes will build the necessary confidence for DNOs to deviate from traditional approaches. It should, however, be recognised that there is a need for further research into the integration of existing or emerging technologies onto a distribution network in terms of management of the communication and control systems.

To date in the UK, Orkney RPZ project, Central Networks' RPZ and GenAVC are the only projects 'on the ground' that are taking this active approach. A DNO has the obligation of managing the risks that are brought about by network power flows. It is a risk in itself to implement pilot schemes and more incentives need to be shown to allow the development of ANM. Only full deployment of such schemes, over time, would provide on looking DNOs with the confidence and trust of such operating methods.

2.9 Active Power Flow Management and Current Commercial Connection Agreements

The requirement of an ANM scheme being flexible and extensible in nature requires the system and the functionality to operate with either no re-configuration or minimal re-configuration in light of new operating and/or contractual agreements. The current connection principle, for 'non-firm' generation, practiced in the UK today is a last-in, first-off (LIFO) disconnection order. This requires the last historically connected generator to reduce its output, during a network constraint violation, in an attempt to resolve the infringement and return the network to a secure state. Where this performed action is not sufficient to resolve the problem the next historically connected generators would be called upon, in succession, until the disconnection list is exhausted. Conventional system planning would ensure that with no DG connected the network limits would not be encroached under normal operating conditions. Only under severe or unexpected system events would a control engineer be able to justify deviating from the LIFO arrangement to preserve overall system security.

The LIFO scheme was introduced to protect network security while ensuring that the revenues of the first connected generators were exposed to less risk in terms of maintaining their revenue. This can be justified in the sense that these first generators had less (or no) incentive to operate other than business profitability, took higher risks due to early deployment into a fairly unknown area of business and therefore

should not be penalised because they took the lead role. However, with an increase in the number of connected DG units, this access rule may hinder further investments as newly connected units may face frequent disconnections. It is important to note that LIFO arrangements had an important and positive role in the initial stage of DG investments but as there is a growing need to increase the proportion of electricity generated by renewable low carbon technologies, in order to fulfil obligations from the EU 20-20-20 target [2.41]. The structured development process acknowledged that DG connection principles will evolve however the focus of this thesis is to discuss and investigate the role that the chosen techniques can play in the active management of DG within the current LIFO commercial framework. Although, the current LIFO agreement will be used the core functionality will be deployed in a manner that it is easily re-configurable (i.e. the core solution functions remain the same but inputs/bounds of the problem will change to reflect changes in commercial contracts) hence taking cognisance of the future potential and extensibility of the PFM techniques. This is in line with the European Smart Grid Technology Platform's [2.38] interest in building up a "toolbox of proven techniques that can be quickly and economically deployed".

2.10 Chapter 2 Review

It has been found that traditional methods of planning or control are either not economically feasible or sufficient to support the numbers of renewable generator units required to meet national targets. Therefore, these evolving distribution networks require new monitoring and control strategies to manage the increasing numbers of DG units expected to connect in the coming years. Adopting an active approach to the management of multiple DG units to mitigate distribution network technical issues has been shown to reduce capital expenditure in network infrastructure, grant increased access to existing DG units and release capacity for greater number of future DG unit connections. The following chapter introduces the 'Specification of Requirements' and the 'Functional Requirements' derived from the structured development process for the active management of the PFM problem. The two techniques are then discussed that were applied to the power flow management problem and the testing environment that is used to demonstrate that ANM can provide, through incremental deployment steps, the functionality for fully operational smart grids.

2.11 Chapter 2 References

[2.1] Department for Business, Enterprise and Regulatory Reform (BERR), "Atlas of UK Marine Renewable Energy Resources: Technical Report", May 2008

[2.2] Office of the Gas and Electricity Markets (Ofgem), " 2008/09 Electricity Distribution Quality of Service Report", Annual Report, December 2009

[2.3] Engineering Recommendation P.2/5, The Electricity Council Chief Engineers' Conference: Security of Supply, System Design and Development Committee, October 1978

[2.4] Engineering Recommendation P.2/6, Energy Networks Association, "Security of Supply", July 2006

[2.5] G. Strbac, N. Jenkins, M. Hird, P. Djapic, G. Nicholson, "Integration of Operation of embedded generation and distribution networks", DTI Pub URN 02/1145, 2002

[2.6] G.W. Ault, R.A.F. Currie, J.R. McDonald, "Active Power Flow Management Solutions for Maximising DG Connection Capacity**",** IEEE PES General Meeting, Montreal, October 2006

[2.7] J. Mutale, "Benefits of Active Management of Distribution networks with Distributed Generation", IEEE PES Power Systems Conference and Exposition, October 2006

[2.8] Embedded Generation Working Group, "Report into Network Access Issues"; Volume 1, Main Report and Appendices, January 2001

[2.9] Embedded Generation Working Group, "Assessment of Embedded Generation Contributions to Network Performance", November 2000

[2.10] Embedded Generation Working Group, "Future Network Design, Management and Business Environment", December 2000

[2.11] A. Collinson, F. Dai, A. Beddoes, Crabtree, J. "Solutions for the Connection and Operation of Distributed Generation"; DTI Distributed Generation Programme (Contractor: EA Technology) K/EL/00303/00/01/REP; 2003

[2.12] HM Government , "Energy White Paper 2003: Our Energy Future – Creating a Low Carbon Economy", Department of Trade and Industry (DTI), February 2003

[2.13] HM Government, "Energy White Paper 2007: Meeting the Energy Challenge", Department of Trade and Industry (DTI), May 2007

[2.14] Office of the Gas and Electricity Markets (Ofgem), "Creating a Britain's Low Carbon Future. Today", Low Carbon Network Fund (LCNF), November 2011, available at http://www.ofgem.gov.uk/Media/FactSheets/Documents1/LCNF%20brochure%202011.pdf, accessed 6th May 2012

[2.15] Office of the Gas and Electricity Markets (Ofgem), "Electricity Distribution Price Control Review – Final Proposal", 7th December 2009, available at http://www.ofgem.gov.uk/Networks/ElecDist/PriceCntrls/DPCR5/Documents1/FP_1_Core%20document%20SS%20FINAL.pdf, accessed 6th May 2012

[2.16] Office of the Gas and Electricity Markets (Ofgem), "RIIO – A New Way to Regulate Energy Networks", October 2010, available at http://www.ofgem.gov.uk/Media/FactSheets/Documents1/re-wiringbritainfs.pdf, accessed 6th May 2012

[2.17] Office of the Gas and Electricity Markets (Ofgem), "RIIO-T1: Final Proposals for SP Transmission Ltd and Scottish Hydro Electric Transmission Ltd", April 2012, available at http://www.ofgem.gov.uk/NETWORKS/TRANS/PRICECONTROLS/RIIO-T1/CONRES/Documents1/SPTSHETLFP.pdf, accessed 6th May 2012

[2.18] Department of Energy and Climate Change (DECC), "Electricity Market Reform White Paper 2011 – Planning Our Electric Future: A White Paper for Secure, Affordable and Low Carbon Electricity", July 2011, available at http://www.decc.gov.uk/assets/decc/11/policy-legislation/EMR/2176-emr-white-paper.pdf, accessed 6th May 2012

[2.19] United Nations, "Kyoto Protocol to the United Nations Framework Convention on Climate Change", 1998

[2.20] Jenkins, N., Allan, R., Crossley, P., Kirschen, D. and Strbac, G. (2000); "Embedded Generation"; IEE Power and Energy Series 31, The Institution of Electrical Engineers, London, United Kingdom

[2.21] DTI Distributed Generation Programme (Contractor: EA Technology); "The Performance of Networks Using Alternative Network Splitting Configurations"; Contract Number: DG/CG/00031/00/00, URN Number: 04/1475; 2004

[2.22] X. Wu, J. Mutale, N. Jenkins, G. Strbac, 2003, "An Investigation of Network Splitting for Fault Level Reduction", Tyndall Centre for Climate Change Research Working Paper 25

[2.23] C.E.T. Foote, G.W. Ault, J.R. McDonald, A.J. Beddoes, "The Impact Of Network Splitting On Fault Levels and Other Performance Measures", CIRED, 18th International Conference on Electricity Distribution, June 2005.

[2.24] R.A.F. Currie, G.W. Ault, J.R. McDonald, "Initial Design and Specification of a Scheme to Actively Manage the Orkney Distribution Network", CIRED, 18th International Conference on Electricity Distribution, June 2005.

[2.25] R.A.F. Currie, G.W. Ault, J.R. McDonald, "Methodology for determination of economic connection capacity for renewable generator connections to distribution networks optimised by active power flow management", IET Generation, Transmission and Distribution, IEE Proceedings, July 2006

[2.26] R.A.F. Currie, G.W. Ault, J.R. McDonald, "Active power-flow management utilising operating margins for the increased connection of distributed generation", IET Generation, Transmission and Distribution, IEE Proceedings, January 2007

[2.27] Centre for Sustainable Electricity & Distributed Generation (SEDG), available at www.sedg.co.uk (accessed on 27/07/2011)

[2.28] S.C.E. Jupe, P.C. Taylor, C. Berry, "Assessing the Value of Active Constrained Connection Managers for Distribution Networks", CIRED Seminar 2008: SmartGrids for Distribution, Frankfurt, June 2008.

[2.29] S.C.E. Jupe, P.C. Taylor, "Strategies for the Control of Multiple Distribution Schemes", CIRED 20th International Conference on Electricity Distribution, Prague, June 2009.

[2.30] S.C.E. Jupe, P.C. Taylor, A. Michiorri, "Coordinated output control of multiple distributed generation schemes", IET Renewable Power Generation, 2010.

[2.31] S.C.E. Jupe, P.C. Taylor, "Distributed generation output control for network power flow management", IET Renewable Power Generation, 2009.

[2.32] R.A.F. Currie, G.W. Ault, C.E.T. Foote, N.M. McNeill, A.K. Gooding, "Smarter Ways to Provide Grid Connections for Renewable Generators", IEEE PES General Meeting, Minneapolis, July 2010

[2.33] R. MacDonald, R.A.F. Currie, G.W. Ault, "Register of Active Management Pilots, Trials, Research, Development and Demonstration Activities", Advanced Electrical Systems Research Group, University of Strathclyde, January 2008. Available at: http://webarchive.nationalarchives.gov.uk/20100919181607/http:/www.ensg.gov.uk/index.php?article=95 (accessed 27/072011)

[2.34] E.on, Central Networks, "Regulatory Report for DG Incentives, RPZs & IFI", Regulatory Year 2008/09. Available at: http://www.ofgem.gov.uk/Networks/Techn/NetwrkSupp/Innovat/ifi/Documents1/Central%20Networks%20IFI%20Report%202008-09.pdf (accessed 27/072011)

[2.35] V. Thornley, J. Hill, P. Lang, D. Reid, "Active Network Management of Voltage Leading to Increased Generation and Improved Network Utilisation", CIRED Seminar 2008: SmartGrids for Distribution, Frankfurt, June 2008

[2.36] Majiec Fila, "Modelling, Evaluation and Demonstration of Active Voltage Control Schemes to Accommodate Distributed Generation in Distribution Networks", Brunel University, Ph.D. Thesis, October 2010

[2.37] Electric Power Research Institute, Technical Report, "Profiling and Mapping of Intelligent Grid R&D Programs", December 2006

[2.38] European Technology Platform for Electricity Networks of the Future: SmartGrids, "Vision and Strategy for European Electricity Networks of the Future", 2006

[2.39] European Technology Platform for Electricity Networks of the Future: SmartGrids, “Strategic Research Agenda”, 2007

[2.40] European Technology Platform for Electricity Networks of the Future: SmartGrids, “Strategic Deployment Document for Europe's electricity networks of the future”, 2010

[2.41] European Commission, “Combating Climate Change: The EU Leads the Way”, 2007. Available at (accessed 27/07/2011): http://ec.europa.eu/publications/booklets/move/70/index_en.htm

Chapter 3

Proposed Power Flow Management Techniques and Closed Loop Steady-State Simulation Environment

3.1 Summary of Chapter 3

In Chapters 1 and 2 the proposed techniques to tackle the power flow management problem have been stated and the PFM problem has been discussed in terms of the evolving distribution networks, respectively. This chapter introduces the developed requirements of an active PFM solution and discusses the OPF and CSP approaches in the context of the power sector and states their general formulation.

Also presented within this chapter are the hardware and software requirements developed to test the defined PFM software characteristics discussed in Chapter 1. The modular software functional blocks are explained and an overview of the test environment's communication interfaces and protocols is specified enabling the assembly of a real-time test environment on which the software algorithms can be embedded.

In addition, the two carefully selected different case study networks and their respective load and generation profiles that are utilised to evaluate the PFM algorithms' real-time performance are presented.

Having established the need for power flow management, in the previous two chapters, this chapter introduces the two candidate solutions and the test environment and its inputs used to evaluate the approaches. The subsequent chapters describe modelling the PFM problem around these candidate approaches and present results based upon the closed loop simulations.

3.1.1 Specification of Requirements

The requirements specification was developed to clearly set out what the ANM functionality was to achieve and what attributes a user may require the functionality to possess e.g. the general, the control and operation, the interface and the user requirements.

The general requirements relate to what the ANM system must conform to and the behaviour of its operation. In this respect the ANM scheme must be:

- Safe – it must operate in a safe manner to ensure the safety of personnel and not subject network operations to adverse control decisions.
- Secure and available – the use of available communications channels will be secure and ensure the ANM scheme is not compromised.
- Flexible and extensible – the flexible nature will ensure that the scheme is easily reconfigurable for future network changes. As such the core functionality remains the same with only the inputs for the control decision making elements having to be updated. Network events that would entail such revisions are:

    - Change in network topology
    - Plant renewal (changes in equipment rating)
    - Addition or removal of DG units
    - Inclusion or removal of further controllable devices e.g. energy storage systems
    - Addition or removal of monitoring/measurement equipment
    - Changes in existing protection and control operations
    - Changes in contractual arrangements

    The extensible trait will allow for better or improved network control functions to replace the existing functionality without having to redesign the system architecture. This is equally applicable to the addition of new control functions.
- Tolerant against failure – the ANM system would need to guarantee that every effort was explored to ensure that the control decisions were carried out by the associated power system's plant. Should the instruction not be carried out, perhaps through communications failure, then the scheme should be

aware and offer the instruction via another medium. The final and undesirable remedy would be the operation of traditional protection schemes.

- Graceful degradation – it is highly desirable that sensor or measurement errors do not compromise the integrity of the deployed functions. Examination of the resilience and fallback position of the applied algorithms to model error is required.

The operation and control requirement of the PFM functionality is defined as operating the power system within thermal limits. The requirements of the PFM function are that it will support the existing management of the network's constrained DG connections and comply with DNO optimisation strategies i.e. maximise DG outputs where possible.

System interface requirements define the incorporation of the ANM scheme into the DNO existing Distribution Management System (DMS) allowing the ANM status to be relayed back to a central control centre. In addition, the ability to switch the system off, override functionality or issue commands via the system's infrastructure is essential. Any ANM scheme will need to interface with field devices, e.g. DG units, measurement and monitoring equipment, which will inevitably employ various legacy standards. Therefore, the solution must interface with these current standards and protocols while extending to support other interfacing standards.

The user requirements identify the way in which users would interface with the ANM scheme. The relevant personnel that would necessitate such actions are the control engineers, the DG operators and the field engineers. The level of access will vary between users. Control engineers require:

- The ability to switch the ANM system functionality 'on' or 'off'
- The ANM system to recognise that a user action has taken place and suspend actions accordingly
- The ANM system to generate an alarm at the control centre when it recognises the need to carry out an action and when that action is carried out

- The ANM system to provide transparency of the autonomous control decisions
- The ANM system to allow its decisions to be overridden

DG operators require:

- Advance warning, in the form of an alarm, that the ANM scheme is going to carry out an autonomous control decision
- The ANM system will provide a signal that alleviates the network constraint to the DG plant e.g. ramp-up, ramp-down, run unconstrained or trip.

Field engineers require:

- The ANM system's functionality to be switched 'on' or 'off' locally
- A warning that a control action is about to be carried out

3.1.2 Functional Specification

Having established the ANM system and user requirements the next stage entailed clearly defining the functionality necessary to meet the requirements. This is the role of the functional specification stage and describes *what* the ANM system will accomplish rather than *how* it will accomplish the requirements. Preparation of a functional specification is an iterative process that will ultimately draw out what functionality is required and available to meet the requirements. Starting from the definition, in this case 'operation of the power system within thermal limit', functional blocks are identified and distilled down in an acyclic graph. Adopting this approach enables under-defined or undefined functionality to be highlighted and refined, Figure 4.

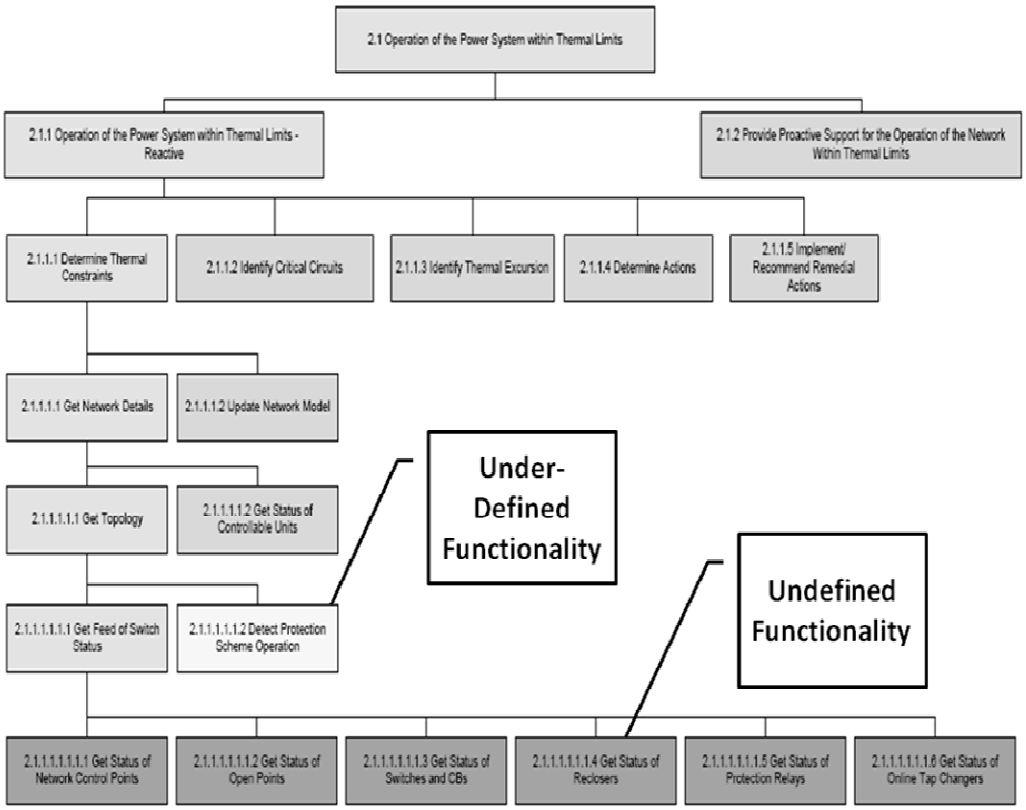

Figure 4 - Hierarchy of Functionality used to Establish Under-defined and Undefined Functionality

After refining the functional graph the information held within can be tabularised and any common functionality identified, i.e. the functionality that could be used by other functions (Figure 5).

Requirement 2.1 – Operation of power system within thermal limits					
No.	Name	Description/Comments	Inputs	Outputs	Equivalents
2.1	Operation of power system within thermal limits	Ensure network is kept within thermal limits	-	-	
2.1.1	Operation of power system within thermal limits - Reactive	Ensure network is kept within thermal limits in response to network events	-	-	
2.1.1.1	Determine Thermal Constraints	To determine all thermal constraints real time data and DNO/Manufacturer data must be gathered	-	Updated network model Topology	
2.1.1.1.1	Get current network details *(System state?)*	Get information related to system topology and status	-	Current network details	2.2.1.2 (partial) 2.2.1.2.3 (partial) 2.3.1.1 (partial) 2.5.1.3.1.1
2.1.1.1.1.1	Get topology	-	-	Topology	2.5.1.3.1.1.1
2.1.1.1.1.1.1	Get feed of switch status	Get switch status in order to establish correct topology	-	Status of CBs, switches, reclosers, protection, tap changers	2.2.1.2.3 (partial) 2.3.1.1.1 2.5.1.3.1.1.1.1
2.1.1.1.1.1.1.1	Get status of network control points	*Manual switches?*	-	Status: Open/closed	2.2.1.2.3 (partial) 2.3.1.1.1 2.5.1.3.1.1.1.1.1
2.1.1.1.1.1.1.2	*Get status of open points*	-	-	Status: Open/closed	2.2.1.2.3 (partial) 2.3.1.1.1 2.5.1.3.1.1.1.1.2
2.1.1.1.1.1.1.3	Get status of switches and CBs	-	-	Status: Open/closed	2.2.1.2.3 (partial) 2.3.1.1.1 2.5.1.3.1.1.1.1.3
2.1.1.1.1.1.1.4	*Get status of reclosers*	-	-	Status: Open/closed (timings)	2.2.1.2.3 (partial) 2.3.1.1.1 2.5.1.3.1.1.1.1.4
2.1.1.1.1.1.1.5	Get status of protection relays	-	-	Status: Tripped/not tripped (timings)	2.5.1.3.1.1.1.1.5
2.1.1.1.1.1.1.6	Get status of online tap changer	-	-	Status: Tap positions/ratios Max no. of taps	2.3.1.1.6 2.5.1.3.1.1.1.1.6
2.1.1.1.1.2	Detect protection scheme operation (*Protection*	Current network model must be updated if	Protection scheme status SCADA sweep (depending	Interlock Protection status	

Functionality shared with other requirements

Figure 5 - Table of Functionality used to Establish Common and Shared Functionality

From the defined functionality a detailed description of what is necessary to meet the functional requirements was compiled in the form of a functional specification document. This document is subjected to numerous iterations until the description of the functions and sub-functions are deemed appropriate and achievable.

Therefore, the requirements of an ANM scheme's functionality and hence the attributes of any autonomous PFM approach should have the ability to solve present power flow issues whilst being easily reconfigurable for energy networks of the future. PFM functionality should have the following characteristics, summarised from the structured development process:

- Applicable to any network configuration / topology (network agnostic)
- Abide by commercial contracts / restrictions
- Be able to operate in a safe and secure manner
- Be a flexible and extensible solution

- Inbuilt graceful degradation or a requirement for an alternative
- Have the ability to solve for exploitation in a real-time environment
- Be transparent at control centres
- Be robust when faced with sensor / measurement and model error

The following sections introduce the two candidate PFM approaches and the test environment established to examine each of the approach's ability in meeting the 'Functional Requirements'.

3.2 Optimal Power Flow (OPF)

Optimal Power Flow [3.1][3.2][3.3] is a well established technique used for power system operation and planning problems that can be formulated as an optimisation problem but is used primarily as an off-line planning tool. OPF algorithms are, in essence, generation dispatch algorithms. The algorithms were derived from the earlier optimisation technique of economic dispatch (ED) using the equal incremental cost method (EICM) that minimised the objective cost function with the only equality constraint being that of satisfying the power balance equations. This is achieved by recognising that the cost of generation varies between generators and therefore the incremental or marginal cost of supplying generation to a particular load is different for each generator. The ED process returns the most cost effective combination of generation. OPF took ED a step further, in that, more network constraints were introduced in the form of equality and inequality constraints. Typically, the goal is to minimise system operation costs or maximise social welfare, subject to system operating constraints such as power balance, generation loading limits and network capacity constraints. There are, however, various modifications of the objective function such as minimisation of original control schedule deviation or bilateral contact curtailments [3.4] for which OPF has been formulated. OPF has been investigated for evaluating the maximum connection capacity of renewable DG units [3.5] and as a real-time strategy for minimising load curtailment to remove thermal congestion [3.6] and these are related to the problem tackled in this thesis.

However, those previous applications of OPF do not consider its use in a real-time multiple generator control situation as is the focus of the application described in this thesis

3.2.1 The General Optimal Power Flow (OPF) Formulation

OPF is formulated from control variables and an objective function that is subject to constraints. These constraints, in the form of equality and inequality constraints are used to model the power system's power balance and operating limits criteria. The equality constraints must be enforced and are 'binding' constraints. The inequality constraints may or may not be 'binding', that is to say, a generator might not be operating at its real or reactive limits or a line may or may not be at its MVA limit. The objective function for an OPF is at the heart of the computation and usually involves maximising or minimising a particular attribute or associated cost (or a combination) of the power system and can include:

- Minimising cost
- Minimising control actions
- Minimising network losses
- Maximising revenue
- Maximising DG output

The purpose of the OPF is therefore to assign the power system control variables with values that take into account the equality and inequality constraints that meet the goals (one or more of the above attributes) of the objective function.

Typically, the OPF problem seeks to minimise system operation costs. In vertically integrated system operation costs reflect true costs of operating a unit, while in systems where electricity markets are introduced, minimisation is based on generating unit offers submitted to a centralised market.

In general, the OPF formulation is as follows:

$$\min_{\mathbf{P}_g,\mathbf{Q}_g,\mathbf{V},\delta} \sum_{n=1}^{N} \Omega_{gi}(P_{gi}) \qquad (3.1)$$

Subject to bus constraints:

- Power balance equations

$$P_{gi} - P_{di} = P_i(V,\delta) = \sum_{\substack{j=1 \\ j\neq i}}^{N_{lines}} P_{ij}(V,\delta) \qquad (3.2)$$

$$Q_{gi} - Q_{di} = Q_i(V,\delta) = \sum_{\substack{j=1 \\ j\neq i}}^{N_{lines}} Q_{ij}(V,\delta) \qquad (3.3)$$

} Equality constraints

- Generation limits

$$P_{gi}^{\min} \le P_{gi} \le P_{gi}^{\max} \qquad (3.4)$$

$$Q_{gi}^{\min} \le Q_{gi} \le Q_{gi}^{\max} \qquad (3.5)$$

- Voltage limits

$$V_i^{\min} \le V_i \le V_i^{\max} \qquad (3.6)$$

} Inequality constraints

And subject to line inequality constraints:

- Thermal limits

$$|S_{ij}| \le S_{ij}^{\max} \qquad (3.7)$$

Where at bus i:

$\Omega_{gi}(P_{gi})$	Offer function of a generator at bus i
P_{gi}, Q_{gi}	Active and reactive generation outputs
P_{di}, Q_{di}	Active and reactive system demands
$P_{gi}^{\max}$, $P_{gi}^{\min}$	Generator real power limits
$Q_{gi}^{\max}$, $Q_{gi}^{\min}$	Generator reactive limits

P_{ij} , Q_{ij}	Active and reactive power flows
$V_i^{\max}$, $V_i^{\min}$	Voltage magnitude limits at bus *i*

And at line *i* to *j:*

$S_{ij}^{\max}$	Apparent power thermal limit for a transformer/line $i\ j$.

Under some conditions the voltage and thermal inequality constraints can be enforced as equality constraints. This is desirable if a particular voltage setpoint is required to be met and if it is necessary for a line or transformer to meet a designated level of loading. For the purpose of these studies the thermal constraints will remain as inequality constraints and the voltage constraints will be omitted due to the distributed nature of control being focused on PFM. PowerWorld's OPF solver [3.7], available with version 11 of the software, has the ability to solve the optimal power flow problem as described above and was used in conjunction with the PFM software and hardware. Within the PowerWorld package, the minimum cost objective function is used and is subject to the above equality and inequality constraints, (3.2) – (3.7). The OPF package iterates between the standard ac power flow engine and a primal linear programme that is a fast and efficient tool for ensuring feasible solutions are optimised.

3.3 Constraint Satisfaction Problem (CSP)

In this section the previous research into and the subsequent applications of the Constraint Satisfaction Problem (CSP) are discussed. Tsang, 1993, [3.8] and Apt, 2003, [3.9] have published very comprehensive books on constraint programming (CP) and the Constraint Satisfaction Problem (CSP) which forms the basis of the introduction to CP and CSP within the next section.

3.3.1 Constraint Programming (CP) and the Constraint Satisfaction Problem (CSP)

Constraint Programming (CP) was introduced as a means of applying constraints to the variables of a specific problem initially embedded within the logic programming field. The nature of this declarative programming approach allows a user to define the bounds of a problem in terms of constraints on the variables by describing the 'world' that can be searched for feasible solutions without actually defining the search procedures or process. The solutions are only valid when all the variables have values such that the constraints of the problem are met. CP is used to solve the Constraint Satisfaction Problem (CSP). The CSP has been a well known technique to computer scientists working on artificial intelligence (AI) applications [3.9] and has been applied in many areas including, resource allocation, scheduling, planning and in agriculture.

There are several classes of CSP (Boolean, integer, linear, finite, mixed) and research into CP has led to the development of a growing set of algorithms (backtracker, local search, constraint propagation) for solving these different problems [3.9]. The particular class of CSP discussed in this thesis is a finite discrete domain CSP. The benefit of the CSP is its ability to define a problem whilst placing restrictions on potential solutions. The CSP follows no specific steps or procedures since the properties of a solution are pre-determined i.e. declarative programming. Thus, the goal is specified without giving the route to achieving that goal. Under different applications a CSP might be required to find a single solution, a finite number of solutions or all solutions where the solutions may be ranked optimally against certain criteria or constraints. The size of the search space and the associated computation time to arrive at the required number of solutions to be returned depend on the CSP properties.

There are few examples of its use within the power sector. The interpretation of fault recorder data, which has been modelled as a CSP and then attacked using CP

techniques, is one example from power engineering [3.10] Its use in the thermal unit commitment area, as a means of solving scheduling problems, serves as another example [3.11].

3.3.2 The General Constraint Satisfaction Problem (CSP) Formulation

A CSP comprises of variables, domains and constraints [3.8][3.9]. The variables of a CSP are a set of finite values that can be assigned their values subject to satisfying the criteria specified in their pre-determined associated domains and constraints. The domain of a variable holds the information about what value that particular variable can hold. The constraints of the problem limit the variable values that can be assigned simultaneously. The general problem is therefore defined in terms of the variables (V), domains (D) and constraints (C):

$$(V, D, C) \tag{3.8}$$

Where:
V is the finite set of variable, $V = \{x_{1,}\ x_{2....}\ x_n\}$
D is the domain of variable values, $Dx_1 = \{a, b, c\}$, $Dx_2 = \{d, e\}$, $Dx_n = \{v_1, v_2... v_n\}$
C is the constraint applied to the sets of variables, e.g., C = if $(x_1 = b)$ then $(x_2 \neq d)$

For example, based upon the above variable, domain and constraint declarations, if a variable, x_1, is assigned or labelled with the value a, then a must be within the domain of x_1, Dx_1. If variable x_2, is assigned with value d, then d must be within the domain of x_2, Dx_2. The value 'a' is a member of the set in the domain of x_1 (i.e. $a \in Dx_1$) and 'd' is a member of the set in the domain of x_2 (i.e. $d \in Dx_2$) in the above formulation. Therefore, the simultaneous labelling of x_1 and x_2, i.e. the solution, can be represented as the following compound label:

$$(<x_1, a> <x_2, d>) \tag{3.9}$$

with pre-defined domains, $Dx_1 = \{a, b, c\}$ and $Dx_2 = \{d, e\}$

If the example constraint, C, above, does not allow variable x_2 to hold the value d, when x_1 is b then x_2 can only be e when x_1 is assigned the value b. Therefore, the following constraint function represents this and can be evaluated as either true or false:

$$C = \text{if } (x_1 = b) \text{ then } (x_2 \neq d) \tag{3.10}$$

For the assignment of variable x_1 to value a and variable x_2 to value d, the following compound label is written such that constraint C is satisfied:

$$((<x_1, a> < x_2, d>), (C)) \tag{3.11}$$

The above solution is not the only viable combination of this particular CSP, since constraint C only restricts x_2 being d when x_1 is b. As the constraints limit the values that the variables can hold simultaneously, a permissible set of variables are labelled with values from their associated domains such that the constraints are not violated. The following permutations are also valid, consistent and legal candidate assignments of values to the variables such that the constraint is satisfied:

$$(<x_1, a> <x_2, d>) \quad (<x_1, a> <x_2, e>)$$

$$(<x_1, b> <x_2, e>) \tag{3.12}$$

$$(<x_1, c> <x_2, d>) \qquad (<x_1, c> <x_2, e>)$$

The CSP might be required to find either a single solution, a finite number of solutions or all solutions and may be ranked optimally against certain criteria.

3.3.3 CSP: Search Space Size, Problem Reduction and Searching

The computation time to arrive at the required number of solutions depends on the size of the search space and the methods adopted to reduce and search the space. The following sections discuss these elements.

3.3.3.1 Search Space Size

The initial size of the search space depends on the number of variables and the domain sizes. For the PFM problem this depends on the number of controllable units, i.e. the generators and the number of curtailment bandings for each controllable device. Figure 6 illustrates the extent of the search space for a problem with 3 variables, V = {1, 2, 3}, each with 2 domain values, $D_{1,2\&3}$ = {1, 0}.

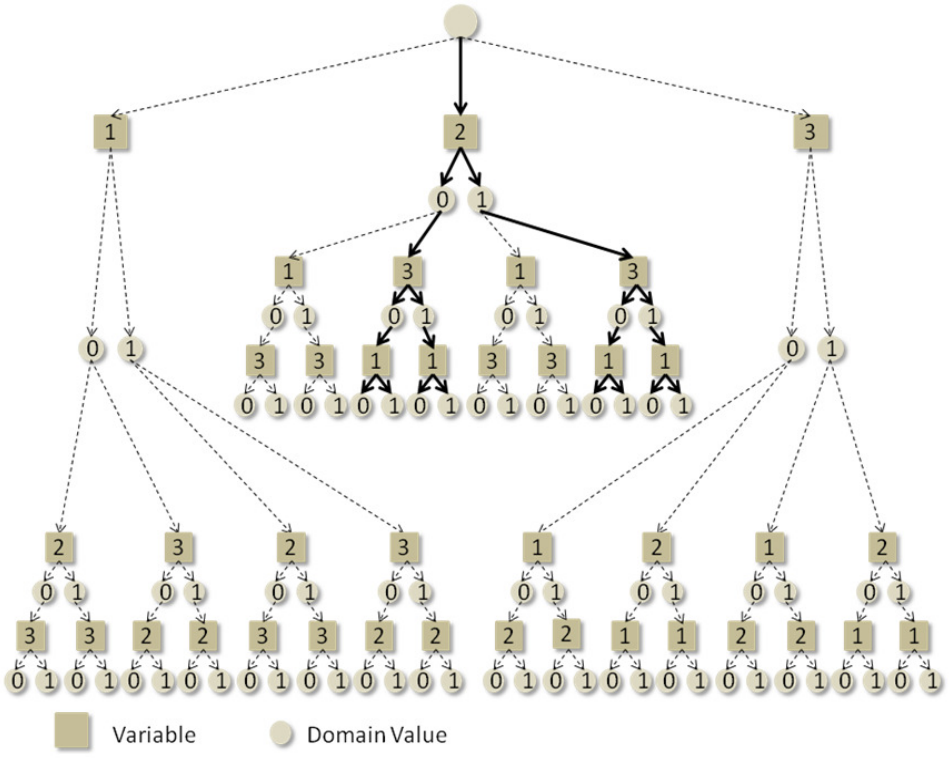

Figure 6 – Example Search Space Showing the Search Branches for a 3 Variable Problem each with 2 Domain Values

The tree of Figure 6 consists of branches and sub-trees, which stem from a root node, that are comprised of internal child nodes (vertices) and leaves. Within the search space there are decision and assignment points at the root node and at each of the child nodes, respectively. In this un-constrained problem from the node of origin there are three branch options to search each leading to a different internal child node or vertex. Each of the branches, in Figure 6, contains the same combinations of the possible solutions however the permutation between state variables in each branch differ. Also, within the sub-tree of each branch there are duplicate solutions due to the possible variable choices that can be made e.g. there are eight possible solutions in the above search space with numerous feasible paths to extracting these possible solutions. The leaves of the search tree are the furthest from the root node and have no child nodes. Therefore, in this search space the leaves of a branch detail the possible variable assignment combinations. The number of solutions, (S_{total}), can be calculated using:

$$S_{total} = |D_{xi}| \times |D_{xj}| \times ...|D_{xn}| \tag{3.13}$$

or approximately by,

$$S_{total} = |D_{Average}|^{n} \tag{3.14}$$

Where '$D_{Average}$' = the average domain size and 'n' = number of problem variables

Figure 7 illustrates the number of possible solutions contained within Figure 6 when the decision to assign variable '2', then variable '3' and finally variable '1' is taken. This search path is highlighted within Figure 6 as solid arrows.

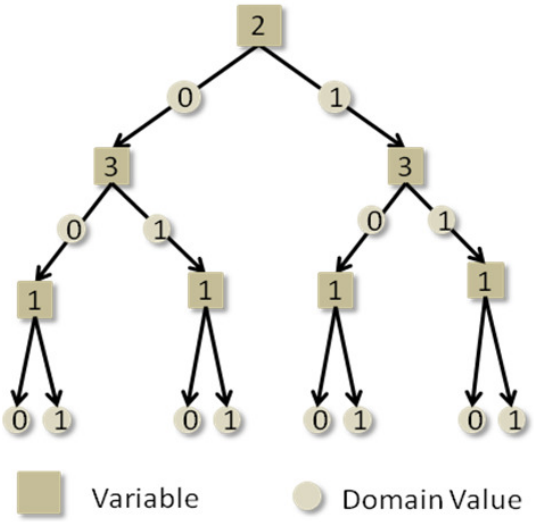

Figure 7 - Number of Solutions based upon the Assumed Ordering of Variables 2, 3 & 1 each with 2 Domain Values

The search space of a CSP has a significant bearing on the computational cost of an algorithm. Ideally, the space should be reduced to the minimal problem, that is, no domain contains redundant values and no constraint contains redundant compound labels. Problem reduction reduces the size of the domains of the variables and therefore reduces or prunes the search space. For any CSP the search space is determined by the number of variables and number of values in their domain.

3.3.3.2 Searching the State Space

Conducting a depth-first search (DFS) requires starting from the root node and selecting a child node to assign a domain value based upon meeting the problem constraints. The space will be searched in a downward direction until all the variables in that path are exhausted and then the next neighbouring child node is selected. Figure 8 illustrates this process. The search direction would move from points ‘a’, ‘b’, ‘c’, ‘d’, ‘e’, ‘f’ and ‘g’.

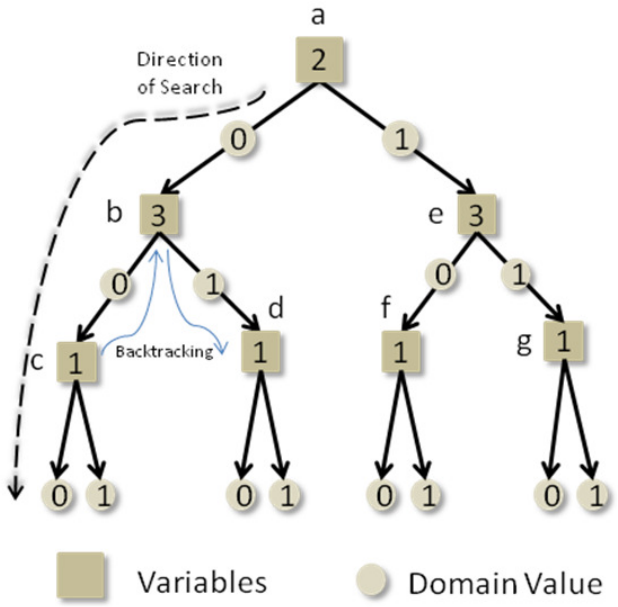

Figure 8 – Illustration of a Depth-First Search with a Backtracking Algorithm in Operation

The use of a backtracking algorithm allows the solver to climb back up the tree should it discover that the domain value assignment to a variable is not permissible. This method allows the solver to return to the last known state that meets the constraints and process the other possible assignments in the search for a solution. Searching for solutions can use the basic backtracking method which takes one variable at time and assigns it a domain value. If the chosen labelled variable (a variable with a domain value assigned) violates a constraint the next available domain value is chosen until all the variables have been assigned values and the problem is solved, with however many solutions that were feasible. If there are no domain variables available then a backtrack operation is performed to the label that was last (the one that previously satisfied all the constraints) and a new domain value is allocated. The next variable is re-assigned its domain value and re-evaluated against the constraints. This procedure continues until all the solutions are found or all possibilities have been exhausted and the CSP deemed insolvable.

Consideration is required when deciding on the quantity of constraints to be considered as too many constraints results in a heavy computational penalty when

carrying out compatibility checks. On the other hand, constraints can be advantageous in pruning the search space.

3.3.3.3 Pruning the Search Space

The ordering of variables halves the depth of the search space. The depth of the space in Figure 6, where no variable ordering took place, is exactly twice the number of variables, i.e. 6. If the variables were to be ordered, say V= {2, 3, 1}, then the depth of the search space becomes 3 (depth = number of variables, when ordering is carried out) due to the decision process (e.g. 'choose 1' or 'choose 2') being removed from the procedure. Figure 9 represents the direct acyclic graph for the ordering of Variables, V= {2, 3, 1}.

Propagation of constraints through the search space enables all the impermissible assignments to be removed from the state space prior to the search commencing. In Figure 9, it was assumed that when 'variable 3' is labelled with the value '0' then 'variable 1' is not permitted to be '1'. Therefore, constraint propagation prior to compound labelling ensures that time is not spent evaluating solutions that would never meet the problem's constraints. Out of the eight possible solutions two can be eliminated immediately. Reduction of the problem that results in no search space signifies that the problem is insolvable.

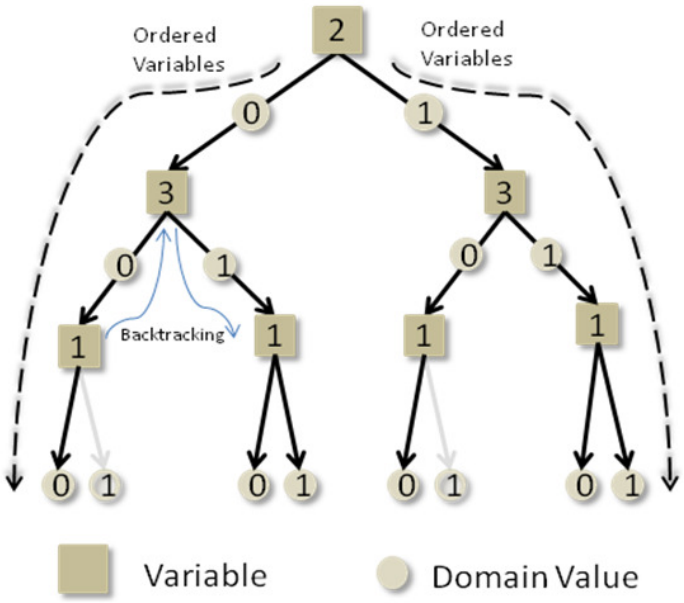

Figure 9 - Illustration of a Depth-First Search with a Backtracking Algorithm in Operation and Pruning of the Space through Constraint Propagation

From the above example it can be observed that the constraints play no role in the physical size of the search space however they do affect the search space that is required to be explored and evaluated. Figure 10 illustrates the general principle of the trade-off between the computational effort required to search the entire space and the amount of effort put into reducing the problem.

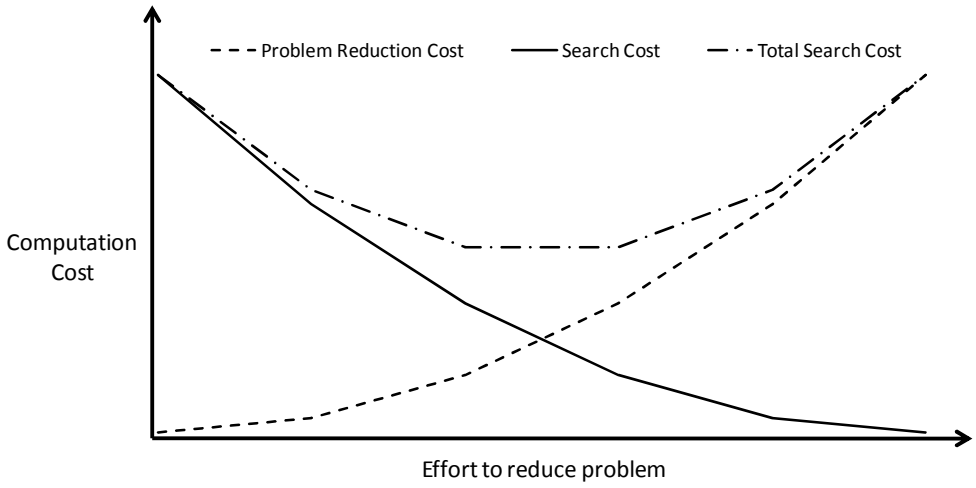

Figure 10 – Illustration of the General Principle of the Trade-Off between Total Computational Cost and Problem Reduction Costs [3.8]

3.4 The Steady-State Test Environment

To evaluate the real-time performance of the developed PFM algorithms an appropriate steady-state test platform was built up. Test scenarios implemented via the steady-state test environment enable the computation time and levels of DG curtailment to be measured for each of the candidate PFM techniques for different network topologies and presumed LIFO arrangements. Furthermore, the robustness of the algorithms when presented with model error through measurement and sensor errors can be examined. The communication standards for device connectivity are described for the simulation environment in terms of their particular ability to flag communication failures and unexpected data. The elements of the real-time test environment are described below.

3.4.1 Substation Computing Hardware

The available substation computing hardware used for the development and testing was ABB's COM6xx series substation automation product, Figure 11. The COM6xx is a Windows XP Embedded industrial computer that offers a powerful substation computing platform that ANM schemes and control functionality can be deployed on. It is robust in the sense that it has no moving parts and its design includes functionality that uses OPC and translates between IEC 61850 and other legacy communication protocols.

Figure 11 - ABB's COM6xx Series Substation Automation Computer

Therefore, the COM6xx offers itself as a gateway for mapping monitoring, control and protection signals from remote devices, the intelligent electronic devices (IEDs e.g. generators, transformers, protection relays), into the substation as long as the protocol used is supported by the COM6xx. A full description of ABB's COM6xx series hardware can be found at [3.12]. Figure 12, shows the architecture of the differing protocols combined on a COM6xx unit cross referenced and re-modelled by the IEC 61850 data model. The subsequent sub-sections describe OPC and the IEC 61850 standard.

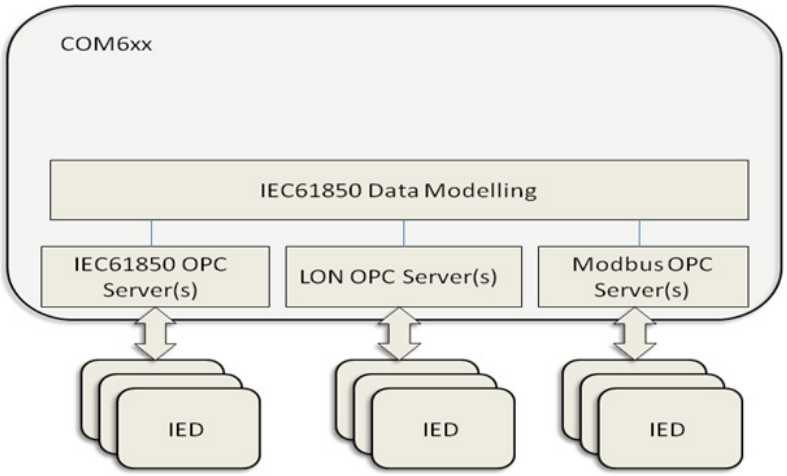

Figure 12 – Example of the COM6xx's OPC Servers using IEC61850 Cross Referencing for Legacy Protocols

3.4.1.1 OPen Connectivity / Object Linking and Embedding for Process Control (OPC)

OPC was developed in conjunction with Microsoft and automation manufacturers/suppliers to overcome interoperability issues with process control hardware. The development of a common interface to the hardware was necessary to ensure processes were conducted in an efficient and regulated manner and remove the labour intensive need for proprietary communication drivers developed by vendors. The OPC Foundation, formed in 1994 [3.13], maintains the seven current

non-proprietary open standards specifications, that are either completed or being created, and is a widely accepted set of industrial standards. The first and most common specification, released in 1996, is OPC Data Access (OPC DA) which defines the interface requirements for the client/server connection. OPC DA essentially allows for the reading and writing of data among PLCs, PACs, RTUs and desktop software in real-time on either local or remote networks. Each OPC item (the address of the data not the physical device) has a value, quality and time-stamp attribute. This standard therefore provides the necessary connectivity to devices in the field and is used to collate data within the real-time test environment.

OPC allows some degree of certainty to be attained for the measurements collected. A 'value', 'quality of value' and 'timestamp' element is associated to each measurement. The 'quality of value' enables a value to be flagged as 'good', 'uncertain' or 'bad' and is assigned values to an 8-bit binary identifying the quality, sub-status and limits in the form, 'QQSSSSLL'. The first two bits 'QQ' gives the quality 'string' (e.g. 00 = 'bad', 01 = 'uncertain' & 11 = 'good'). The next 4-bits, 'SSSS' return the reason for the 'quality' label (e.g. if the quality was 'bad' and the next 4-bits read '0110' then this indicates that the reason for the 'bad' assignment is due to loss of communications to the device). Other OPC sub status ('SSSS') field codes enable 'Device Failure', 'Configuration Error' and 'Sensor Error' to be identified. The last 2-bits detail whether an upper or lower limit has been hit or whether a constant value has unexpectedly changed and can therefore be used for diagnostics. Thus the use of the OPC standard, for device connectivity, enables loss of communications, lack of measurements or unexpected measurements to be detected and postpone the service of the power flow management algorithms until such time all data is 'flagged as good'.

3.4.1.2 IEC 61850 – Communications Network and Systems in Sub-Stations

There are numerous substation automation communication protocols with differing semantics and this poses a significant problem to the interoperability of automation

devices supplied by different manufacturers. Many of these protocols are proprietary and the International Electrotechnical Commission (IEC) recognised the barrier presented by this and created the IEC 61850 standard as a single protocol for substation automation design. The standard differs from previous substation automation standards in that it has been developed, over the last decade, in such a way as to be flexible and future proof [3.14].

3.4.2 Power Flow Management (PFM) Software and Power Systems Simulator

The Power Flow Management (PFM) software and a power systems simulator package are embedded within the COM6xx platform. The power system simulator package is used to ensure that a representative network model is maintained through updated data transfer from field IEDs. The load flow engine is called each time the complete set of data is received. The PFM software monitors and evaluates the line and plant MVA flows to identify thermal constraints and operates, for the purpose of the simulations, in a three second loop. When thermal excursions are identified the PFM solver is called to return DG curtailment solutions (from either the CSP solver [3.15] or the OPF solver [3.7]). The control solutions are then sent to corresponding DG unit's IED to carry out the instruction. This process is further explained in Chapters 4 and 5.

Figure 13, represents a software overview of the COM6xx with the detection and control functionality incorporated and connected to IEDs in the field. It also highlights the modular approach utilised and the extensible trait of enabling functions to be easily replaced or updated.

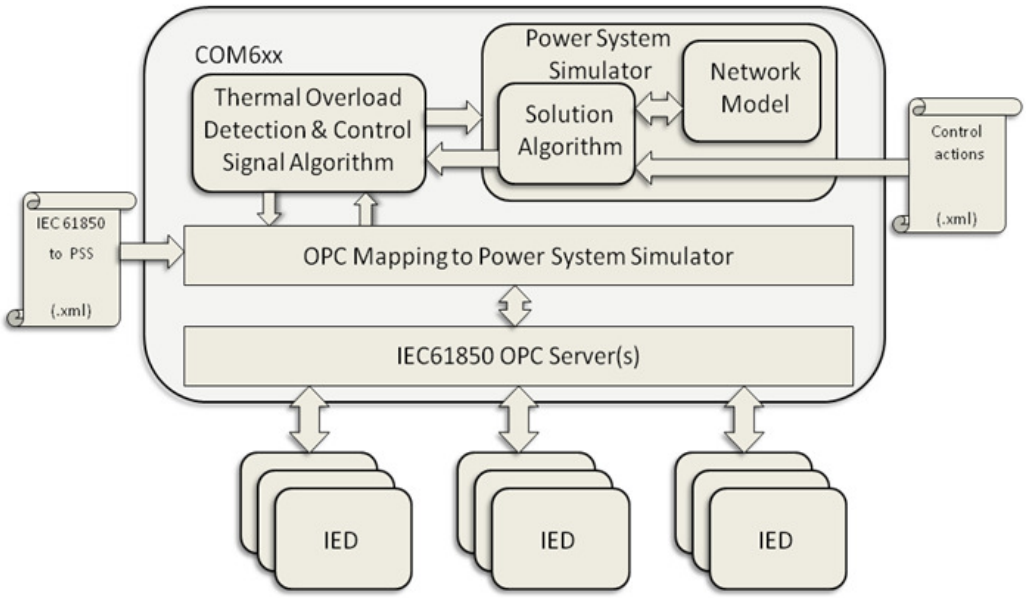

Figure 13 – Illustration of the COM6xx with Control Software Embedded, the External Inputs and Connected IEDs

To ensure that the ANM scheme is flexible external (.xml) files are used to enable the system to be easily reconfigured in the event that new DG connections are made or DG connections are removed from the network. The purpose of the xml files are to define DG limits, their connection order and map the power system simulator representation to the IED.

3.4.3 Sequential Steady-State Simulator

A means of emulating the data transfer from network Intelligent Electronic Devices (IEDs) to the COM600 substation platform was developed to provide a test platform for closed-loop control testing. The sequential steady-state simulator software runs on a dedicated PC and calls upon data files that hold load and generation profiles (.csv files). These profiles are used to represent the system steady-state conditions over a time period. The simulator uses IEC 61850 and OPC to interface with one or more COM6xx units. This emulates measurements that would be provided by IEDs in the field and also provide a simulated response to the control signals issued by the COM6xx.

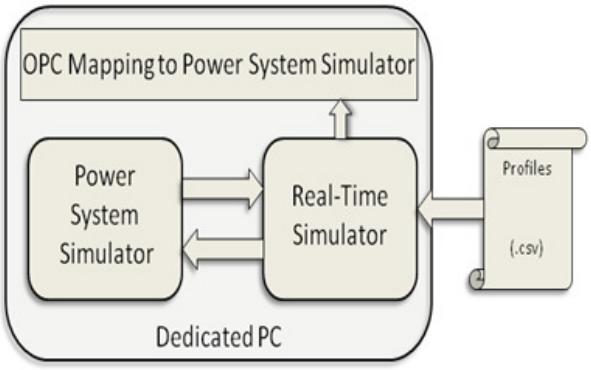

Figure 14 – Illustration of the Sequential Steady State Simulator with Generation and Load Profile Inputs

Within the steady-state simulator are embedded controller functions that simulate network control responses and include: tap-changers; circuit breakers; real power set-point control responses; and power factor set-point control responses. For the purpose of this investigation only the circuit-breaker, real power set-point control and DG trim/trip controls were utilised. This allows topological changes by setting the status of circuit breakers to enable 'normal' and 'n-1' conditions to be evaluated in terms of the post-analysis response of the DG units reacting to a real power control signal that includes DG unit ramp rates. The steady-state simulator accepts data from the csv files and updates the network model embedded within the COM6xx once a second. Figure 15 depicts the functional overview of the COM6xx test environment platform and the steady-state simulator.

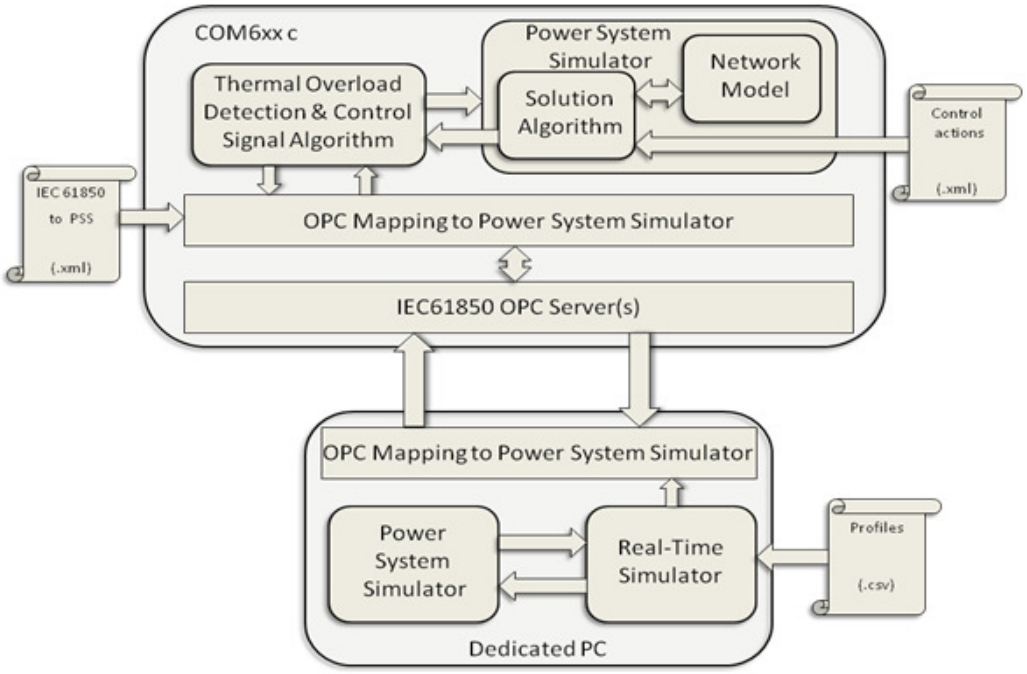

Figure 15 – Illustration of the Sequential Steady State Simulator Connected to the COM6XX Substation Computing Platform

The system and computer specifications for the COM6xx and the dedicated PC used for the sequential steady state simulator are presented in Table 1.

Table 1 - COM6xx and Dedicated PC Specifications

Platform	System	Computer
COM600	Microsoft Windows XP Embedded, Version 2002, SP2	Intel(R) Pentium(R) M Processor 1600MHz. 1.6GHz, 992MB of RAM
Dedicated PC	Microsoft Windows XP Professional, Version 2002, SP2	Intel(R) Pentium(R) 4 CPU 3.00GHz 2.99GHz, 504MB of RAM.

3.5 Case Study Networks

In order to meet the requirement of being a network agnostic solution two actual and disparate networks were chosen. These contrasting networks offer different DG penetration levels connected at various voltage levels and hence have dissimilar network topologies and technical attributes. The real 11kV radial and 33kV

interconnected medium voltage distribution networks are described in the following sections.

3.5.1 11kV Radial Distribution Network

The first case study network is a section of standard 11kV radial distribution network with two DGs connected to one feeder, shown in Figure 16.

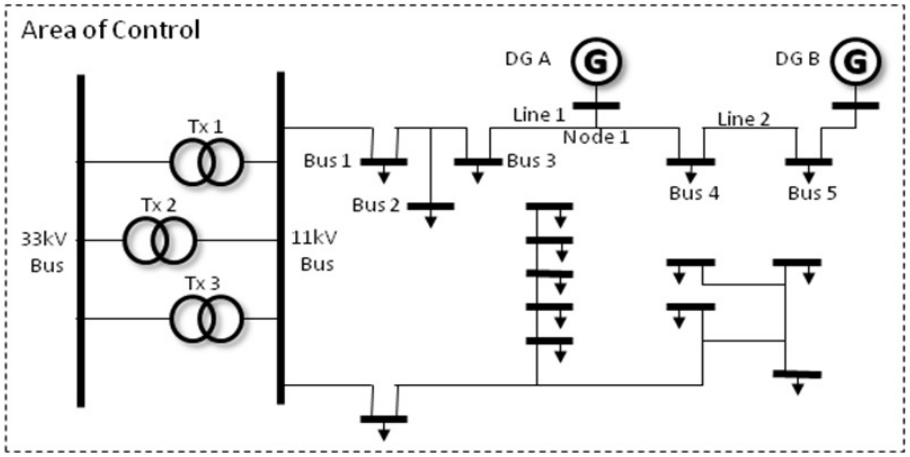

Figure 16 - 11kV Radial Distribution Case Study Network

Common practice in planning LV networks entailed tapered feeders that met the feeder load, voltage and prospective fault current constraints with strategically placed open points to achieve necessary levels of network security. This limits the potential connection capacity on 11kV feeders. Table 2 tabulates the connected DG capacity of this case study.

Table 2 – DG Unit Capacity Connected to the 11kV Network

DG Unit	MW Capacity
DG A	1.6
DG B	2
Generation Total	3.6

The DG units are connected, via single circuit connections, to the 11kV feeder. Traditional inter-tripping schemes would be in place for each of the unit's associated circuit breaker. Circuit breaker trip operations would be enforced during any abnormal event that results in voltage or thermal excursions arising on the connected feeder. Although in the radial distribution network case the constraint management schemes will be fewer. The available measurement points are also fewer due to the expense in deploying equipment at LV levels. It is therefore assumed for the purpose of this thesis that all necessary measurements are available, in the first instance, to evaluate the performance of the PFM algorithms.

3.5.1.1 11kV Network Profiles

Pre-simulation power flow analysis was carried out on the 11kV network to identify scenarios that would ensure thermal constraints arose on a particular cable section of the feeder with the DG units connected. Profiles were developed, based on the analysis, that would ensure thermal violations occur. Figure 17 depicts the DG units' outputs. DG A was assumed to have a constant output value of 1.6MW while DG B's output was varied to represent a small wind farm.

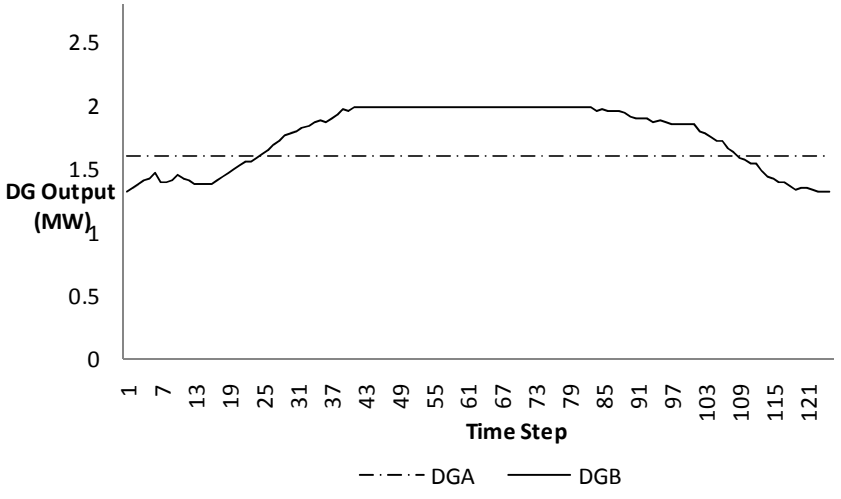

Figure 17 - 11kV Network: DG Input Profile for the Sequential Steady State Simulator

In addition to the DG unit profiles the load at ‘Bus 5’ was varied thus allowing the thermal limits to be manipulated to allow an excursion on either ‘Line 1’ or 'Line 2’. The load profile at ‘Bus 5’ is shown in Figure 18 and depicts a ‘perfect’ measurements case scenario.

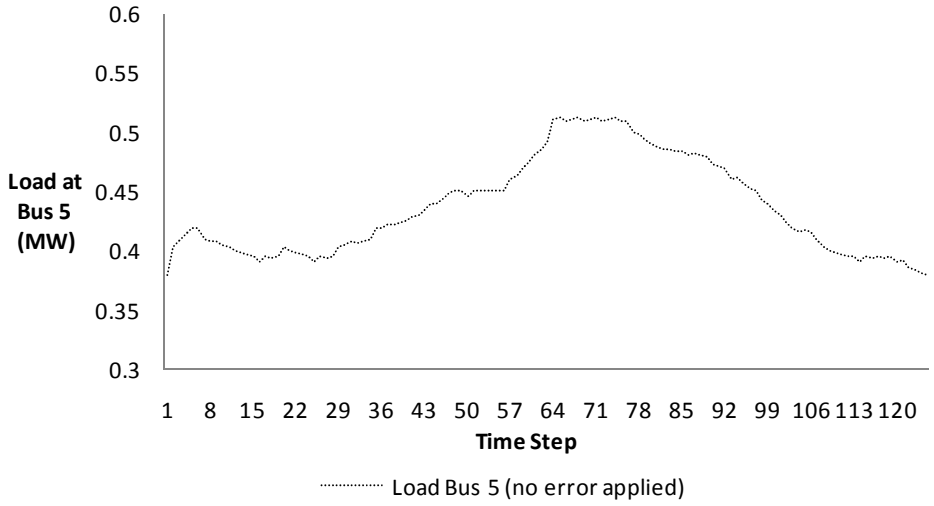

Figure 18 - 11kV Network: 'Bus 5' Loading, with No Error, Input Profile for the Sequential Steady State Simulator

To enable the evaluation of the control algorithms when presented with erroneous data the profile of Figure 18 was applied with a 1% randomised error. This profile is shown in Figure 19.

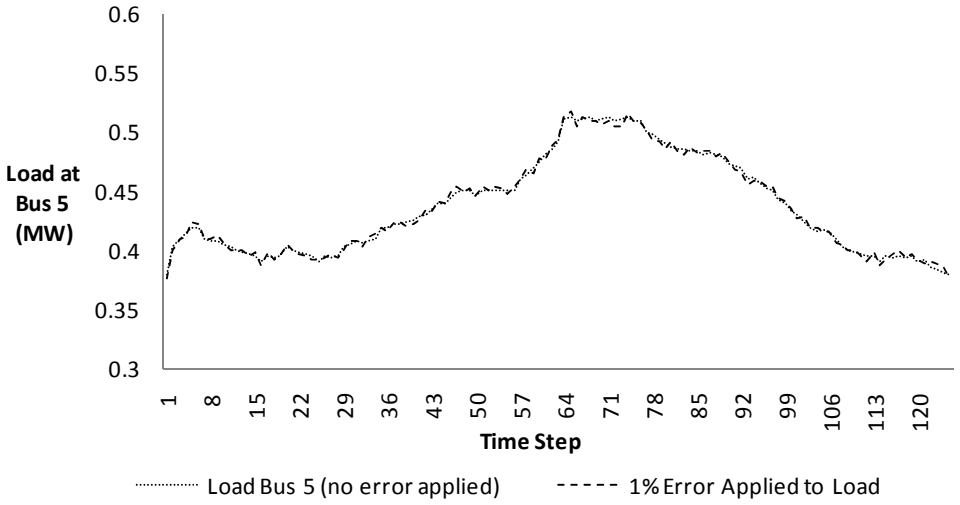

Figure 19 - 11kV Network: 'Bus 5' Loading, with 1% Error, Input Profile for the Sequential Steady State Simulator

Figure 20 shows the load profile with an exacerbated error of 6% applied. The 6% error applied is scaled up from that of the 1% error case.

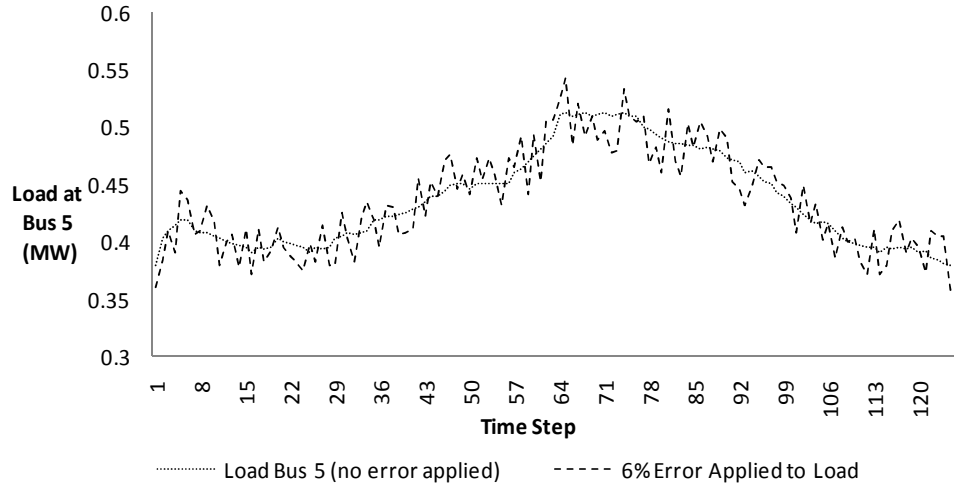

Figure 20 - 11kV Network: 'Bus 5' Loading, with 6% Error, Input Profile for the Sequential Steady State Simulator

The above profiles are the input csv files for the steady-state test environment of Figure 15.

3.5.2 33kV Interconnected Distribution Network

The second of the case study network is the 33kV interconnected network depicted in Figure 21. This network is supplied via two 132kV circuits from 'Substation X'. These terminate into two 45MVA 132/33-kV transformers at 'Substation A' and 'Substation B'. These two substations operate as an interconnected group at 33-kV via 3 circuits. A further two 33kV circuits radiate northerly to supply loads and generation to the north and these circuits have normally open points midway along their lengths at 'Substation E' and 'Substation B'.

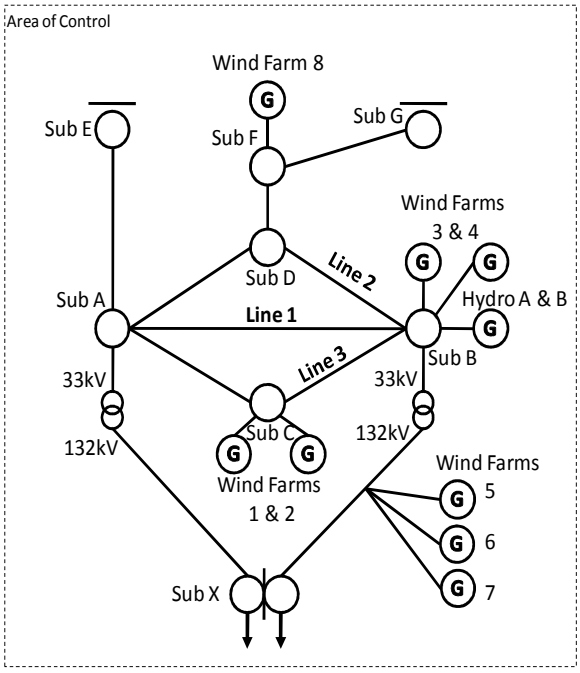

Figure 21 - 33kV Interconnected Case Study Distribution Network

This network has eight connected generator units. Table 2 shows the MW rated capacity of the connected generator units. The generation potential for this case exceeds that of a standard planning connection policy [3.16] i.e. local generation should equal the networks export capacity plus minimum local load.

Table 3 – DG Capacity Connected to the 33kV Network

DG Unit	MW Capacity
DG 1	5
DG 2	4.35
DG 3	2.4
DG 4	2
DG 5	23.5
DG 6	23.5
DG 7	12
DG 8	10.2
Generation Total	82.95

3.5.2.1 33kV Network Profiles

Pre-simulation power flow analysis was also carried out on the 33kV network to identify scenarios that would ensure thermal constraints arose on a particular line. For the 33kV case study, Figure 21, the profiles developed held all generation at a constant level equal to the maximum rated DG outputs, $P_{gi}^{\max}$ (Table 3), with the exception of unit DG 5. By increasing the load at 'Sub A' and the varying output of DG 5 it is possible to create a scenario that contributed to an overload on 'Line 1'. DG 5 output and the load at 'Sub A' is shown in Figure 22, where the DG unit's MW output is shown on the primary vertical axis and the loading of 'Sub A' shown on the secondary vertical axis.

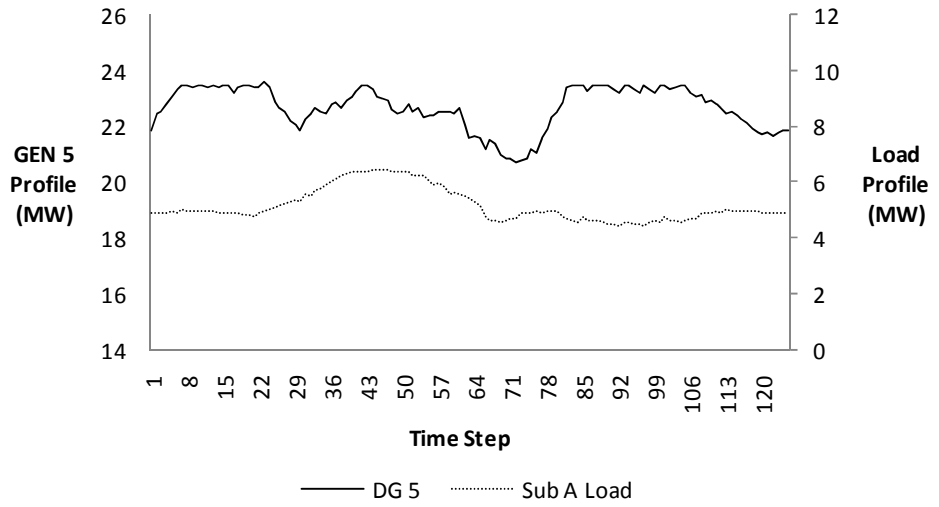

Figure 22 - 33kV Network: DG 5 and Sub A Input Profiles for the Sequential Steady State Simulator

The above load and DG 5 profiles are used as the csv input files for the steady-state test environment (Figure 15). The remaining DG units and network loads are held constant within the csv files.

3.6 Chapter 3 Review

This chapter has introduced the general properties of the OPF and CSP techniques that will be used within the next two chapters to model the PFM problem. A detailed description of the real-time test environment that will allow test scenarios to be comprehensively evaluated has been introduced along with the case study networks and the associated load and generation profiles for each of them.

The modular approach to the proposed ANM schemes offers extensibility in the sense that new or updated functions can be easily integrated into the system software. In terms of flexibility the input files can be viewed as easily reconfigurable in terms of adding or removing controllable devices as well as offering the ability to change the contractual priority order.

3.7 Chapter 3 References

[3.1] J. Carpentier, “Optimal power flow”, International Journal of Electrical Power and Energy Systems 1, pp. 3–15, 1979

[3.2] J. Carpentier, “Contribution a l'Etude du Dispatching Economique”. Bulletin de la Society Francaise des Electricien 8 3, pp. 431–447, 1962

[3.3] H. Dommel and W.F. Tinney, “Optimal power flow solutions”. IEEE Transactions on Power Apparatus and Systems PAS-87, pp. 1866–1876, 1968

[3.4] I. Kockar ,F.D. Galiana, "Combined Pool/Bilateral Dispatch - Part 2: Curtailment of Firm and Non-Firm Contracts", IEEE Transactions on Power Systems, vol. 17, no. 4, pp. 1184 – 1190, November 2002

[3.5] L. F. Ochoa, C. J. Dent, and G. P. Harrison, “Distribution Network Capacity Assessment: Variable DG and Active Networks”. IEEE Transactions on Power Systems, VOL. 25, NO. 1, pp. 87 – 95, February 2010

[3.6] F. Capitanescu, L. Wehenkel, “Optimal Power Flow Computations with a Limited Number of Controls Allowed to Move”. IEEE Transactions on Power Systems, VOL. 25, NO. 1, pp. 586 – 587, February 2010

[3.7] PowerWorld Corporation, “PowerWorld Simulator version 11 Manual”, available at http://www.powerworld.com/Document%20Library/pw110UserGuide.pdf, accessed 6th May 2012

[3.8] E.P.K. Tsang, “Foundations of Constraint Satisfaction”, Academic Press, London and San Diego, 1993

[3.9] K. R. Apt., “Principles of Constraint Programming”, Cambridge University Press, 2003

[3.10] M. Chantler, P. Pogliano, A. Aldea, G. Tornielli, T. Wyatt, A. Jolley. “Use of fault-recorder data for diagnosing timing and other related faults in Electricity Transmission Networks” IEEE Trans. on Power Systems, Vol. 15, No. 4, pp. 1388-1393, November 2000

[3.11] Kun-Yuan Huang Hong-Tzcr Yang, Ching-Lien Huang, A New Thermal Unit Commitment Approach Using Constraint Logic Programming, IEEE Transactions on Power Systems, Vol. 13, No. 3, pp. 936-945, August 1998

[3.12] ABB Product Website: http://www.abb.com/Product/seitp328/3cc7d0b2a99f2f40c1257188002facd2.aspx?productLanguage=us&country=00, accessed on 03/08/2011

[3.13] OPC Foundation: Available at https://www.opcfoundation.org/Default.aspx, accessed on 03/08/2011

[3.14] M. Adamiak , D. Baigent (GE Digital Energy), R. Mackiewicz (SISCO), “IEC 61850 Communication Networks and Systems In Substations: An Overview for Users”, 2009. Available at: http://www.gedigitalenergy.com/multilin/journals/issues/Spring09/IEC61850.pdf, accessed on 03/08/2011

[3.15] Gustavo Niemeyer , “Python Constraint”, available at: http://niemeyer.net/python-constraint, accessed 03/08/2011

[3.16] Energy Networks Association (2004); “Guidelines for Actively Managing Power Flows associated with the Connection of a Single Distributed Generation Plant”, Working draft: Engineering Technical Report 124 (ver-005), February 2004

Chapter 4

Power Flow Management with Optimal Power Flow

4.1 Summary of Chapter 4

Within this chapter the first approach to active power flow management (PFM) using Optimal Power Flow (OPF) is discussed in terms of modelling the PFM problem as an OPF formulation. The practical implementation issues of dealing with the last in first off (LIFO) contractual arrangements and generator set-points for intermittent sources of generation are discussed within the presentation of the problem formulation. Utilising the steady-state test environment, case study networks and profiles, introduced in Chapter 3, results from the OPF approach to PFM are documented in terms of the number of control signals issued to DG units and the computation timescales. The scenario to which the technique is applied is introduced prior to the presentation of the results. These results are summarised in the chapter conclusion with regards to performance within a real-time control environment.

4.2 Developing Optimal Power Flow (OPF) as a Technique for Power Flow Management (PFM) in Distribution Systems

The general OPF formulation defined by (3.1) – (3.7), in Chapter 3, is typically used for operation of high voltage transmission systems with larger generating units. This is a complex problem with a large number of decision variables. The system operator has a set of well established rules and ancillary service arrangements to help maintain secure system operation. These rules are reflected in the OPF formulation. With increasing numbers of DG at distribution level and multiple, bespoke and overlying constraint management schemes, OPF offers a possible consolidating solution to managing multiple DG units due to being able to handle large numbers of decision variables. However, management of non-conventional intermittent plant at distribution level brings about some fundamentally different problems and restrictions as discussed within the next sections.

As discussed previously, significant increases in the connection of DG on distribution networks are expected bringing an inherent increase in bi-directional power flow magnitudes. Since the distribution networks were not designed to operate with DG, this can lead towards a more uncertain and congested situation than previously. This, therefore, requires novel network management solutions to facilitate increased DG connections. As such, DG developments at distribution levels are relatively recent and thus the role of the DG in distribution network operations is less defined than it is for the generating units in the transmission system. As a result, the effect of DG units on the networks calls for operational techniques that will better reflect these uncertainties and bi-directional flows.

The aim of the OPF-LIFO approach for PFM proposed in this thesis is to offer a solution that will help better operate such distribution networks. Since LIFO arrangements are currently applied by the UK DNO, the proposed method seeks to closely follow this LIFO access principle for the majority of operating conditions. However, it will deviate from LIFO only to avoid disconnecting or curtailing an unnecessary level of generator outputs. In that way the application of OPF-LIFO will allow for better utilisation of DG resources and network infrastructure.

The proposed OPF-LIFO method is based on the general OPF formulation (3.1) – (3.7) in Chapter 3, with the only change being in the definition and formulation of the individual generation cost terms, $\Omega_{gi}(P_{gi})$, in the objective function (3.1) and the omission of the voltage constraint (3.6). While in the general OPF formulation these terms, $\Omega_{gi}(P_{gi})$, reflect either true costs associated with the electricity production, or the offer curves that generators submit when selling energy on the market, in the OPF-LIFO formulation $\Omega_{gi}(P_{gi})$ terms reflect the order of the generators' connections. Thus, each generator is assigned a constant cost function defined as:

$$\Omega_{gi}(P_{gi}) = \pi_{gi} P_{gi} \tag{4.1}$$

Where, π_{gi} is a constant allocated to each generating unit to reflect its connection order. This means that in order to prioritise the utilisation of generators that were connected first, they will be assigned the lower value of π_{gi}, while those connected last will be assigned the highest values. Note that the constant π_{gi} in (4.1) does not reflect actual generation costs (or offers), but, as mentioned above, is rather used to indicate a connection order which would be considered for resolving any network constraint.

Such modification of generation costs means that the solution of the defined OPF will seek to maintain LIFO arrangements as long as such an approach is curtailing generators that can relieve the congestion. However, if the curtailment of the particular generator does not address line overloads, the proposed OPF-LIFO will leave the output of this generator unmodified. Thus, by curtailing outputs of only generators that actually affect the congestion, the OPF-LIFO approach can help in increasing the level of renewable generation outputs while seeking to maintain LIFO rights.

In the case when deviation from the LIFO rule gives a solution that enforces less overall DG curtailment, the OPF-LIFO formulation will automatically yield the improved generation dispatch. This means that the developed OPF-LIFO formulation may help DNOs automatically decide in which situations it would be beneficial for the overall system performance to forfeit LIFO arrangements.

Furthermore, as in the case of other ANM schemes, in the proposed OPF approach a specific area of the distribution system is controlled with one or more interface points to the rest of the network. This means that when the generation output from all of the DGs is greater than the demand in the given area, the surplus power is exported into the rest of the network through the interfacing nodes. Similarly, if the DG output is not suffice to supply the area demand, power balance will be maintained by importing necessary power through the interfacing nodes. In order to account for both cases, any such nodes are modelled as a generator bus that can have both a positive and negative generation output. In addition, each of these outputs will have

its separate values of parameters π_{gi}, however the value assigned to the latter would be lower in order to maximise DG outputs and encourage export into the other part of the network. This cost allocation is representative of the negative generation bus being the first historically connected generator and maintains the LIFO regime of the connected DG units. In fact, one of the aims of the DG installation is to reduce energy input from the grid, and here proposed OPF-LIFO is seeking to minimise this import or maximise the export. This is in the interest of all of the DG units in that area, but financial gains could be allocated to cover the possible losses of some generators. These additional financial arrangements, however, are not the subject of this thesis because they will not affect the results of this real-time application of OPF. The formulation of the OPF-LIFO presented in this section is general. However, due to the modular nature of the ANM scheme that was influenced by the practical aspects of the DNOs' operation strategies, OPF-LIFO application was intended only for relieving congestion due to thermal line limits. Therefore, the above formulation can omit voltage constraints (3.6) as they will be managed through another module specifically designed for the voltage control [4.1][4.1]. This simplification enables application of the commercially available PowerWorld (version 11) tool [4.2] which is included into the steady state test platform, as discussed in the subsequent sections.

4.2.1 Practical Considerations for Implementing Optimal Power Flow (OPF) as a Power Flow Management (PFM) Scheme

Traditionally, OPF has been used for generation dispatch where a calculated operating point can be allocated and achieved by conventional, larger scale generators. The intermittent nature of renewable DG units introduces problems in defining and allocating power output set-points. In a congested network it is straightforward to calculate a curtailment level for a generating unit assuming that generator output measurements would be available.

Under congested operation the proposed constraint detection algorithm identifies any congested circuits violating the condition $|S_{ij}| \leq S_{ij}^{max}$. The generator cost models are then sent to the OPF engine which returns generator outputs ($P_{gi}^{OPFCalculated}$) based upon the solved OPF. When curtailing generation that is operating in an unconstrained manner, the machine's rated power output variable (P_{gi}^{max}) is set to the actual generator's power output (P_{gi}) to ensure that the calculated output set point value ($P_{gi}^{OPFCalculated}$) is not higher than what the generator can supply. $P_{gi}^{OPFCalculated}$, together with the generator's actual rated output value (P_{gi}^{max}), are passed to the algorithm to calculate the generator control signals (CS_{gi}). These curtailment factors are sent to the corresponding generator units, pictured in Figure 23, as a proportion of its rated output:

$$CS_{gi} = P_{gi}^{OPFCalculated} \div P_{gi}^{Max} \tag{4.2}$$

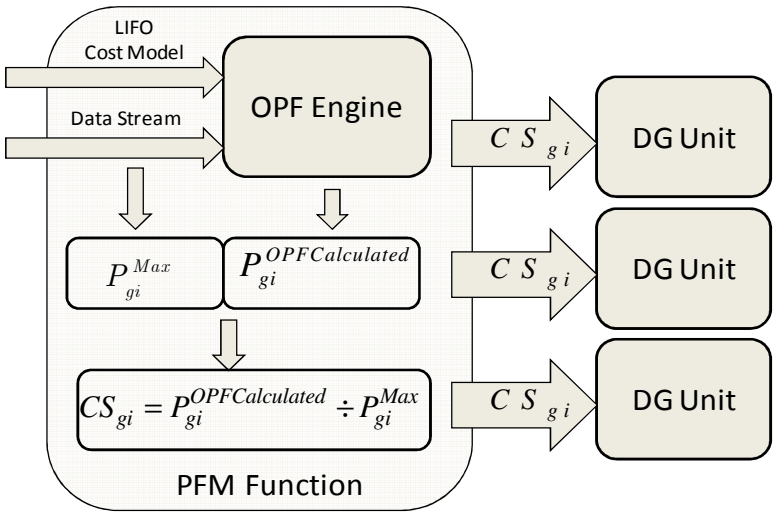

Figure 23 – Illustration of the Inputs, Computation and Issue of Individual Control Signals to DG Units

Restoring the permissible generation output defined by the current network limits and after the curtailment signal has been sent is, however, more problematic. This is

due to the fact that potential unconstrained outputs, defined by availability of the primary renewable resources (i.e. wind, waves, etc.), is unlikely to be known by the control scheme. The difficulty is in how to recognise when a constraint has passed and the curtailment of the DG unit can be relaxed. This is because it cannot be known what level of output the DG unit will achieve once curtailment is released. If the primary renewable resource is not known then DG units can only output what is available and not what the OPF solution requests or permits.

To overcome this issue a condition was formulated that identified whether an output curtailment could be relaxed or removed from the constrained generators. Without knowing the potential output of the renewable DG units the value of the curtailed generator's maximum rated output ($P_{gi}^{\max}$) must be used to obtain the level of relaxation with the variation in network loading. Therefore, when a DG unit is subjected to a curtailment command, the DG unit's rated output variable ($P_{gi}^{\max}$) is set to the actual rated output of the machine. This is in contrast to the case when a DG unit is operating unconstrained, where $P_{gi}^{\max}$ is set to the generator's prevailing output (P_{gi}), discussed above. A comparison of the new result ($P_{gi}^{OPFCalculated}$) with the current curtailment signal determines whether an updated control signal (CS_{gi}), either releasing or further curtailing output, can be sent to the corresponding generators as defined in (4.2). In reality, this level of output may not be attainable by a renewable DG unit since the achievable output might be less than $P_{gi}^{OPFCalculated}$, as discussed above. However, in order to maintain the system within thermal limits the generator output cannot exceed $P_{gi}^{OPFCalculated}$ i.e. generation output is capped. In the case where $P_{gi}^{OPFCalculated} = P_{gi}^{\max}$, the control signal (equal to 1) informs the DG unit that it can run unconstrained at whatever level of generation resources permit as defined by (4.2).

4.2.2 Analysis and Results of the OPF-LIFO Technique

To achieve network management with the OPF-LIFO approach, a new algorithm was developed. The algorithm identifies thermal constraint violations, updates DG cost models and calls upon the OPF engine to solve the congestion constraint whilst following connection and operating constraints. The outputs from running the OPF-LIFO algorithm are the control signals for the corresponding generating units i.e. updated set points. The PowerWorld power systems analysis software package provided the functionality to solve the OPF problem defined previously. The additional software provides the algorithms for congestion detection, cost models representing LIFO and the control signal processing. The attributes of the OPF-LIFO approach was embedded within the real-time test environment, illustrated in Figure 24.

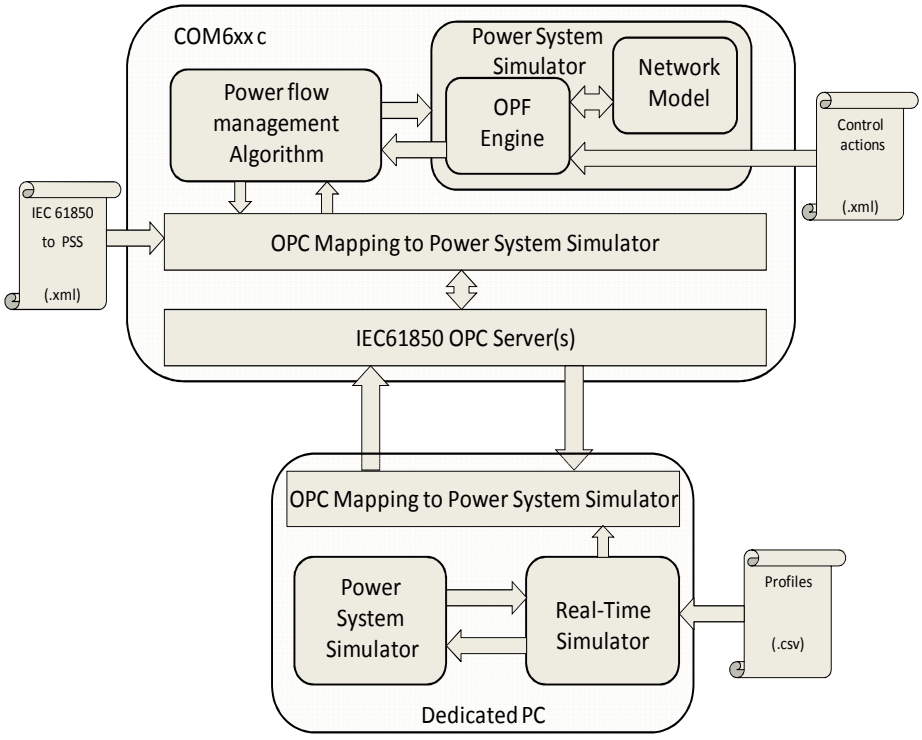

Figure 24 – Illustration of the OPF-LIFO Software Embedded within the COM6xx Substation Computer and Connected to the Sequential Steady State Simulator

The following sections present the results of the OPF-LIFO control approach when applying the profile based scenarios to the steady-state simulation environment. These profiles were updated once a second and monitored, for thermal excursions, every three seconds, for the 'Test Scenarios' described prior to the associated results.

4.3 OPF-LIFO: 11kV and 33kV Case Study Results

For the two case study networks the algorithm performance will be discussed in terms of the control signals issued to generators, the MW output from the DG units, the MW curtailment levels and the computation time to calculate solutions.

For Case Study A, Figure 25, the load and generation profiles were used to demonstrate algorithm performance with:

- Perfect measurement;
- 6% measurement error superimposed onto the load profile; and
- 1% measurement error superimposed onto the load profile (aligned with the 6% error)

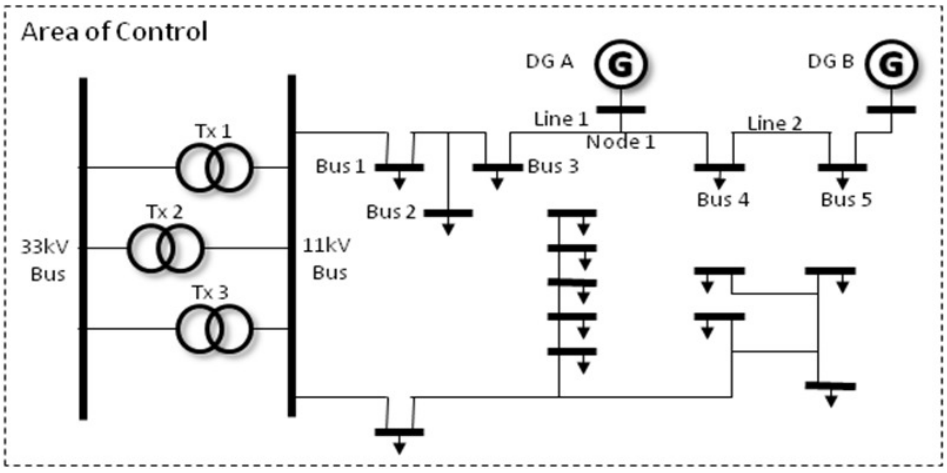

Figure 25 – Case Study A - 11kV Radial Distribution Network

For Case Study B, Figure 26, load and generation profiles were utilised to demonstrate the algorithm's behaviour with:

- Perfect measurement;
- Increased loading on the 33kV network (twice the load profile); and
- Single circuit outage on the 33kV network.

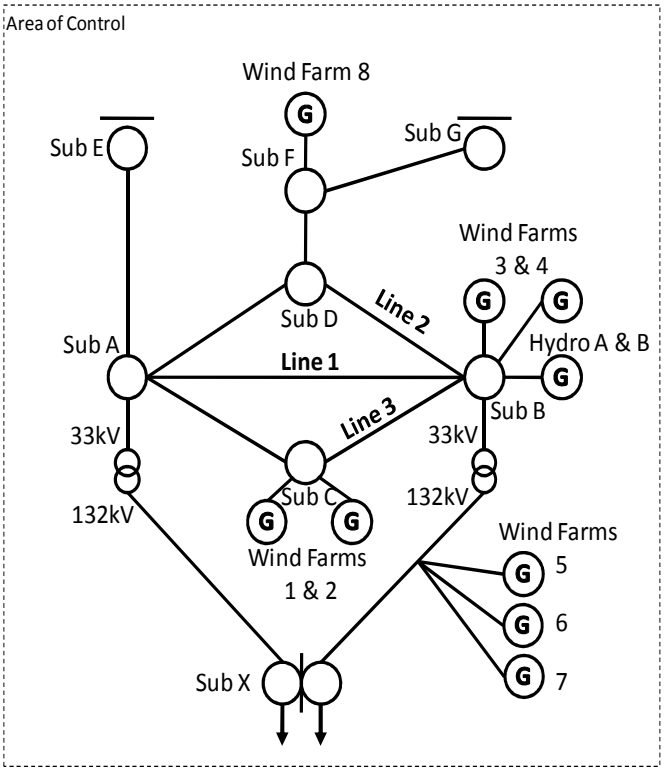

Figure 26 – Case Study B - 33kV Interconnected Distribution Network

4.4 Case Study A – 11kV Radial Distribution Network

In the following 'Test Scenarios' the DG cost models are updated to represent a change in DG contractual arrangements. Table 4 illustrates an example of the cost models enforced to allow DG A to have network access over DG B. The costs associated with DG A and DG B is reversed when DG B is deemed to have priority over DG A in the following 'Test Scenarios'. Thus the LIFO arrangement can be represented via the generator cost models.

Table 4 - OPF Piecewise Cost Models. DG B has the Highest Cost and is Deemed to be Last Historically Connected Unit

Slack bus		DG A		DG B	
Breakpoint (MW)	Cost (£/MWh)	Breakpoint (MW)	Cost (£/MWh)	Breakpoint (MW)	Cost (£/MWh)
-9999	10.01	0	1	0	2
-0.01	10.01	0.5	1	0.66	2
0.01	11.01	1	1	1.3	2
9999	11.01	1.6	1	2	2

For the 'Test Scenarios', described in the sections below, the assumed connection orders for the DG units is presented in Table 5.

Table 5 - Generator Connection Priority

Generator ID	Prioity (Test Scenario 1 - Figure 28)	Prioity (Test Scenario 2 - Figure 34)	Prioity (Test Scenario 3 - Figure 40)	Priority (Test Scenario 4 - Figure 59)
DG A	**2**	1	**2**	1
DG B	1	**2**	1	**2**

The priority numbers in bold, in Table 5 above, are highlighted as they are the generators that are curtailed for the following 'Test Scenarios'.

The above cost representation results in a step increase in cost when moving from one DG unit to the next, illustrated in Figure 27. Prior studies, where the costs were changed by different factors, illustrated that this linear cost representation was effective in maintaining the LIFO principle under normal network conditions. However, further investigation could be conducted to examine whether exponentially increasing the costs, to represent LIFO, results in maintaining the LIFO principle for all network conditions (i.e. single circuit outage conditions).

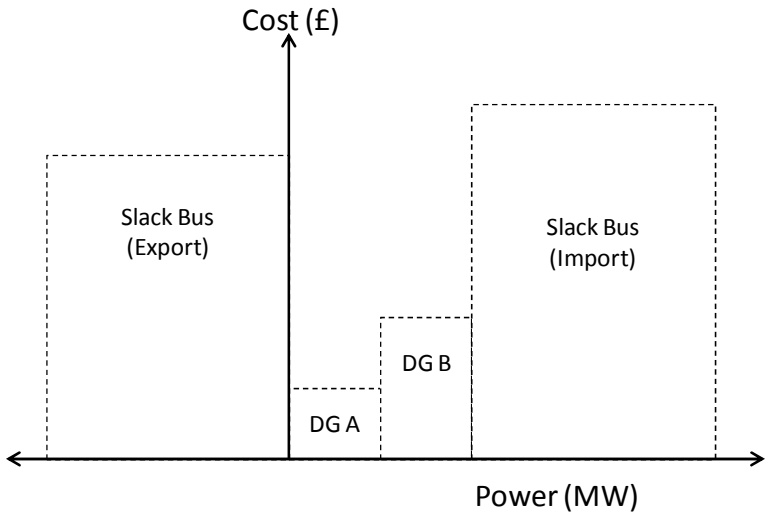

Figure 27 - Illustration of Step in DG Cost

4.4.1 Test Scenario 1: 11kV Radial Distribution Network with 'Line 1' Overloaded and DG A being the Last Historically Connected DG Unit

Test Scenario 1 consists of applying the network load and generation profiles, introduced in Chapter 3, such that the overloading of 'Line 1' of Figure 25 is achieved.

The OPF cost models are set such that DG A has the highest cost to represent DG A being the last historically connected DG unit and therefore the first unit to be curtailed under a network overload condition. Figure 28 shows that DG A is required to be curtailed to 0.956302 of maximum rated output at 'time step 42'. The curtailment can be relaxed at 'time step 68' whereby a control signal of 0.994764 is issued to the DG unit. A further control signal is issued at 'time step 72' indicating that load conditions are such that DG A can run unconstrained for the duration of the simulation. There is no requirement placed upon DG B to reduce its output.

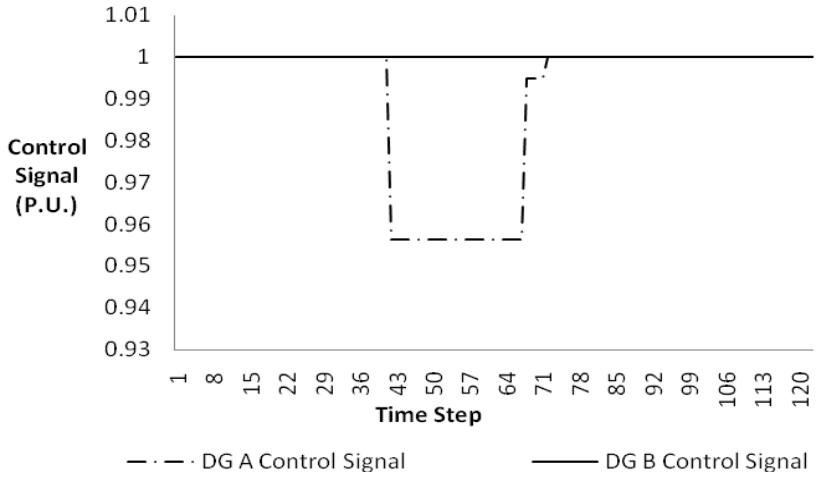

Figure 28 - Case Study A - Line 1 Overloaded with DG A having the Lowest Priority

In Figure 29 the line loading and limit is shown for the inputted DG and load profiles. The case is shown for the algorithm taking no action and therefore the line running overloaded. The line loading is also depicted for the above case when DG control actions are carried out to alleviate the thermal overload. It is clear that when the above control actions are carried out the line remains within thermal limits and DG is only brought back on as and when loading permits.

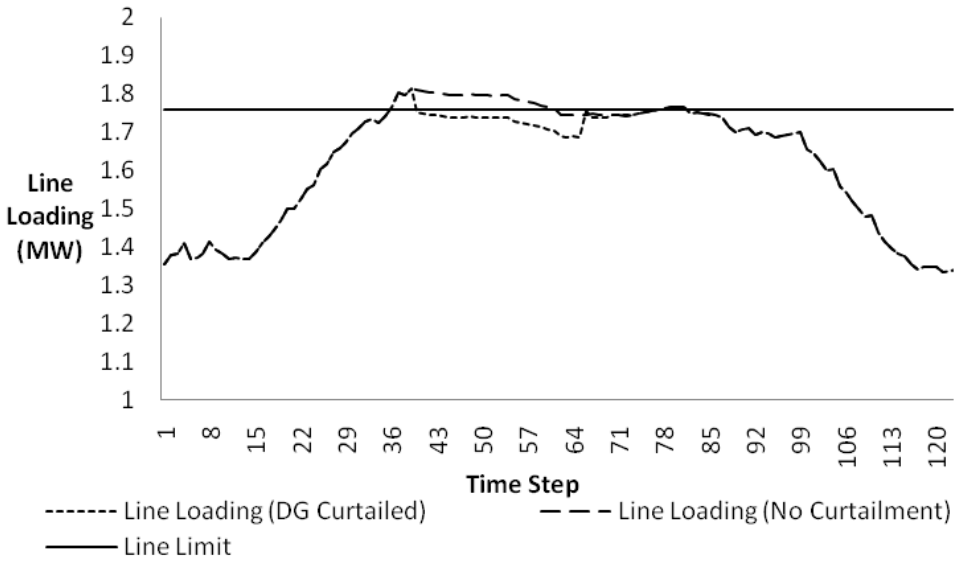

Figure 29 - Line Loading with and without DG Curtailed

Figure 30 illustrates the change in resulting control signals sent to DG A when a 6% erroneous measurement is applied to the load profile. The overload detection occurs at 'time step 41' and a deeper level of curtailment is required. The control signal restricting DG A to output at a maximum of 0.949528 of rated output is issued to the unit at this time step. This slight change in detection time, from that of the perfect measurement case, may be attributed to the three second monitoring and detection loop. It is however apparent that measurement error contributes to the relaxation signals at 'time step 57 and 66' when the DG unit is allowed to prematurely relax its curtailed output. The control signals of 0.989761 and 1 are sent at these time steps, respectively. DG B can run unconstrained for the duration of this simulation.

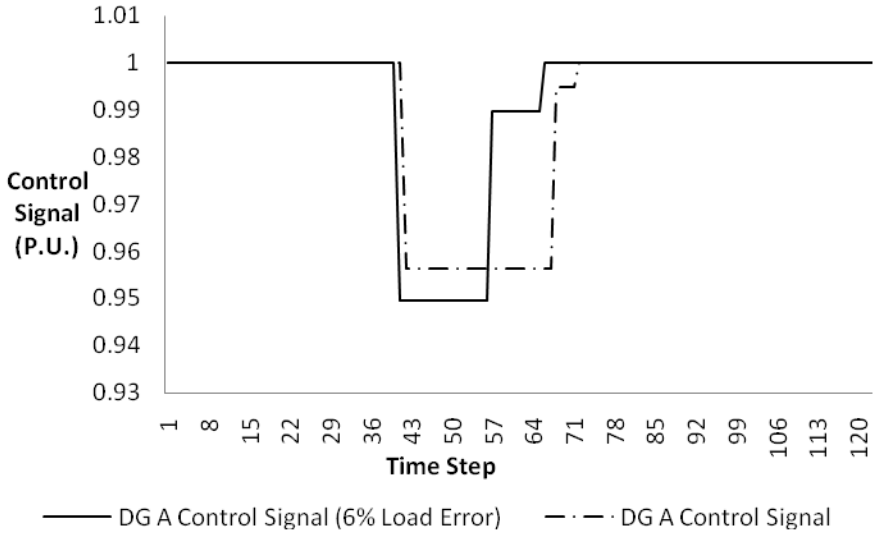

Figure 30 - Case Study A - Line 1 Overloaded with DG A having the Lowest Priority with and without 6% Erroneous Load Measurements

The same scenario is run with the exception that the load profile is subjected to a 1% measuremetn error. Figure 31 shows the control signal issued to DG A for the 1% load error case and the perfect measurement scenario. It can be observed from Figure 31 that the overload was detected at 'time step 45', three seconds after that of the perfect measurement case of Figure 28. This may be down to the detection loop that cycles every three seconds. At the point of detection a deeper limitation is placed upon DG A than that of the perfect measurement case whereby a control signal of 0.950341 is sent. The control signal is relaxed at 3 further intervals. At 'time step 73' the generator can increase output to a maximum of 0.994379 of rated output until at 'time step 77' the control signal of 0.997603 is issued allowing the DG unit to further increase its output. These control signals are 5 seconds behind that of the perfect measurement case indicating that measurement error is attributable to the delay in relaxing the constraint on the DG unit. The unit is allowed to run uncurtailed at 'time step 87' – 15 seconds after that of the perfect measurement case.

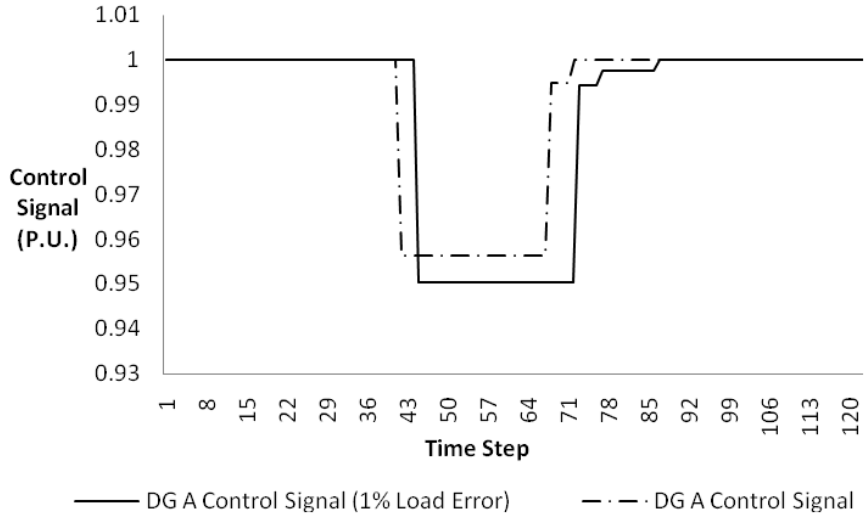

Figure 31 - Case Study A - Line 1 Overloaded with DG A having the Lowest Priority with and without 1% Erroneous Load Measurements

In Figure 32 DG A's MW output is shown on the primary vertical axis for the perfect measurement case and the 6% load error case. For the same cases the secondary vertical axis shows the MW curtailment of generation for the duration of the overload detection period.

It can be observed that for the perfect measurement case output is constrained to 1.530083MW following the control signal of 0.956302 being issued to DG A, where maximum rated output of DG A is 1.6MW. This level of output is further increased to 1.591622 when the 0.994764 control signal is sent. When the unit is allowed to operate unconstrained rated output of 1.6MW is resumed. The total MW curtailment over this period is 1.85MW.

For the 6% load error case, the reduction in DG output can be seen to be 1.519244MW when the 0.949528 signal is issued. This output increases to 1.583618MW when the 0.989761 control signal is sent. Operation at rated output resumes when the control signal of 1 is transmitted to the DG unit. Total MW curtailment over this period accumulates to 1.42MW.

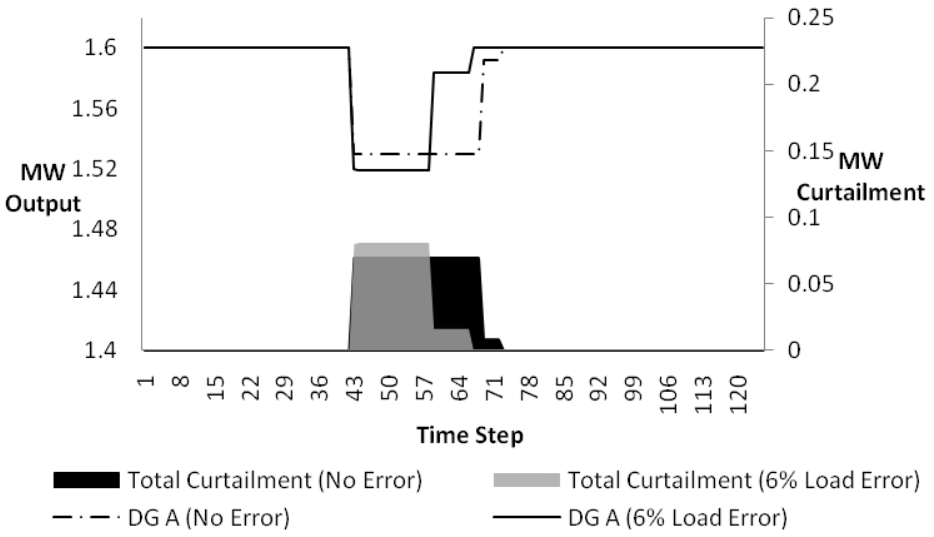

Figure 32 - Case Study A - Line 1 Overloaded with DG A having the Lowest Priority. DG A MW Output and Curtailment Graphed for 'Perfect' and 6% Erroneous Load Measurements

Figure 33 shows DG A's MW output on the primary vertical axis for the 1% load error case compared to the perfect measurement case. The secondary vertical axis shows the MW curtailment of generation for the duration of the overloaded period. The summary of Figure 32 for the perfect measurement case applies to Figure 33.

It can be observed that the MW output of DG A, for the 1% load error case depicted in Figure 33, is constrained to 1.520546MW when sent a control signal of 0.950341. The curtailment can be viewed as being relaxed to 1.591006MW for the 0.994379 signal and again to 1.596164MW for the 0.997603 control signal. DG A resumes rated output when it receives a control signal of 1. The total curtailment of DG A over this overload period is 2.21MW.

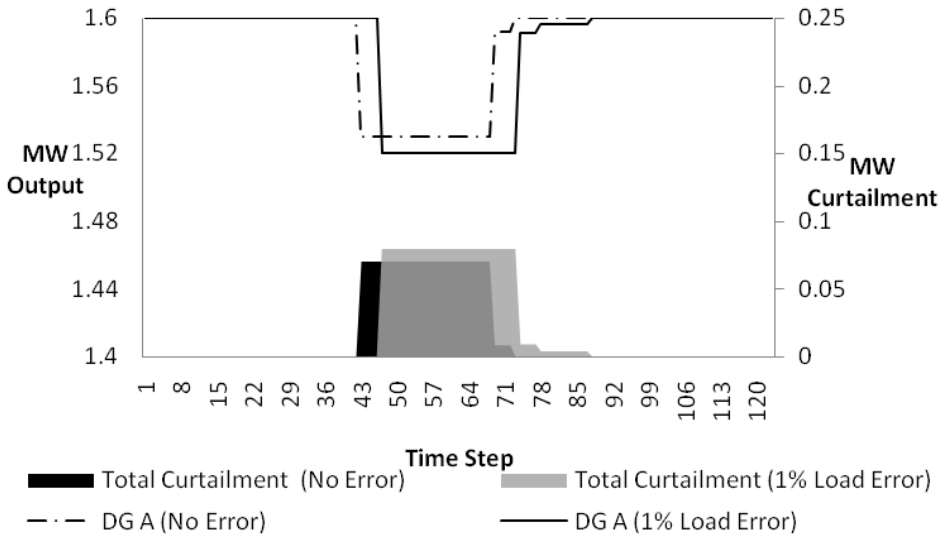

Figure 33 - Case Study A - Line 1 Overloaded with DG A having the Lowest Priority. DG A MW Output and Curtailment Graphed for 'Perfect' and 1% Erroneous Load Measurements

4.4.2 Test Scenario 2: 11kV Radial Distribution Network with 'Line 1' Overloaded and DG B being the Last Historically Connected DG Unit

Test Scenario 2 consists of applying the network load and generation profiles, introduced in Chapter 3, such that overloading of 'Line 1' of Figure 25 is achieved. However, this scenario reverses the assumed DG contractual arrangements. The OPF cost models are set such that DG B has the highest cost to represent DG B being the last historically connected DG unit and therefore the first unit to be curtailed under a network overload condition.

Figure 34 shows the control signals issued to DG B that ensures the overload is removed from the network. The initial detection occurs at 'time step 44' when a signal constraining DG B to 0.95308 is issued to the DG unit. Control signals are then issued to the DG unit to relax its curtailed operation at 'time step 72 and 77', the signals being 0.990692 and 0.991891, respectively. At 'time step 81' DG B can operate unconstrained and resume an output up to full rated output. For the duration of this scenario DG A can operate uncurtailed.

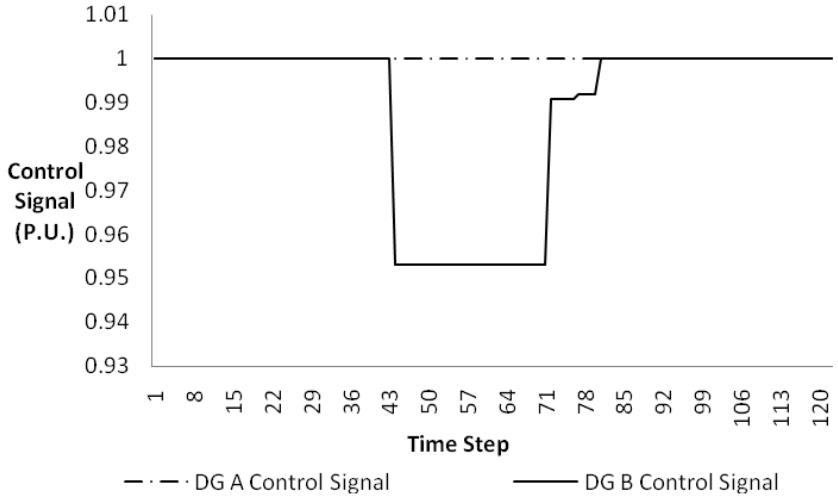

Figure 34 - Case Study A - Line 1 Overloaded with DG B having the Lowest Priority

In Figure 35 the line loading and limit is shown for the inputted DG and load profiles. The case is shown for the algorithm taking no action and therefore the line running overloaded. The line loading is also depicted for the above case when DG control actions are carried out to alleviate the thermal overload. It is clear that when the above control actions are carried out the line remains within thermal limits and DG is only brought back on as and when loading permits.

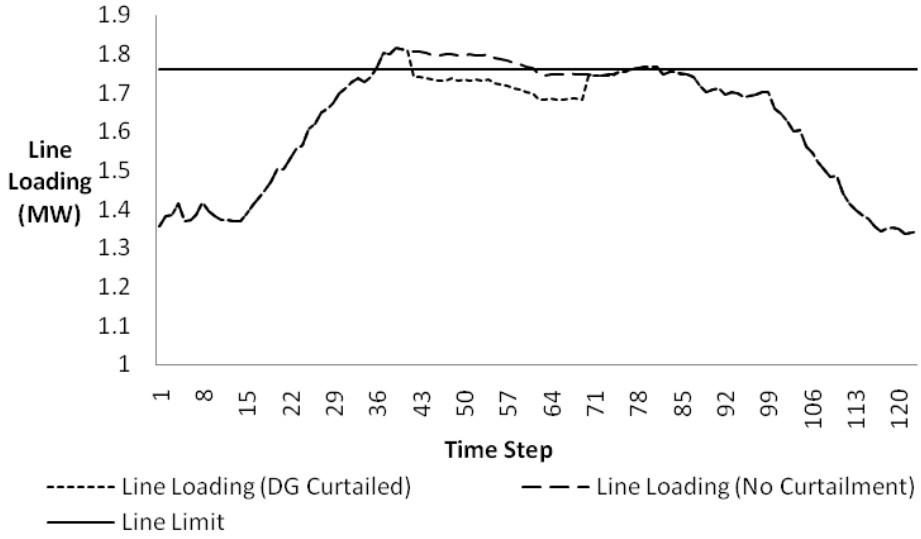

Figure 35 - Line Loading with and without DG Curtailed

The same scenario was run with 6% measurement error applied to the load profile. Figure 36 shows the control signals issued to DG B under this condition and compares them to that of the perfect measurement case. At 'time step 40' the overload is detected and generation, at DG B, reduced to a maximum of 0.939145 of rated output (a deeper level of curtailment than that of the perfect case). This occurs 4 seconds prior to that of the perfect measurement case and is outwith the three second monitoring and detection loop timeframe therefore indicating that measurement error plays a role in the early detection of the thermal overload. The level of curtailment is relaxed, ahead of time, at 'time step 61 and 65 when the signals of 0.971828 and 0.983011 are sent to DG B, respectively. The curtailment is removed at 'time step 69' when the unit is allowed to operate up to its rated value.

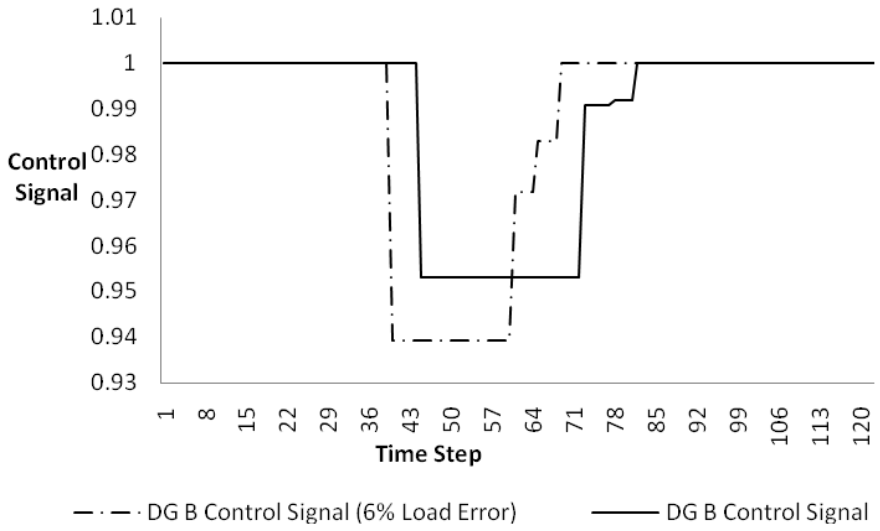

Figure 36 - Case Study A - Line 1 Overloaded with DG B having the Lowest Priority with and without 6% Erroneous Load Measurements

In Figure 37 the control signal for the perfect measurement case is compared to that of two simulations of the 1% erroneous load measurement case, named 'Run 1' and 'Run 2'. This highlights the role that the three second monitoring and detection loop cycle has on the period that the control actions are issued and also the level of curtailment required. The main differences between 'Run 1' and 'Run 2' are due to the manual nature of running the simulations, whereby the PFM algorithm is started on the substation computer prior to starting the software that passes the load and generation profiles to the monitored model. Therefore, the subsequent detection and control actions calculated are dependent on how long the simulation has to wait before the PFM software checks for overloads and what profiles values are present in the model at that particular period.

It can be observed, from Figure 37, that 'Run 1' of the 1% erroneous load case detects the thermal overload at 'time step 41' and requests a deeper curtailment, of 0.946114, than that of the perfect measurement case. This is three seconds prior to the detection in the perfect measurement case and therefore measurement error may not be directly at fault (as indicated in the 'Run 2' case). Two signals are later issued to DG B at 'time step 68 and 73' to relax the level of curtailment to a maximum of

0.982663 and 0.990312 of DG B's rated output, respectively. At 'time step 77' network load conditions are such that the constraint on DG B's output can be completely lifted i.e. a control signal of 1 is issued to the unit.

For the 'Run 2' simulation of the 1% load error case the control signal levels and issue times correspond very closely to that of the perfect measurement case as illustrated in Figure 37. The thermal overload is detected at the same instant as the perfect measurement case, 'time step 44'. The signal sent requires DG B to reduce output to no more than 0.952007 (compared to 0.95308 for the perfect measurement case) of rated output value. At 'time step 72' the signal is relaxed to 0.991572 the same time step that the perfect measurement case requests a 0.990692 restraint on DG output. The curtailment of DG B is completely removed at 'time step 79' compared to that of 'time step 77' for the perfect measurement case.

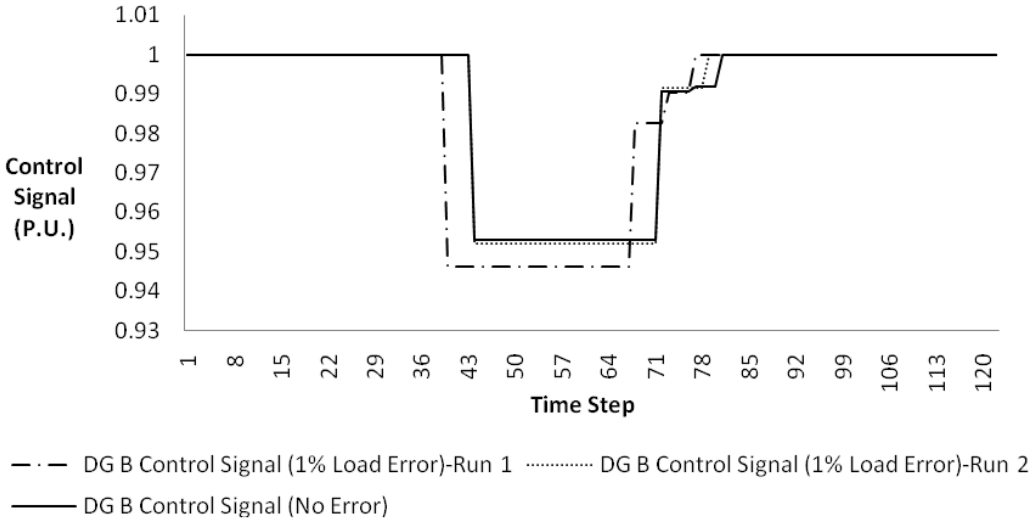

Figure 37 - Case Study A - Line 1 Overloaded with DG B having the Lowest Priority with and without 1% Erroneous Load Measurements

In Figure 38 DG B's MW output is shown on the primary vertical axis for the perfect measurement case and for the 6% load error case. For the same cases, the secondary

vertical axis shows the MW curtailment of generation for the duration of the overload period.

It can be viewed, from Figure 38, that for the perfect measurement case when the initial signal of 0.95308 is sent to DG B the unit ramps down to 1.90616MW. At the point where the 0.990692 and the 0.991891 signals are sent the DG unit increases output up to 1.981384MW and 1.983781MW, respectively. When the curtailment is removed the DG unit can operate up to maximum rated output of 2MW however at this point the unit can only output 1.96MW due to the profile input.

From the same Figure 38 the output of DG B for the 6% erroneous load measurement case is presented. The level of DG B's initial curtailment for the 0.939145 signal is 1.878289MW. This level is increased to 1.943655MW and 1.966022MW as the DG constrained connection is relaxed to 0.971828 and 0.983011, respectively. When the curtailment constraint is released, via the control signal of 1, the DG resumes output up to its rated value (2MW). At that moment in time the unit can only output 1.984MW.

Data skew within Figure 38 is noticeable towards the end of the profiles and would have a slight impact upon the detection and control signal calculation. However the discrepancy between the scenarios would be predominantly down to the 6% erroneous load measurement. For the perfect measurement case a total of 2.22MW was removed from the network compared with 2.4MW for the 6% load error case.

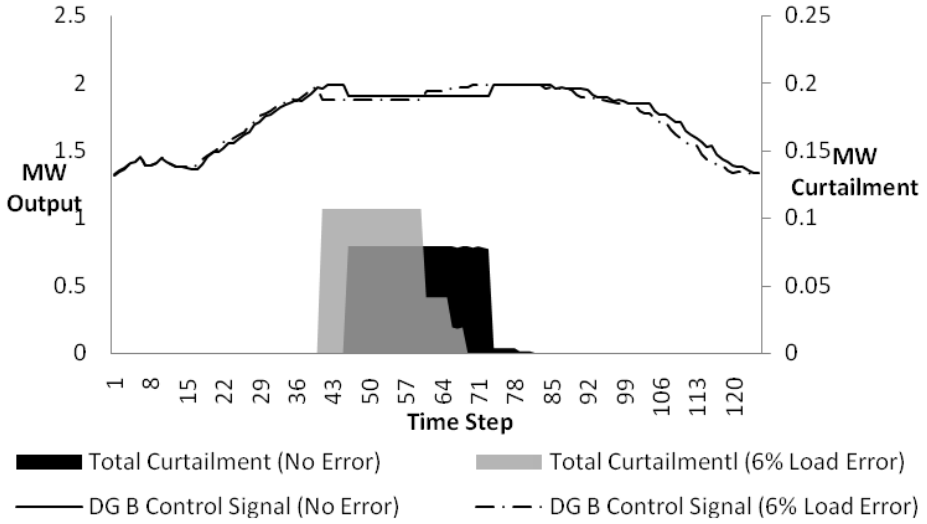

Figure 38 - Case Study A - Line 1 Overloaded with DG B having the Lowest Priority. DG B MW Output and Curtailment Graphed for 'Perfect' and 6% Erroneous Load Measurements

Figure 39, below, presents the MW output of DG B and the level of total curtailment for the perfect measurement case and for both 'runs' of the 1% load error case. The perfect measurement scenario is as described above for Figure 38.

For the 1% erroneous load measurement 'Run 1' case, Figure 39, DG B reduces output to 1.89228MW when instructed by the 0.946114 control signal. The relaxation of curtailment allows the DG unit to ramp up to 1.965325MW and 1.980624MW when issued with the controls signals 0.982663 and 0.990312, respectively. When network loading is such that the curtailment can be completely removed the unit outputs what is available, 1.985MW.

For the 1% erroneous load measurement 'Run 2' case it is difficult to observe the trace on Figure 39 due to the output very closely resembling that of the non-erroneous case. However, when DG B is signalled to curtail its output with the 0.952007 control signal it responds and ramps down to 1.904013MW. The signal is then relaxed to 0.991572 where the generator increases output up to 1.983144MW. At the time where network loading permits the curtailment to be removed DG B returns to the output it is capable of delivering, 1.985MW.

Total curtailment over these cases is recorded as 2.22MW for the perfect measurement scenario, 2.71MW for the 1% load error 'Run 1' case and 2.27MW for the 1% load error 'Run 2' case.

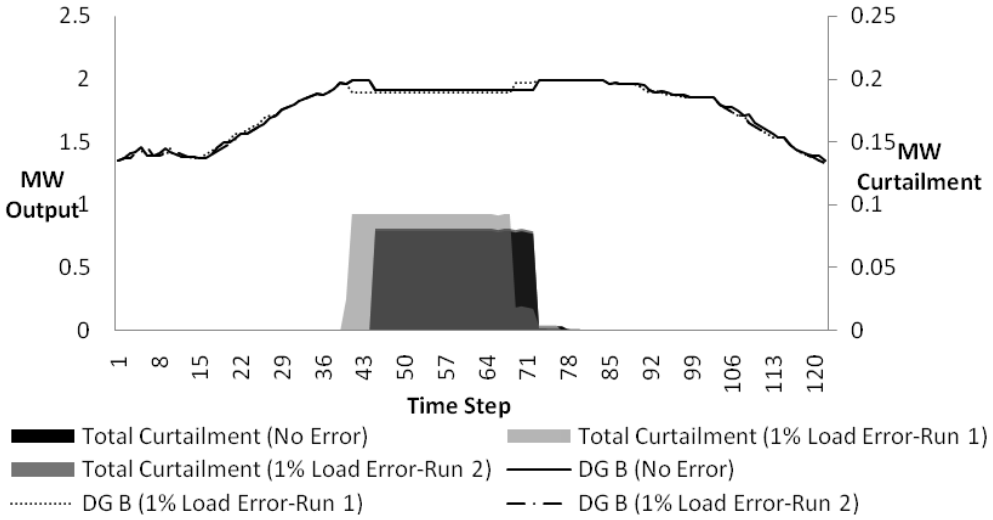

Figure 39 - Case Study A - Line 1 Overloaded with DG B having the Lowest Priority. DG B MW Output and Curtailment Graphed for 'Perfect' and 1% Erroneous Load Measurements

4.4.3 Test Scenario 3: 11kV Radial Distribution Network with 'Line 2' Overloaded and DG A being the Last Historically Connected DG Unit

Test Scenario 3 consists of applying the network load and generation profiles, introduced in Chapter 3, such that overloading of 'Line 2' of Figure 25 is achieved. The OPF cost models are set such that DG A has the highest cost to represent DG A being the last historically connected DG unit and therefore the first unit to be curtailed under a network overload condition.

Figure 40 shows the control signals for DG A and DG B for 'Line 2' being overloaded. This scenario shows that although DG A should be constrained under the LIFO connection agreement it is technically infeasible as DG A is not feeding into the overloaded line. Therefore, control signals are issued to the only unit capable of alleviating the network thermal constraint, DG B, thus deviating from the contractual arrangement. At 'time step 43' the thermal excursion is detected and DG B is sent a ramp down signal of 0.959016. The signal is relaxed at 'time step 69' where DG B can operate at up to 0.99908 of rated output. This maximum output is further restricted to 0.998571 of rated output at 'time step 74' before being allowed to operate unconstrained at 'time step 79'.

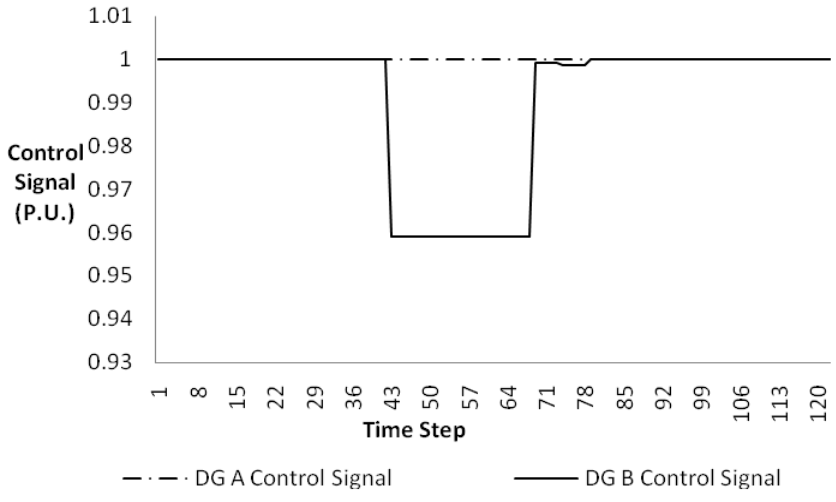

Figure 40 - Case Study A - Line 2 Overloaded with DG A having the Lowest Priority

In Figure 41 the line loading and limit is shown for the inputted DG and load profiles. The case is shown for the algorithm taking no action and therefore the line running overloaded. The line loading is also depicted for the above case when DG control actions are carried out to alleviate the thermal overload. It is clear that when the above control actions are carried out the line remains within thermal limits and DG is only brought back on as and when loading permits.

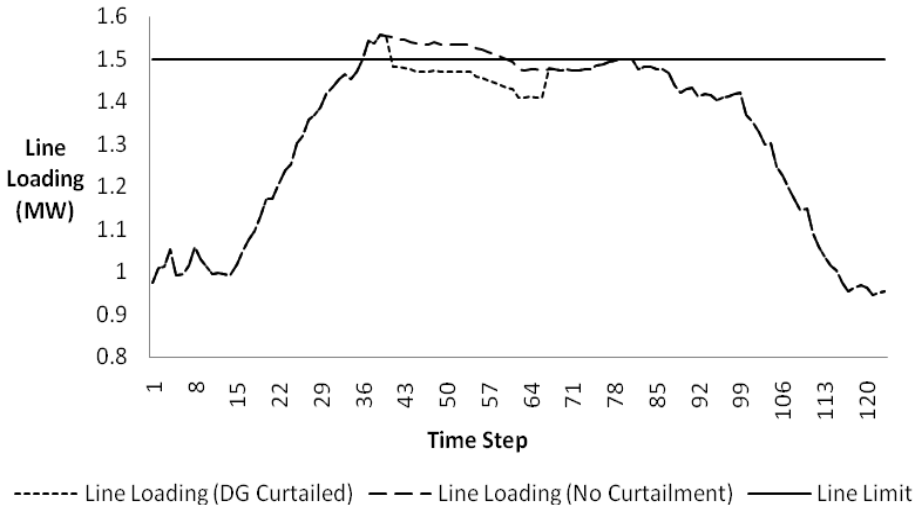

Figure 41 - Line Loading with and without DG Curtailed

In Figure 42 the same scenario is run using the 6% erroneous load data. The initial control signal is sent, when the thermal breach is detected, at 'time step 44'. DG B is restricted to output a maximum of 0.954988 of rated value at this time step. The restriction is removed at 'time step 49' whereby the unit can output up to maximum rated value. Measurement error for this case bears a significant impact on the level of curtailment.

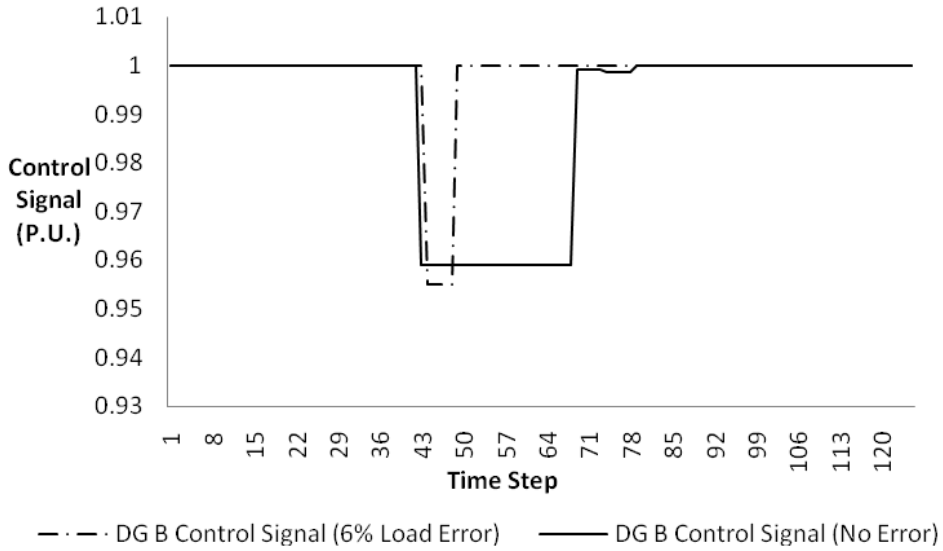

Figure 42 - Case Study A - Line 2 Overloaded with DG A having the Lowest Priority with and without 6% Erroneous Load Measurements

Figure 43 shows this same case run with 1% measurement error. The thermal overload is detected at 'time step 46'. This is three seconds after that of the perfect measurement case and may be attributable to the three second monitoring and detection cycle. The initial curtailment signal sent to DG B requires it to output no greater than 0.964618 of its rated output. The level of curtailment is relaxed at 'time step 69' to 0.991037 then again at 'time step 74' to 0.998361. DG B can output unconstrained at 'time step 79' when network loading is such that the thermal excursion has dissipated.

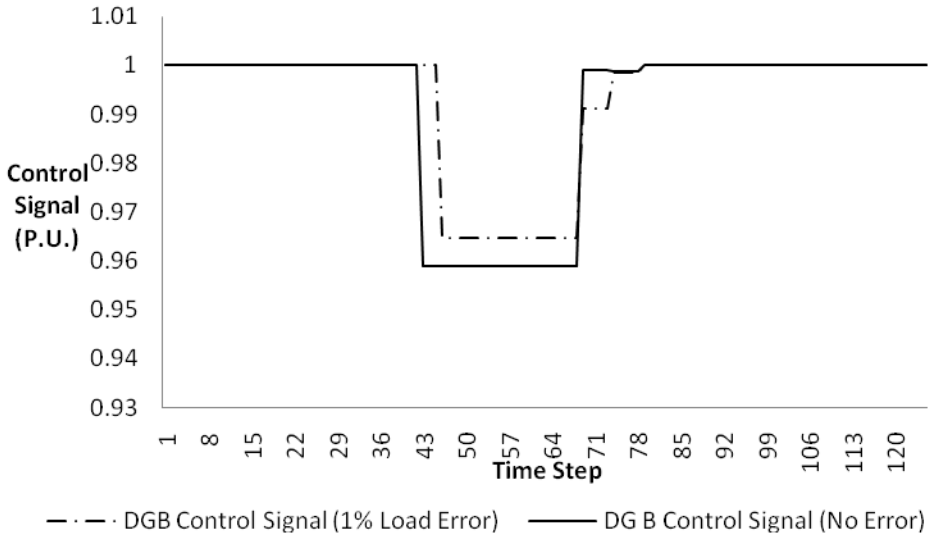

Figure 43 - Line 2 Overloaded with DG A having the Lowest Priority with and without 1% Erroneous Load Measurements

In Figure 44 the MW output of DG B can be observed on the primary vertical axis and the total MW curtailment on the secondary vertical axis. The perfect measurement case is presented alongside the 6% load error measurement case.

For the perfect measurement case DG B (rated at 2MW) is seen to ramp down to 1.918031MW when instructed to do so via the 0.959016 initial control signal. The next two signals allow the unit to operate up to 1.99816MW (for the 0.99908 signal) and 1.997142MW (for the 0.998571 signal). At these time steps the DG output sits at 1.984MW and 1.985MW, respectively, due to the intermittency of the generator reflected through the unit's profile. This can also be viewed when the DG unit is allowed to run unconstrained. Rather than outputting at the rated level of 2MW the unit outputs what it is capable of doing, 1.985MW.

The 6% erroneous case presented in Figure 44 shows that when DG B's output is constrained, to 0.954988 of rated value, the unit reduces output to 1.909976MW. When DG B receives the control of 1 and can therefore output up to 2MW the unit outputs what it can at a level of 1.985MW.

The total curtailment for the perfect measurement case was 1.74MW and only 0.3MW for the 6% load error case. There is no significant impact upon this scenario from skewed data.

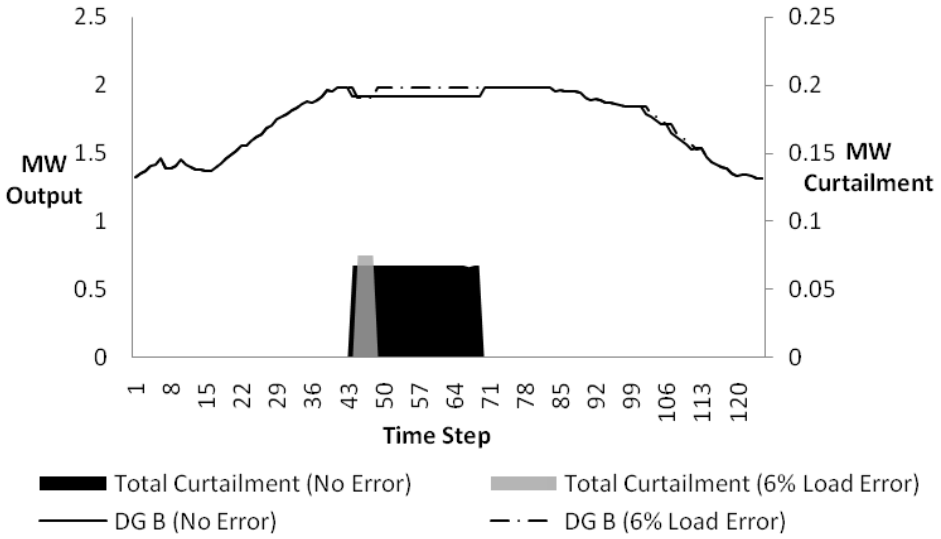

Figure 44 - Case Study A - Line 2 Overloaded with DG A having the Lowest Priority. DG B MW Output and Curtailment Graphed for 'Perfect' and 6% Erroneous Load Measurements

For the perfect measurement case and the 1% load error measurement case the MW output of DG B can be observed on the primary vertical axis and the total MW curtailment on the secondary vertical axis of Figure 45. The perfect measurement case is the same as that described above in Figure 44.

Examining the 1% erroneous measurement case presented in Figure 45 it can be observed that DG B, when requested by the initial 0.964618 signal, curtails its output to 1.929235MW and increases output to 1.982074MW when the 0.991037 control signal is received. When the DG unit receives the 0.998361 signal its output is restricted to a maximum of 1.996722MW however under the conditions of the units

profile it outputs what is available, 1.985MW. This same output is only achievable when the unit can run unconstrained when issued with a control signal of 1.

The total curtailment for the 1% load error case is 1.29MW compared to 1.74MW for the perfect measurement case. In this scenario slight data skew can be observed towards the end of the simulation which may have a small bearing on the results for the 1% load error case.

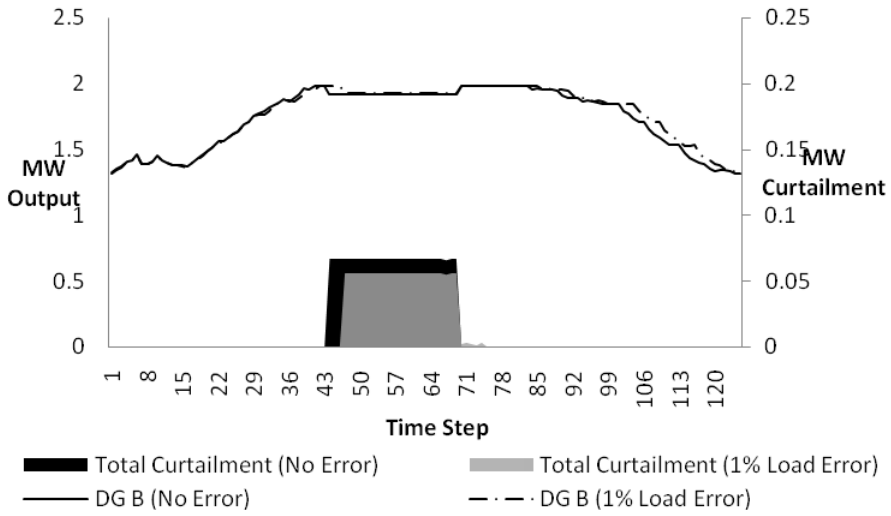

Figure 45 - Case Study A - Line 2 Overloaded with DG A having the Lowest Priority. DG B MW Output and Curtailment Graphed for 'Perfect' and 1% Erroneous Load Measurements

4.4.4 Test Scenario 4: 11kV Radial Distribution Network with 'Line 2' Overloaded and DG B being the Last Historically Connected DG Unit

Test Scenario 4 consists of applying the network load and generation profiles, introduced in Chapter 3, such that overloading of 'Line 2' of Figure 25 is achieved. However, this scenario reverses the assumed DG contractual arrangements from that of the previous 'Test Scenario 3'. The OPF cost models are set such that DG B has the highest cost to represent DG B being the last historically connected DG unit and therefore the first unit to be curtailed under a network overload condition.

Figure 46 shows that at 'time step 44' only DG B is sent a reduction signal due to being the last historically connected generator and being the only unit feeding into the overloaded line. The signal constraining DG B at this time step is 0.961518. This level of curtailment is relaxed at 'time step 69' when the unit is sent a signal limiting its output to 0.999078 of rated output. DG B is further constrained to 0.998569 of rated output at 'time step 74' before being allowed to operate unconstrained (at 'time step 80') for the duration of the simulation. DG A operated with an unconstrained output for the entirety of the simulation.

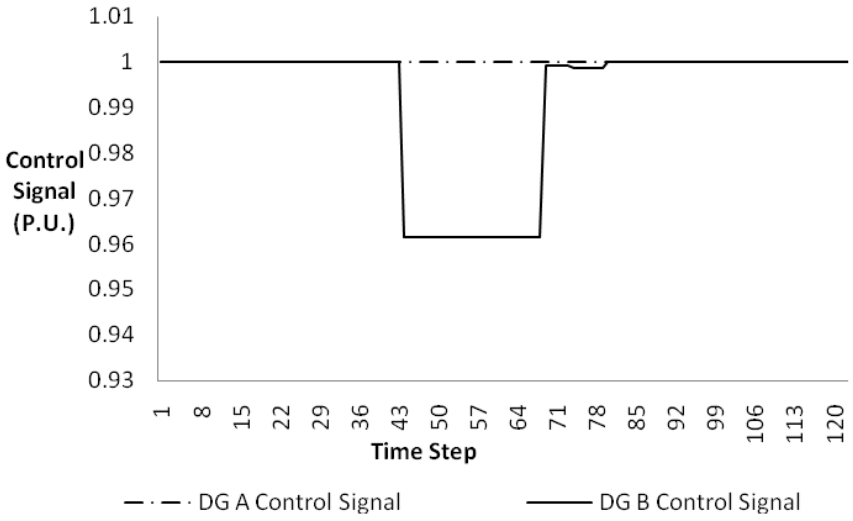

Figure 46 - Case Study A - Line 2 Overloaded with DG B having the Lowest Priority

In Figure 47 the line loading and limit is shown for the inputted DG and load profiles. The case is shown for the algorithm taking no action and therefore the line running overloaded. The line loading is also depicted for the above case when DG control actions are carried out to alleviate the thermal overload. It is clear that when the above control actions are carried out the line remains within thermal limits and DG is only brought back on as and when loading permits.

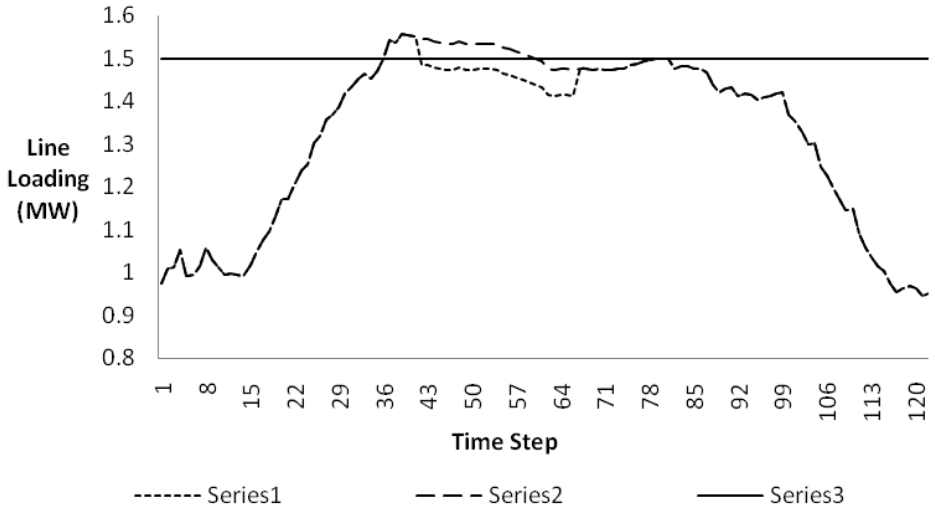

Figure 47 - Line Loading with and without DG Curtailed

Figure 48 presents the control signals for the 6% erroneous load case alongside the perfect measurement case. The thermal overload is detected at 'time step 42', 2 seconds prior to that of the perfect measurement case. This may be attributable to the three second detection loop cycle however a deeper level of curtailment is requested by the 0.947523 control signal. This deep curtailment is relaxed at two following time intervals, 'time step 54 and 58', where the control signals of 0.973539 and 0.980295 are issued to DG B, respectively. DG B can operate unconstrained at 'time step 66'.

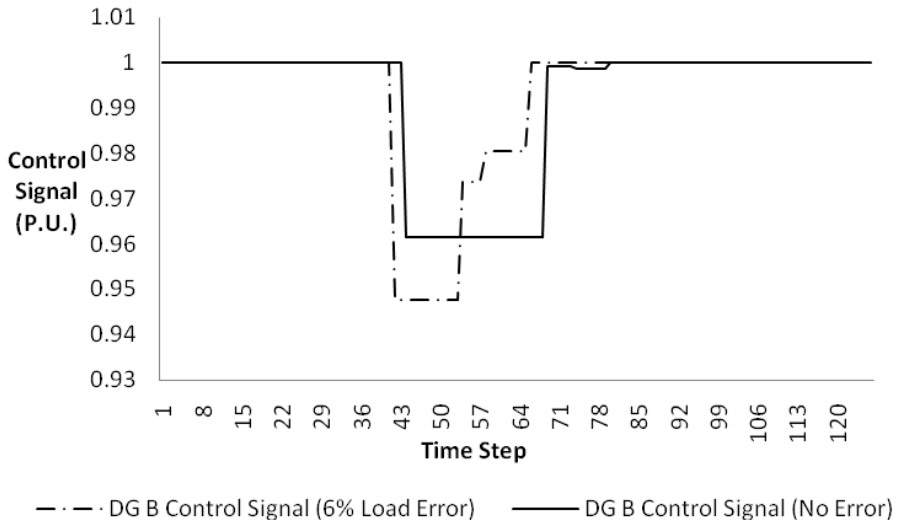

Figure 48 - Case Study A - Line 2 Overloaded with DG B having the Lowest Priority with and without 6% Erroneous Load Measurements

In Figure 49 the control signals for the 1% load error case is illustrated next to the perfect measurement case. The three second monitoring and detection loop picks up the thermal breach at 'time step 42' and issues the curtailment command of 0.954595 to DG B. Two further signals relax this curtailment to 0.991048 and 0.999929 of full rated output at 'time step 71 and 74', respectively. At 'time step 79' network load is such that the curtailment instruction on DG B can be removed.

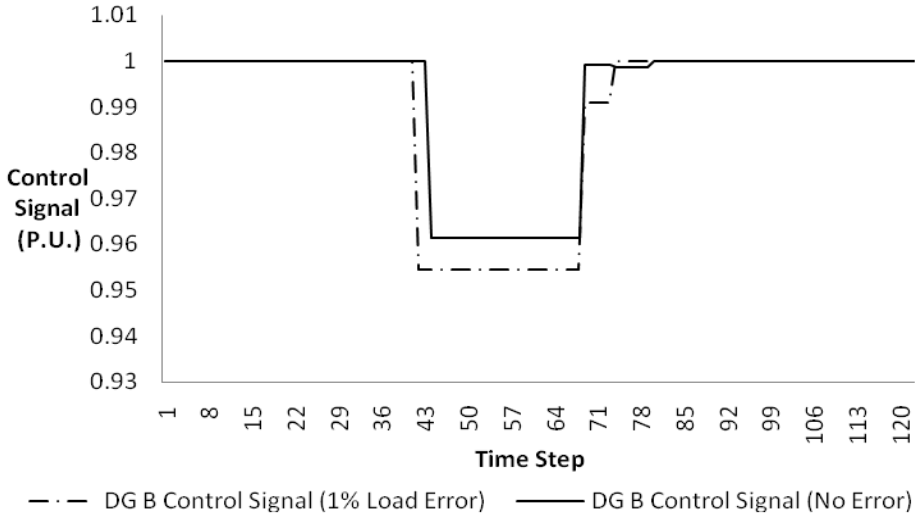

Figure 49 - Case Study A - Line 2 Overloaded with DG B having the Lowest Priority with and without 1% Erroneous Load Measurements

Figure 50 shows the MW output of DG B on the primary vertical axis and the total MW curtailment can be observed on the secondary vertical axis. The perfect measurement case is presented alongside the 6% load error measurement case.

For the perfect measurement case, depicted in Figure 50, the output of DG B can be seen to be reduced when instructed by the 0.961518 control signal to 1.923035MW. When the curtailment is relaxed to 0.999078 the DG unit can run at a maximum of 1.998156MW however this value is greater than the profile allows and the unit operates at 1.984MW. The same situation arises for the next two control signals. When issued with the 0.998569 signal DG B can output a potential 1.997138MW however the intermittent nature of this unit, as reflected in the profile, only permits it to output 1.985MW. The final signal sent allows DG B to operate up to maximum rated output (2MW) but can only achieve 1.985MW at this time step.

The 6% erroneous load case, also presented in Figure 50, shows DG B output reducing to 1.895046MW when commanded to do so by the 0.947523 control signal. The two subsequent relaxations of the control signals, 0.973539 and 0.980295, permit the unit to operate at 1.947078MW and 1.96059MW, respectively. When

network conditions are such that the unit can commence operation uncurtailed (2MW) the unit resumes an output that it is capable of producing, 1.985MW.

The total curtailment for the perfect measurement case for this scenario was 1.55MW and for the 6% load error the total curtailment was recorded as 1.4MW.

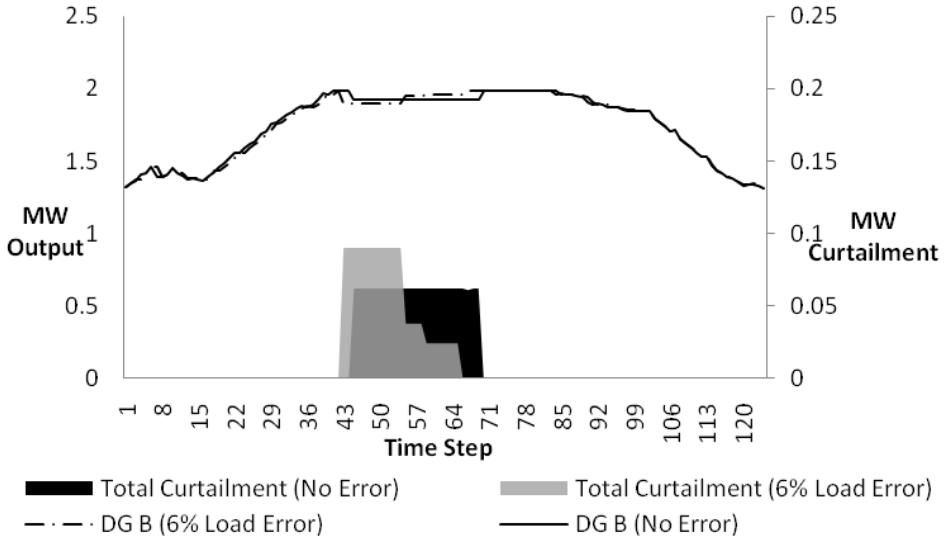

Figure 50 - Case Study A - Line 2 Overloaded with DG B having the Lowest Priority. DG B MW Output and Curtailment Graphed for 'Perfect' and 6% Erroneous Load Measurements

For the perfect measurement case and the 1% load error measurement case the MW output of DG B can be observed on the primary vertical axis and the total MW curtailment on the secondary vertical axis of Figure 51. The perfect measurement case is the same as that described above in Figure 50.

It can be observed, from Figure 51, for the 1% erroneous load case that DG B ramps down to 1.90919MW when issued with the 0.954595 curtailment signal. When the 0.991048 signal is received the output of DG B ramps up to 1.982095MW. The next two control signals sent to DG B, 0.999929 and 1, allow the unit to operate up to 1.999858MW and 2MW, respectively. The DG unit is not capable of reaching these

limits and continues to output what is available, 1.983MW and 1.985MW, respectively.

The total curtailment of DG B accumulates to 2.13MW over this period. This compares to 1.55MW for the perfect measurement case.

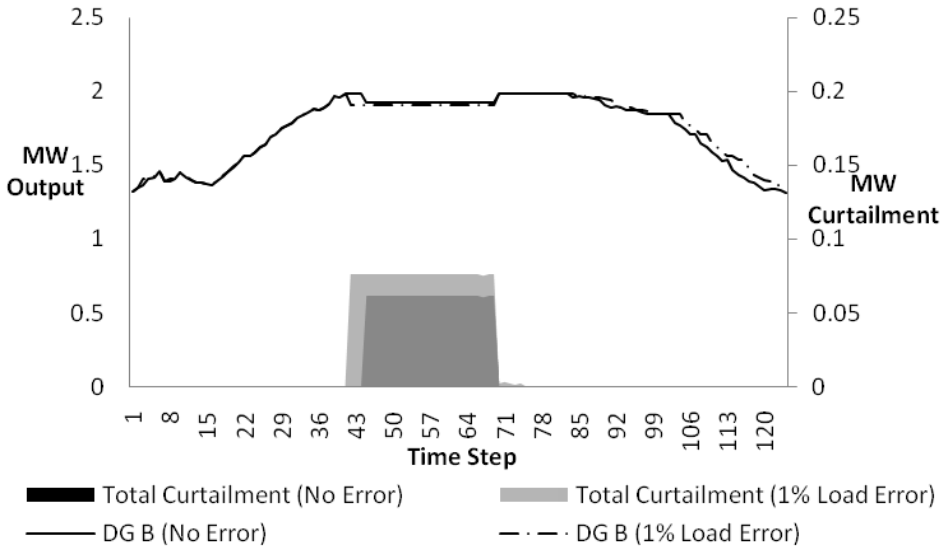

Figure 51 - Case Study A - Line 2 Overloaded with DG B having the Lowest Priority. DG B MW Output and Curtailment Graphed for 'Perfect' and 1% Erroneous Load Measurements

4.4.5 Case Study A: Test Scenario Computation Times for the 11kV Radial Distribution Network

For the above 'Test Scenarios' the computation time was recorded for the calculation of each control signal when the OPF engine was called following the identification of curtailment or the relaxation or removal of the constraint on the DG output. The fastest computation time was recorded at 44.675ms with the slowest taking 172.16ms to compute the solution.

Figure 52, below, shows the average time to compute the solutions over the simulation period for all the 'Test Scenario' cases presented. The x-axis corresponds to the 'Test Scenario' figures within this chapter.

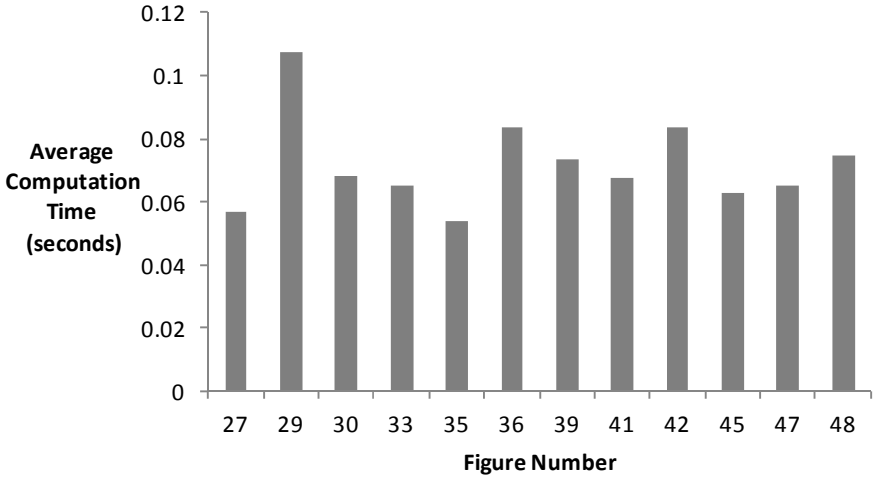

Figure 52 - Average Solution Computation Time for Case Study A

4.5 Case Study B – 33kV Interconnected Distribution Network

In the following 'Test Scenarios' the DG cost models are updated to represent a change in their contractual arrangements. Table 6 illustrates an example of the cost models used to enforce DG 1 having network access priority over DG N and DG N+1 and DG N having access rights over DG N+1. Thus the LIFO arrangement can be represented via the generator cost models. The approach illustrated in Table 6 is used to update the cost models of the ten generator units shown in Figure 26 to enable the LIFO connection order to be represented within the simulations. In order to change the connection order the costs of the generators can be updated to reflect these changes.

Table 6 - OPF Piecewise Cost Models. DG N+1 has the Highest Cost and is Deemed to be Last Historically Connected Unit

Slack bus		DG 1		DG N		DG N+1	
Breakpoint (MW)	Cost (£/MWh)	Breakpoint (MW)	Cost (£/MWh)	Breakpoint (MW)	Cost (£/MWh)	Breakpoint (MW)	Cost (£/MWh)
-9999	10.01	0	1	0	2	0	DG N +1
-0.01	10.01	5	1	1	2	a	DG N +1
0.01	11.01	10	1	2	2	b	DG N +1
9999	11.01	15	1	3	2	c	DG N +1

For the 'Test Scenarios', described in the sections below, the assumed connection orders for the DG units is presented in Table 7.

Table 7 - Generator Connection Priority

Generator ID	Prioity (Test Scenario 5 - Figure 53)	Prioity (Test Scenario 6 - Figure 55)	Prioity (Test Scenario 7 - Figure 58)	Priority (Test Scenario 8 - Figure 59)
Hydro A	1	1	1	1
Hydro B	2	2	2	**2**
DG 1	3	4	4	4
DG 2	4	5	5	5
DG 3	5	**10**	**10**	**10**
DG 4	6	9	**9**	**9**
DG 5	**10**	8	**8**	**8**
DG 6	9	7	7	7
DG 7	8	6	6	6
DG 8	7	3	3	3

The priority numbers in bold, in Table 7 above, are highlights as they are the generators that are curtailed for the following 'Test Scenarios'.

4.5.1 Test Scenario 5: 33kV Interconnected Distribution Network with 'Line 1' Overloaded and DG 5 being the Last Historically Connected DG Unit

With 'Line 1' de-rated and through increasing the load at 'Sub A' it is possible to force a thermal excursion on 'Line 1' of the interconnected distribution network in Figure 26. In this scenario it is assumed that DG 5 has been the last historically connected DG unit and therefore the first unit in the priority list to attempt to alleviate the thermal excursion.

In Figure 53, DG 5 had the largest costs in its OPF cost model to represent being last the last connected generating unit, and hence was the first unit curtailed when 'Line 1' experiences a thermal constraint. The primary vertical axis in Figure 53 shows the MW level of curtailed and the potential generation, while the secondary vertical axis depicts the set point control signal sent to the DG unit. The horizontal axis shows the simulation time steps.

It can be observed, from Figure 53, that DG 5 is sent four control signals during the thermal overload period. The initial control signal (at 'time-step 36') requires DG 5 to ramp down to 0.911881 of its rated output value, 21.4292MW. At 'time step 65 and 69' this level of curtailment is relaxed to 0.963396 and 0.993505, respectively. These control signals would limit DG 5's output to a maximum of 22.6398MW and 23.3473MW however as the primary wind resource is not present (i.e. insufficient wind speed) the actual generating unit output level is lower to reflect the unavailability of the wind. At these periods the actual DG output is 21.2MW and 20.89MW. The same situation arises when the generator unit is allowed to operate unconstrained (23.5MW) and is only able to provide an output of 20.87MW at 'time step 73'.

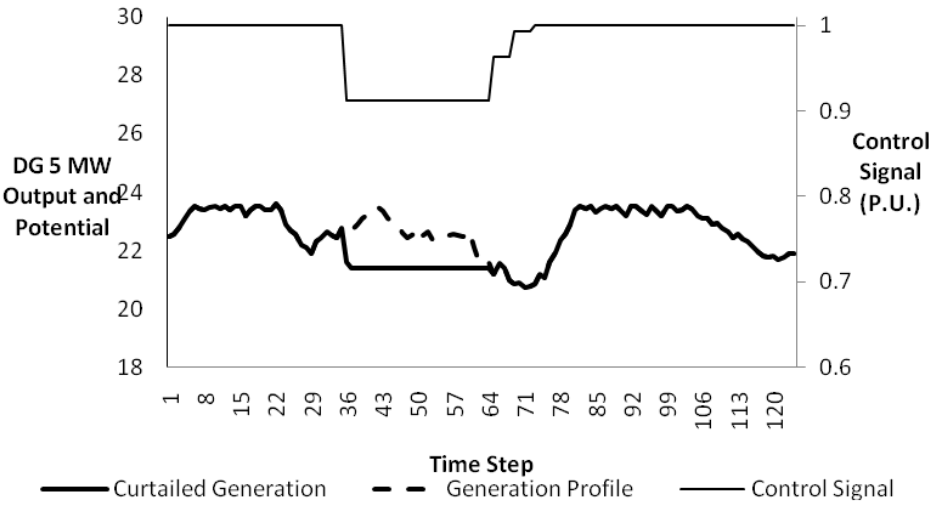

Figure 53 - Case Study B - Line 1 Overloaded with DG 5 having the Lowest Priority

Figure 54 is representative of the line loading for the inputted DG and load profiles. The case is shown for the algorithm taking no action and therefore the line running overloaded. The line loading is also depicted for the above case when DG control actions are carried out to alleviate the thermal overload. It is clear that when the above control actions are carried out the line remains within thermal limits and DG is only brought back on as and when loading permits.

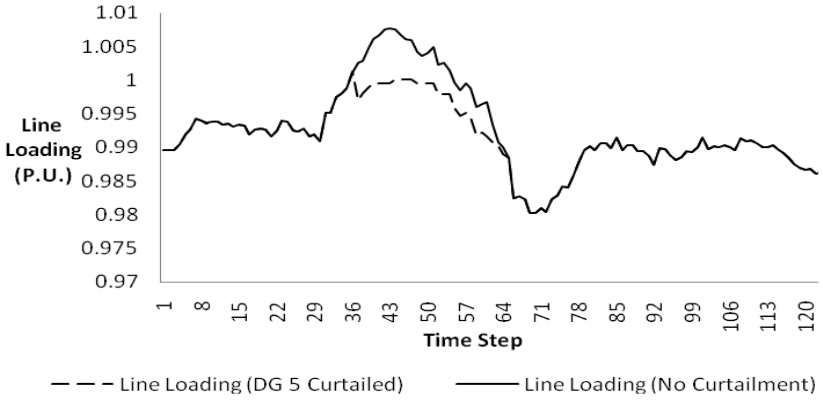

Figure 54 - Line Loading with and without DG Curtailed

For the above 'Test Scenario 5' the four control signals, shown in Figure 53, are calculated in 48.6, 83.1, 50.5 and 55.9ms, respectively.

4.5.2 Test Scenario 6: 33kV Interconnected Distribution Network with 'Line 1' Overloaded and DG 3 being the Last Historically Connected DG Unit

The effect that the order of priority has on the curtailment results is tested by applying the same profiles with the exception that DG 3 is deemed to be the last historically connected unit. Figure 55 shows the control signals (secondary vertical axis), the MW output and the potential DG output (primary vertical axis) for DG 3.

In this case there are five initial curtailment signals between 'time-step 37 and 41'. These control signals are revised as congestion on 'Line 1' increases with the increase of load at 'Sub A'. The control signals calculated and sent are 0.715, 0.6813796, 0.641525, 0.5878112 and 0.5310767. When the first control signal is sent DG 3 starts to reduce its output to the desired level of 1.716MW in incremental steps of 0.12MW per time step to represent the generator's ramp down rate. This ramp rate is deemed to be 5% of rated output per time step (and is reconfigurable within the software) to simulate the response of a controlled DG unit. The time steps are of one second duration for the purpose of the simulation, however these simulations could represent hourly/daily profiles depending on the resolution of monitoring set by the DNO. For the purpose of these one second time steps the cycling of the monitoring and detection algorithm every three seconds is appropriate, however this can be reconfigured by a DNO to any cycle deemed appropriate for the network's assets. This set point is superseded by the other revised control signals and the generator continues to ramp down to meet the last control signal's desired output limit, 1.274584MW. The unit remains at this level until the curtailment can be relaxed. At 'time step 53' the level of curtailment can be reduced to 0.7424158 and the unit can output up to 1.78179MW. This is not reached as another control signal, 0.8123496 sent at 'time step 57', superseding this previous set point and allowing the unit to export up to 1.949639MW. A further relaxation in curtailment is permitted at 'time step 61' when the signal of 0.9527575 is received by DG 3 enabling the unit to ramp up to 2.2866MW. The curtailment is fully removed at 'time step 65'.

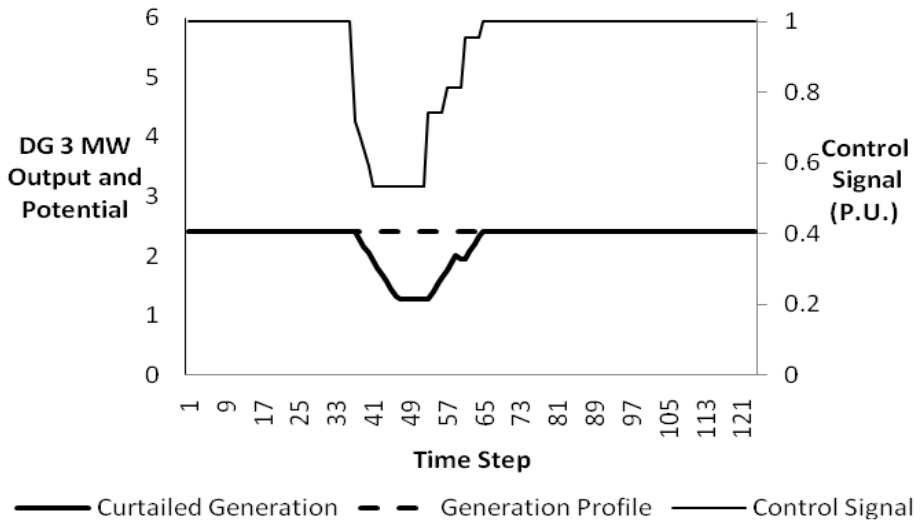

Figure 55 - Case Study B - Line 1 Overloaded with DG 3 having the Lowest Priority

In Figure 56 the line loading is shown for the inputted DG and load profiles. The case is shown for the algorithm taking no action and therefore the line running overloaded. The line loading is also depicted for the above case when DG control actions are carried out to alleviate the thermal overload. It is clear that when the above control actions are carried out the line remains within thermal limits and DG is only brought back on as and when loading permits.

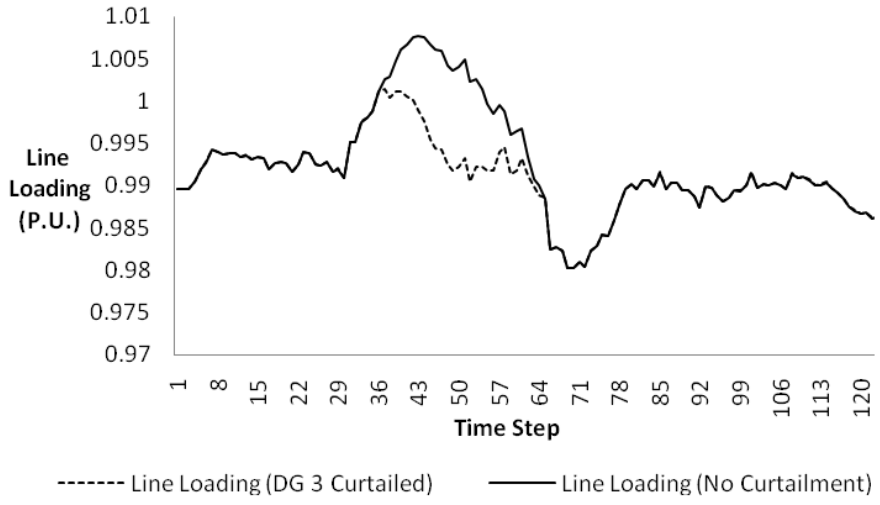

Figure 56 - Line Loading with and without DG Curtailed

The computation times to arrive at the solutions for ‘Test Scenario 6’ are detailed within Table 8, below.

Table 8 - 'Test Scenario 6' Solution Computation Times

Control Signal	Computation Time (ms)
1	63.77
2	60.76
3	61.36
4	92.58
5	91.03
6	70.38
7	94.20
8	92.78
9	97.78

It is notable from Figure 57, below, that for the same overload condition differing levels of curtailment were required due to the geographic location of the DG units. For ‘test scenario 5’ a total of 34.12MW were curtailed throughout the thermal overload. In ‘test scenario 6’ the resultant curtailment totalled 19.04MW.

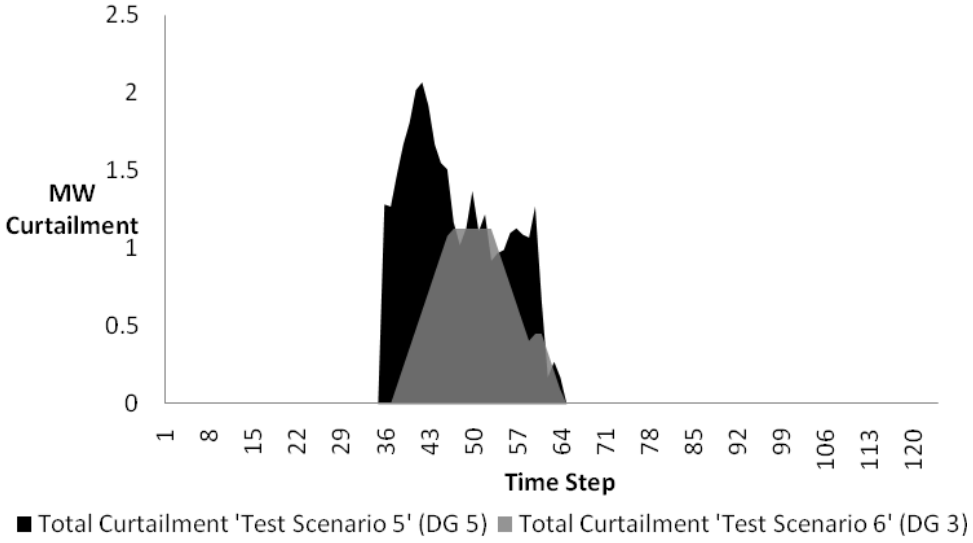

Figure 57 - Total Curtailment for 'Test Scenario 5 & 6'

4.5.3 Test Scenario 7: 33kV Interconnected Distribution Network using Double the Load Profile to Overload 'Line 1'

With the same connection priority maintained as that of 'Test Scenario 6' the load at 'Sub A' is doubled to increase the magnitude of the thermal constraint. The DG units' connection order list now has to be used more extensively by the OPF-LIFO algorithm to manage the congestion. DG units 3, 4 and 5, prioritised as 10th, 9th and 8th respectively (Table 7), are curtailed in the appropriate order to keep the network within thermal limits, Figure 58. As system loading changes, these generating units are brought back on in the reverse order. With DG 3 offline and DG unit 5 operating at maximum rated output the DG unit 4 control signal fluctuates against the network conditions to ensure that thermal limits are adhered to. In this case loading is such that DG unit 3 must remained offline.

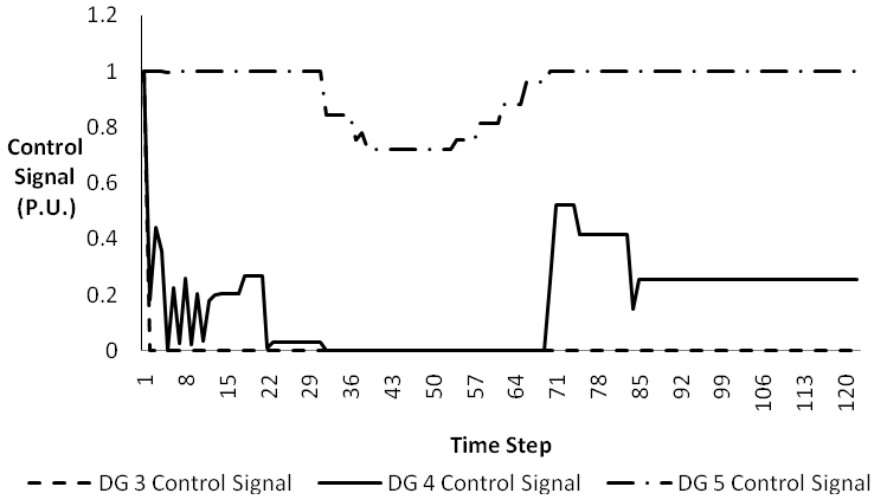

Figure 58 - Case Study B - Line 1 Overloaded due to Increasing 'Sub A' Load Twofold with DG 3, DG 4 & DG 5 having the Lowest Priorities, Respectively

4.5.4 Test Scenario 8: 33kV Interconnected Distribution Network under a Single Circuit Outage Condition

In this further test scenario the original load profiles were used whilst maintaining the connection priority set in 'Test Scenario 6', Table 7. To evalute the OPF PFM approach perfomance under a first circuit outage condition 'Line 1' was removed from service forcing a thermal overload on 'Lines 2 & 3', (Figure 26) and later returned back into service to show the resultant control actions.

Figure 59 illustrates the calculated DG unit control signals when 'Line 1' is switched out of service at 'time step 14'. The result of this line outage is a step change in network states and under this system event the order of curtailment is DG units DG 4, DG 3, DG 5 and Hydro B. These units are prioritised as 9^{th}, 10^{th}, 8^{th} and 2^{nd} respectively. This breaks the cost modelled LIFO connection order due to the severity and step change of the states within this situation however the result is less curtailment than enforcing LIFO under this event.

At 'time-step 40' the 'Line 1' is returned back into service. Hydro B station is the first to be allowed back on, followed by units 4 and 5, simultaneously, and then as load levels drop DG 3 ('time step 45') is signalled to run unconstrained. This relaxation of DG curtailment follows the LIFO connection agreement i.e. generators with the lowest priority are brought back online first.

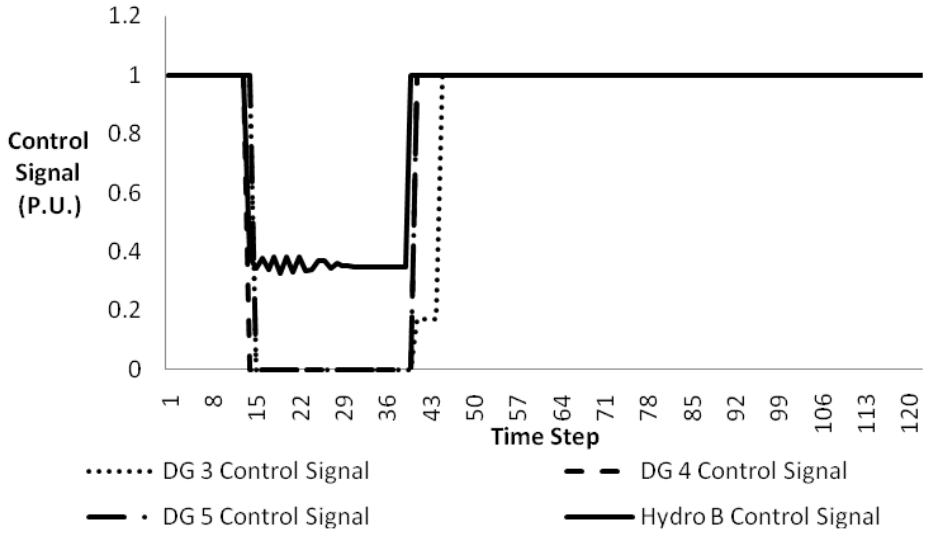

Figure 59 - Case Study B - Line 1 Switched Out DG 3, DG 4, DG 5, DG 6 & DG7 having the Lowest Priorities, Respectively

4.6 Chapter 4 Review: OPF-LIFO Conclusions

The closed loop simulation results presented above demonstrate that the novel application of OPF combined with prototype PFM algorithms, running on a commercially available substation computer platform, has the potential to operate in an online and real-time environment. The OPF-LIFO algorithm successfully detected and offered solutions to manage network thermal constraints. Furthermore, the algorithm recognised when network loading was such that DG curtailment signals could be relaxed and removed. The solution computation times are in the tens of milliseconds range for moderately sized distribution network areas and are therefore well within the timeframe required for thermal overload control.

The overload detection loop is a reconfigurable user input and for the purpose of these studies cycled in a three second loop. This resulted, for the controlled test environment, in slight discrepancies in the actual detection point of the thermal excursion. This is shown in Test Scenario 2 where two runs of the 1% measurement

error case are presented. For practical implementation care would be required to ensure that this potential delay in detection does not breach the short-term/emergency overload ratings of the network plant/circuits.

Continuous monitoring and control leads to progressive DG set point control signals allowing for the LIFO representation to be maintained and for good resolution DG set points to be calculated in contrast to the DG unit capacity blocks proposed in other PFM scheme designs. Under network outage conditions and other more onerous operation conditions a solution to the circuit congestion is found through DG unit constraint control but the LIFO connection agreements are not honoured. The outcome in this case allows greater energy yields across the DG units than that of conventional methods i.e. inter-tripping of all 'non-firm' DG units. This non-conformity of the LIFO principle of access demonstrates the potential for OPF to be used under different connection principles such as DG bids for access to distribution network capacity or some form of access sharing to enhance DG access.

In summary, the novel OPF-LIFO approach has been found, through implementation and testing, to be viable in terms of robustness (find a practical solution under all test cases), speed of computation and the ability to represent existing (i.e. LIFO) and alternative principles of access to distribution network capacity.

.

4.7 Chapter 4 References

[4.1] P. C. Taylor, T. Xu, S. McArthur, G. Ault, E. Davidson, M. Dolan, C. Yuen, M. Larsson, D. Botting, D. Roberts, and P. Lang, “Integrating voltage control and power flow management in AuRA-NMS," CIRED Seminar 2008: Smart Grids for Distribution, Frankfurt, 2008

[4.2] P. C. Taylor, T. Xu, N. S. Wade, M. Prodanovic, R. Silversides, T. Green, E. M. Davidson, S. D. J. McArthur. “Distributed voltage control in AuRA-NMS” IEEE Power Engineering Society General Meeting, July 2010, pp. 1-7

[4.3] PowerWorld Corporation, “PowerWorld Simulator version 11 Manual”, available at: http://www.powerworld.com/Document%20Library/pw110UserGuide.pdf, accessed 6th May 2012

Chapter 5

Power Flow Management with the Constraint Satisfaction Problem

5.1 Summary of Chapter 5

This chapter details the modelling approach of the second technique to active power flow management (PFM) using the Constraint Satisfaction Problem (CSP). The characteristics of the CSP are described in terms of their relevance to the formulation of the PFM technique. Utilising the steady-state test environment, case study networks and profiles introduced in Chapter 3, results from the CSP-LIFO approach to PFM are documented in terms of the number of control signals issued to DG units and the computation timescales. The scenarios to which the approach is applied are introduced prior to the presentation of the results and are identical scenarios to those used in chapter 4 for the OPF-LIFO approach to PFM. Conclusions are then drawn from the case study results with regards to the approach's performance within a real-time control environment.

5.2 Developing the Constraint Satisfaction Problem (CSP) as a Power Flow Management (PFM) Technique in Distribution Systems

In Chapter 3 the general concept and properties of the CSP were examined in terms of their variables, domains and constraints. This section describes the variables, domains and constraints required for a power flow management CSP-LIFO algorithm.

5.2.1 Modelling Power Flow Management (PFM) as a Constraint Satisfaction Problem (CSP)

To model the power flow management problem as a CSP the problems would be expressed as a set of *variables* with finite discrete *domains* and a set of *constraints*. In the case of PFM, it is assumed that the problem to be solved is concerned with deciding what control actions to take in order to maintain flows within the thermal

limits (i.e. constraints) of the network. The *variables* of the CSP are the controllable generating plant power output set-points. Associated with each generator set-point is a *domain* of discrete values which are the maximum values that the generator output may be set to. However, DG operation is such that its output is continuous up to this discrete set-point value.

Generators can therefore be sent discrete trim/trip control signals. This means the generator can "run without curtailment", i.e. generate as much or as little real power as it wishes or as is available. Alternatively, the generator must "run curtailed" and reduce its output to below a given threshold to avoid thermal overloading. Each generator is given a number of discrete curtailment bandings, e.g. 80% rated output, 50% rated output, 0% rated output etc. The curtailment bandings represent a generator variable's *domain*, e.g. **{***1, 0.8, 0.5, 0***}**, where 1 represents operation without curtailment and 0 represents the tripped state. Utilising discrete bands in this way enables the definition of a simple contract between the host DNO and the generator in which the generator can clearly distinguish the actions that the DNO is permitted to take. The CSP approach places no restriction on what the domain values represent. For the PFM problem, they represent generator real power set-points.

In addition to *variables* and their *domains*, the *constraints* on the solution must be modelled. For the PFM problem the following *constraints* have been defined in this research*:*

- **Power flow constraints.** Any potential solution in the form of control actions sent to generators must fulfil a power flow constraint, i.e. a given set of control actions will not result in the thermal overload of any plant given the current network conditions. This constraint can be checked using a suitable network model and load flow engine, if loads at key network points can be measured or estimated and generator output is measured.

- **Contractual constraints**. Generator access rights place further constraints on possible solutions. Non-firm DG units in some countries are typically connected to the network with LIFO network access rights (e.g. in the UK). These access rights can be expressed as a constraint or set of constraints.

- **Preference constraints**. For a given situation, there may be many sets of control actions which meet the constraints above. For example, due to the network design rules, thermal overloads are unlikely to occur when all generation is tripped (unless another contingency has occurred). As a result the CSP solver requires a preference constraint or set of preference constraints to capture information about what solutions have greater value in a similar way to the objective function in optimisation. Preference constraints are used by the CSP solver to decide when one solution is better than another and guide the search for solutions. In the case of PFM, a preference constraint can be used to make the CSP solver check potential solutions that maximise DG access, while meeting contractual constraints.

Applying the PFM problem to the general CSP definition and incorporating the specific constraints. PFM modelled as a CSP can be represented as:

$$(V_{gens}, D_{Gens}, C) \tag{5.1}$$

Where:

$$V_{gens} = \{Gen_{1,} Gen_{2,....,} Gen_{n}\} \tag{5.2}$$

$D_{Control\ Signal}$ is:

$$D_{Gen1}=\{1,...,0\},\ D_{Gen2}=\{1,...,0\},\ D_{Genn}=\{v_1.., v_n\} \tag{5.3}$$

And:

C is the constraint applied to the sets of variables:

$$C_{\text{Power Flow}} = \{ -S_{ij}^{\max} \leq S_{ij} \leq S_{ij}^{\max} \} \quad (5.4)$$

$$C_{\text{Contractual}} = \{Gen_1 = 3, Gen_2 = 2, Gen_n = 1\} \quad (5.5)$$

$$C_{MaxDG} = \left\{\max \sum_{n=1}^{NGens} P_{Geni}\right\} \quad (5.6)$$

5.2.2 Constraint Satisfaction Problem (CSP) Search Space and reducing Computation Time

The initial size of the search space depends on the number of variables and the domain sizes. For the PFM problem this depends on the number of controllable units, i.e. the generators and the number of curtailment bandings for each controllable device. By applying constraints to the search space, it is possible to search the space efficiently and hence reduce the computation times to return a solution or all solutions. In the case of PFM, the introduction of the contractual constraint, i.e. the least computationally expensive, enables feasible solutions to found quicker by only running the load flow engine on feasible solutions that meet the contractual constraint, i.e. the solution meets the LIFO generator arrangements. Checking the contractual constraints in essence orders the variables and therefore the path through the state space can be defined. It is then possible to return all solutions that meet both the contractual constraint and the load flow constraint. In addition, this approach allows the preference constraint to be met by selecting the first solution found for implementation, i.e. the solution that maintains the maximum DG access to the network. As the contractual constraint has pruned the search space, in terms of running load flows, the load flows need only be run at each variable's domain value. If the load flow constraint returns false, the next variable's domain value is checked and evaluated. In doing so, the number of feasible solutions within the search space can be approximated by k^G. Where k is the average size of the domain and G is the number of generators. This presents an exponential increase in the state space when further generators are added into the problem. This combinatorial explosion in size of the search space also has implications on the computation time involved in searching

the space. One method of achieving a reduced computation time is to limit the number of discrete domain values i.e. the discrete curtailment bands.

The conditions for labelling the variables are: when the contractual constraint returns true for all variable assignments and when a load flow returns true for the assigned variables (the variables will be labelled with the domain value that passed the load flow constraint); and when a variable's domain is exhausted (the last domain value will be assigned).

It can be noted that for the PFM problem, modelled in this manner, that all solutions below the initial assignment are also valid, down to the solution where all generation is tripped off. This is due to network planning that ensures all demand can be met from traditional central generation plants. For this reason the use of backtracking is not required to search the state space. This characteristic of the CSP inherently builds-in graceful degradation, where, if the first 'optimal' solution fails due to model or measurement error then the next successive solutions can be implemented until all power flows are within thermal limits.

Figure 60 depicts the search space for a 2 generator (variable) case with domain values for each generator equal to 0, 0.5, 0.8 and 1. Generator A is deemed to be the last historically connected unit in this case. The subsequently described steps show that only load flows are run when the priority constraint is met.

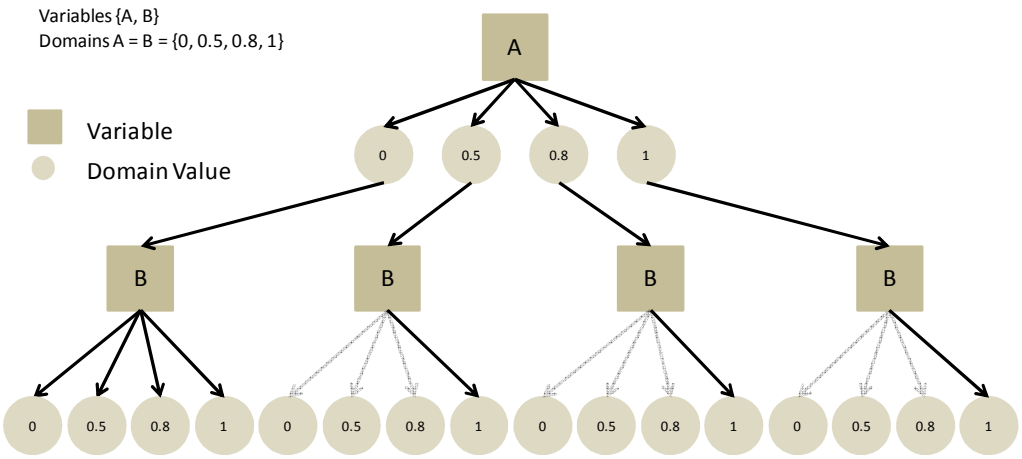

Figure 60 – Illustration of CSP-LIFO Search Space

For the search space in Figure 60, the search steps are presented below, illustrating that the least computationally expensive priority constraint is evaluated for each assignment of variable values (from the respective domains) prior to running the more computationally expensive load flow constraint. Therefore, the load flow constraint is only run on valid variable assignments.

Step 1: Evaluate A = 1 & B = 1 against priority constraint – passes
Step 2: Assign A = 1 & B = 1 – Load flow fails as these are the starting conditions
Step 3: Evaluate A = 1 & B = 0.8 against priority constraint – Fails
Step 4: Evaluate A = 1 & B = 0.5 against priority constraint – Fails
Step 5: Evaluate A = 1 & B = 0 against priority constraint – Fails
Step 6: Branch search exhausted move to next branch
Step 7: Evaluate A = 0.8 & B = 1 against priority constraint – passes
Step 8: Run load flow and check for overloads (pass = solution, fail = continue)
Step 9: Evaluate A = 0.8 & B = 0.8 against priority constraint – Fails
Step 10: Evaluate A = 0.8 & B = 0.5 against priority constraint – Fails
Step 11: Evaluate A = 0.8 & B = 0 against priority constraint – Fails
Step 12: Search Branch exhausted move to next branch
Step 13: Evaluate A = 0.5 & B = 1 against priority constraint – Passes
Step 14: Run load flow and check for overloads (pass = solution, fail = continue)

Step 15: Evaluate A = 0.5 & B = 0.8 against priority constraint – Fails

Step 16: Evaluate A = 0.5 & B = 0.5 against priority constraint – Fails

Step 17: Evaluate A = 0.5 & B = 0 against priority constraint – Fails

Step 18: Search branch exhausted move to next branch

Step 19: Evaluate A = 0 & B = 1 against priority constraint – Passes

Step 20: Run load flow and check for overloads (pass = solution, fail = continue)

Step 21: Evaluate A = 0 & B = 0.8 against priority constraint – Passes

Step 22: Run load flow and check for overloads (pass = solution, fail = continue)

Step 23: Evaluate A = 0 & B = 0.5 against priority constraint – Passes

Step 24: Run load flow and check for overloads (pass = solution, fail = continue)

Step 25: Evaluate A = 0 & B = 0 against priority constraint – Passes

Step 26: Run load flow and check for overloads (pass = solution, fail = no solution)

The CSP-LIFO PFM software functionality was achieved by developing the PFM algorithm in combination with an off-the-shelf constraint solver [5.1] and load flow engine [5.2] (TNEI's IPSA software). The constraint solver is an open-source Python library called 'Python Constraint' [5.1]. This module hosts solvers for the finite discrete domain CSPs and currently has backtracking, recursive backtracking and minimum conflict solving capability. The PFM software, written in Python, interfaces with the load flow engine (mapping load and generation data from each of the devices IEDs) to provide the thermal overload detection functionality. In addition, the PFM software integrates with the CSP solver as a means of evaluating the contractual, preference and load flow constraints. Figure 61 shows the required inputs, the software interactions and the resultant output of the CSP-LIFO PFM algorithm.

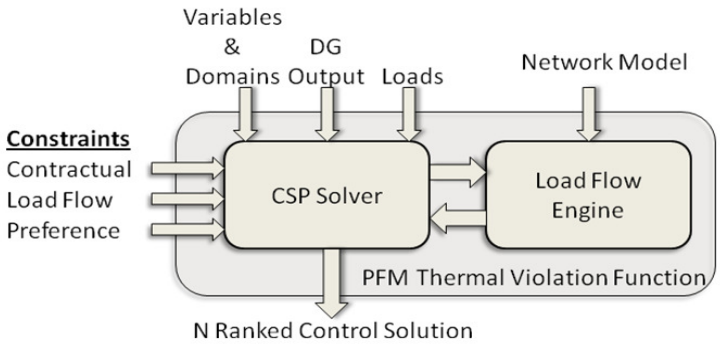

Figure 61 - Inputs and Outputs of the Software Interactions for PFM Modelled as a CSP

When a thermal overload is detected and a solution found, the PFM software maps the calculated control signals to the appropriate DG units and returns the solution back to the dedicated pc for implementation. These attributes of the CSP-LIFO PFM approach were embedded within the real-time test environment, illustrated in Figure 62, with profile data being inputted in the IEC61850 standard via OPC from the dedicated PC.

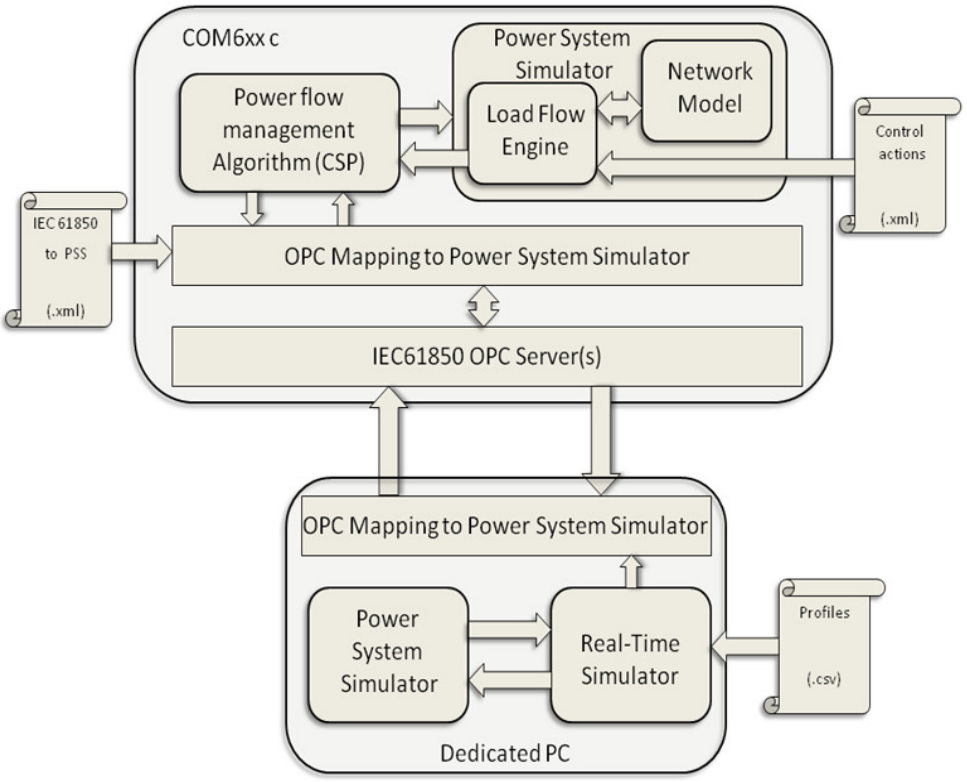

Figure 62 - Hardware and Software Interface and Function Interactions

The following sections present the results of the CSP-LIFO control approach when applying the profile based scenarios to the simulation environment. These profiles were updated once a second and monitored, for thermal excursions, every three seconds, for the 'Test Scenarios' described prior to the associated results (the same 'Test Scenarios' conducted for the OPF-LIFO approach to PFM).

5.3 CSP-LIFO: 11kV and 33kV Case Study Results

For the two case study networks the algorithm performance will be discussed in terms of the control signals issued to generators, the MW output from the DG units, the MW curtailment levels and the computation time to calculate solutions.

For Case Study A, Figure 63, load and generation profiles were used to demonstrate algorithm performance with:

- Perfect measurement;
- 6% measurement error superimposed onto the load profile; and
- 1% measurement error superimposed onto the load profile (normalised against the 6% error)

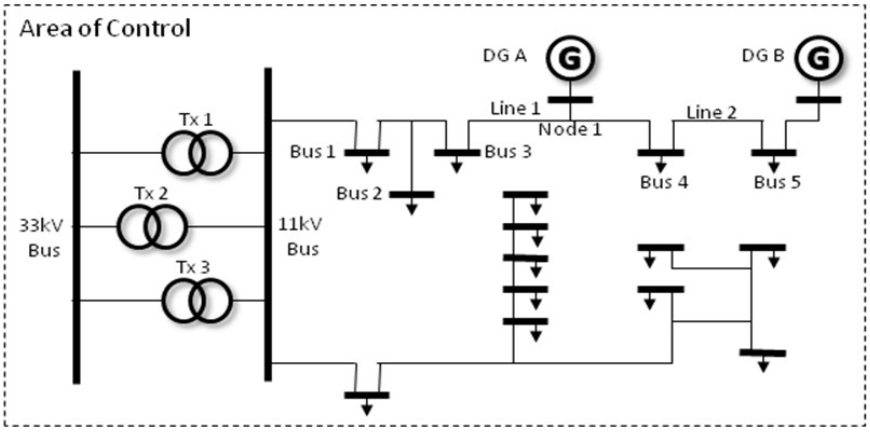

Figure 63 – Case Study A - 11kV Radial Distribution Network

For Case Study B, Figure 64, load and generation profiles were utilised to demonstrate the algorithm's behaviour with:

- Perfect measurement;
- Increased loading on the 33kV network (twice the load profile); and
- Single circuit outage on the 33kV network.

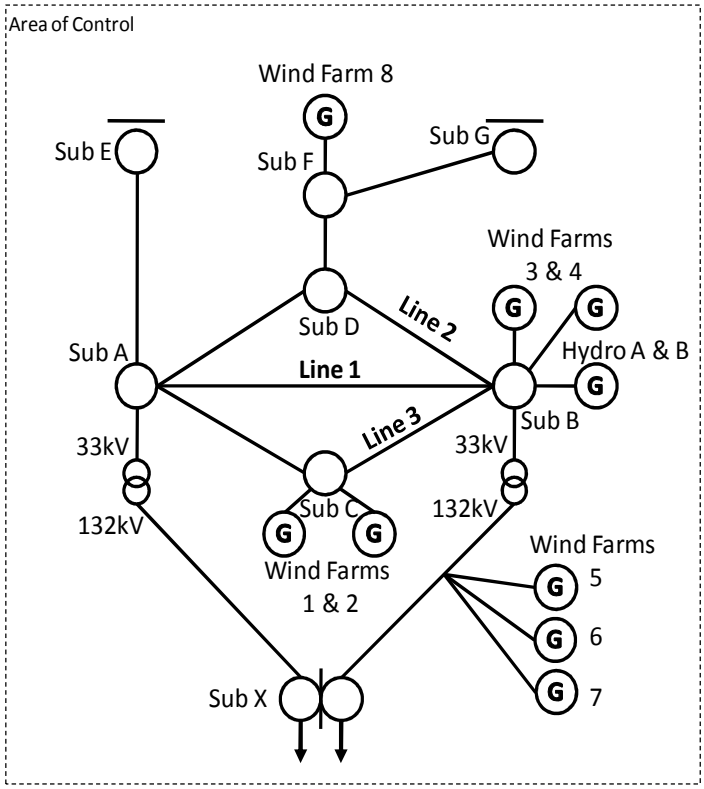

Figure 64 – Case Study B - 33kV Interconnected Distribution Network

5.4 Case Study A – 11kV Radial Distribution Network

In each of the following test scenarios the variables and domains remain constant with only the priority constraint being changed. Variables and domains are as follows:

$V_{gens} = \{DG\ A = 1.6MW, DG\ B = 2MW\}$

$D_{DG\ A} = \{1, 0.8, 0.5, 0.2, 0\}$ & $D_{DG\ B} = \{1, 0.8, 0.5, 0.2, 0\}$

i.e. DG A can operate uncurtailed at 1.6MW, or curtailed at (1.6MW x 0.8), (1.6MW x 0.5), (1.6MW x 0.2) or tripped at (1.6MW x 0). DG B can operate with the same bandings with the exception that its rated output is 2MW.

The solutions must meet the load flow constraint:

$$C_{\text{Power Flow}} = \{ -S_{ij}^{\max} \leq S_{ij} \leq S_{ij}^{\max} \}$$

With either of the assigned priority constraints depending on the presumed order of connection for each of the 'Test Scenarios':

$C_{Contractual} = \{\text{DG A} = 1, \text{DG B} = 2\}$ or $C_{Contractual} = \{\text{DG A} = 2, \text{DG B} = 1\}$

In the above formulation a '1' ranks the DG unit as being the first historically connected unit and therefore the last unit that is required to respond to the thermal constraint.

In the following 'Test Scenarios' there is no need to utilise the preference constraint as the first 'optimal' solution is found and implemented. However, it is an important characteristic of the CSP approach as severe measurement error or failure of one of the DG units to respond to a control signal may require the next best 'ranked' solution to be implemented.

5.4.1 Test Scenario 1: 11kV Radial Distribution Network with 'Line 1' Overloaded and DG A being the Last Historically Connected DG Unit

With 'Line 1' de-rated and DG A (Figure 63) deemed to be the last historically connected DG unit the non-erroneous load and DG profiles are applied via the simulation environment which results in a thermal limit breach on 'Line 1'.

Figure 65 shows the resultant control signals sent to DG A whereby a 20% reduction in output is instructed on two separate occasions. At 'time step 40' variable DG A is assigned the value '0.8' from its finite domain set and is therefore constrained to output 80% of its maximum output until the network conditions change such that the control signal can be relaxed. Network loading is such at 'time step 68' where the domain value of '1' is assigned to variable and a signal is sent to allow the generator to run unconstrained. A further 80% reduction is required at 'time step 80' until the DG unit is allowed to operate unconstrained at 'time step 89'. It can be noted that DG B, for this case, can operate uncurtailed for the duration of the simulation.

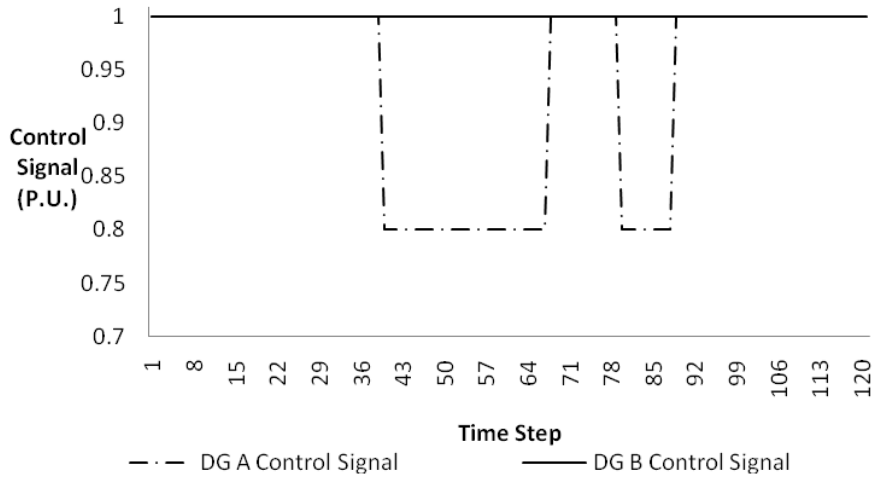

Figure 65 - Case Study A - Line 1 Overloaded with DG A having the Lowest Priority

In Figure 66 the line loading and limit is shown for the inputted DG and load profiles. The case is shown for the algorithm taking no action and therefore the line running overloaded. The line loading is also depicted for the above case when DG control actions are carried out to alleviate the thermal overload. It is clear that when the above control actions are carried out the line remains within thermal limits and DG is only brought back on as and when loading permits.

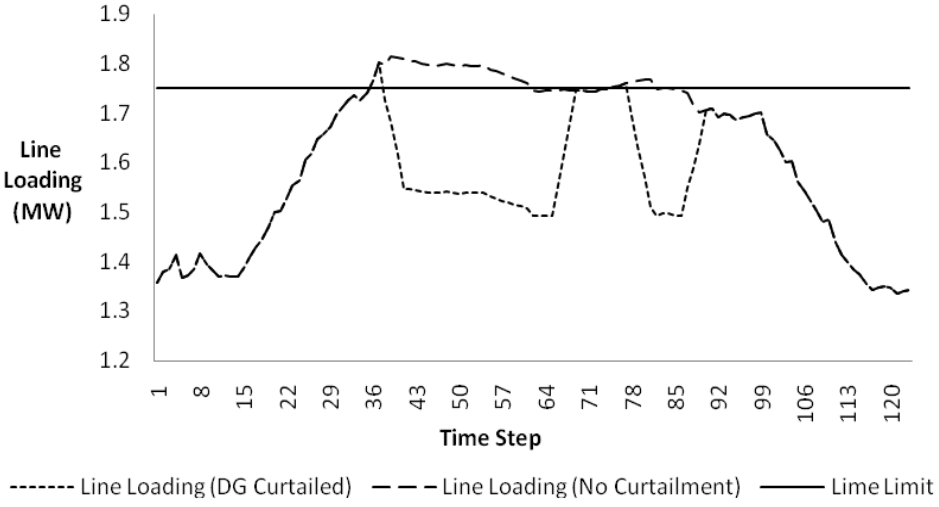

Figure 66 - Line Loading with and without DG Curtailed

The same scenario was run with the 6% error applied to the load profile. The impact of measurement error is illustrated against the result of the 'perfect' measurement case. It can be observed that, for the 6% load error, there was a delay ('time step 45') in the initial detection of the thermal excursion. The detection algorithm looped in a three second cycle therefore it is not clear whether the measurement error is completely at fault for the delay or whether the detection cycle exacerbates the delayed response. However the same level of curtailment, 20%, is issued via the control signal to the DG unit. At 'time step 70' curtailment of the DG unit is relaxed and the unit can operate up to maximum rated output. The next 20% reduction is required at 'time step 76' – 4 seconds in advance of the 'perfect' measurement scenario. Again, it is unclear whether measurement error is solely at fault or whether

the detection loop plays a role. However, it is apparent that measurement error is responsible for allowing the DG unit to run unconstrained during the thermal overload between 'time step 83 and 89'. At 'time step 93 generator DG A can run unconstrained for the duration of the simulation.

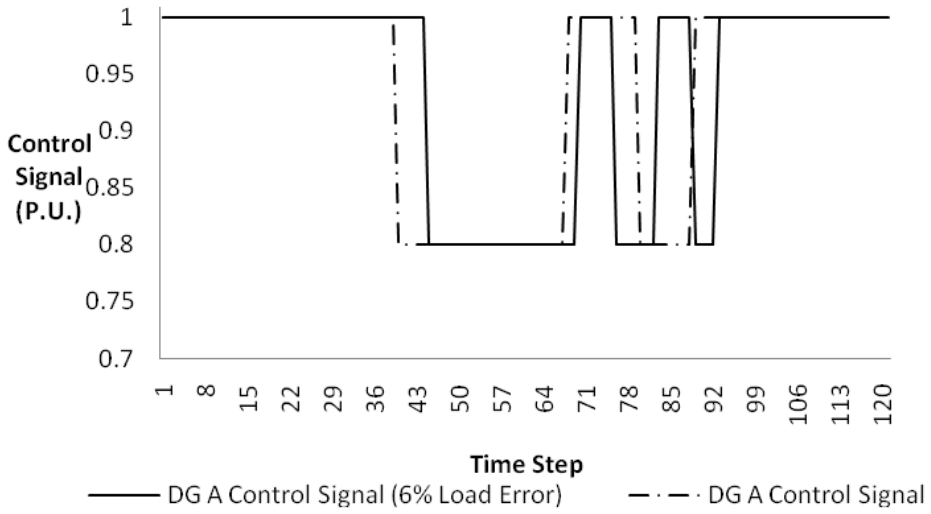

Figure 67 - Case Study A - Line 1 Overloaded with DG A having the Lowest Priority with and without 6% Erroneous Load Measurements

Figure 68 illustrates the same situation of DG A having the lowest priority and 'line 1' being subjected to a thermal overload however the 1% erroneous load measurements are used. For the 1% load error case there was little deviation in actual time steps that control signals were sent to the DG unit from that of the 'perfect' measurement scenario. The initial, of the four control signals, 20% reduction was signalled at 'time step 40' – the same instant as the 'perfect' scenario. The three subsequent control signals were sent 1 second prior (next two) and 1 second after (final signal) that of 'perfect' measurement case. It is therefore unclear as to whether or not a 1% measurement error is totally attributable to the small deviations or whether the detection loop cycle plays a positive or negative role.

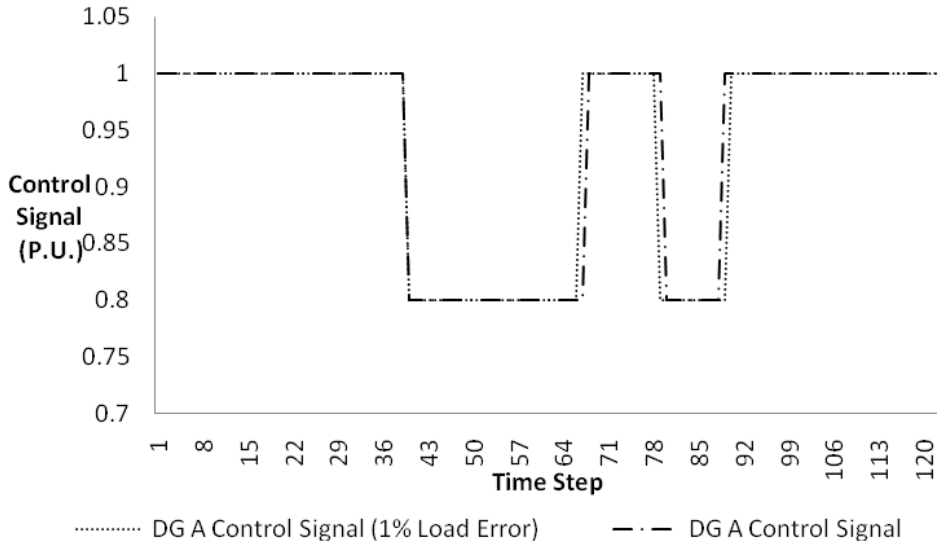

Figure 68 - Case Study A - Line 1 Overloaded with DG A having the Lowest Priority with and without 1% Erroneous Load Measurements

The impact of false signals being transmitted to DG A is illustrated in the following two figures. In each of the figures the primary vertical axis shows the MW output of DG A as the control signals are sent while the secondary vertical axis plots the MWs curtailed. Both axes show the cases with and without measurement error.

In Figure 69, from the primary vertical axis, it can be observed that when the DG unit is constrained to operate at a maximum of 80% of its rated output it ramps down to 1.28MW from 1.6MW (rated output). Output fluctuates between these values until the DG unit can finally operate at rated output. In terms of the MW curtailment levels, from the secondary vertical axis, the 'perfect' measurement case has a total of 11.44MW that are trimmed off during the simulation. For the 6% erroneous load case a total of 10.88MWs are curtailed.

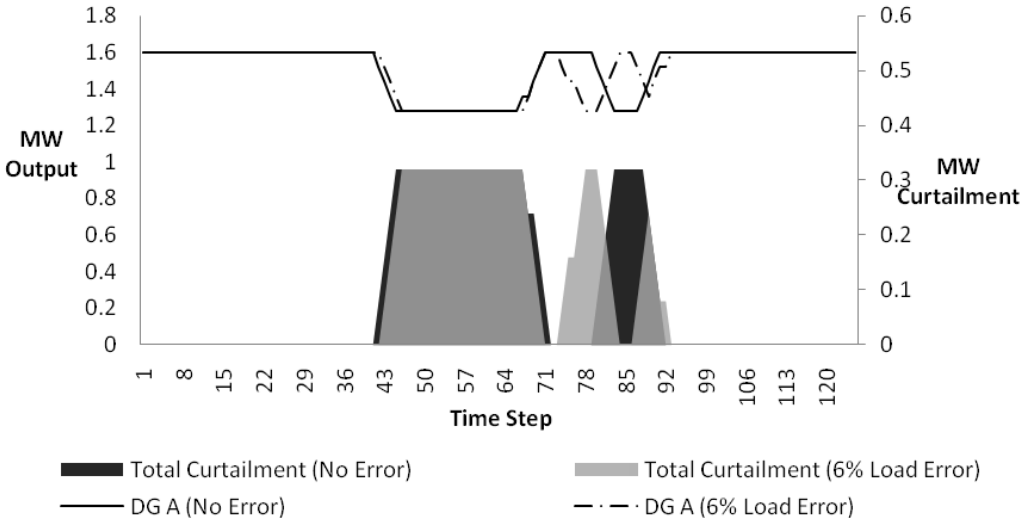

Figure 69 - Case Study A - Line 1 Overloaded with DG A having the Lowest Priority. DG A MW Output and Curtailment Graphed for 'Perfect' and 6% Erroneous Load Measurements

In Figure 69 the DG unit can be seen to ramp down to 80% of its rated output value – from 1.6MW to 1.28MW – on the two occasions that control signals are issued. From the secondary vertical axis the curtailment totals can be examined. The 1% load error case curtails a total of 11.68MW compared with that of 11.44MW for the 'perfect' measurement case.

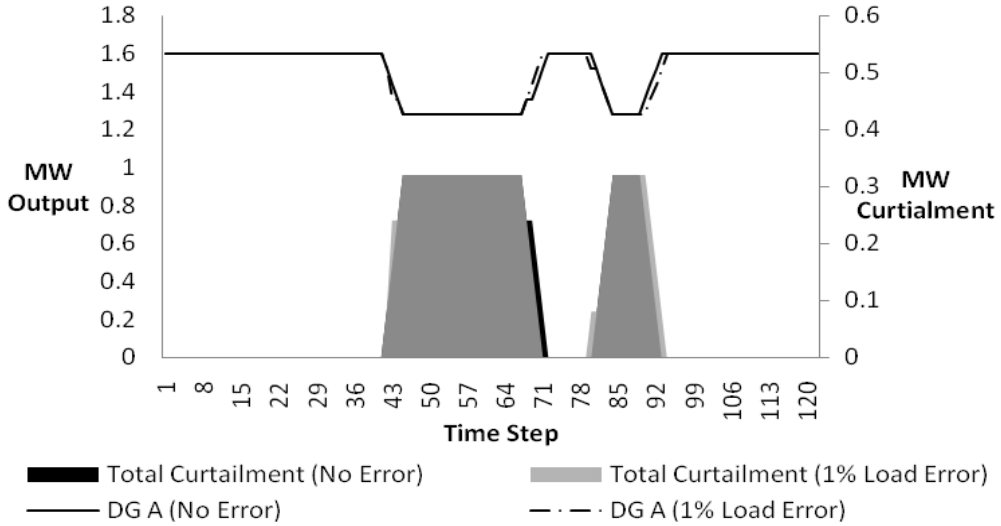

Figure 70 - Case Study A - Line 1 Overloaded with DG A having the Lowest Priority. DG A MW Output and Curtailment Graphed for 'Perfect' and 1% Erroneous Load Measurements

5.4.2 Test Scenario 2: 11kV Radial Distribution Network with 'Line 1' Overloaded and DG B being the Last Historically Connected DG Unit

With 'Line 1' de-rated and now DG B (Figure 63) deemed to be the last historically connected DG unit the non-erroneous load and DG profiles are applied via the simulation environment which results in a thermal limit breach on 'Line 1'.

Figure 71 shows the control signals issued to DG B for this overloaded scenario without load error. The thermal excursion is detected at 'time step 40' – the same detection point that 'Test Scenario 1', without load error, encountered the network constraint. Under this connection arrangement DG B is sent one control signal limiting DG output to 80% of its rated output for the duration of the simulation. DG A can operate uncurtailed for the entire test case.

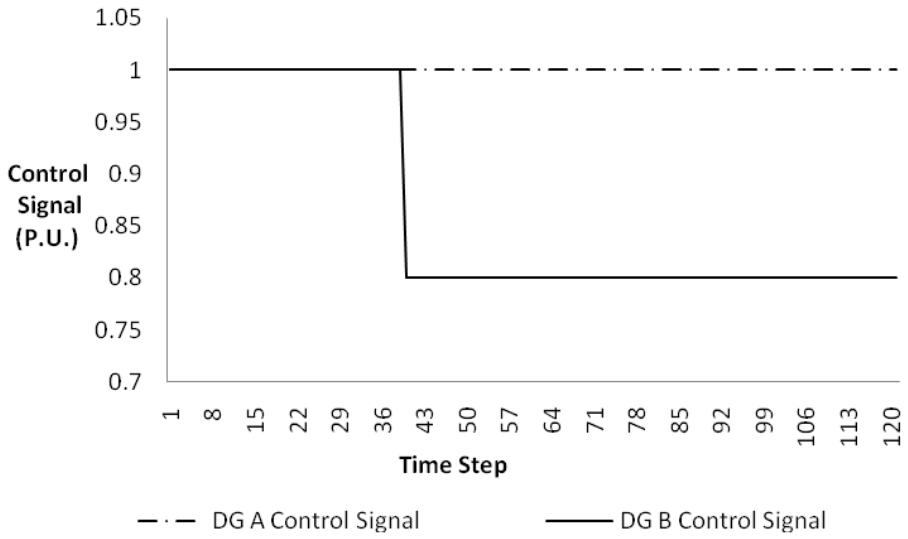

Figure 71 - Case Study A - Line 1 Overloaded with DG B having the Lowest Priority

In Figure 72 the line loading and limit is shown for the inputted DG and load profiles. The case is shown for the algorithm taking no action and therefore the line

running overloaded. The line loading is also depicted for the above case when DG control actions are carried out to alleviate the thermal overload. It is clear that when the above control actions are carried out the line remains within thermal limits and DG is only brought back on as and when loading permits.

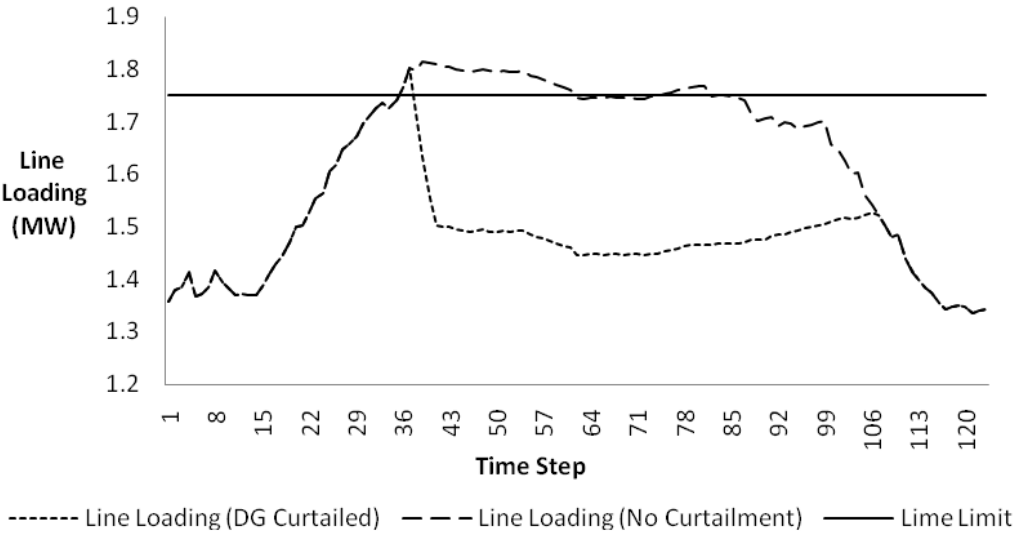

Figure 72 - Line Loading with and without DG Curtailed

Figure 73 illustrates the same scenario but with the 6% erroneous load measurements simulated. The inclusion of measurement error, at this level, entails a delay in the detection that occurs at 'time step 42', thereafter DG B is curtailed to 80% of rated output. Due to the detection loop cycle it is unclear as to whether or not measurement error is solely responsible for this delay in the control signal being issued. However, DG B is allowed, on two occasions, to operate unconstrained during the thermal event at 'time step 67 and 76' thus feeding into the overloaded line, 'Line 1'. These two occurrences are directly attributable to the 6% erroneous load measurements.

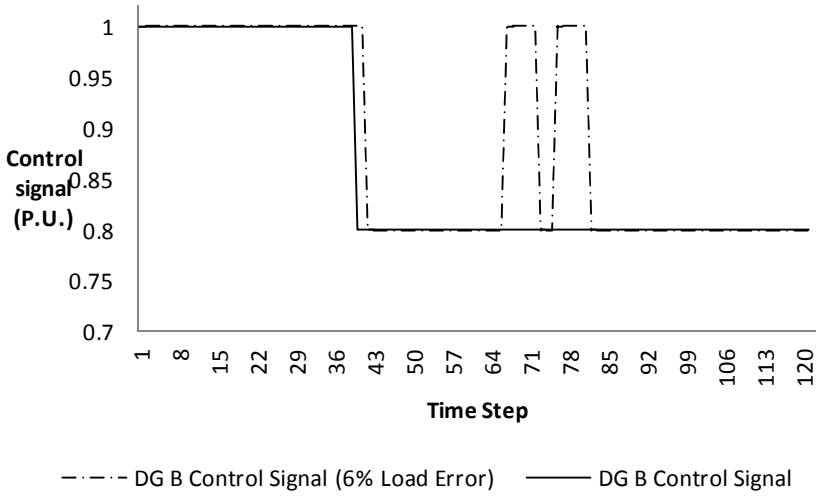

Figure 73 - Case Study A - Line 1 Overloaded with DG B having the Lowest Priority with and without 6% Erroneous Load Measurements

Figure 74 shows that with a measurement error of 1% the detection and curtailment is equal to that of the perfect measurement scenario. At 'time step 40' the overload is detected and DG B remains constrained at 80% output for the duration of the simulation.

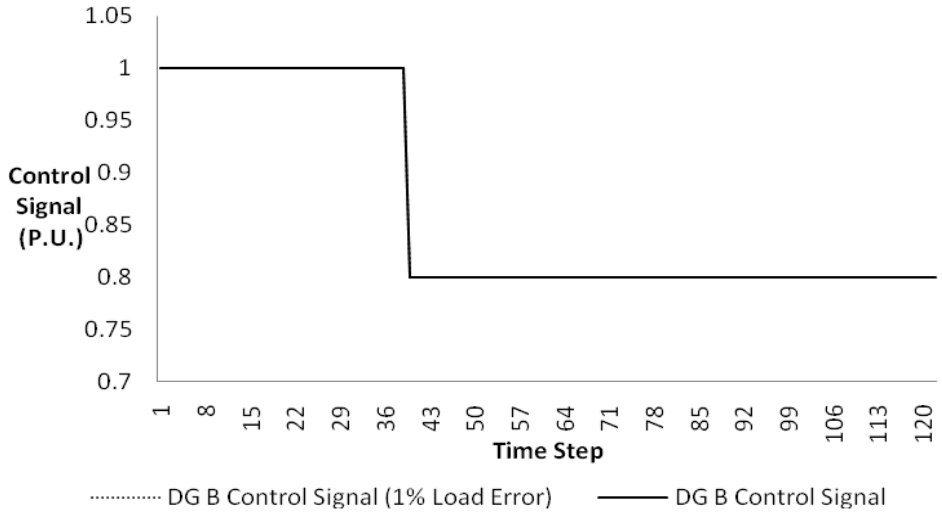

Figure 74 - Case Study A - Line 1 Overloaded with DG B having the Lowest Priority with and without 1% Erroneous Load Measurements

The impact of false signals being issued to DG B is illustrated in the following two figures. In each of the figures the primary vertical axis shows the MW output of DG B as the control signals are sent while the secondary vertical axis plots the MWs curtailed. Both axes show the cases with and without measurement error.

The MW output of DG B can be seen, Figure 75 primary vertical axis, to ramp up and down as and when the control signals are issued to the unit. The DG unit is rated at 2MW and is constrained to 1.6MW (80% of rated output) during the thermal violation. From this trace there is no evidence of data skew from the DG unit's profile. Both MW output traces drop below 1.6MWs at the end of the scenario, even though they are constrained to 80% output for the entire case duration, due to the intermittency of the renewable unit being represented in its profile. Therefore, as a stochastic DG unit it can only provide power available from its intermittent source, in this case wind. The total curtailment level differs substantially from the 'perfect' measurement case and the 6% load error case. From the secondary vertical axis the total MWs curtailed for the 'perfect' scenario is 22.24MW and the 6% load error case totals only 16.54MW.

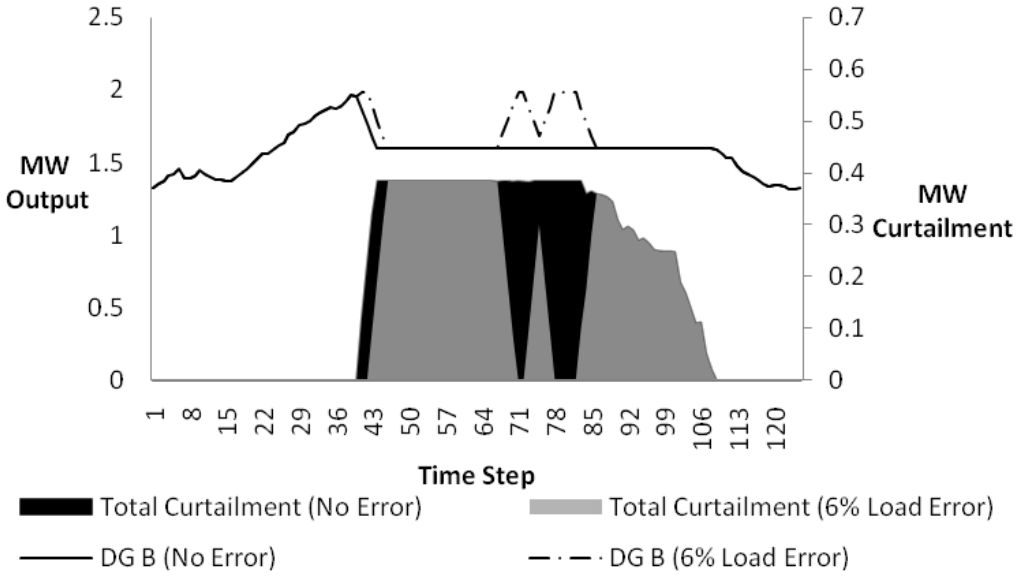

Figure 75 - Case Study A - Line 1 Overloaded with DG B having the Lowest Priority. DG A MW Output and Curtailment Graphed for 'Perfect' and 6% Erroneous Load Measurements

DG B's output trace, shown in Figure 76 primary vertical axis, is seen to be constrained to 80% of its maximum output capability. As with the above case the output is lower than the constrained 1.6MW, towards the end of the study, due to the intermittent nature of wind generation. In this case data skew can be observed within the DG unit output trace. The total curtailment for the 1% load error case sits at 22.18MW compared with 22.24MW from the 'perfect' measurement scenario. Therefore, measurement error at this level, for this case, does not have a significant impact on the curtailed MWs. However, data skew may indeed have an impact – either positive or negative in this case.

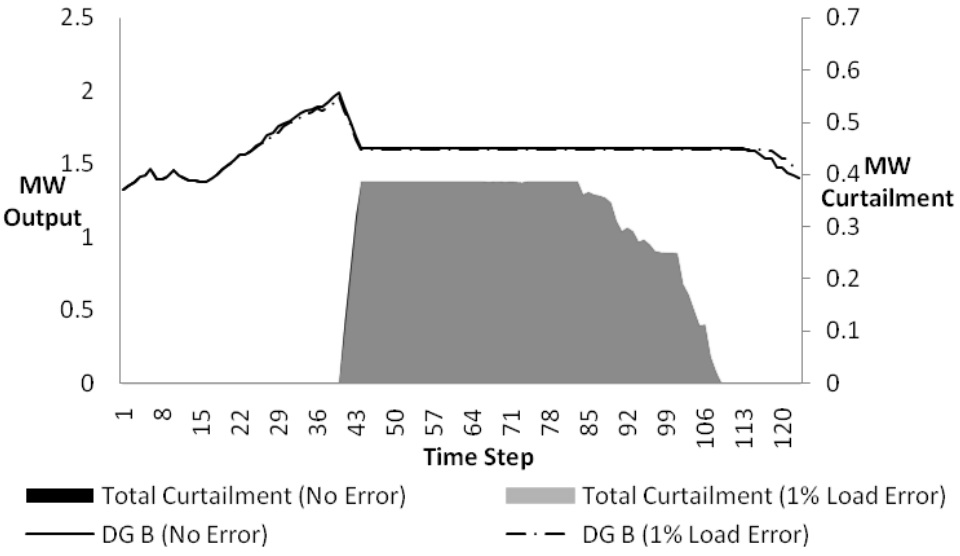

Figure 76 - Case Study A - Line 1 Overloaded with DG B having the Lowest Priority. DG A MW Output and Curtailment Graphed for 'Perfect' and 1% Erroneous Load Measurements

5.4.3 Test Scenario 3: 11kV Radial Distribution Network with 'Line 2' Overloaded and DG A being the Last Historically Connected DG Unit

De-rating of 'Line 2' and applying the DG and 'perfect' load measurement profiles via the simulation environment results in a thermal limit breach on 'Line 2'. For this scenario the DG A (Figure 63) has been assumed to be the last historically connected DG unit and therefore the first to be trimmed to ensure power flow limits are met.

The results in Figure 77 show the curtailment signals sent to both DG units when DG A has the lowest priority order. In this situation even though DG A is not directly contributing to the thermal excursion it is tripped off due to DG B having the higher connection precedence. At 'time step 42 and 43' DGs A and B are curtailed respectively. DG A is sent a control signal that enforces the DG unit is tripped whilst DG B is curtailed to 80% of rated output. When network loading is such that the overload ceases, at 'time step 66', both DG units are instructed that uncurtailed operation can resume.

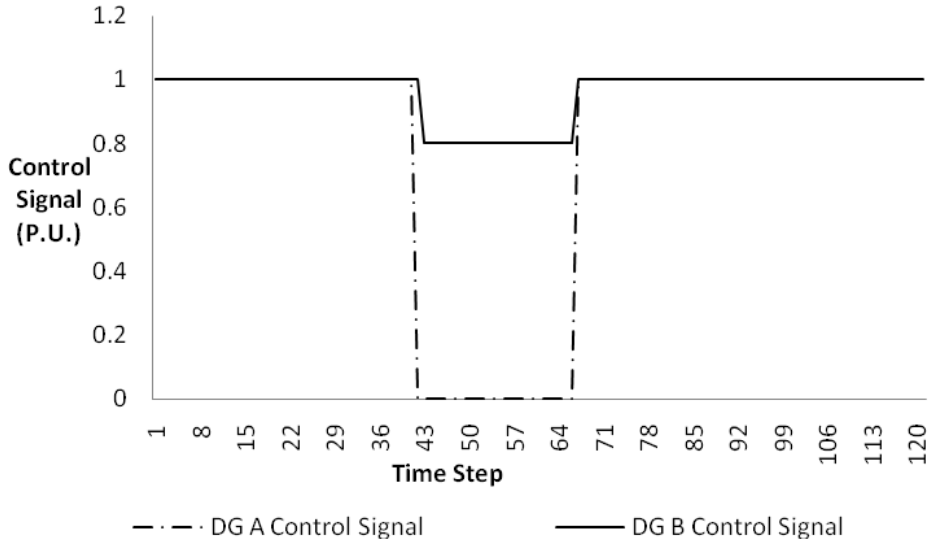

Figure 77 - Case Study A - Line 2 Overloaded with DG A having the Lowest Priority

In Figure 78 the line loading and limit is shown for the inputted DG and load profiles. The case is shown for the algorithm taking no action and therefore the line running overloaded. The line loading is also depicted for the above case when DG control actions are carried out to alleviate the thermal overload. It is clear that when the above control actions are carried out the line remains within thermal limits and DG is only brought back on as and when loading permits.

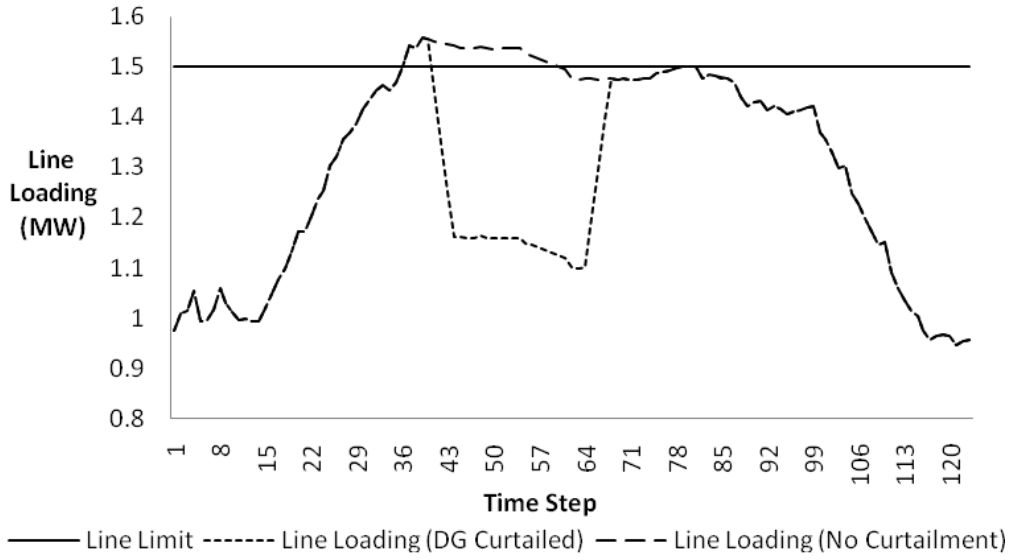

Figure 78 - Line Loading with and without DG Curtailed

The erroneous 6% load profile was applied to 'test scenario 2' and the resulting curtailment signals depicted in Figure 79 where the thermal excursion occurs on 'Line 2'. The detection loop picks up the network constraint at 'time step 42' where both DG units are constrained and then relaxed at 'time step 64' (2 seconds prior to that of the 'perfect' measurement case) when both DG units are allowed to operate unconstrained. It can be noted that the algorithm curtailed generation for most of the time period when the thermal overload was present and it is unclear whether measurement error or the detection cycle (or both) contribute to the early relaxation of the control signals. However, there is a further control signal sent at 'time step 85'

that called upon the unnecessary curtailment of both generators lasting up to 'time step 92'.

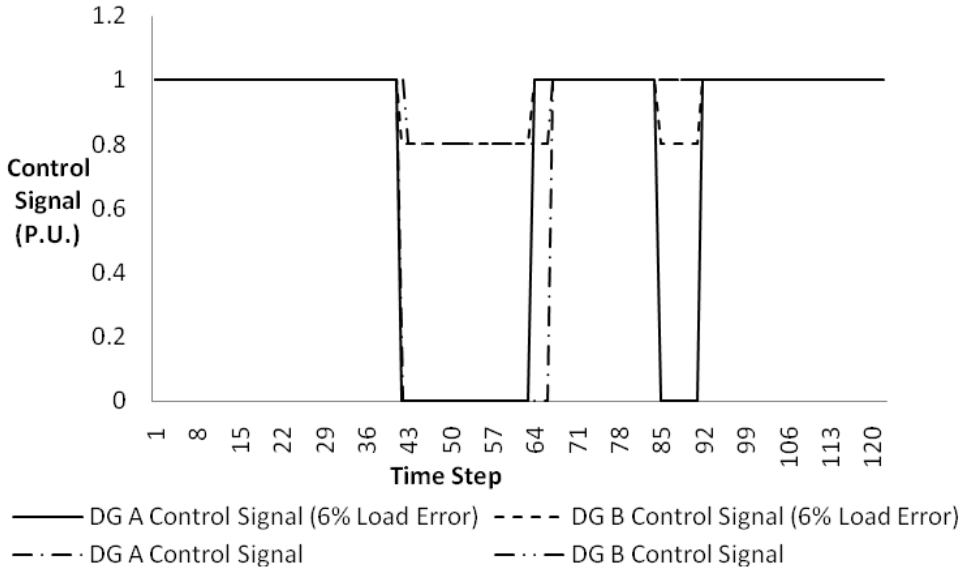

Figure 79 - Case Study A - Line 2 Overloaded with DG A having the Lowest Priority with and without 6% Erroneous Load Measurements

For the 1% load error case for this scenario the control signals sent closely resemble that of the ones sent for the perfect measurement case. Figure 80 shows DG A being constrained at 'time step 40' and DG B being constrained at 'time step 41'. Each curtailment signal is sent 2 seconds prior to that of the 'perfect' measurement case. The signals sent to relax the constraints on the DG units are given at 'time step 65' – 1 second prior to that of the 'perfect' measurement case. The signals for the 1% erroneous and 'perfect' measurement scenarios are within three seconds and therefore the difference may be attributable to the three second detection loop time rather than the erroneous measurements.

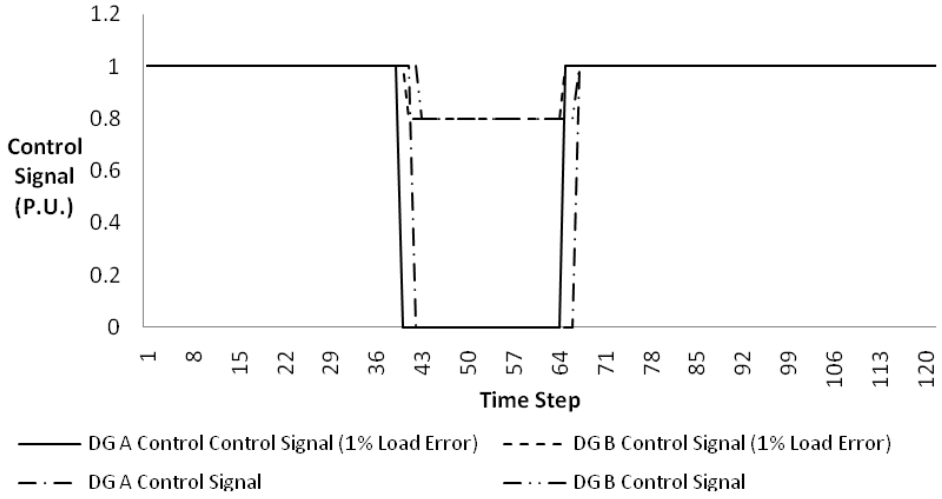

Figure 80 - Case Study A - Line 2 Overloaded with DG A having the Lowest Priority with and without 1% Erroneous Load Measurements

The impact of false signals being sent to DGs A and B is illustrated below in the four figures. For clarity the DG's MW outputs are graphed separately from the DG'S MW curtailment levels for the 'perfect' and erroneous measurement cases.

Figure 81, shows both DG responses as control signals are issued to alleviate the thermal excursion on 'Line 2'. For the 'perfect' measurement case DG A is tripped off and DG B is curtailed to output up to 80% of rated value. As network loading changes and the thermal breach is no longer present the detection algorithms allows the DG units to run unconstrained. With the 6% load error case it can be observed that the DG units are required to ramp down – DG A is once again tripped and DG B is restricted to 80% output. DG A having being sent a control signal equal to '0' does not reach zero output as the relaxation signal is issued only a few time steps later that allows the DG unit to resume unconstrained operation.

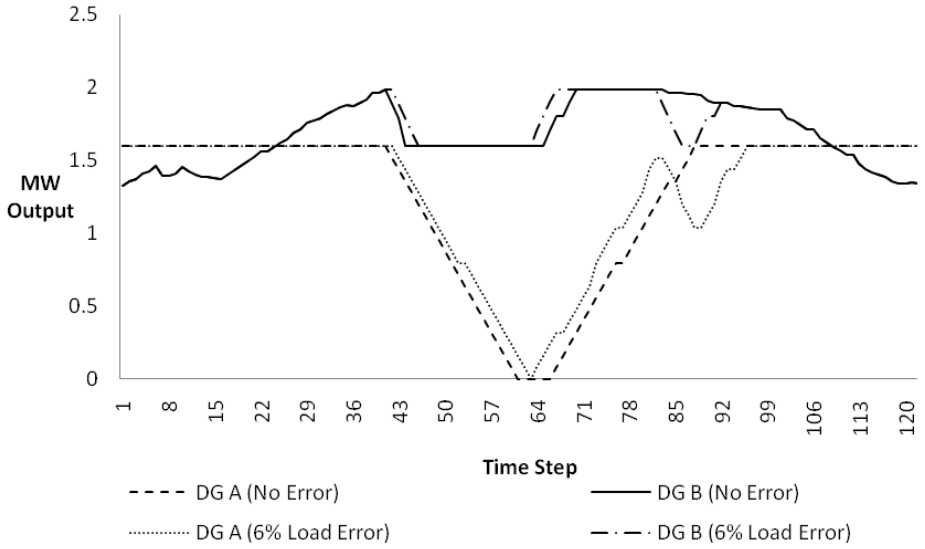

Figure 81 - Case Study A - Line 2 Overloaded with DG A having the Lowest Priority. DG A & DG B MW Output for 'Perfect' and 6% Erroneous Load Measurements

The DG output traces for DGs A and B for 'perfect' measurement and 1% erroneous load measuremetns are shown in Figure 82. The 1% load error responses are similar to that of the 'perfect' measurement case. It is noticable from Figure 82 that data skew creeps into the simulation and may therfore impact upon the results.

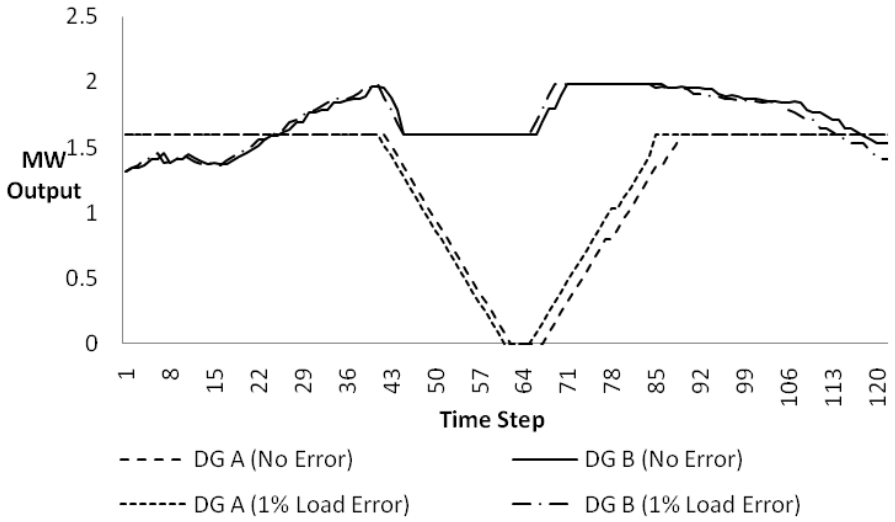

Figure 82 - Case Study A - Line 2 Overloaded with DG A having the Lowest Priority. DG A & DG B MW Output for 'Perfect' and 1% Erroneous Load Measurements

In Figure 83 the total curtailment for the 'perfect' and 6% load measurement cases is illustrated. The total curtailment for the 'perfect' case is 50.55MW and for the 6% load measurement case is 47.68MW.

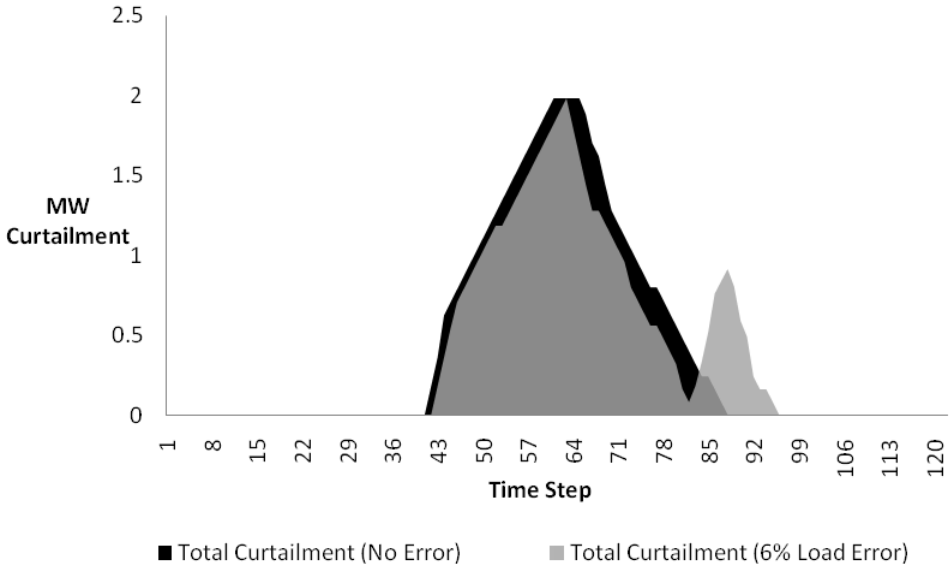

Figure 83 - Case Study A - Line 2 Overloaded with DG A having the Lowest Priority. DG A & DG B MW Curtailment for 'Perfect' and 6% Erroneous Load Measurements

The total curtailment for the 1% load error case is 48.12MW, as shown in Figure 84, compared with that of the 50.55MW for the 'perfect' measurement case.

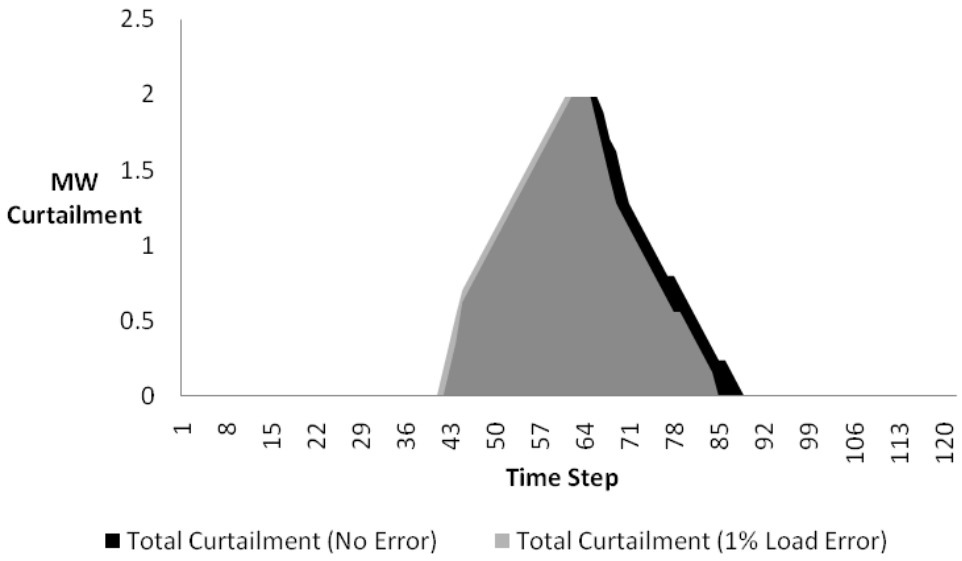

Figure 84 - Case Study A - Line 2 Overloaded with DG A having the Lowest Priority. DG A & DG B MW Curtailment for 'Perfect' and 1% Erroneous Load Measurements

5.4.4 Test Scenario 4: 11kV Radial Distribution Network with 'Line 2' Overloaded and DG B being the Last Historically Connected DG Unit

Similar to 'test scenario 3', 'Line 2' was de-rated and the perfect profiles applied via the simulation environment applied which results in a thermal limit breach on 'Line 2'. For this scenario the DG connection arrangement was reversed such that DG B (Figure 63) was assumed to be the last historically connected DG unit and therefore the first to be trimmed to ensure power flow limits are met.

Figure 85 shows that at 'time step 44' only DG B is sent an 80% reduction signal due to being the last historically connected generator and being the only unit feeding into the overloaded line. The overload is clear at 'time step 71' and DG B can resume operation up to its maximum capable output. This relaxation differs by 5 seconds from that of 'test scenario 3' (the same overload condition) and is attributable to data skew. Data skew is more apparent in this case as DG B's varying output does not mask the issue such as DG A's constant output does. In the previous 'test scenarios' data skew was mitigated through multiple runs of the simulations for the purpose of evaluating the performance of the algorithm. However, data skew plays an important role in the accuracy of the network model used as the basis of the curtailment decisions. Therefore, data skew is incorporated and discussed within this scenario.

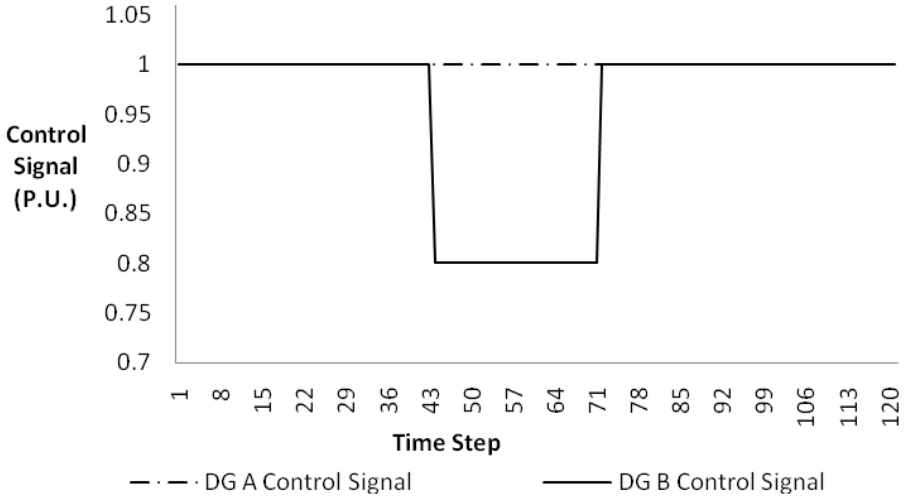

Figure 85 - Case Study A - Line 2 Overloaded with DG B having the Lowest Priority

In Figure 86 the line loading and limit is shown for the inputted DG and load profiles. The case is shown for the algorithm taking no action and therefore the line running overloaded. The line loading is also depicted for the above case when DG control actions are carried out to alleviate the thermal overload. It is clear that when the above control actions are adhered to the line remains within thermal limits and DG is only brought back on as and when loading permits.

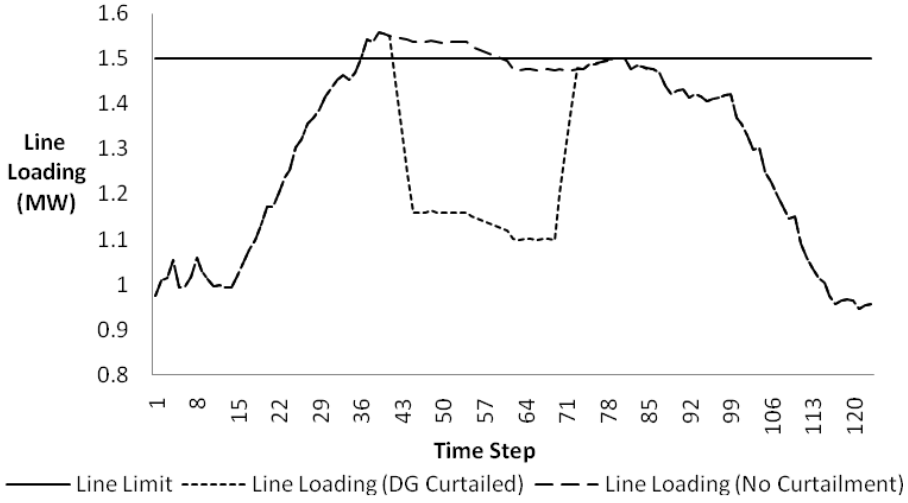

Figure 86 - Line Loading with and without DG Curtailed

Applying the 6% measurement error to the above scenario results in the curtailment signals shown in Figure 87. The overload is detected between 'time step 41 and 66' however generation is allowed to run un-curtailed before the network conditions are such that the thermal breach is no longer – as far as the data presented to algorithm indicates. A further thermal excursions is detected between 'time step 75 and 78' and DG control signals are sent to compensate against the mistaken limit violation.

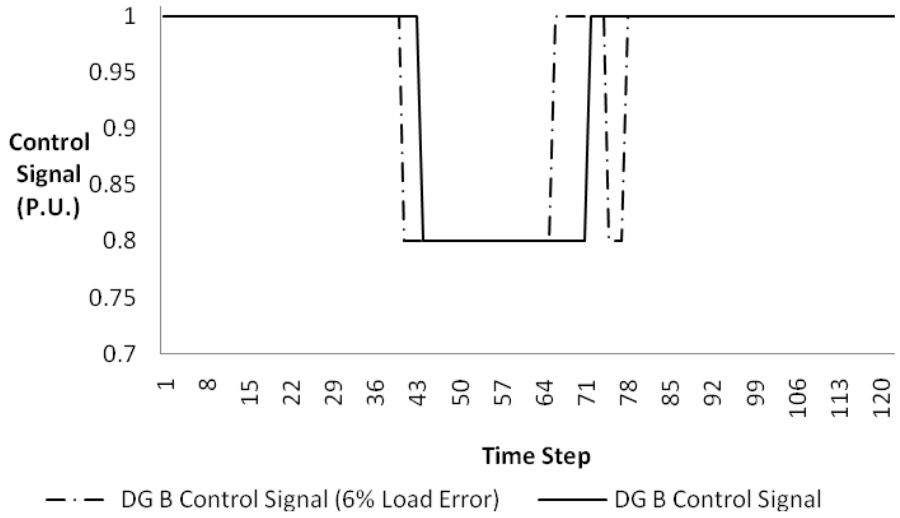

Figure 87 - Case Study A - Line 2 Overloaded with DG B having the Lowest Priority with and without 6% Erroneous Load Measurements

From Figure 88 it can be observed that after DG B's curtailment has been relaxed the generator MW output data from the 'perfect' case and the 1% load error case are out of synchronisation and gradually deteriorate as time evolves. This highlights the importance of having accurate time stamped data when applying real-time control algorithms. The impact appears to be minimal over the duration of the thermal excursion however it cannot be ruled out that data skew has played a role along with erroneous measurements to the early relaxtion of the control signal and the folloing false detection.

The MW curatilment levels, taken from Figure 88, shows that for the 'perfect' measurement case 10.6MW were curtailed over the simulation period. This is in contrast to the 6% load error case where 10.96MW required to be trimmed from the potential output. From a DG operators perspective this is not a drastic difference however the they would be apprehensive of any autonomous control action that results in unnecessary curtailment. Equally, the DNO would be concerned about the unit feeding into and contributing to overloading their assets.

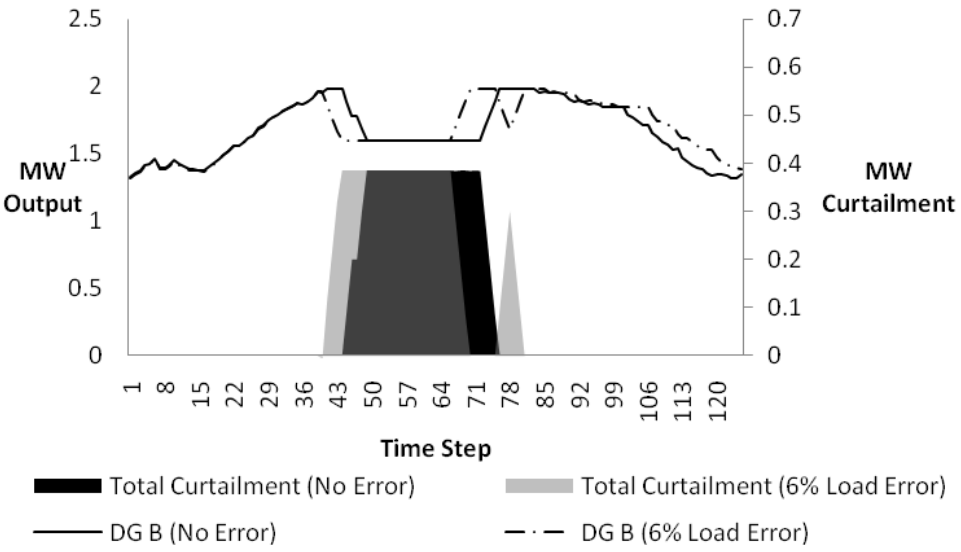

Figure 88 - Case Study A - Line 2 Overloaded with DG B having the Lowest Priority. DG A MW Output and Curtailment Graphed for 'Perfect' and 6% Erroneous Load Measurements

For the 1% erroroneous load case, Figure 89, the thermal violation was detected at the same time step ('44') as that of the perfect measurment scenario with the same level of signal issued. The relaxation of the control signal is sent 5 seconds prior to the non-erroneous case, at 'time step 66' therfore the error or data skew (or both) have an influence on the precise timing of the control signal.

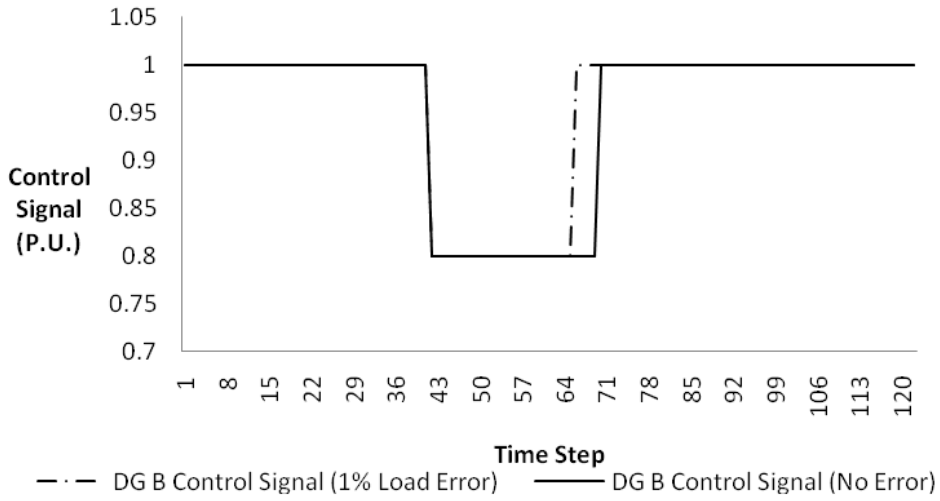

Figure 89 - Case Study A - Line 2 Overloaded with DG B having the Lowest Priority with and without 1% Erroneous Load Measurements

In Figure 90, data skew can be noticed after the relaxation signal has been issued to DG B. It is therefore evident that data skew, the detection cycle and erroneous measurements may all contribute to the false computation of control signals. The curtailed MWs for the 'perfect' measurement scenario totalled 10.6MW with 9.4MW trimmed over the simulation period for the 1% erroneous load measurement scenario.

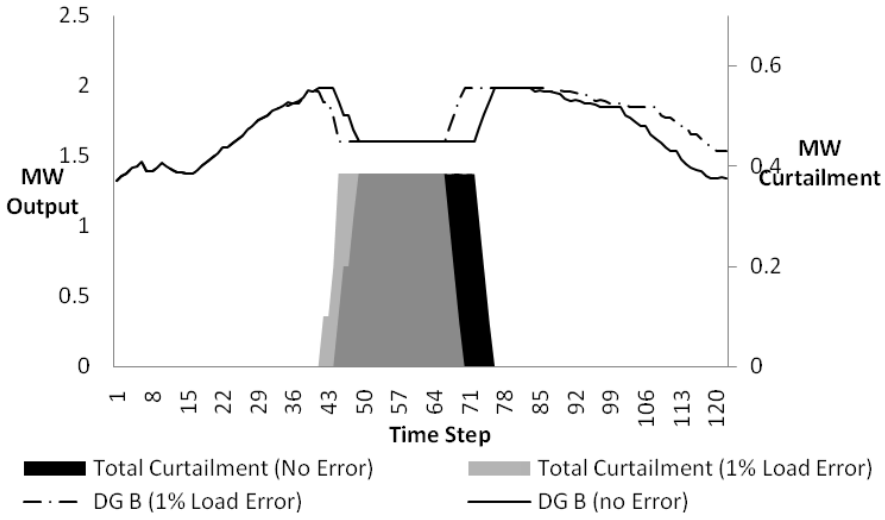

Figure 90 - Case Study A - Line 2 Overloaded with DG B having the Lowest Priority. DG A MW Output and Curtailment Graphed for 'Perfect' and 1% Erroneous Load Measurements

5.4.5 Case Study A: Test Scenario Computation Time

The computation time involved in calculating valid solutions is crucial in a real-time autonomous ANM scheme. The computation time clock starts when the CSP solver is called upon, post overload detection, and stopped when the first solution is found. For each scenario, the time for the solver to compute every control action was recorded. The fastest time recorded was 52ms with the slowest time being logged as 131ms.

Figure 91 shows the average computation time to compute the solutions in each of the Case A scenarios above. The x-axis corresponds to the 'Test Scenario' figures within this chapter.

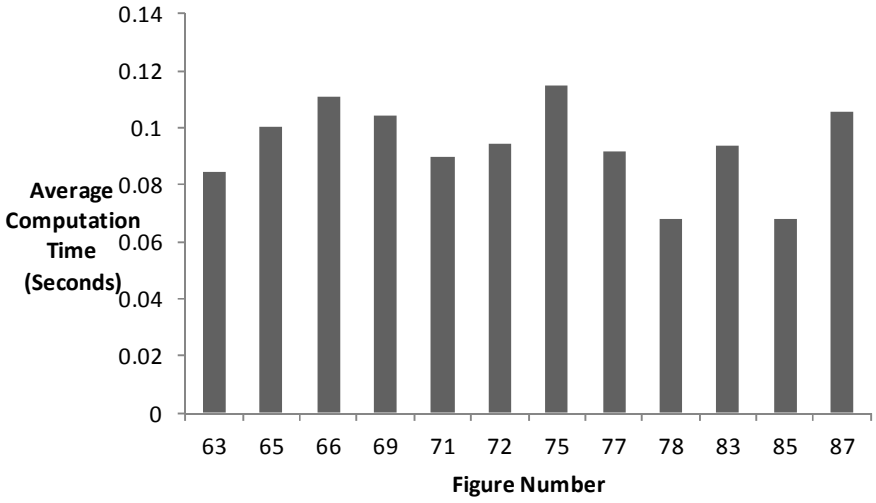

Figure 91 - Average Solution Computation Time for Case Study A

5.5 Case Study B – 33kV Interconnected Distribution Network

In each of the following test scenarios the variables and domains remain constant with only the priority constraint being changed. The variables and corresponding domains are as follows:

V_{gens} = {
Hydro A = 20MW,
Hydro B = 20MW,
DG 1 = 5MW,
DG 2 = 4.35MW,
DG 3 = 2.4MW,
DG 4 = 2MW,
DG 5 = 23.5MW
DG 6 = 23.5MW,
DG 7 = 12MW,
DG 8 = 10.2MW,
}

D_{gens} = {
$D_{Hydro\ A}$ = {*1, 0.8, 0.5, 0.2, 0*}
$D_{Hydro\ B}$ = {*1, 0.8, 0.5, 0.2, 0*}
$D_{DG\ 1}$ = {*1, 0.8, 0.5, 0.2, 0*}
$D_{DG\ 2}$ = {*1, 0.8, 0.5, 0.2, 0*}
$D_{DG\ 3}$ = {*1, 0.8, 0.5, 0.2, 0*}
$D_{DG\ 4}$ = {*1, 0.8, 0.5, 0.2, 0*}
$D_{DG\ 5}$ = {*1, 0.8, 0.5, 0.2, 0*}
$D_{DG\ 6}$ = {*1, 0.8, 0.5, 0.2, 0*}
$D_{DG\ 7}$ = {*1, 0.8, 0.5, 0.2, 0*}
$D_{DG\ 8}$ = {*1, 0.8, 0.5, 0.2, 0*}
}

e.g. DG 1 can operate uncurtailed at 5MW, or curtailed at (5MW x 0.8), (5MW x 0.5), (5MW x 0.2) or tripped at (5MW x 0). The other units can operate with the same bandings with the exception that their rated output differs.

The solutions must meet the load flow constraint:

$$C_{\text{Power Flow}} = \{ -S_{ij}^{\max} \leq S_{ij} \leq S_{ij}^{\max} \}$$

And the assigned priority constraints as per Table 9 for each of the 'Test Scenarios', e.g.:

$$C_{\text{Contractual}} = \{Hydro\ A = 1, Hydro\ B = 2, \ldots, \text{DG } 8 = 10\}$$

In the above formulation a '1' ranks the DG unit as being the first historically connected unit and therefore the last unit that is required to respond to the thermal constraint.

Table 9 - Generator Connection Priority

Generator ID	Prioity (Test Scenario 5 - Figure 92)	Prioity (Test Scenario 6 - Figure 94)	Prioity (Test Scenario 7 - Figure 97)	Priority (Test Scenario 8 - Figure 98)
Hydro A	1	1	1	1
Hydro B	2	2	2	2
DG 1	3	4	4	4
DG 2	4	5	5	5
DG 3	5	**10**	**10**	**10**
DG 4	6	9	**9**	**9**
DG 5	**10**	8	**8**	**8**
DG 6	9	7	7	**7**
DG 7	8	6	6	**6**
DG 8	7	3	3	3

Therefore, for $C_{Contractual}$ for 'Test Scenario 5', where DG 5 is deemed the last historically connected unit, would be:

$$C_{Contractual} = \{Hydro\ A = 1, Hydro\ B = 2, \text{DG } 1 = 3, \text{DG } 2 = 4, \text{DG } 3 = 5,$$
$$\text{DG } 4 = 6, \text{DG } 5 = 10, \text{DG } 6 = 9, \text{DG } 7 = 8, \text{DG } 8 = 7\}$$

The priority numbers in bold, in Table 9 above, are highlighted as they are the generators that are curtailed for the following 'Test Scenarios'.

In the following 'Test Scenarios' there is no need to utilise the preference constraint as the first 'optimal' solution is found and implemented. However, it is an important characteristic of the CSP approach as severe measurement error or failure of one of the DG units to respond to a control signal may require the next best 'ranked' solution to be implemented.

5.5.1 Test Scenario 5: 33kV Interconnected Distribution Network with 'Line 1' Overloaded and DG 5 being the Last Historically Connected DG Unit

With 'Line 1' de-rated and through increasing the load at 'Sub A', Figure 64, it is possible to force a thermal excursion on 'Line 1' of the interconnected distribution network. In this scenario it is assumed that DG 5 has been the last historically connected DG unit and therefore first unit in the priority list to attempt to alleviate the thermal excursion.

Figure 92 displays the MW output and the potential output for DG 5 on the primary vertical axis. The control signal sent to DG 5 is presented on the secondary vertical axis. It can be seen that at 'time step 51' DG 5 is required to reduce output by 20% in order to remove the thermal breach on 'Line 1'. At this time period the MW output of DG 5 is reduced from maximum rated output (23.5MW) to 18.8MW and is held at this value until network load allows the DG to run unconstrained at 'time step 83'. The dashed trace shows the potential wind generation had the unit not been constrained.

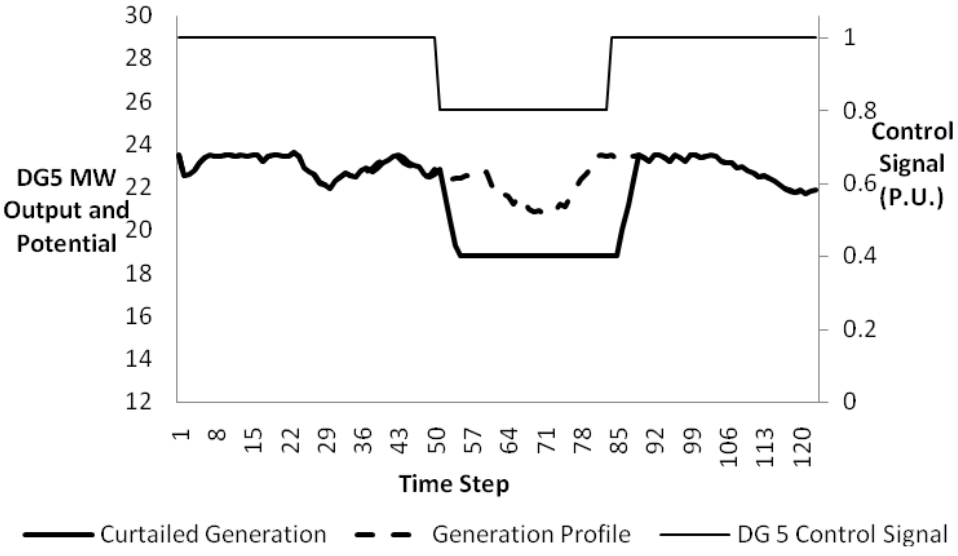

Figure 92 - Case Study B - Line 1 Overloaded with DG 5 having the Lowest Priority

In Figure 93 the line loading and limit is shown for the inputted DG and load profiles. The case is shown for the algorithm taking no action and therefore the line running overloaded. The line loading is also depicted for the above case when DG control actions are carried out to alleviate the thermal overload. It is clear that when the above control actions are carried the line remains within thermal limits and DG is only brought back on as and when loading permits.

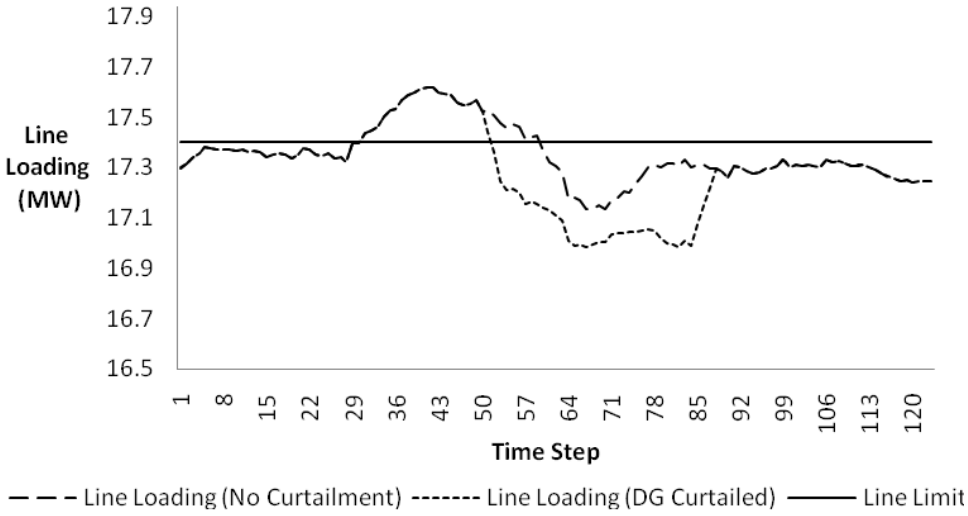

Figure 93 - Line Loading with and without DG Curtailed

The effect of the computation time is evident within Figure 93 where the line loading can be viewed to be above the prescribed limit while the constraint is being solved. The computation time to calculate the curtailment signal and the subsequent relaxation of that signal is approximately 14.1 seconds for this scenario.

5.5.2 Test Scenario 6: 33kV Interconnected Distribution Network with 'Line 1' Overloaded and DG 3 being the Last Historically Connected DG Unit

Applying the same profile with the exception that DG 3 is deemed to be the last historically connected unit, the control signal, the MW output, and the potential output are depicted below in Figure 94. Two control signals are sent to DG 3, at 'time step 52 and 66', to curtail the output and relax the curtailment. The signals set the DG output to a maximum of 50% and then 80% of rated output until network conditions allow the curtailment to be removed whereby the unit can run unconstrained ('time step 80'). The MW output is reduced from 2.4MW (rated output) to 1.2MW and then allowed to increase up to 1.92MW until the curtailment is released.

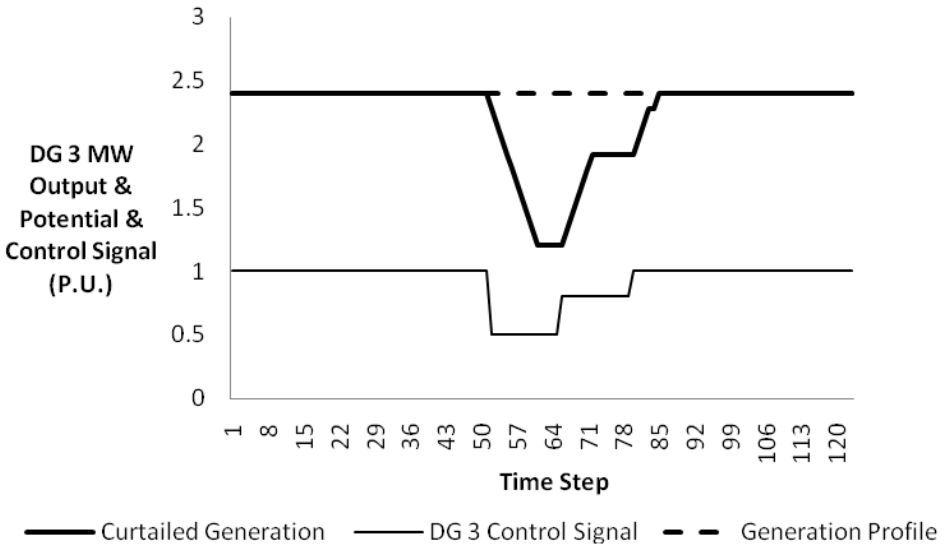

Figure 94 - Case Study B - Line 1 Overloaded with DG 3 having the Lowest Priority

In Figure 95 the line loading and limit are shown for the inputted DG and load profiles. The case is shown for the algorithm taking no action and therefore the line running overloaded. The line loading is also depicted for the above case when DG

control actions are carried out to alleviate the thermal overload. It is clear that when the above control actions are carried the line remains within thermal limits and DG is only brought back on as and when loading permits.

Again the effect of the computation time is evident within Figure 95 where the line loading is above the prescribed limit while the constraint is being solved. The computation times to calculate the curtailment signal and the subsequent relaxation of that signal are approximately 13.2 and 14 seconds, respectively.

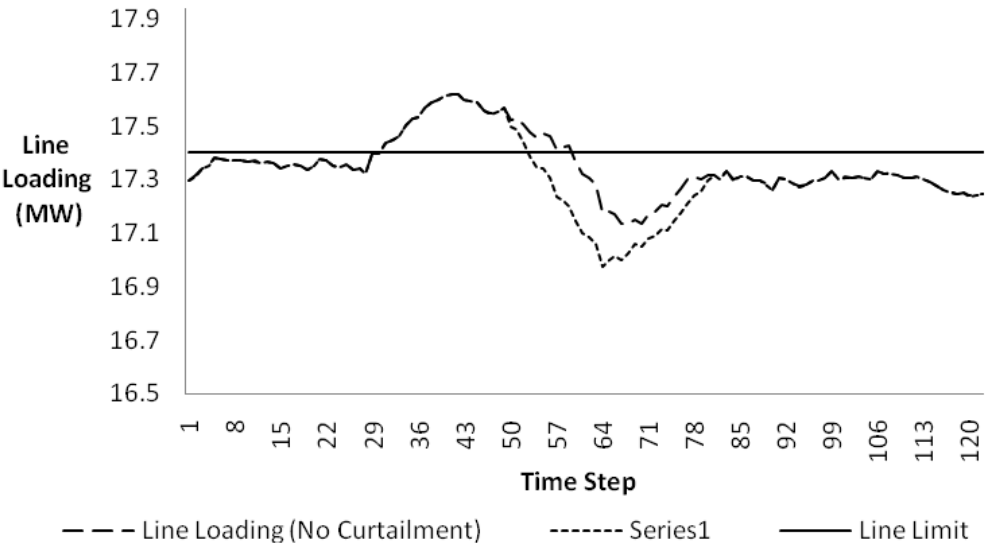

Figure 95 - Line Loading with and without DG Curtailed

It is notable from Figure 96, below, that for the same overload condition differing levels of curtailment were required due to the geographic location of the DG units. For ‘test scenario 5’ a total of 112.6MW were curtailed throughout the thermal overload. In ‘test scenario 6’ the resultant curtailment totalled 30MW.

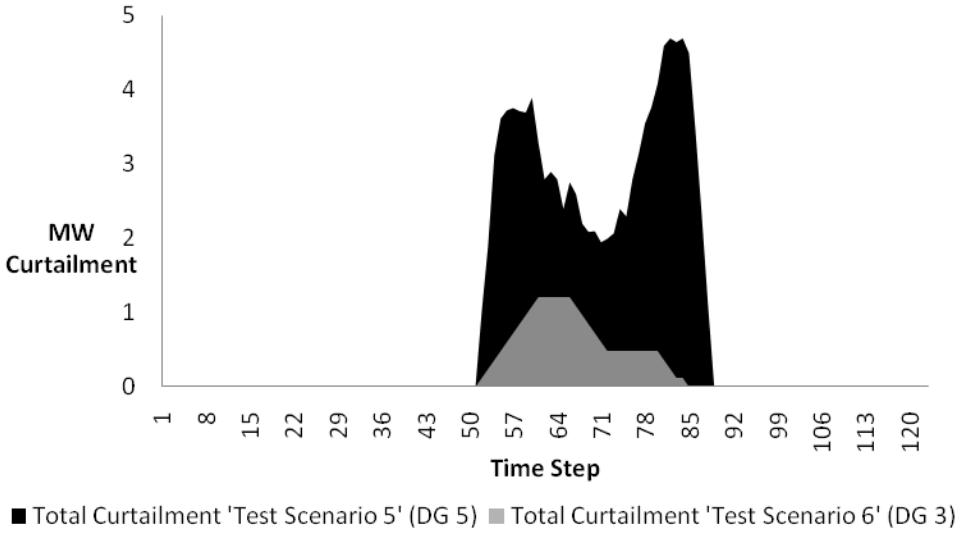

Figure 96 - Total Curtailment for 'Test Scenario 5 & 6'

5.5.3 Test Scenario 7: 33kV Interconnected Distribution Network using Double the Load Profile to Overload 'Line 1'

To examine the algorithm's solution for a deeper level of thermal overload the load profile was doubled at each time step. The connection order for the DG units called upon to alleviate the thermal overload was assumed to be DG 3, DG 4 and DG 5 with DG 3 having the lowest connection priority and DG 5 having the highest.

In Figure 97 the control signals are displayed for DG 3, DG 4 and DG 5 for the scenario of doubling the load profile at 'Sub A'. It can be observed that at the point of detection of this increased overload condition DG 3 and DG 4 are immediately tripped from the network while DG 5 is curtailed to 80% of rated output. Throughout the duration of the scenario, as network load varies, DG 5's control signal is altered to ensure that thermal limits are maintained. DG 5 is eventually allowed to run uncurtailed however DGs 3 and 4 remain tripped for the duration of the profile.

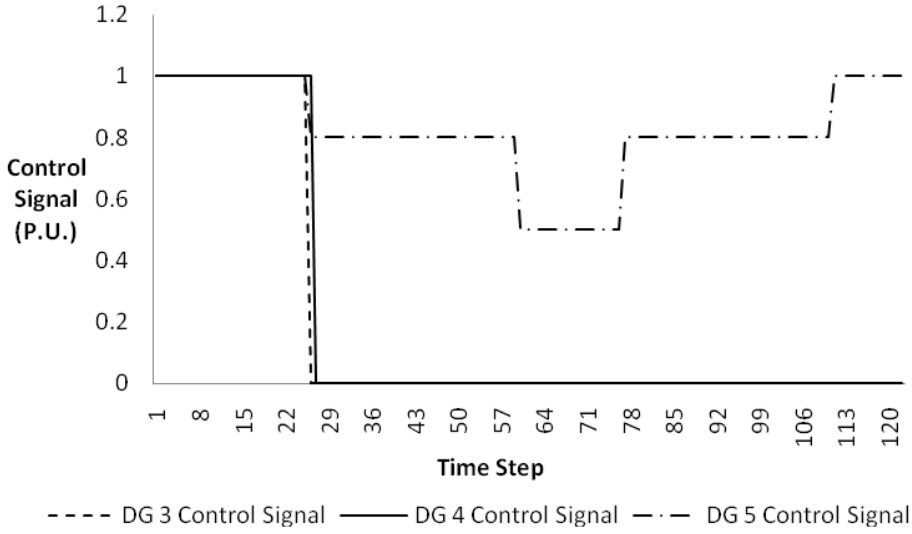

Figure 97 - Case Study B - Line 1 Overloaded due to Increasing 'Sub A' Load Twofold with DG 3, DG 4 & DG 5 having the Lowest Priorities, Respectively

5.5.4 Test Scenario 8: 33kV Interconnected Distribution Network under a Single Circuit Outage Condition

To evalute the CSP PFM approach's perfomance under a first circuit outage condition 'Line 1' was removed from service forcing a thermal overload on 'Lines 2 & 3', Figure 64) and later returned back into service to show the resultant control actions.

The DG connection order for the controlled units of this scenario was deemed to be DG 3, 4, 5, 6, and 7 with DG 3 being the last historically connected unit and DG 7 being the most recent. Figure 98 displayes the control signals sent to DG units 3, 4, 5, 6, and 7. At 'time step 63' all units were tripped from the network. After switching 'Line 1' back into service all the DG units, except for DG 3, were issued a run unconstrained command at 'time step 77'. At this period DG 3 was issued a signal allowing it to operate up to 50% of rated output until network loading allowed a signal to be re-issued (at 'time step 89') to enable DG 3 to operate unconstrained. This scenario highlights the ability of the algorithm to follow the last-in, first-off (LIFO) connection principle for curtialing units and bringing them back online.

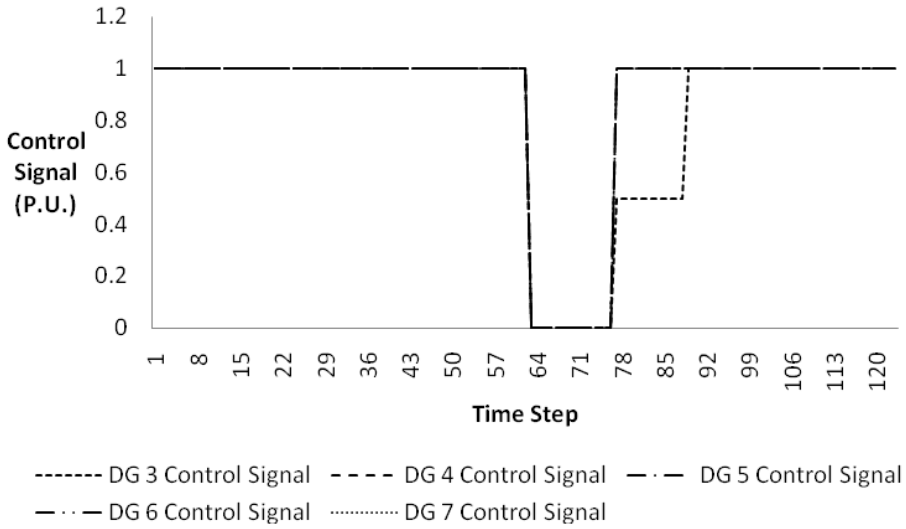

Figure 98 - Case Study B - Line 1 Switched Out DG 3, DG 4, DG 5, DG 6 & DG7 having the Lowest Priorities, Respectively

5.5.5 Case Study B: Test Scenario Computation Time

The computation time, for Case Study B, under normal network operation ranged from 13 to 15 seconds. However, under a first circuit outage condition, the worst case planning criterion, this time increased to approximately 56 seconds.

5.6 Chapter 5 Review: CSP-LIFO Conclusions

The closed loop simulation results presented above, using the CSP approach and applying it to distribution network PFM, demonstrated that this novel application has the ability to operate in an online and real-time control environment. The CSP-LIFO approach successfully detected and provided solutions to operate the case study networks within thermal limits. It was also demonstrated that the CSP-LIFO algorithm recognised when network loading conditions allowed curtailment signals to be relaxed or removed. When running the prototype PFM algorithm, on a commercially available substation computer platform combined with the steady-state simulator, it was shown that CSP-LIFO is a scalable solution but with evident implications on the computation time when modelled, in this way. Computation time ranged from 58 milliseconds to 56 seconds under the test conditions. For both normal network operations (i.e. all lines in service) and for the single circuit outage condition the solutions were returned in a timescale sufficient to meet the requirements of a real-time PFM algorithm.

The algorithm can be easily re-configured to reduce the number of discrete curtailment bands to speed computation time when more generation connects to a network or alternatively increase the curtailment bands for finer resolution control that maximises DG power output. It was observed that adhering to the common last-in first-off (LIFO) connection arrangements has a detrimental impact on the output of DG units not directly contributing to a thermal limit violation. The flexibility of the CSP-LIFO approach does allow for additional constraints to be added mitigating some of these negative effects of the LIFO curtailment regime.

Analyses of the results from the 6% load measurement error scenarios highlights the importance of ensuring the network model is representative of current network conditions as erroneous control actions (of relatively insignificant magnitude and duration in the simulated cases) could result. A load error of 1% produced very small deviations in DG curtailment from that of the perfect measurement cases and this shows that deployment of sensors categorised within this tolerance band are capable of delivering measurements suitable for this approach. An important feature of active distribution network control intended to work in autonomous or semi-autonomous mode is robustness. Should the first (highest preference) solution of the CSP-LIFO approach fail to resolve the thermal overload (e.g. for reasons of lack of DG response, communications failure, etc.) then the next best solution can be implemented thus offering 'graceful degradation'.

In summary, the simplicity of control actions when applying the CSP-LIFO method to the PFM problem ensures discrete control signals are sent to multiple DG units to dynamically manage their outputs in real time. Under these 'Test Scenarios' the approach has been found to be viable in terms of robustness (to measurement error) as a practical solution was found for each case and the speed of computation and the ability to represent existing (i.e. LIFO) commercial contracts has been proven. In terms of extensibility the CSP-LIFO approach can be easily re-configured without changing the core functions, to take into consideration additional DG units or the removal of existing DG units or indeed other controllable devices e.g. energy storage systems. With this technique there are some options to manage scalability issues in that domain sizes can be reduced as DG connections increase. The ability of this approach to build in graceful degradation is an important characteristic for real-time operation to aid dealing with uncertainty.

5.7 Chapter 5 References

[5.1] Gustavo Niemeyer , “Python Constraint”, available at: http://niemeyer.net/python-constraint, accessed 03/08/2011

[5.2] TNEI IPSA, Available at: http://www.ipsa-power.com, accessed 03/08/2011

Chapter 6

Discussion and Comparative Analysis of Results

6.1 Summary of Chapter 6

In Chapters 4 and 5 the OPF and CSP LIFO methods of PFM were demonstrated to meet the goal of detecting and alleviating network thermal overloads through the control of multiple DG units in sufficient timescales for real time control. In addition, the algorithms were able to relax control signals, issued to the DG units, when loading on the network was such that DG output could be increased.

This chapter further examines and discusses the results from the steady-state closed loop test environment in terms of the duration of curtailment and the impact of measurement error on the volume of curtailed generation. These levels of curtailment are then used to obtain an indication of the accuracy of the approaches from both the DNO's (under-curtailment) and DG operator's (over-curtailment) perspective.

6.2 Discussion

The following discussion is split into two main sub-sections.

The first sub-section examines the periods of curtailment to ascertain the actual duration of the detected thermal overload(s) for each algorithm. This breakdown along with the curtailment levels extracted from the results, presented in Chapters 4 and 5, forms the discussion of the ability of the proposed techniques to retain more DG power output into the network, during the constraint period, than that of a traditional inter-tripping scheme.

The second sub-section uses the erroneous data cases, presented in Chapters 4 and 5, to ascertain the levels of 'over' and 'under' curtailment issued to DG units when the control signals are calculated with measurements that have been subjected to errors. These erroneous cases are compared against the 'perfect' measurement scenario, as the coupled base case, to provide a breakdown of the accuracies of the algorithms when measurement error is present.

6.2.1 Curtailment Duration

The following two sub-sections tabularise and discuss the curtailment periods, one sub-section for each of the PFM approaches, for each of the case study networks' test scenarios. These values allow a comparison of the MW curtailment to be carried out for a traditional inter-trip scheme. These MW curtailment values are presented in the final sub-section summarising both candidate PFM approaches.

A short description of the '***Test Scenarios'*** are contained within each of the tables presented.

6.2.1.1 OPF-LIFO Curtailment Duration

In Table 10 the curtailment durations can be examined for ***Test Scenarios 1 - 8*** for the OPF-LIFO power flow management algorithm.

For ***Test Scenario 1*** and ***Test Scenario 2*** the duration of curtailment, 30 and 37 'time steps', respectively, differs by 7 'time steps'. This is due to ***Test Scenario 1*** controlling the smaller of the two DG units (1.6MW) therefore in ***Test Scenario 2*** the algorithm has to wait until network loading is lower to enable a control signal to be sent that brings on the full rated generation capacity (i.e. 2MW).

Test Scenario 3 and ***Test Scenario 4*** are essentially the same scenarios with the exception that for ***Test Scenario 3*** DG A is in front of the thermal excursion and cannot be used to alleviate the thermal overload. Therefore in both cases the OPF-LIFO algorithm requires DG B to respond thus deviating from the commercial arrangements. It can be observed that the curtailment duration for both these cases were the same with only a small discrepancy at the point of thermal detection and control signal relaxation.

Table 10 - Total Curtailment Duration for the 'Perfect' Measurement Case (OPF-LIFO)

OPF-LIFO with 'Perfect' Measurements	Curtailment ('Time Step')	Curtailment Released ('Time Step')	Duration of Curtailment ('Time Steps')
***Test Scenario 1**: 11kV Radial Distribution Network with 'Line 1' Overloaded and DG A being the Last Historically Connected DG Unit*			
OPF-LIFO	42	72	30
***Test Scenario 2**: 11kV Radial Distribution Network with 'Line 1' Overloaded and DG B being the Last Historically Connected DG Unit*			
OPF-LIFO	44	81	37
***Test Scenario 3**: 11kV Radial Distribution Network with 'Line 2' Overloaded and DG A being the Last Historically Connected DG Unit*			
OPF-LIFO	43	79	36
***Test Scenario 4**: 11kV Radial Distribution Network with 'Line 2' Overloaded and DG B being the Last Historically Connected DG Unit*			
OPF-LIFO	44	80	36
***Test Scenario 5**: 33kV Interconnected Distribution Network with 'Line 1' Overloaded and DG 5 being the Last Historically Connected DG Unit*			
OPF-LIFO	36	73	37
***Test Scenario 6**: 33kV Interconnected Distribution Network with 'Line 1' Overloaded and DG 3 being the Last Historically Connected DG Unit*			
OPF-LIFO	37	65	28
***Test Scenario 7**: 33kV Interconnected Distribution Network using Double the Load Profile to Overload 'Line 1'*			
OPF-LIFO	2	Not Fully Released	118
***Test Scenario 8**: 33kV Interconnected Distribution Network under a Single Circuit Outage Condition*			
OPF-LIFO	14	45	31

Test Scenario 5 and ***Test Scenario 6*** have the same overload conditions with the exception that in ***Test Scenario 6*** the assumed DG connection order is changed to reflect that a smaller rated unit (2.4MW), that is geographically closer to the overloaded line, is the last historically connected unit. The longer duration of curtailment (36 'time steps') resulting from ***Test Scenario 5***, compared to that of ***Test Scenario 6*** (28 'time steps'), is due to waiting for line loading to reduce significantly in order to allow the larger unit (23.5MW) to run unconstrained.

Test Scenario 7 does not fully restore all generation to an uncurtailed level due to the doubling of the load profile. Therefore, the duration of the thermal overload is taken to be 118 'time steps'.

In ***Test Scenario 8*** all DG is restored, to run unconstrained, after 31 'time steps'.

6.2.1.2 CSP-LIFO Curtailment Duration

In Table 11 the curtailment durations can be examined for ***Test Scenarios 1 - 8*** for the CSP-LIFO power flow management algorithm.

Table 11 - Total Curtailment Duration for the 'Perfect' Measurement Case (CSP-LIFO)

CSP-LIFO with 'Perfect' Measurements	Curtailment ('Time Step')	Curtailment Released ('Time Step')	Duration of Curtailment ('Time Steps')
***Test Scenario 1**: 11kV Radial Distribution Network with 'Line 1' Overloaded and DG A being the Last Historically Connected DG Unit*			
CSP-LIFO	*40 & 68*	*80 & 89*	61
***Test Scenario 2**: 11kV Radial Distribution Network with 'Line 1' Overloaded and DG B being the Last Historically Connected DG Unit*			
CSP-LIFO	*40*	*Not Released*	80
***Test Scenario 3**: 11kV Radial Distribution Network with 'Line 2' Overloaded and DG A being the Last Historically Connected DG Unit*			
CSP-LIFO	*42*	*66*	24
***Test Scenario 4**: 11kV Radial Distribution Network with 'Line 2' Overloaded and DG B being the Last Historically Connected DG Unit*			
CSP-LIFO	44	71	27
***Test Scenario 5**: 33kV Interconnected Distribution Network with 'Line 1' Overloaded and DG 5 being the Last Historically Connected DG Unit*			
CSP-LIFO	51 (14secs, 37)	83 (14secs, 68)	32
***Test Scenario 6**: 33kV Interconnected Distribution Network with 'Line 1' Overloaded and DG 3 being the Last Historically Connected DG Unit*			
CSP-LIFO	52 (14secs, 38)	80 (14secs, 66)	28
***Test Scenario 7**: 33kV Interconnected Distribution Network using Double the Load Profile to Overload 'Line 1'*			
CSP-LIFO	25 (15secs, 10)	Not Fully Released	95
***Test Scenario 8**: 33kV Interconnected Distribution Network under a Single Circuit Outage Condition*			
CSP-LIFO	63 (56secs)	89 (13secs)	26

A similar situation is witnessed (as in the first two OPF-LIFO scenarios) for the CSP-LIFO ***Test Scenario 1*** and ***Test Scenario 2*** cases. For ***Test Scenario 1*** the

1.6MW DG unit can run unconstrained at two occasions whereas for the second case, ***Test Scenario 2***, the algorithm is unable to release the curtailment on the 2MW unit.

Test Scenario 3 and ***Test Scenario 4*** display similar curtailment durations, thermal detection points and control signal relaxation points. The difference in these would be attributable to the fact that in ***Test Scenario 4*** the algorithm is trying to push the 2MW unit (i.e. the larger machine) to run unconstrained.

Test Scenario 5 and ***Test Scenario 6*** have very similar curtailment durations, 32 'time steps' and 28 'time steps' respectively, due to examining the same thermal overload but with different DG connection priorities. For ***Test Scenario 6*** the curtailment duration is shorter due to the geographically closer proximity and smaller rating (2.4MW) of the unit to the thermally overloaded line compared to that of ***Test Scenario 5*** (where the machine rating is 23.5MW). For both these scenarios there is a delay of approximately 14 seconds, from when the thermal overload is detected and from when it is realised that the curtailment can be relaxed, due to the solution computation time. Therefore, the actual detection of the thermal breach occurs at 'time steps' 37 and 38 which is supported by the results of the OPF-LIFO algorithm's detection 'time steps' (36 and 37). This is illustrated in Figure 99 where the time series response of the CSP-LIFO and the OPF-LIFO is graphed for ***Test Scenario 5 –*** the 14 second delay due to computation time is highlighted. The shift in curtailment occurs due to the computation time to calculate the curtailment signal and latterly to calculate the relaxation signal.

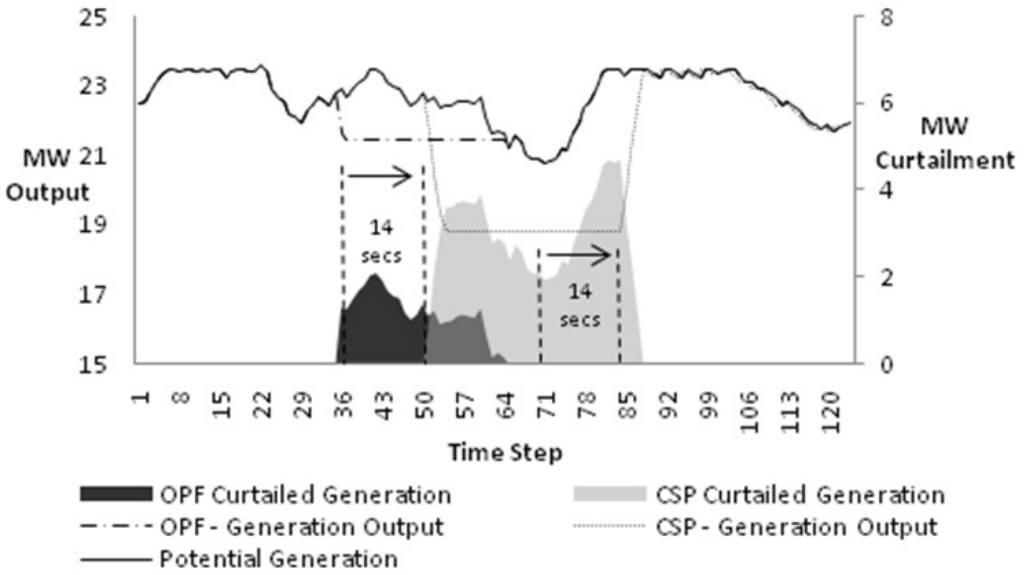

Figure 99 - OPF & CSP LIFO Results for Test Scenario 5

In ***Test Scenario 7*** the DG units are not all allowed to run uncurtailed for the duration of the simulation. The duration of curtailment is 95 'time steps'. Again, due to the computation time of the algorithm, of approximately 15 seconds, there is a delay in the actual detection of the overload and the issuing of the control signal by exactly the time taken to compute the solution.

Test Scenario 8 all units are allowed to run uncurtailed after a duration of 26 'time steps'. In this scenario a deeper search of the search space was required that resulted in a 56 second delay in the actual overload detection to the control signal command. The releasing of curtailment was subject to a delay of approximately 13 seconds.

6.2.1.3 Comparison of Curtailment Duration

The curtailment durations for each test scenario and PFM algorithms discussed in the previous two sub-sections enables a comparison of these candidate approaches, through MW curtailment levels, with a traditional inter-tripping scheme.

The inter-tripping rules applied to determine the equivalent level of curtailment are as follows. The assumptions are made that the DG owner/operator does not comply with a DNO instruction to regulate wind farm output, therefore requiring the inter-trip scheme to operate, and that the inter-trip delay and the ANM computation and communication delays are equivalent.

At the point of overload detection (taken from Table 10 and Table 11), for each of the test scenarios, all DG is tripped off following the LIFO connection order. The DG units are brought back online, based on the time steps in Table 10 and Table 11, in increments of 5% of rated output until each unit reaches its desired output (i.e. either rated output or below depending on the generator's resource profile). This follows the same assumed ramp rate that the OPF and CSP-LIFO approaches apply.

The results of applying these rules based upon each of the scenario's duration of curtailment for the OPF-LIFO approach are shown in Table 12.

The calculated curtailed energy shown in Table 12 is based upon the level of MWs curtailed over the 120 time steps in the simulation. Each time step equates to one second therefore the curtailed energy over the simulation period is MWh = MW x (120/3600).

Table 12 – OPF-LIFO and Inter-trip Curtailment Levels

Test Scenario	OPF Curtailed Generation (MWh)	Inter-trip Equivalent (MWh)	Increased DG Access through ANM (factor)
1	0.062	2.11	34.16
2	0.074	3.33	45.04
3	0.058	3.003	51.78
4	0.0517	3.003	58.12
5	1.137	33.34	29.31
6	0.6347	3	4.73
7	19.64	75.686	3.85
8	34.72	110.66 (All NFG Tripped) 64.084 (OPF DG Tripped)	3.19 1.84

For the OPF-LIFO approach to PFM it can be observed that significant amounts of DG are retained during the thermal overload compared to that of having to rely on a traditional inter-trip arrangement. For system 'normal' conditions (***Test Scenario 1-7***) the amount of DG being allowed access to the network ranges from 3 times up to 58 times more access to that of the inter-trip equivalent. For the single circuit outage case (***Test Scenario 8***) it is normal practice to disconnect all non-firm DG units. This results in the OPF-LIFO algorithm keeping approximately 3 times as much DG connected to the network. However, if the OPF-LIFO algorithm was used in an offline decision support mode then system operators could identify and invoke the relevant inter-tripping schemes, therefore, not having to remove all DG units. If this was the case then system operators could retain 1.84 times as much DG during this particular network condition.

Again, these assumed inter-trip rules were applied to the CSP-LIFO 'time steps' and curtailment durations for each of the test scenarios. The results of which are presented in Table 13.

The calculated curtailed energy shown in Table 13 is based on the MW output curtailed over the 120 time steps in the simulation. Each time step equates to one second therefore the curtailed energy over the simulation period is MWh = MW x (120/3600).

Table 13 – CSP-LIFO and Inter-trip Curtailment Levels

Test Scenario	CSP Curtailed Generation (MWh)	Inter-trip Equivalent (MWh)	Increased DG Access through ANM (factor)
1	0.381	2.912	7.63
2	0.741	5.249	7.08
3	1.685	3.932 (LIFO) 2.147 (Trip DG B)	2.33 1.27
4	0.353	2.343	6.63
5	3.753	30.758	8.19
6	1	3	3
7	27.263	85.55	3.14
8	23.018	96.21 (All NFG Tripped) 46.28 (CSP DG Tripped)	4.18 2.02

The CSP-LIFO approach to PFM also increases the amount of DG unit outputs during the thermal overload than that of the traditional inter-trip scheme. When following the LIFO connection principle, under network 'normal' conditions (***Test Scenario 1 - 7***), the CSP-LIFO algorithm retains approximately two to eight times as much DG access to the network compared to the inter-trip equivalent. ***Test Scenario 3*** is a two DG study case and it is likely that any traditional tripping scheme for this overload would be tied to only the unit that can alleviate the problem. In this case, where only DG B is tripped, the CSP-LIFO approach curtails 1.27 times less DG than the inter-trip equivalent. Interestingly, if the CSP-LIFO approach could identify that it could break the LIFO arrangement for this case it would curtail 9.51MW over the thermal excursion period. This equates to 0.317MWh (9.51MW x 120/3600) curtailed and results in approximately 7 times less energy curtailed (2.147/0.317 = 6.77) than that of the inter-tripping only DG B. Again, for the single circuit outage case (***Test Scenario 8***) it is normal practice to disconnect all non-firm DG units. The CSP-LIFO algorithm keeps around 4 times as much DG online compared to the inter-trip equivalent. If the CSP-LIFO algorithm was used as an offline decision support tool the system operators could identify and trip only the relevant inter-tripping schemes that were identified by the CSP-LIFO approach (e.g. not all non-firm DG units need to be tripped). If this was the case the system operator could retain twice as much DG during this particular network condition.

6.2.1.4 Curtailment Duration Summary

Current financial incentives are leading the way and are stimulating increased DG applications and as a result the expectation is that DG connections, at distribution level, will significantly increase. Taking an active approach to PFM by regulating the real power output from currently connected DG units and by utilising existing network capacity can significantly increase the power sourced from renewable and intermittent generation. The future facilitation of DG connections can be included in the PFM approaches thus avoiding or deferring the high capital reinforcement costs traditionally required for new DG connections.

The OPF-LIFO PFM technique offered higher levels of DG penetration compared with that of the CSP-LFO approach. This is due to the continuous nature of the parameters in the OPF solution compared to that of the discrete power set point bandings used within the CSP approach. Higher DG access levels can therefore be achieved using an OPF-LIFO approach. However, with this approach there is no fallback position should a solution fail as there is for CSP-LIFO where the use of discrete curtailment bandings intrinsically builds in an operational margin and should the initial solution fail to resolve the thermal breach a fall back situation exists. The CSP solver can retrieve 'some' or 'all' solutions and rank them in order of maximising DG access using the 'preference constraint'.

The reduced curtailment levels achieved by these algorithms are a positive advancement for active PFM techniques.

6.2.2 Curtailment Accuracies

The level of DG curtailed and the accuracy of the curtailment to alleviate thermal overloads affects both the DG owner/operator and the DNO. The DG owner would want to export as much real power to the network in order to maximise revenue and would therefore not welcome any unnecessary over-curtailment. On the other hand, DNOs have an obligation to provide a safe and secure supply to customers while facilitating renewable generation and protecting the lifetime of network assets for security and business reasons. As such, the DNO would not want to encounter under-curtailment as this could allow network assets to run overloaded with potential short and long term implications. The accuracy of measurement sensors, the reliability of the communications network and the quality of the network model used in active network management are therefore crucial in meeting the demands of the DNO and DG operator.

Taking the 'perfect' measurement case, for each of the applied techniques and for each of the ***Test Scenarios***, gives a DG curtailment base case for comparison of

under-curtailment and over-curtailment when the techniques were subjected to measurement errors. The following two sub-sections tabularise and discuss the 'over' and 'under' curtailment levels for each of the candidate PFM approach. The 'over' and 'under' curtailment values are derived from the ***Test Scenarios*** that were subjected to erroneous data input and based upon the control signals that succumbed to the erroneous data. That is, the number of error related signals is defined as the signals sent either when the thermal overload is not present (i.e. forcing over-curtailment) or when signals are sent relaxing DG output during the thermal excursion (i.e. forcing under-curtailment). To exclude the false labelling of control signals only the control signals that can be attributed to erroneous measurements are logged i.e. the control signals that are greater than three seconds (either side) from that of the perfect measurement case are counted. This ensures that the monitoring and detection loop, operating in a three second cycle, does not play a role in the labelling of error related signals. Furthermore, under-curtailment is defined as uncurtailed generation during the thermal overload or generation not curtailed compared to that of the 'perfect measurement' case. Over-curtailment is defined as curtailed generation outwith the thermal overload or a deeper level of curtailment during the thermal overload from that of the perfect measurement case. These definitions are illustrated in Figure 100.

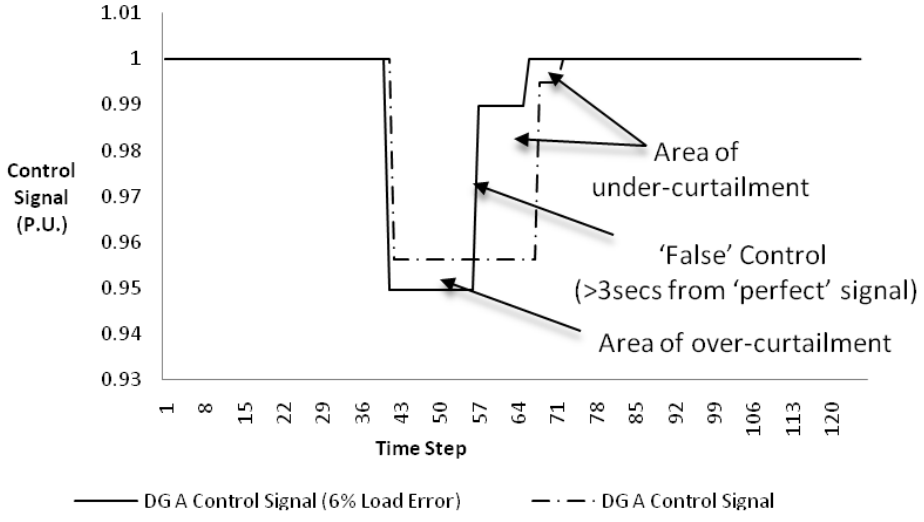

Figure 100 - Illustration of Definition of Terms used in the Following Sub-Sections

A short description of the '***Test Scenarios'*** are contained within each of the tables presented in the following sub-sections.

6.2.2.1 OPF-LIFO Curtailment Accuracies

This section summarises the results of the ***Test Scenarios 1 – 4*** for the OPF-LIFO algorithms in terms of the apparent accuracies when subjected to measurement error. The tables for each ***Test Scenario***, below, present the number of control signals sent to the DG units, the number of error related signals sent to the DG units and the overall curtailment. The overall curtailment is then subdivided into 'under-curtailment' and 'over-curtailment' to allow conclusions to be drawn on the accuracy of the algorithms from a DNO's perspective and the DG operator's viewpoint.

In Table 14 for ***Test Scenario 1*** it is shown that, as expected, the 1% error case delivered a solution with a smaller net percentage error than that of the 6% case. For the 6% error case, the algorithm returned results that from the DG operators point of view was 90.66% accurate and from the DNO's point of view was 67.48% accurate. For the 1% error case this perceived accuracy was reversed for each stakeholder. The DG operator would have viewed the accuracy at 64.98% due to the amount of over-curtailment. With less under-curtailment the DNO would perceive the accuracy to be 84.89%.

Table 14 – Test Scenario 1 (OPF-LIFO Curtailment Accuracy)

Test Scenario	***Test Scenario 1**: 11kV Radial Distribution Network with 'Line 1' Overloaded and DG A being the Last Historically Connected DG Unit*								
	No. of Control (Error Related) Signals	Net Curtail-ment (MW)	Under Curtail-ment (MW)	Over Curtail-ment (MW)	Net Error Curtail-ment (%)	Under Curtail-ment (%)	Over Curtail-ment (%)	Overall % Accuracy (DG Viewpoint)	Overall % Accuracy (DNO Viewpoint)
Perfect	3(-)	1.85	-	-	-	-	-	100	100
6% Error	3(2)	1.42	0.6016	0.1727	23.2	32.52	9.34	90.66	67.48
1% Error	4(3)	2.21	0.2797	0.6479	19.45	15.11	35.02	64.98	84.89

In Table 15 the ***Test Scenario 2*** inaccuracies can be observed. The 'Run 1' case, for the 1% erroneous data, yielded a higher net error in curtailment than that of the 6% error case. The 'Run 2' case for the 1% error case produced less percentage error than that of the other two erroneous cases. This highlights that the different thermal detection and relaxation 'time steps' (due to the three second loop) coupled with the erroneous data can increase the net error under certain conditions. The 6% erroneous case produced results that indicated that the algorithm was 57.14% accurate from the DG operator's viewpoint and 64.19% accurate from the DNO's perspective. The 'Run 1' case, for 1% measurement error, showed accuracies higher than that of the 6% error case. 66.96% (DG operator's viewpoint) and 89.03% (DNO's viewpoint) resulted from the simulations. The 'Run 2' case, for 1% erroneous data, returned results of a very high accuracy that would not significantly impact the DG operator (97.27%) or the DNO (99.5%).

Table 15 - Test Scenario 2 (OPF-LIFO Curtailment Accuracy)

Test Scenario	***Test Scenario 2**: 11kV Radial Distribution Network with 'Line 1' Overloaded and DG B being the Last Historically Connected DG Unit*								
	No. of Control (Error Related) Signals	Net Curtail-ment (MW)	Under Curtail-ment (MW)	Over Curtail-ment (MW)	Net Error Curtail-ment (%)	Under Curtail-ment (%)	Over Curtail-ment (%)	Overall % Accuracy (DG Viewpoint)	Overall % Accuracy (DNO Viewpoint)
Perfect	4(-)	2.22	-	-	-	-	-	100	100
6% Error	4(4)	2.40	0.7789	0.9516	8.11	35.09	42.86	57.14	64.91
1% Error ('Run 1')	4(2)	2.71	0.2439	0.7334	22.07	10.97	33.04	66.96	89.03
1% Error ('Run 2')	3(1)	2.27	0.0112	0.0607	2.25	0.5	2.73	97.27	99.5

For ***Test Scenario 3***, Table 16 , the 1% erroneous case issued instructions with substantially less net percentage error than that of the 6% erroneous case. For the 1% and the 6% error cases the accuracy (98.15% and 99.39%, respectively) of the algorithm was high from the DG operators point of view due to very little over-

curtailment commands. However, the 6% error case produced unsatisfactory results as there was substantial under-curtailing of DG that resulted in a very low accuracy from the DNOs point of view, 15.39%. The 1% error case produced an accuracy of 73.65% from the DNO's viewpoint.

Table 16 - Test Scenario 3 (OPF-LIFO Curtailment Accuracy)

Test Scenario	***Test Scenario 3**: 11kV Radial Distribution Network with 'Line 2' Overloaded and DG A being the Last Historically Connected DG Unit*								
	No. of Control (Error Related) Signals	Net Curtail-ment (MW)	Under Curtail-ment (MW)	Over Curtail-ment (MW)	Net Error Curtail-ment (%)	Under Curtail-ment (%)	Over Curtail-ment (%)	Overall % Accuracy (DG Viewpoint)	Overall % Accuracy (DNO Viewpoint)
Perfect	4(-)	1.74	-	-	-	-	-	100	100
6% Error	2(1)	0.3	1.4723	0.0322	82.76	84.61	1.85	98.15	15.39
1% Error	4(0)	1.29	0.4585	0.0106	25.86	26.35	0.61	99.39	73.65

The results of ***Test Scenario 4***, Table 17, show a reversal in the net percentage errors for the erroneous cases. Under these test conditions the 1% erroneous case is in fact the one that presents the highest net percentage error compared to the 6% error case. ***Test Scenario 4*** is fundamentally the same test case as ***Test Scenario 3*** as the OPF-LFO algorithm ignores the LIFO arrangements, for ***Test Scenario 3***, as DG A cannot resolve the thermal constraint. Data skew is apparent in the 1% error case, from the results in Chapter 4, and as such this discrepancy points to skewed data. In terms of the perceived accuracies the 6% erroneous data simulation resulted in 70.34% precision from the DG operator's outlook and 60.91% accurate from the DNOs viewpoint. For the 1% error case the result was 62.38% and 100% accuracy from the DG operator and DNOs point of view, respectively.

Table 17 - Test Scenario 4 (OPF-LIFO Curtailment Accuracy)

Test Scenario	***Test Scenario 4**: 11kV Radial Distribution Network with 'Line 2' Overloaded and DG B being the Last Historically Connected DG Unit*								
	No. of Control (Error Related) Signals	Net Curtail-ment (MW)	Under Curtail-ment (MW)	Over Curtail-ment (MW)	Net Error Curtail-ment (%)	Under Curtail-ment (%)	Over Curtail-ment (%)	Overall % Accuracy (DG Viewpoint)	Overall % Accuracy (DNO Viewpoint)
Perfect	4(-)	1.55	-	-	-	-	-	100	100
6% Error	4(3)	1.4	0.6059	0.4597	9.68	39.09	29.66	70.34	60.91
1% Error	4(0)	2.13	0	0.5831	37.42	0	37.62	62.38	100

When examining these error cases to gauge algorithm accuracy it is highlighted that wide variations can occur when not using high precision time stamped data. The impact of the detection loop cycle and the time steps that the thermal constraint is detected also introduces slight error to the cases.

The following sub-section examines the same scenarios to identify the CSP-LIFO approach's resilience to measurement error.

6.2.2.2 CSP-LIFO Curtailment Accuracies

This section summarises the results of the ***Test Scenarios 1 – 4*** for the CSP-LIFO algorithms in terms of the apparent accuracies when subjected to measurement error. The tables for each ***Test Scenario***, below, present the number of control signals sent to the DG units, the number of error related signals sent to the DG units and the overall curtailment. The overall curtailment is then subdivided into 'under-curtailment' and 'over-curtailment' to allow conclusions to be drawn on the accuracy of the algorithms from a DNO's perspective and the DG operator's viewpoint.

In ***Test Scenario*** 1 the results of Table 18 demonstrate that the 1% erroneous case delivers solutions that result in less net percentage error than the 6% error case. This case illustrates the high levels of accuracy attained with 1% erroneous measurements

(>95%) and even for the 6% load error (where the accuracy > 80%). The 6% erroneous cases yielded results favourable to DG operator, where less over-curtailment was recorded, whereas the 1% case offered solutions more in line with the DNO's expectations (less under-curtailment).

Table 18 - Test Scenario 1 (CSP-LIFO Curtailment Accuracy)

Test Scenario	***Test Scenario 1**: 11kV Radial Distribution Network with 'Line 1' Overloaded and DG A being the Last Historically Connected DG Unit*								
	No. of Control (Error Related) Signals	Net Curtail-ment (MW)	Under Curtail-ment (MW)	Over Curtail-ment (MW)	Net Error Curtail-ment (%)	Under Curtail-ment (%)	Over Curtail-ment (%)	Overall % Accuracy (DG Viewpoint)	Overall % Accuracy (DNO Viewpoint)
Perfect	4(-)	11.44	-	-	-	-	-	100	100
6% Error	4(3)	10.88	2.24	1.68	4.895	19.58	14.69	85.31	80.42
1% Error	4(0)	11.68	0.24	0.48	2.1	2.1	4.2	95.8	97.9

In ***Test Scenario 2***, Table 19, again the 1% erroneous load case delivered results with far less net percentage error than the 6% error case. For both erroneous simulations no 'over' curtailment commands were instructed giving positive results for the DG operator (i.e. 100% accurate). In terms of the DNO, the accuracy of the 6% load error stands at approximately 75% whereas the 1% error simulation produced results very close to the perfect measurement scenario (99.73% accurate).

Table 19 - Test Scenario 2 (CSP-LIFO Curtailment Accuracy)

Test Scenario	***Test Scenario 2**: 11kV Radial Distribution Network with 'Line 1' Overloaded and DG B being the Last Historically Connected DG Unit*								
	No. of Control (Error Related) Signals	Net Curtail-ment (MW)	Under Curtail-ment (MW)	Over Curtail-ment (MW)	Net Error Curtail-ment (%)	Under Curtail-ment (%)	Over Curtail-ment (%)	Overall % Accuracy (DG Viewpoint)	Overall % Accuracy (DNO Viewpoint)
Perfect	1(-)	22.24	-	-	-	-	-	100	100
6% Error	5(3)	16.54	5.698	0	25.63	25.63	0	100	74.37
1% Error	1(0)	22.18	0.06	0	0.27	0.27	0	100	99.73

For ***Test Scenario 3***, Table 20, the 1% error case produces results that are marginally better in terms of net percentage error than the 6% case. For both cases, the algorithm favours the DG operator however both deliver solutions to a high degree of accuracy. The 6% error case is 89.77% accurate from the DG operator's viewpoint and 84.09% accurate from the DNOs outlook. The perceived accuracies for the 1% error case are more precise. 97.74% and 95.44% were recorded from the DG operators and DNOs perspective, respectively.

Table 20 - Test Scenario 3 (CSP-LIFO Curtailment Accuracy)

Test Scenario	***Test Scenario 3**: 11kV Radial Distribution Network with 'Line 2' Overloaded and DG A being the Last Historically Connected DG Unit*								
	No. of Control (Error Related) Signals	Net Curtail-ment (MW)	Under Curtail-ment (MW)	Over Curtail-ment (MW)	Net Error Curtail-ment (%)	Under Curtail-ment (%)	Over Curtail-ment (%)	Overall % Accuracy (DG Viewpoint)	Overall % Accuracy (DNO Viewpoint)
Perfect	2(-)	50.55	-	-	-	-	-	100	100
6% Error	4(2)	47.68	8.044	5.172	5.68	15.91	10.23	89.77	84.09
1% Error	2(0)	48.12	2.306	1.14	5.05	4.56	2.26	97.74	95.44

In Table 21 the results are tabularised for ***Test Scenario 4***. In this simulation significant data skew reverses the net percentage error for the erroneous cases with the 1% case achieving less accuracy overall. For the 6% error case the algorithm is more supportive of the DNO requirement delivering a 78.2% accurate solution. From the DG operators outlook this error was marginally less and was calculated to be 74.67%. For the 1% erroneous data case the DG operator would perceive the algorithm to be 82% accurate whereas from the DNOs point of view the 1% error case delivered a poor result of only 59.16% due to large under-curtailment taking place.

Table 21 - Test Scenario 4(CSP-LIFO Curtailment Accuracy)

Test Scenario	*Test Scenario 4: 11kV Radial Distribution Network with 'Line 2' Overloaded and DG B being the Last Historically Connected DG Unit*								
	No. of Control (Error Related) Signals	Net Curtail-ment (MW)	Under Curtail-ment (MW)	Over Curtail-ment (MW)	Net Error Curtail-ment (%)	Under Curtail-ment (%)	Over Curtail-ment (%)	Overall % Accuracy (DG Viewpoint)	Overall % Accuracy (DNO Viewpoint)
Perfect	2(-)	10.6	-	-	-	-	-	100	100
6% Error	4(3)	10.96	2.311	2.685	3.39	21.8	25.33	74.67	78.2
1% Error	2(1)	9.4	4.329	1.9	11.32	40.84	17.92	82.08	59.16

6.2.2.3 Curtailment Accuracy Summary

When error is applied to the measurements varying levels of accuracy of the algorithm's response, compared to that of the base case, is observed. Data skew and the time step in which the detection loop catches the thermal excursion and point at which the curtailment is released also have a bearing on the accuracy of the algorithms.

In Table 22 the average accuracy of the OPF-LIFO approach is tabularised. These values indicate the precision of the algorithm over all the erroneous ***Test Scenarios (1-4)*** and categorise the relative accuracies from the perspective of the DG operators and the DNOs. For the 6% erroneous case the average accuracy as perceived by the DG operator was 79.07% with a much lower result for the DNO of 52.17%. This latter result is pulled down by the poor results of ***Test Scenario 3***.

For the 1% error cases there are two values recorded for each of the stakeholders viewpoints due to the two simulations conducted for ***Test Scenario 2*** to examine the influence of the detection and the erroneous data. The less accurate of the cases (using the 'run 1') resulted in an accuracy of 73.43% and 86.89% from the outlook of the DG operator and the DNO, respectively. The 'run 2' scenario contributed to higher levels of accuracy for the DG operator and DNO (81.01% and 89.51% respectively).

Table 22 - Average Accuracy (OPF-LIFO)

Test Scenario	Average % Accuracy (DG Viewpoint)	Average % Accuracy (DNO Viewpoint)
Perfect	100	100
6% Error	79.07	52.17
1% Error (Run '1')	73.43	86.89
1% Error (Run '2')	81.01	89.51

The average accuracies for the CSP-LIFO approach are logged in Table 23. From the 6% measurement error case it can be viewed that overall the algorithm returned a high precision of accuracy. From the DG operators point of view the accuracy was 87.44% and from the DNOs it was 79.27% accurate. The 1% error case returned even higher levels of precision. The average overall accuracy from the DG operator's point of view was 93.91% and 88.06% from the DNO's outlook.

Table 23 - Average Accuracy (CSP-LIFO)

Test Scenario	Average % Accuracy (DG Viewpoint)	Average % Accuracy (DNO Viewpoint)
Perfect	100	100
6% Error	87.44	79.27
1% Error	93.91	88.06

The CSP-LIFO results illustrate that the discrete nature of CSP curtails DG to the required level as to retain the line flows within limits. The DG is maximised in the sense that the first discrete domain band that removes the thermal constraint is implemented. As and when network loading permits the DG output set point is moved to a higher band, in the pre-defined discrete steps, until DG can operate uncurtailed.

The OPF-LIFO results illustrate that the continuous nature of OPF curtails DG to the required level that maximises line flows and therefore also maximises the export of DG onto the network. The same can be observed when relaxing the DG control signals. A good resolution of DG maximum output signals are issued when network loading is such that the system can accommodate further DG exports without breaching thermal constraints.

In general, the CSP-LIFO algorithm curtails higher levels of DG output compared to that of the OPF-LIFO approach however the CSP approach yields more consistent accuracies for both parties. It can be observed that, for the high majority of cases, the CSP-LIFO algorithm has a lower net percentage error than OPF-LIFO. This increased level of accuracy, when subjected to measurement error, comes with the cost of larger amounts curtailment due to the discrete nature of the CSP-LIFO.

Chapter 7

Conclusions and Future Work

7.1 Conclusion

Within this concluding section the higher level implementation issues along with the ability of each of the PFM approaches to meet the general and user requirements (Chapter 1) is presented based upon the findings of the laboratory closed loop testing.

Finally, the potential areas of future interest for this research are documented.

7.1.1 Modelling and Problem Formulation

Successful modelling, problem formulation and implementation of the OPF and CSP LIFO approaches to PFM have been discussed and demonstrated. The results section has shown that the algorithms are capable of detecting thermal overloads and solving the particular network constraints. Curtailment signals can be sent to multiple DG units that cap the output of the associated unit allowing the generator to operate up to that permissible output. When the network loading conditions allow DG outputs to be increased the algorithms successfully recognise this condition and relax the curtailments signals appropriately. The formulations do not have to discriminate against current 'firm' and 'non-firm' generator connection agreements in that both can be intrinsically included within the formulation. That is, the 'firm' DG units can be included within the problem but would be have a higher connection priority so that they are called upon once all 'non-firm' DG units have been tripped from the network.

7.1.2 Computation Timescales

The operation and control of the PFM functions require detection and curtailment of DG real power in timescales appropriate to a real time control environment as a fundamental requirement to an ANM scheme. The approaches demonstrated within this thesis exhibit these traits. Under normal network topology the algorithms found

solutions ranging from tens of milliseconds up to tens of seconds. Even under an n-1 condition the maximum solution calculation time, for the CSP-LIFO approach, was in the region of 56 seconds. These timescales are well within the required computation times for solving thermal excursions.

7.1.3 Connection Principle Constraint

In addition, the PFM functions support the existing management of constrained DG connections and comply, in most cases, with the current connection agreement strategy. The CSP-LIFO approach adheres strictly to the last in, first off connection philosophy for all cases presented. From a commercial perspective this is a positive characteristic but from the operational sense some subtleties, such as, when a DG unit is not directly contributing to an overload (Test Scenario 4), are not realised. Therefore, under some circumstances rigid conformity to the LIFO principle may not maximise DG outputs from the technical and operational perspective although the CSP-LIFO algorithm delivers the best solution in terms of maximised DG output based upon it meeting all of the constraints (e.g. the commercial agreements). On the other hand, the OPF-LIFO approach provides solutions to thermal excursions but with the benefit that it does not take into account the LIFO arrangements when a DG unit clearly cannot have a direct impact on solving the network constraint. Additionally, when large step changes occur in system states, as observed when a line is switched out of service, the OPF-LIFO approach breaks the LIFO order when curtailment signals are sent but resumes the LIFO contracts when bringing DG back online.

7.1.4 Flexibility and Extensibility

The general requirements highlighted that the ANM system must be flexible and extensible. To be a flexible solution it must be easily reconfigurable to accommodate changes to the network in which it is controlling without redesign of the core functionality or architecture. The flexibility of the algorithms was demonstrated by

running successful test cases on two topologically different case study networks. In addition, both the algorithms adapted to dynamic topological changes by ensuring that circuit breaker status was updated and represented within the monitored network model. In terms of the addition or removal of controllable devices (other DG units or energy storage systems) this can easily be represented within the network model with plant ratings changed to reflect the change. The control bands (for CSP) and the LIFO arrangements (for both approaches) can easily be updated within the configuration files (.xml input files) without having to recode the core functions. Should monitoring or measurement devices on the network be altered then the network model can be updated to include the additional monitored circuits.

The extensible feature of replacing the functionality without having to redesign the system architecture has been demonstrated in that two PFM management approaches were evaluated within the closed-loop testing architecture. These, evaluations only required the PFM algorithms to be changed and configured while the other functionality and software remains the same. This results in a 'plug and play' architecture for the two tested algorithms and any others implemented using similar principles. Therefore, any future updated algorithms, based upon these examples or other developed methods, can easily replace legacy PFM techniques.

7.1.5 Robustness

Tolerance against failures, resulting from no measurement received or loss of communications, and resilience to erroneous measurement error is an inherent problem within closed-loop control systems such as an ANM scheme. Within the system architecture the OPC (Object linking and embedding for Process Control) communications standard was utilised to allow some degree of certainty to be attained for the measurements collected. A 'value', 'quality of value' and 'timestamp' element is associated to each measurement. The 'quality of value' enables a value to be flagged as 'good', 'uncertain' or 'bad'. Deployment of such a scheme would require examination of the communications standards and protocols to be used to identify what attributes are available for ascertaining the quality of data.

Consequently, any robustness issues such as loss of communications, lack of measurements or unexpected measurements to be detected and postpone the service of the power flow management algorithms until such time that a greater level of confidence in the data is achieved.

In terms of measurement error, each of the algorithms displayed varying resiliencies and the results illustrated the requirements of each of the approaches. Accurate measurements are essential to having a representative network model to ensure under curtailments and over curtailments are minimised. The response of the algorithms would be no worse than manual operations conducted, based on the visibility that a control engineer has of the network, with varying degrees of sensor tolerances. Furthermore, in the event that sensor or measurement errors occur the CSP-LIFO approach offers the characteristic of graceful degradation in that multiple ranked solutions can be returned. Therefore, if the first solution (that maximises DG output for the given thermal excursion) fails the next best solution can be implemented.

7.2 Conclusion and Discussion Summary

In general, the closed loop simulation results presented demonstrate that the novel application of OPF and CSP combined with prototype PFM algorithms, running on a commercially available substation computer platform, has the potential to operate in an online and real-time environment. The feasibility has been explored on two different network topologies and voltage levels. This demonstrated that practical solutions can be found for all 'Test Scenarios' and that the applied approaches have a network agnostic feature.

The OPF-LIFO approach showed faster response times with less overall curtailment of DG than that of the CSP-LIFO approach. This accuracy appears to be negatively impacted upon when presented with erroneous measurements due to the continuous nature of the optimisation problem. This approach also deviated from the LIFO connection constraint for two of the study cases. This non-conformity of the LIFO

principle of access demonstrates the potential for OPF-LIFO to be used under different connection principles such as DG bids for access to distribution network capacity or some form of sharing. One drawback of the OPF-LIFO approach is that no secondary solution can be offered in the event that the initial solution fails and hence this technique does not degrade in a graceful manner.

The CSP-LIFO technique demonstrated slower response times and higher levels of DG curtailment compared to the results of the OPF-LIFO approach. Due to the discrete nature of the CSP this technique was more resilient to measurement errors. Under all test conditions the CSP-LIFO approach reflected DG contractual arrangements by maintaining the LIFO principle. However, unnecessary generation curtailment was observed when DG units, further down the LIFO priority stack, were not directly contributing to a thermal overload. Due to the nature in which the CSP state space is searched, the algorithm can offer graceful degradation. If the first solution fails, from sensor errors or communications failure, then the next solution can be implemented until a satisfactory solution is found.

In conclusion, the developed and tested OPF-LIFO and CSP-LIFO approaches have been found to be viable in terms of robustness (practical solutions under all test cases have been found), speed of computation and the ability to represent existing (i.e. LIFO) and alternative principles of access to distribution network capacity. Active power flow management, utilising these approaches, allows greater energy yields across the DG units than that of conventional methods i.e. inter-tripping of 'non-firm' DG units and removes or at least defers the need for expensive capital investments to accommodate future DG connections.

In addition, the ANM algorithms presented can form part of the toolbox of proven technical solutions that can be deployed rapidly and cost effectively in future smart grids. The flexible and extensible characteristics enable augmentation as and when more controllable devices become available through active participation of consumers and generators. Rigorous testing and deployment of such ANM approaches aid the delivery of the required confidence, to DNOs and other network

stakeholders, in the ability of real-time control of today's networks. Employing ANM approaches require communication and hardware deployments and as such can offer the incremental steps required to achieve the full smart grid operating vision.

7.3 Future work

In conducting this research further developments have been highlighted in terms of research contributions and algorithm refinements. This section presents these the areas of interest that would be supported through the current regulatory environment and incentives offered for DG connections.

- Future work can take the work presented in this thesis from the closed loop-simulation environment and deploy the scheme within an operational platform to ensure that such a scheme can integrate and operate safely and securely with other power system automation and protection products [7.1]. Devices such as auto-reclosers and reconfiguration schemes would need to be included within the modelling capability to ensure the algorithms had sufficient visibility of network conditions. ANM operating criteria based upon these system events requires to be defined. Follow on research in this area will be conducted at the University of Strathclyde's Microgrid laboratory before moving the algorithms to a fully operational test environment at the Power Network Demonstration Centre (PNDC) in Cumbernauld. PNDC offers an opportunity to embed these novel ANM algorithms in a controlled operational environment that will enable the capture of all relevant data to conduct open loop evaluations under a number of different emulated communication channel scenarios. This data will provide useful benchmark information for conducting further investigations of the approaches under different operating conditions prior to closing the loop in the operational environment. The outcome of this research would generate new interoperability knowledge, communication channel information and identify specific algorithm refinements.

- The OPF-LIFO approach to PFM delivered high precision control actions for all of the DG units [7.2]. In practical circumstances it may not be desirable for the DG units to change their outputs frequently and to a high degree of accuracy (yielding small changes to DG output), particularly if there is uncertainty in the quality of data. Further investigations into the implementation of a 'deadband' for the OPF-LIFO approach should be considered. Studies into quantifying/stating these practical benefits of operating at different 'deadband' values against the reduced 'optimality' of the solutions (i.e. levels of DG access) and the impact on the communication channels would be an area of future research work.

- CSP-LIFO was shown to be a scalable solution for the case study networks [7.3]. There is an evident implication on the increased computation time when the number of controllable units is increased due to the exponential increase in the size of the state space. Further investigation into constraint propagation, the introduction of heuristics and utilising other solver algorithms (backtracking, recursive backtracking, local search, forward checking, branch and bound, minimum conflict) would be beneficial to identify faster or better ways to search or reduce the problem as the search space exponentially expands with increased controllable units. Quantifying the trade-offs between the time taken to prune the state space and the time it would take to search the entire state space with different solvers would be highly valuable. In addition to examining efficient methods of searching/reducing the state space, another area of future work would be to examine the 'zones' of control and investigate how to implement distributed constraint satisfaction approaches and draw out the benefits and potential limitations to this approach.

- Further evaluation of the system interface requirements for ANM schemes into the DNO's existing Supervisory Control and Data Acquisition (SCADA) system and Distribution Management System (DMS). This future research

area would entail the incorporation of the ANM scheme into the existing DMS that may result in additional functionality that allows:

  - The ANM status to be relayed back to a central control centre
  - ANM override capability at local and central levels (ANM 'on', 'off' or 'reject' solution)
  - Enable the ANM system to recognise that a user action has taken place and suspend actions accordingly
  - Provision of alarms to the control centre when the ANM scheme recognises the need to carry out an action and confirm what action and when that action is carried out
  - Control centre commands issued via the ANM scheme
  - Local warning of control action taking place

- Measurements on the distribution network are currently limited and due to the expansive nature of distribution systems it may not be financially possible to deploy sensor and measurement devices to record all required data and system state. Therefore, research that would investigate the role of distribution state estimation as the primary measurement source for ANM schemes is required to identify the operating characteristics when presented with estimated measurements.

- Research to investigate alternative controller options that would enable energy storage systems or demand side management schemes to be easily embedded within a network as a controllable device would be highly beneficial. Additional, controllable devices that allow the active participation of other network control devices and consumers is in line with the future energy network vision. Characteristics such as, accurate state of charge, charge and discharge cycles (energy storage and domestic thermal storage) that can define the level of support (and limitations) on offer by a particular device is important for any ANM scheme incorporating these devices to allow effective and efficient management of network constraints.

- Research into the implementation of dynamic line ratings and dynamic detection limits within the ANM scheme to identify the benefit in terms of increased DG access. Research outputs could entail investigating the frequency in which the real-time computation and updating of the model's line ratings is required to achieve higher levels of DG through higher utilisation of network lines and plant.

- Further investigation is required into the role that the PFM approaches could take on with different DG connection principles [7.4]. Research into the capability of the OPF's technique to represent alternative principles of DG access is required to determine the techniques feasibility and flexibility for future connection arrangements. In addition, the ease in which future connection agreements can be implemented in software for the CSP approach requires further research.

- Research into a 'preventative' power flow management function using forecasting capabilities to determine the depth and duration of a thermal overload could result in the decreased curtailment of DG. Research could investigate the benefits/drawbacks of setting DG outputs prior to the envisaged excursion to avoid the overload condition. In addition, identifying whether a forecast can be used to postpone the ANM scheme issuing control actions to alleviate a thermal overload of short duration and depth would be of interest.

7.4 Chapter 7 References

[7.1] Federico Coffele, Michael J. Dolan, Campbell Booth, Graham W. Ault, Graeme Burt, "Co-ordination of Protection and Active Network Management for Smart Distribution Networks", CIRED Workshop 2012, May 2012, Paper No. 0031

[7.2] Michael J. Dolan, Euan M. Davidson, Ivana Kockar, Graham W. Ault, Stephen D. J. McArthur, "Distribution Power Flow Management Utilising an Online Optimal Power Flow Technique", IEEE Transactions on Power Systems, *in pres*

[7.3] Michael J. Dolan, Euan M. Davidson, Graham W. Ault, Stephen D. J. McArthur, Keith Bell, "Distribution Power Flow Management Utilising an Online Constraint Programming Technique", IEEE Transactions on Smart Grid, *under review*

[7.4] Ivana Kockar, Euan M. Davidson, Graham W. Ault, Michael J. Dolan, "Distributed Generation Access and Power Flow Management", IEEE PES General Meeting, Minneapolis, July 2010